The roles of RNA Polymerase I and III subunits Polr1a, Polr1c, and Polr1d in craniofacial development

BY

Kristin Emily Noack Watt

Submitted to the graduate degree program in Anatomy and Cell Biology and to the Graduate Faculty of The University of Kansas Medical Center in partial fulfillment of the requirements for the degree of Doctor of Philosophy.

Paul Trainor, Co-Chairperson

Brenda Rongish, Co-Chairperson

Brian Andrews

Jennifer Gerton

Tatjana Piotrowski

Russell Swerdlow

Date Defended: January 26, 2016

The Dissertation Committee for Kristin Watt

certifies that this is the approved version of the following dissertation:

The roles of RNA Polymerase I and III subunits Polr1a, Polr1c, and Polr1d in craniofacial development

Paul Trainor, Co-Chairperson

Brenda Rongish, Co-Chairperson

Date approved: February 2, 2016

Abstract

Craniofacial anomalies account for approximately one-third of all birth defects. Two examples of syndromes associated with craniofacial malformations are Treacher Collins syndrome and Acrofacial Dysostosis, Cincinnati type which have phenotypic overlap including deformities of the eyes, ears, and facial bones. Mutations in *TCOF1*, *POLR1C* or *POLR1D* may cause Treacher Collins syndrome while mutations in *POLR1A* may cause Acrofacial Dysostosis, Cincinnati type. *TCOF1* encodes the nucleolar phosphoprotein Treacle, which functions in rRNA transcription and modification. Previous studies demonstrated that *Tcof1* mutations in mice result in reduced ribosome biogenesis and increased neuroepithelial apoptosis. This diminishes the neural crest cell (NCC) progenitor population which contribute to the development of the cranial skeleton. In contrast, apart from being subunits of RNA Polymerases (RNAP) I and/or III, nothing is known about the function of POLR1A, POLR1C, and POLR1D during embryonic and craniofacial development. I therefore examined zebrafish with mutations in *polr1a*, *polr1c*, and *polr1d* to understand the function of RNAPI during embryogenesis. Remarkably, these genes are dynamically expressed during embryonic development and display enriched expression in craniofacial regions, such as the pharyngeal arches, demonstrating that they may have tissue specific functions. Homozygous mutant *polr1a, polr1c*, and *polr1d* zebrafish display reduced cranial cartilage formation due to elevated *tp53*-dependent cell death of NCC progenitors and a diminished population of cranial NCC. In addition, mutant embryos have altered ribosome biogenesis, as demonstrated by reduced rRNA transcription and polysome profiling, which impact the survival and proliferation of cranial

NCC. Taken together, this suggests diminished ribosome biogenesis, nucleolar stress, and Tp53-dependent neuroepithelial apoptosis underlie the loss of NCC needed to generate the normal cranioskeletal elements, consistent with the *Tcof1* studies. In support of this mechanism, genetic inhibition of *tp53* is one approach for improving the skeletal deficiencies in *polr1c* and *polr1d* mutants. These zebrafish models represent the first study of RNAPI during craniofacial development and demonstrate that tissue specific phenotypes can arise from disruptions of global processes like ribosome biogenesis. The *polr1a, polr1c*, and *polr1d* zebrafish will be useful for further examining RNAPI function as well as finding potential therapies for the prevention of craniofacial anomalies.

Acknowledgements

In the course of my PhD research, I have been helped by so many wonderful people. I would like to thank all those who kindly provided reagents. The Nancy Hopkins lab generated the *polr1a*, *polr1c,* and *polr1d* zebrafish and Dr. Adam Amsterdam kindly provided primers for genotyping. Dr. Tom Schilling provided *sox10:gfp* transgenic zebrafish to aid in my studies of neural crest cells, and Dr. Tatjana Piotrowski provided the tp53 mutant zebrafish for my rescue experiments.

The core facilities at the Stowers Institute were also immensely helpful. I thank the SIMR Aquatics team for zebrafish care and maintenance – especially Jamie, Jessica, Lily, Xia, and Darin – for completion of numerous fin clip requests so I could genotype my fish and maintain the colony. The microscopy team provided excellent training and assistance with confocal microscopy and I especially thank Cindy Maddera for her assistance as well as Richard Alexander for his assistance with image quantification and the IMARIS software. I thank the Molecular Biology core for assistance with qPCR experiments and RNA-Seq, especially Willie, Brian, and Allie. Finally, I thank Chris Seidel for his analysis of the RNA-Seq data.

I would next like to thank our collaborators at University of Southern California, Cynthia Neben and Dr. Amy Merrill-Brugger for their assistance with polysome profiling. I thank Cynthia for running numerous polysome samples, optimizing the protocol, and then kindly showing me the process and Amy for helping to make the collaboration possible and for discussions about ribosome biogenesis.

I thank my committee members for their guidance, support, and suggestions. My project benefited greatly from the input of each of my committee members – to Dr. Piotrowski for her zebrafish expertise, to Dr. Gerton for her expertise in the ribosome field,

Finally, I have to thank my family. My parents, Max and Jeanne, have always stressed the importance of education and worked so hard to provide learning opportunities as I was growing up. They are two of the hardest working people I know and taught me the value of doing the job right and doing it well. Their example, love, and support over the years have helped me become the person I am to which I fell incredibly blessed. I also thank my brother, Ben, for setting an example of being curious about the world. He is one of the most brilliant people I know and so excited about learning. I have enjoyed our conversations about what science is and he always provides an interesting philosophical perspective. Thanks to my dad and brother, chemistry and physics were common topics of conversation at the dinner table, which always challenged me to learn more.

I also owe a great deal to my husband, Joshua, who has supported me throughout grad school. He encouraged me to keep going when I didn't think I could, and put up with all of the late nights and long hours; he made me dinner and brought it to the lab many times so I could make it through another late night. He patiently sat through numerous practice talks, even though biology is not his area, because I needed someone to be an audience. We were also blessed with our daughter, Nora, during this time and it has been a joy to watch her develop. Joshua has been an incredible father to her, and had spent extra time with her so I could work on my thesis. Without his help, I would not have finished writing my thesis.

Dedication

To my parents, Max and Jeanne, and my husband Joshua for their love and support and for making this possible.

Table of Contents

List of Tables

List of Figures

xvii

I. INTRODUCTION

Craniofacial anomalies occur in approximately 1/100 live births and the consequences of these anomalies can require significant medical interventions. Understanding the process of craniofacial development is important for determining the etiology and potential mechanisms for prevention of craniofacial anomalies, which can be isolated or syndromic. Two examples of syndromes with craniofacial anomalies are Treacher Collins syndrome (TCS) and Acrofacial Dysostosis, Cincinnati Type which will be described in detail in Chapters III and IV. TCS may result from mutations in *TCOF1*, *POLR1C*, or *POLR1D* while Acrofacial dysostosis, Cincinnati Type is associated with mutations in *POLR1A*. POLR1A, POLR1C, and POLR1D are all subunits of RNA Polymerase I, which synthesizes ribosomal RNA. These syndromes are characterized as both neurocristopathies and ribosomopathies, which arise from deficiencies in neural crest cells and ribosome biogenesis, respectively. In this thesis, I examine the roles of neural crest cell development and ribosome biogenesis in zebrafish models of TCS and Acrofacial Dysostosis, Cincinnati Type.

Neural Crest Cells and Neurocristopathies

Neural crest cells (NCC) are a migratory stem and progenitor cell population established early in development around the time of gastrulation and continue to develop through late organogenesis. In many vertebrate models, NCC are induced at the neural plate border, which folds to form the neural tube, and the neural crest progenitors reside

in the dorsal portion of the neural tube (Bronner-Fraser, 1994; Le Douarin and Kalcheim, 1999). NCC then undergo an epithelial-to-mesenchymal transition and migrate out of the neural tube to distant sites throughout the embryo, eventually contributing to a number of different tissues. These tissues include the bones, cartilage, and connective tissue in the head and face, pigment cells, and neurons and glia (Le Douarin and Kalcheim, 1999; Knecht and Bronner-Fraser, 2002) (See Figure I-1). Since the NCC contribute to such a wide array of tissues, they have been called a fourth germ layer (Hall, 2000). The phases of NCC development can be generally categorized into formation, migration, and differentiation. Perturbation of NCC development at any of these stages can result in a number of disorders classified as neurocristopathies, which are defined by disrupted development of NCC or NCC-derived tissues. The craniofacial anomalies present in TCS and Acrofacial dysostosis, Cincinnati type are indicative of altered NCC development, as the craniofacial skeleton is primarily derived from NCC, and these syndromes are therefore classified as neurocristopathies. Portions of this introduction were published as a book chapter on neurocristopathies (Watt and Trainor, 2014). In the following sections, I describe NCC development, with an emphasis on their roles in zebrafish, and use neurocristopathies to demonstrate the importance of NCC formation, migration, and differentiation during embryogenesis.
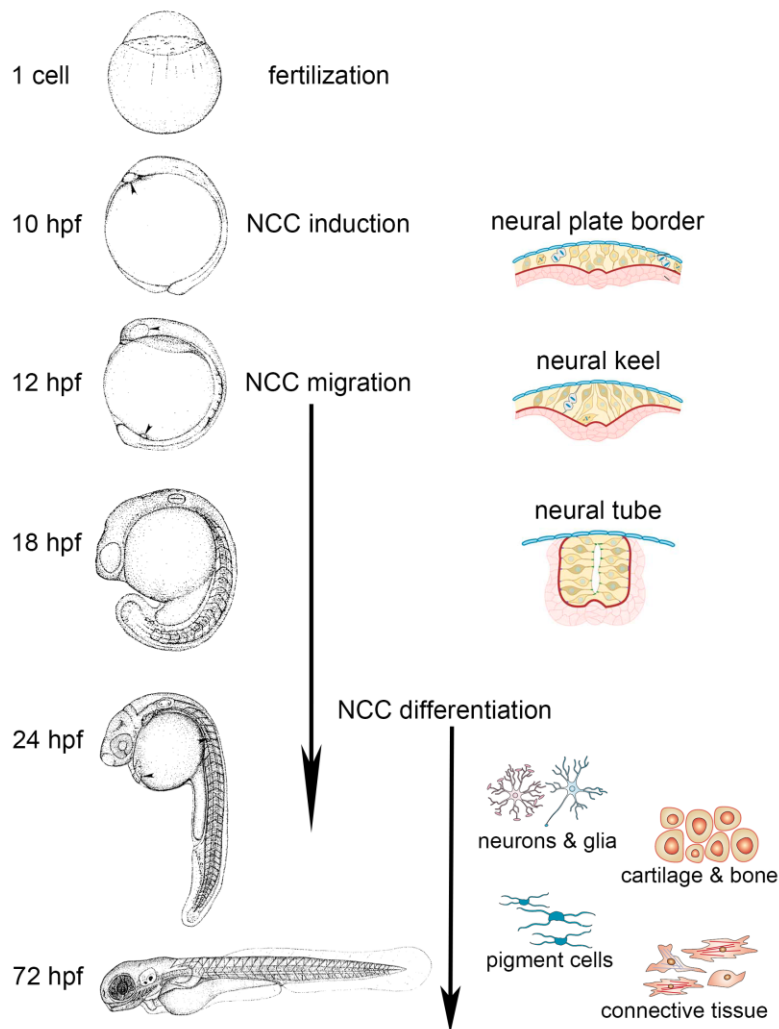
Figure I-1 Neural crest cell development occurs during zebrafish embryogenesis.
NCC development begins with the induction of NC specifiers at the neural plate border at approximately 10 hours post fertilization (hpf). The neural plate thickens to form the neural keel and NCC begin migration around 12 hpf as they delaminate out from dorsal regions of the neural keel. The neural keel folds together to form the neural rod, which then hollows to form the neural tube by 18 hpf. Migration continues and overlaps with the beginning of NCC differentiation at about 24 hpf. At this time, NCC are being specified towards different lineages including bone, cartilage, connective tissue, neurons, glia, and pigment cells. These tissues continue to develop into the larval stages of zebrafish development (beyond 72 hpf). Images adapted from (Kimmel et al., 1995), (Araya et al., 2015) and (Knecht and Bronner-Fraser, 2002).

3

NCC Formation

NCC formation requires a complex series of signaling and tissue interactions in the developing embryo. In this section, I describe the induction of NCC and the tissues and signals involved in this process.

NEURAL INDUCTION

NCC formation begins during gastrulation stages in which the three germ layers - endoderm, mesoderm, and ectoderm - are established and give rise to the majority of the tissues in the body. Cellular movements during gastrulation generate these different germ layers, and in zebrafish embryos this process begins at approximately 5 hours post fertilization (hpf) and is completed around 10 hpf (Kimmel et al., 1995; Gilbert, 2010). Establishing polarity across the embryo is important for the generation of the different germ layers. For example, Nodal signaling is important for establishing mesoderm (Schier and Talbot, 2001), while different levels of BMP are important in establishing ectoderm (Nguyen et al., 1998; Schumacher et al., 2011). The ectoderm is segregated into neural and non-neural regions, with NCC induction occurring at the border between these regions. The neural ectoderm gives rise to the neural plate, which will eventually become the central nervous system, while the non-neural ectoderm will become the epidermis.

In zebrafish, formation of the neural plate occurs during gastrulation and can be observed along the anterior-posterior axis of the embryo by 10 hpf (Figure I-1) (Kimmel et al., 1995). In contrast to avian or frog embryos, in which the neural plate folds in a process called primary neurulation (Le Douarin and Kalcheim, 1999), the zebrafish neural

4

plate undergoes a process called secondary neurulation. The neural plate thickens towards the midline to form the neural keel, which is observed at 12 hpf (Araya et al., 2015). At 12 hpf, two layers are visible in the head: the dorsal ectoderm, which will produce NCC, and the ventral mesoderm/endoderm (Schilling and Kimmel, 1994). By 15 hpf, the neural keel has folded into a neural rod, and a lumen forms in the neural rod to form the neural tube by 17-18 hpf with the NCC progenitors located in the dorsal portion of the neural tube (Figure I-1) (Raible et al., 1992; Lowery and Sive, 2004; Araya et al., 2015).

TISSUES AND SIGNALS IN NCC FORMATION

The induction of the genetic program for neural plate border (NPB) and NCC specification requires the appropriate production of signaling molecules from the surrounding tissues. Signals from the three germ layers are integrated for the induction of NCC (LaBonne and Bronner-Fraser, 1999). Bone morphogenetic protein (BMP) is one particular signal which has been implicated in formation of NCC, however, BMP alone is not sufficient to induce NCC (LaBonne and Bronner-Fraser, 1998; LaBonne and Bronner-Fraser, 1999). Additional signals required include Wnts, fibroblast growth factors (Fgfs), and retinoic acid (RA) although the timing, location and amount of these signals varies between organisms (Streit et al., 2000; Mayor and Aybar, 2001; Villanueva et al., 2002; Lewis et al., 2004).

Formation of the neural plate and NPB in zebrafish requires intermediate levels of BMP signaling and a combination of Fgf and Wnt signals (Figure I-2) (Garnett et al., 2012). Studies in Xenopus embryos show a gradient of BMP patterns the ectoderm, in which low

levels lead to neural plate formation, intermediate levels lead to NCC induction, and high levels lead to epidermis formation (Mayor and Aybar, 2001). In addition, expression of BMP antagonists within the mesoderm help modulate levels of BMP (Marchant et al., 1998). Studies of BMP pathway mutations in zebrafish also demonstrate that a gradient of BMP is established and intermediate levels are required for NCC generation (Schumacher et al., 2011). For example, mutation of the BMP ligand *bmp2b* results in a failure of NCC induction and demonstrates a requirement for BMP in the generation of NCC (Nguyen et al., 1998). Surprisingly, the presence of mesoderm is not absolutely required for NCC induction in zebrafish. Upon elimination of mesoderm using Nodal signaling mutants, NCC specifier genes are still expressed; however, the domains of expression are altered and the levels of migratory NCC are reduced in mutant embryos (Ragland and Raible, 2004). This suggests that there may be important roles for mesoderm at later stages of NCC development such as in migration and differentiation. In addition to BMP, Fgf signaling also functions to pattern the early zebrafish embryo, as inhibition of Fgf signaling results in expansion of *bmp2b* expression (Fürthauer et al., 2004). This expansion of *bmp2b* expression would then be expected to alter BMP levels and impact NCC induction, however NCC were not investigated in this study. In a separate study, NCC induction was investigated in response to alterations in Wnt signaling at specific times using a heat-shock inducible Wnt inhibitor. Inhibition of Wnt signaling specifically at the end of gastrulation (approximately 10 hpf), prevented expression of the NCC specifier *foxd3* (Lewis et al., 2004).

Recently, the integration of BMP, Wnt, and Fgf signals in establishing the NPB and NCC progenitors was investigated. Experiments using heat-shock activation of *dkk1*, a Wnt antagonist, and heat-shock activation of *bmp2b* at 6 hpf and 8 hpf revealed that both Wnt and BMP signaling were required for accurate expression of *zic3*, a NPB specifier gene (Garnett et al., 2012). However, *pax3a* expression, another NPB specifier gene, was not strongly affected by *dkk1* over-expression, suggesting a different responsiveness to Wnt signaling (Garnett et al., 2012). Fgf signaling is known to be important in NPB formation in *Xenopus*, so its role in zebrafish NPB was investigated using the Fgf inhibitor SU5402. Expression of *pax3a* was reduced upon SU5402 treatment, but *zic3* levels were not affected (Garnett et al., 2012). Altogether, this indicates a different responsiveness to the Wnt, Fgf, and BMP signals during NPB specification, but that all of these signals play a role in the proper expression of the NPB specifier genes – both the domain as well as the levels of expression.

Thus, the combination of BMP, Wnt, and Fgf signals are required at the proper time and at the correct level in order for the NBP to become competent to generate expression of NCC specifiers and form NCC. The transcription factors *tfap2a* and *foxd3*, which also have roles in NCC migration and differentiation, are two of the earliest NCC specifiers in zebrafish. Expression of *foxd3* is observed during gastrulation at the NPB (Odenthal and Nüsslein-Volhard, 1998), and *tfap2a* expression is observed at gastrulation stages as well (Barrallo-Gimeno et al., 2004). Loss of *tfap2a* alone leads to apoptosis of NCC progenitors, while loss of *foxd3* alone leads to diminished NCC derived tissues such as the craniofacial skeleton and peripheral nervous system (Wang et al., 2011). The combined loss of *tfap2a*

7

and *foxd3* results in the absence of the pre-migratory NCC population, confirming a role for these factors in NCC induction (Wang et al., 2011). Tfap2a and Foxd3 then function to activate a series of NCC specifier genes which have roles in NCC development and migration and will be discussed in the next section.
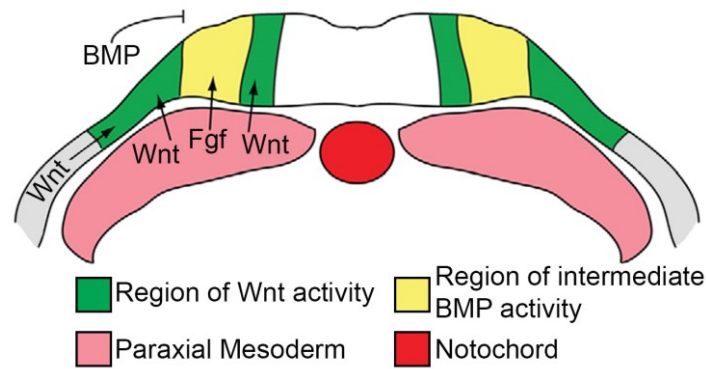
Figure I-2 A model of zebrafish neural plate formation.
The neural plate (white) is established while the border regions (green) receive Wnt, Fgf, and BMP signals. An intermediate level of BMP is necessary for induction of NCC from the NPB. Regions beyond the NPB will form the epidermis (gray). Figure adapted from Garnett et al., 2012.

NCC Migration

The migration of NCC involves initiation of NCC specifier genes followed by an epithelial to mesenchymal transition (EMT) which enables the NCC to migrate out from the neural tube and into specific regions of the embryo. In this section I highlight the migration of the cranial NCC, the *hox* and *dlx* signaling complexes involved in patterning the head, and some of the NCC specifier genes and other signaling molecules involved in NCC migration.

NCC SPECIFIER GENES

Cell autonomous expression of NCC specifier genes are required to generate migratory NCC (Reviewed in (Betancur et al., 2010; Rogers et al., 2012). Many of the NCC specifier genes have multiple roles during NCC development including NPB specification, migration, and differentiation. Some of these genes are *Sox9, Sox10, Foxd3, Twist,* and *Snail2*. *Sox9* has been shown to be important in NCC specification in *Xenopus* (Spokony et al., 2002) and then later in the differentiation of NCC into cartilage in zebrafish and mice (Yan et al., 2002) (Bi et al., 2001; Mori-Akiyama et al., 2003). Zebrafish have two copies of the *sox9* gene, *sox9a* and *sox9b,* which are both capable of functioning as transcription factors. These genes are expressed in distinct, though overlapping, patterns during zebrafish development. *sox9b* is expressed within premigratory NCC at 14 hpf, while *sox9a* is expressed within the somites. *sox9a* expression is not required for NCC specification or migration in zebrafish (Yan et al., 2002), but mutations in *sox9b* lead to diminished expression of other migratory NCC markers (Yan et al., 2005). At 24 hpf, both

sox9a and *sox9b* are expressed in similar regions of the brain, however, only *sox9a* is expressed in the cranial mesenchyme which will contribute to the formation of the pharyngeal arches and thus the craniofacial skeleton. At later stages (2-3 dpf) both *sox9a* and *sox9b* are expressed in the craniofacial cartilage condensations, although *sox9a* is expressed at a higher level (Chiang et al., 2001). Zebrafish with mutations in *sox9a* have little expression of *col2a1* and almost no craniofacial skeleton; zebrafish with mutations in *sox9b* have slightly more craniofacial cartilage, while double mutants have no pharyngeal skeleton (Yan et al., 2002). Corresponding with a more important role in skeletal differentiation, mutations in *SOX9* in humans lead to the disorder campomelic dysplasia which is characterized by underdevelopment of the skeleton, bent long bones, cleft palate, and micrognathia (Wagner et al., 1994).

Another *Sox* gene, *Sox10,* has roles in NCC formation, maintenance, and differentiation (Kelsh, 2006). It is expressed early in development in humans (Bondurand et al., 1998), mice (Kuhlbrodt et al., 1998; Southard-Smith et al., 1998), zebrafish (Dutton et al., 2001), chick (Cheng et al., 2000), and frog (Honoré et al., 2003). *Sox10* has multiple roles during NCC development including formation of pigment cells and enteric ganglia (Bondurand et al., 1998; Kuhlbrodt et al., 1998; Southard-Smith et al., 1998; Dutton et al., 2001; Aoki et al., 2003) as well as maintaining multipotency of neural crest stem cells (Kelsh, 2006), influencing fate decisions of the melanocyte lineage (Bondurand et al., 2000; Potterf et al., 2000; Elworthy et al., 2003), and maintaining pluripotency in migrating enteric nervous system progenitors (Bondurand et al., 2006). In zebrafish, *sox10* is expressed in the premigratory NCC at the NPB at the 1-somite stage and is maintained in

migratory NCC (Dutton et al., 2001). At later stages, *sox10* is expressed in melanocyte, neuron, and glial precursor cells, but not within the craniofacial cartilage. However, ectopic Sox10 expression is observed in craniofacial cartilage in some transgenic lines such as Tg(7.2kb-*sox10:gfp*) (Hoffman et al., 2007). Consistent with the expression within melanocytes and neurons, the zebrafish *sox10* mutant, known as *colorless*, fails to develop the enteric nervous system and lacks the majority of pigment cells (Dutton et al., 2001). This is in agreement with the roles for *SOX10* in humans where mutations in *SOX10* can result in Waardenburg syndrome (WS). WS is characterized by pigmentation defects of the skin and hair and sensorineural hearing loss and is frequently associated with Hirschsprung disease, which is classified by varying degrees of colonic aganglionosis (Pingault et al., 2010). In the zebrafish, the NCC that would normally adopt non-ectomesenchymal NCC fates, such as melanocytes, fail to migrate and differentiate and instead undergo apoptosis resulting in the *sox10* mutant phenotype (Dutton et al., 2001; Elworthy et al., 2005).

NCC must undergo an EMT to segregate and migrate away from the neural tube. This transition requires down-regulation of cell adhesion molecules such as E-cadherin and N-cadherin, and interactions with signaling molecules. Some of the NCC specifiers have roles in EMT such as *Foxd3* and *Snail2* (*snai2* in zebrafish).

Foxd3 is expressed in premigratory and migratory NCC in mice (Labosky and Kaestner, 1998; Yamagata and Noda, 1998). Early in development, *Foxd3* acts to specify NCC and is required for maintenance of multipotent NCC progenitors (Dottori et al., 2001). Activation of cell adhesion molecules, such as N-cadherin, Cadherin7, Laminin, and Integrinb1, by Foxd3 is necessary for NCC migration (Cheung et al., 2005). *Foxd3* is also

expressed in the forming dorsal root ganglion (Lister et al., 2006) and suppresses the development of the melanocyte lineage (Thomas and Erickson, 2009). In zebrafish, *foxd3* is expressed within the NPB and then in the premigratory NCC, but is downregulated in migratory NCC, and is also found in the somites as development proceeds (Stewart et al., 2006). Zebrafish with mutations is *foxd3* show normal NCC induction, but diminished expression as well as a disrupted pattern of the migratory NCC markers *sox10* and *crestin* (Stewart et al., 2006). At later stages, *foxd3* mutants have deficiencies in the NCC-derived neurons and craniofacial cartilage (Stewart et al., 2006). NCC-derived tissue defects are the result of increased cell death in a subpopulation of the premigratory NCC within the hindbrain region and potentially also the reduced ability of NCC to migrate in the correct pattern. These results emphasize the importance of *foxd3* expression within the premigratory NCC population and suggest a role for *foxd3* in activating genes important for NCC migration and survival.

Snail2 (also known as Slug) primarily functions in NCC specification and initiation of EMT and is expressed in migratory NCC, but not premigratory (Jiang et al., 1998). In mouse cell lines, Snail was shown to repress *E-cadherin* (Cano et al., 2000) while studies in chick embryos showed that Snail2 directly represses *Cadherin6,* a cell adhesion molecule, enabling NCC migration (Taneyhill et al., 2007). Zebrafish snail genes include *snail1a, snail1b* (previously named *snail2*), and *snai2. snai2* expression can be found at the neural plate border as well as paraxial mesoderm (Thisse et al., 2001). After gastrulation, *snail1a* is expressed in muscle pioneer precursors (Thisse et al., 1993) while *snail1b* is expressed at the neural plate border, including within NCC precursors, and is

later expressed in NCC (Thisse et al., 1995). The distinct but overlapping domains of *snail1a* and *snail1b* expression enable them to function together in the migration of axial mesendoderm (Blanco et al., 2007). Morphilino knockdown of *snail1b* resulted in an increase in Cdh1 (E-cadherin), indicating Snail1b functions as a repressor of E-cadherin and would then function in enabling EMT (Blanco et al., 2007). Another cadherin, *cadherin6* is expressed in hindbrain and NCC of zebrafish embryos and has been shown to function in promoting EMT through regulating F-actin (Clay and Halloran, 2014). The alternate function of *cadherin6* in promoting EMT in zebrafish stands in contrast to the down regulation of Cadherin6 in chick (Taneyhill et al., 2007). These differences illustrate that adhesion molecules like Cadherin6 may have different functions depending on the developmental timing, such as prior to EMT or after EMT, and embryonic context. In humans, mutations in *Snail2* have been reported to cause piebaldism, a disorder characterized by patches of unpigmented skin and hair (Sánchez-Martín et al., 2003). A potential mechanism is that melanocyte precursors are unable to undergo EMT and instead undergo apoptosis, similar to what occurs upon mutation of *sox10*.

In summary, NCC specifier genes including *sox9*, *sox10*, *foxd3* and *Snail2* all have important functions in NCC migration. Expressing NCC specifiers at the appropriate level and time is important for NCC development to proceed. In addition, patterning within the embryo (discussed below) determines whether the NCC will migrate, survive, and differentiate into the correct elements.

CRANIAL NCC MIGRATION

The migratory NCC emerge along the anterior–posterior axis of the embryo and NCC are generally divided into the cranial, vagal, and trunk populations. The cranial NCC are the first to undergo EMT and migrate, with the more posterior populations emerging sequentially. In zebrafish, the premigratory NCC express specifiers such as *sox10* around 12 hpf and then begin migration (Figure I-1). By 15 hpf, migration of cranial NCC can be observed with more posterior regions of NCC, such as the vagal and trunk populations, emerging sequentially (Schilling and Kimmel, 1994; Kimmel et al., 1995). By 24 hpf, some of the cranial NCC have migrated to reach their destinations where they differentiate into a number of different tissues while some of the trunk NCC are still in the process of migrating (Raible and Eisen, 1994; Kimmel et al., 1995). The cranial and trunk NCC migrate in different patterns, but there are common features such as the involvement of similar signaling molecules. The migration of cranial NCC will be discussed below.

Cranial NCC migration requires a complex series of interactions between the NCC and the endoderm, mesoderm, and ectoderm. In the cranial region, NCC migrate out from the developing brain, which is divided into the diencephalon, mesencephalon, and hindbrain. The hindbrain is further divided into segments known as rhombomeres (r). On the ventral side of the embryo, structures called the pharyngeal arches (PA) form, which are a series of paired mesodermal outpocketings surrounded by the surface ectoderm and separated by portions of endoderm, known as the endodermal (or pharyngeal) pouches (Figure I-3). NCC which arise from the dorsal neural tube migrate in conserved pathways into the PA and both proper patterning of the PA and the cranial NCC are needed for normal

craniofacial development (Klymkowsky et al., 2010). This patterning involves both cell-autonomous features of NCC, such as expression of NCC specifiers, as well as non-cell autonomous interactions with the surrounding endoderm, mesoderm, and ectoderm which provide signals to direct migration and differentiation (Cordero et al., 2011). In order for NCC to reach the correct locations, they must express NCC specifier genes and the embryo must be segmented correctly with the proper signals in place.
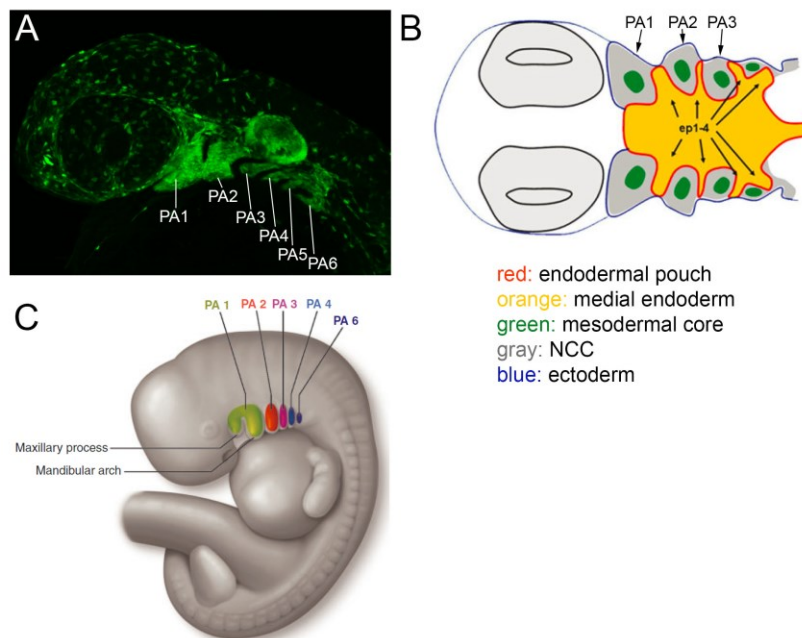
Figure I-3 Pharyngeal arch structure in zebrafish and humans.
A) *sox10:gfp* labels NCC within the pharyngeal arches (PA) in a 36 hpf zebrafish embryo. B) Diagram of a cross-section through a zebrafish embryo reveals the paired structures of the PA. ep: endodermal pouch. Adapted from Kopinke *et al.* (Kopinke et al., 2006). C) Diagram of PA structures in a human embryo. PA1 in humans is divided into a maxillary and mandibular component. Adapted from Frisdal & Trainor (Frisdal and Trainor, 2014).

PATTERNING AND SIGNALING MOLECULES IN NCC MIGRATION

The craniofacial region is patterned by signaling complexes, morphogens, and ligand/receptor interactions, all of which are required to ensure migration of the cranial NCC to the correct locations (Akimenko et al., 1994; Trainor and Krumlauf, 2001; Cordero et al., 2011; Frisdal and Trainor, 2014). Two major signaling complexes in this process are the homeobox (*Hox*) genes which give anterior-posterior positioning information and the distal-less homeobox (*Dlx*) genes which provide dorsal-ventral patterning to the pharyngeal arches (Figure I-4) (Schilling et al., 2001; Medeiros and Crump, 2012). *Hox* genes are expressed in a region-specific manner providing distinct arch identities. During development, the embryo establishes anterior-posterior segmental identity in large part through combinatorial expression of *Hox* genes. The *Hox* expression pattern is well characterized in the hindbrain, which is divided into seven segments called rhombomeres (r) and confers segmental identity to cranial NCC; this identity is critical for forming proper structures after NCC migration (Lumsden et al., 1991; Kontges and Lumsden, 1996). The anterior limits of *Hox* expression vary and there are different combinations of *Hox* expression in different rhombomeres. In zebrafish, *hoxa2* is expressed in r2, while *hoxb3* is expressed in r4, and *hoxb4* in r7 (Prince et al., 1998; Schilling et al., 2001; Hunter and Prince, 2002). NCC which come from the midbrain and r1 have no *hox* expression, while *hoxa2* is expressed in NCC of r2 and r3, both *hoxa2* and *hoxb3* are expressed in r4 and r5 and only *hoxb3* is expressed in r6 (Schilling et al., 2001). These different combinations of *hox* expression persist in the NCC which populate the different PAs and function in the patterning of the elements derived from each arch.

16

Alterations of *Hox* gene expression result in homeotic transformations of NCC derivatives (Trainor and Krumlauf, 2000b; Minoux et al., 2009), whereby the elements of one segment of the embryo are replaced by those characteristic of another. Changes in retinoic acid may alter expression of the *Hox* genes, as exposure to excessive retinoic acid *in vivo* can shift expression of *Hox* genes anteriorly, altering the segmental identity of the embryo, and resulting in homeotic transformations (Kessel and Gruss, 1991). Furthermore, some *Hox* gene enhancer regions contain retinoic acid response elements. These response elements are bound by a heterodimer consisting of a retinoid X receptor (RXR) and a retinoic acid receptor (RAR). RARs are expressed by NCC, with RARα and RARγ being important for development of skeletal structures (Lohnes et al., 1994; Dupé and Pellerin, 2009). This is demonstrated by pharyngeal arch defects in the absence of RA. For example, zebrafish with a mutation in *raldh2*, an enzyme involved in RA synthesis, fail to form cartilage elements from PA 3-7 (Begemann et al., 2001), confirming other studies showing pharyngeal patterning requires RA signaling (Lohnes et al., 1994; Mark et al., 2004). Altogether, this shows that RA signaling and its action on *Hox* gene expression is important in establishing anterior-posterior identity in the embryo.

The dorsal-ventral identity of the pharyngeal aches are patterned by the *Dlx* genes (Minoux and Rijli, 2010; Medeiros and Crump, 2012). Six *Dlx* genes have been identified in mammals which are expressed in overlapping domains within the pharyngeal arches, and their functions in mice have been examined by Depew *et al*. (Stock et al., 1996; Depew et al., 2005). In zebrafish, the *dlx* genes consist of *dlx1a, dlx2a, dlx2b, dlx3b, dlx4a, dlx4b, dlx5a,* and *dlx6a* and are similarly organized to those in mice. These genes are expressed

within different domains in the PA and the combination of *dlx* signals is important for the development of PA structures, most notably the craniofacial skeleton. *dlx1* and *dlx2* are expressed throughout PA 1 and 2, and are the only *dlx* genes expressed in the dorsal most region of the arch (Figure I-4 B). In more ventral domains, *dlx3*, 4, 5, and 6 are expressed in different regions in combination with either *msxe* or *hand2* (see Figure I-4 B). *msxe* is a muscle segment homeobox gene while *hand2* is a transcription factor and both of these genes function downstream of endothelin signaling and are required for ventral cartilage formation (Miller et al., 2003). The combination of different *dlx* genes are necessary for the dorsal-ventral patterning and development of the craniofacial skeleton. The ventral domain is defined by expression of *hand2* and will eventually give rise to Meckel's cartilage, part of the lower jaw, and the ceratohyal, which has homology to the hyoid. The intermediate domain, which contains the jaw joint, is defined by expression of all of the *dlx* genes, with the borders defined by *dlx4a* expression (Talbot et al., 2010). Finally, the dorsal domain is defined by *dlx2a* and *dlx4a* expression and will give rise to skeletal structures including the palatoquadrate and hyomandibula. Alterations of the dorsal ventral gene expression pattern within the arches can result in homeotic transformations. For example, mutations in *hand2* show a duplication of the palatoquadrate, revealing a loss of ventral elements and a gain of dorsal elements (Talbot et al., 2010). Hence, similar to *hox* genes, expression of *dlx* genes in the correct domains is important for proper patterning and development of the pharyngeal arches.

18
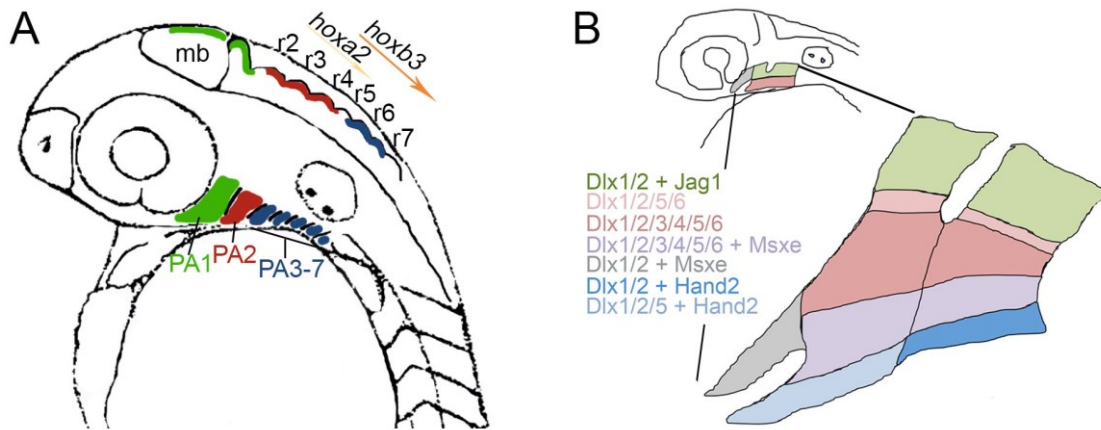
Figure I-4 *hox* and *dlx* expression in the 36 hpf zebrafish embryo.
A) *hox* expression within the zebrafish hindbrain provides anterior-posterior identity and patterns the NCC which populate the pharyngeal arches. PA1 is populated by NCC coming from the midbrain (mb) and rhombomere (r) 1. *hoxa2* expression is in r2-r5 while *hoxb3* is expressed starting in r4. B) *dlx* gene expression within PA1 and PA2 defines dorsal-ventral identity. Adapted from (Medeiros and Crump, 2012).

In addition to *hox* and *dlx* genes, signaling via Fgfs, BMPs, and sonic hedgehog (Shh) from the different germ layers are required to act as guidance cues for proper NCC migration and PA development. In avian embryos, the endoderm serves as a source of BMP7, an inducing signal to form the epibranchial placodes which contribute to formation of the sensory cranial ganglia (Begbie et al., 1999). The mesoderm serves as a source of RA (Deschamps and van Nes, 2005)and provides maintenance signals for *Hox* gene expression (Trainor and Krumlauf, 2000a), while the ectoderm serves as a source of *Fgf8* (Trumpp et al., 1999). Fgfs serve as NCC survival factors (Trumpp et al., 1999; Abu-Issa et al., 2002; Macatee et al., 2003), and as chemoattractants to direct NCC migration (Kubota and Ito, 2000). *Fgf8* has been shown to be important in the specification of NCC

spatial identity in the first pharyngeal arch by establishing anterior posterior polarity (Tucker et al., 1999). Fgf8 together with BMP4 signaling patterns the pharyngeal arches by regulating expression of genes such as *nkx3.2* (previously known as *bapx1*) which contributes to dorsal-ventral patterning and the positioning of the jaw joint (Miller et al., 2003; Wilson and Tucker, 2004). Shh signaling from the endoderm is also part of the signaling network in the head, and can induce expression of *Fgf8* (Haworth et al., 2004; Haworth et al., 2007).

The Fgf, Shh, and BMP signals function to positively or negatively regulate other signaling molecules which have roles in segregating and guiding the cranial NCC streams. These include Endothelin1, Sema/Neuropilin, Sdf1b/Cxcr4, and Eph/ephrin. Endothelin1 (Edn1) is a secreted peptide expressed in the pharyngeal arch ectoderm, mesoderm, and endoderm (Nair et al., 2007) and is induced by BMP shortly after NCC migration (Alexander et al., 2011). The receptor for Edn1, endothelin receptor A (Ednra), is expressed by NCC. Edn1 is thought to serve as a positional signal as well as having a role in the post-migratory NCC (Miller et al., 2000; Kimmel et al., 2001; Kimmel et al., 2003; Walker et al., 2007). Ventral fates are induced by *edn1* expression, and *edn1* is particularly important in determining mandibular versus maxillary identity in the first pharyngeal arch. It does so by activating *Dlx5/Dlx6* which subsequently activate *Hand2*, a ventral marker in the arch (Sato et al., 2008). Negative regulation of *edn1* is mediated by *tbx1,* a transcription factor important in the formation of the aortic arches (Piotrowski et al., 2003), although this has not been shown in mice. Jagged-Notch signaling, which helps determine dorsal skeletal fates, is repressed by Edn1, which is important for ventral skeletal development

(Zuniga et al., 2010) and so the combination of these signals establishes dorsal and ventral domains within the PA.

Sema/Neuropilin signaling is also involved in proper segregation of the cranial NCC streams. In zebrafish, the *nrp2a* and *nrp2b* receptors are expressed in NCC targeting PA 1-3, while ligands *sema3f* and *sema3g* are expressed in NCC-free zones (Yu and Moens, 2005). In mice, *Npn2* (expressed in migrating NCC) and *Sema3F* signaling is also required for cranial NCC development (Gammill et al., 2007). Sema3d has also been shown to have a role in NCC migration through controlling proliferation (Berndt and Halloran, 2006). Cranial NCC migration is also guided by chemokine signaling, which was recently examined in zebrafish. The chemokine, stromal cell derived factor (*Sdf1b,* also known as *Cxcl12*), is expressed in the pharyngeal arch endoderm while the receptor, *Cxcr4*, is expressed in the cranial NCC in zebrafish embryos (Olesnicky Killian et al., 2009). Expression of receptors on NCC while ligands are expressed in endoderm, mesoderm, and/or ectoderm helps guide NCC to the pharyngeal arches.

A fourth example of this is the Eph receptors, which are membrane bound and have tyrosine kinase activity. Eph receptors function in the pattered migration of NCC in the pharyngeal arch streams (Smith et al., 1997; Davy et al., 2004). In Xenopus, EphA4 and EphB1 are expressed in migrating NCC and mesoderm of the third, or third and fourth arches, respectively. The ephrin-B2 ligand, which is also membrane bound and interacts with these receptors, is expressed in the adjacent second arch NCC and mesoderm. Thus ephrin-B2 functions to guide migrating cranial NCC-expressing Eph receptors to their destination in the pharyngeal arches (Smith et al., 1997). Ephrin-B1 acts cell autonomously

in NCC to regulate craniofacial development (Davy et al., 2004). In addition, it has been shown that EphB1 physically interacts with the gap junction protein connexin43, which is required for cell sorting (Davy et al., 2006). However, roles for Eph/ephrin signaling in NCC have not been identified in zebrafish.

Thus, the expression of many genes within the pharyngeal arch region as well as within the NCC themselves are important for guiding cranial NCC to the correct locations. The patterning and migration of NCC involves numerous signals which act both cell autonomously and non-cell autonomously and are expressed in NCC as well as surrounding tissues. *Hox* and *Dlx* genes function to provide anterior-posterior and dorsal-ventral patterning to the pharyngeal arches. Gradients of BMP, Fgf, and Shh expression function to regulate expression of other genes involved in PA patterning. Finally, receptor-ligand interactions including Edn1/Ednra, Sema/Neuropilin, and Cxcr4/Sdf1 are also important in NCC finding the correct migratory path. Mutations in NCC specifier genes or signaling molecules and their receptors may only affect one of the stages of NCC development, or multiple stages. The functions of some of these NCC specifiers in NCC differentiation are discussed in the following section.

NCC Differentiation

NCC migration and differentiation occur simultaneously, with specification of NCC fate sometimes beginning before migration. For example, melanoblasts are specified upon or soon after segregation from the neural tube. Similar mechanisms of differentiation exist in the cranial and trunk NCC populations, with the cranial population being distinguished by the ability to give rise to cartilage and bone. In this section, I discuss the differentiation of three major NCC lineages: neurons, pigment cells, and cartilage/bone.

DIFFERENTIATION OF NEURONS

The peripheral nervous system is one of the major systems formed by NCC. The peripheral nervous system can be subdivided into different systems including the sensory nervous system, which conveys information to the central nervous system about things sensed by the body, and the autonomic nervous system (ANS), which is related to involuntary organ control and functions such as breathing and digestion. The enteric nervous system, sympathetic nervous system, and parasympathetic nervous system are all further subdivisions of the ANS.

Neurons of the sensory nervous system develop in three waves and have different functions. The first wave gives rise to mechanoreceptive (touch) and proprioceptive (movement and spatial position) neurons of larger diameters, the second wave to mechanoreceptive, thermoreceptive (temperature), and nociceptive (pain) neurons of smaller diameters, and the third to nociceptive neurons (Pavan and Raible, 2012). Several genes including the neurogenin (*neurog*) transcription factors are known to have roles early

23

in sensory neuron specification; these function with other factors such as *Brn3a* and *Isl*, which promote expression of genes involved in differentiation such as *Runx1* and *Runx3* (Pavan and Raible, 2012). The neurotrophins (NGF, BDNF, NT3, NT4) and receptor tyrosine kinases (TrkA, TrkB, TrkC) are involved in both sensory and autonomic differentiation. The Trk receptors form homodimers upon ligand binding, leading to transphosphorylation and initiation of a phosphorylation signaling cascade. This cascade will activate AKT, which is important for cell survival, and MAPK, which activates transcription factors to regulate genes involved in survival and neuronal differentiation (Brodeur et al., 2009). For example, the ligand NGF binds to the TrkA receptor and is necessary for the survival and differentiation of sympathetic neurons (Brodeur et al., 2009).

BMP and Wnt signals are important as NCC migrate towards the dorsal aorta to form the dorsal root ganglia and sympathetic ganglia. Constitutively active expression of β-catenin in NCC in mice led to differentiation into ectopic sensory neurons (Lee et al., 2004), which is in contrast to the constitutive activation in zebrafish leading to melanocytes over neural lineages (Dorsky et al., 1998). The differences in these studies may be due to the different organisms and method of increasing β-catenin expression as the timing of Wnt signals is critical in segregating the neural from melanocyte lineages. β-catenin signal activation in premigratory NCC suppresses melanocyte specification, while β-catenin activation in migratory NCC suppresses formation of neural derivatives (Hari et al., 2012). In addition to Wnts, BMP signaling is important in the development of the sympathetic nervous system. BMPs are required for sympathetic neuron differentiation in chick embryos (Schneider et al., 1999) and induce expression of *Phox2b* in neural crest stem cells

24

(Lo et al., 1999), a transcriptional activator which promotes neuronal differentiation (Dubreuil et al., 2008). Conditional deletion of BMP receptor IA in NCC in mice results in diminished levels of *Phox2b* and results in death at the dorsal aorta (Morikawa et al., 2009).

Similar to the sympathetic nervous system, development of the ANS requires several different transcription factors. One of the earliest required factors is the achaete-shute complex (*Mash1* in mice and *zash1* in zebrafish) which is important for neuronal differentiation and maintenance (Guillemot et al., 1993; Sommer et al., 1995). Mash1 is in a feedback loop with Phox2. Downstream of BMP signaling, *Phox2a, Phox2b, Gata2/3,* and *Hand2* all interact in the development of the ANS. Phox2b regulates many of the other transcription factors involved in differentiation including *Gata2/3* (Tsarovina et al., 2004) and binds the *DBH* (dopamine-β-hydroxylase) promoter and indirectly activates *TH* (tyrosine hydroxylase) and *Ret*. TH and DBH are both enzymes involved in the synthesis of the neurotransmitter noradrenaline (Pattyn et al., 1999). Ret is a receptor tyrosine kinase for GDNF (glial cell line derived neurotrophic factor), which promotes neuronal survival. Ret and GDNF are especially important in enteric nervous system development as mutations in these genes can result in Hirschsprung disease (Doray et al., 1998; Shen et al., 2002). Phox2a and Hand2 have both been implicated in the activation of *DBH* and *TH*, and Gata2, which is expressed during later neuronal differentiation, is also known to activate *TH* (Stanke et al., 1999; Tsarovina et al., 2004; Lucas et al., 2006).

The cranial ganglia are a part of the peripheral nervous system and are derived from both NCC and cranial placodes. The cranial placodes are ectodermal thickenings and include the lens, olfactory, trigeminal, otic, and epibranchial placodes; the epibranchial

placodes include the facial, glossopharyngeal, and vagal placodes (Figure I-5). The otic and olfactory placodes give rise to the sensory structures of the ear and nose while the trigeminal and epibranchial placodes contribute to the formation of the cranial ganglia. The cranial ganglia in 5 dpf zebrafish consist of the trigeminal, statoacoustic, facial, vagal, glossopharyngeal, and the anterior and posterior lateral line ganglia (Figure I-5 B). Studies in chick embryos have shown that NCC contribute to the proximal regions of the trigeminal and epibranchial ganglia as well as glial cells (D'Amico-Martel and Noden, 1983). Lineage tracing studies in zebrafish have confirmed that NCC contribute to the cranial ganglia (Kague et al., 2012). Thus the coordinated development of NCC and placodes are important for the formation of the cranial ganglia.

Interactions between placode and NCC populations occur throughout neurogenesis in the developing embryo. The preplacodal region, which gives rise to the placodes, lies adjacent to the anterior neural plate, close to the neural plate border where NCC are specified. This close proximity to NCC continues during development as the further posterior placodes form. Various studies have examined the importance of NCC in placode and ganglia development. In *Xenopus* embryos, ablation of premigratory NCC disrupts the directional migration of the epibranchial placodes (Theveneau et al., 2013). Reciprocally, replacing the placodal region with non-placodal ectoderm inhibits migration of NCC (Theveneau et al., 2013). Similar experiments in mice show that ablating the neural fold leads to a displaced and misshapen trigeminal placode that is missing the NCC component (Stark et al., 1997). The role of NCC in placode and cranial ganglia development are also evidenced my numerous animal models in which cranial ganglia are disrupted as a result

26

of disruptions in NCC development (Vitelli et al., 2002; Dixon et al., 2006; Culbertson et al., 2011; Weaver et al., 2015).

Several signals regulate the interactions between NCC and placodes. BMP and Fgf signaling from the surrounding tissues is important for inducing the factors necessary for placode development (Holzschuh et al., 2005; Nechiporuk et al., 2005; Nechiporuk et al., 2007). In zebrafish, the placodes are defined by expression of *neurog1* starting around 9 hpf (Andermann et al., 2002) and subsequently *pax2a* (Nechiporuk et al., 2007) is expressed within the epibranchial placodes and *foxi1* is expressed in the otic placode (Solomon et al., 2003). Interactions between the migratory NCC and the migrating placodal cells involves multiple signals including Sdf1/Cxcr4 (Olesnicky Killian et al., 2009; Theveneau et al., 2013), Neuropilin/Semaphorin (Gammill et al., 2007; Maden et al., 2012), and Robo/Slit (Shiau et al., 2008). Once the epibranchial ganglia are induced, *phox2a* and *phox2b* are important for their survival and differentiation, as these transcription factors activate genes in the neuronal differentiation cascade such as TH and DBH (Pattyn et al., 1997; Guo et al., 1999; Pattyn et al., 1999).

In summary, NCC contribute to form the peripheral nervous system of the embryo in the trunk and head. In the head, NCC contribute to cranial ganglia formation, which are also partly derived from the cranial placodes. Differentiation of NCC into neurons and glia of the peripheral nervous system requires their migration to the appropriate locations, which is mediated in part by Wnt, Fgf, and BMP signals. These signals are involved in activating the neuronal gene cascade and segregating them from the melanocyte lineage.
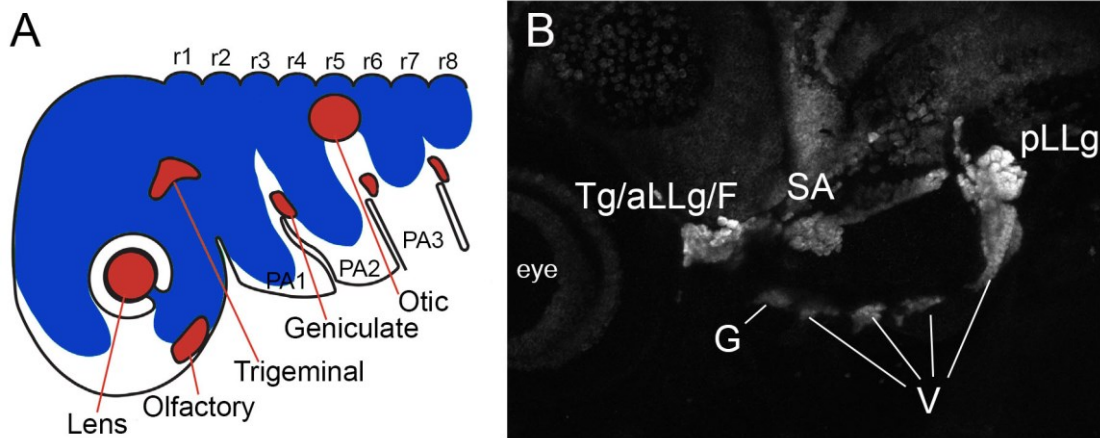
Figure I-5 A model of placode development and cranial ganglia.
A) NCC (blue) and placodes (red) in a generic vertebrate embryo. At this stage NCC are migrating into the PA and interact with the placodes, which are labeled. These cell populations interact in the development of the cranial ganglia. Adapted from (Steventon et al., 2014). B) Cranial ganglia within a 5 dpf zebrafish embryo labeled with pan-neuronal marker Hu. The ganglia are located posterior to the eye and include the trigeminal (Tg), anterior lateral line (aLLg), facial (F), statoacoustic (SA), posterior lateral line (pLLg), glossopharyngeal (G), and vagal (V) ganglia.

DIFFERENTIATION OF PIGMENT CELLS

Pigment cells such as melanocytes are another cell type derived from NCC. Zebrafish have three types of pigment cells: melanocytes, xanthophores, and iridophores. Melanocytes provide black/brown pigmentation, xanthophores are yellow, and iridophores are an iridescent silver. As melanocytes are also found in mammals and their development is the best understood of the pigment cell types, I use them as an example of pigment differentiation. Most melanoblasts, the precursor to melanocytes, are progressively specified during development, with specification occurring upon or soon after exit from the neural tube. The ongoing fate restriction involves a bipotent glia-melanocyte precursor

28

as well as a tripotent melanocyte-neural-adrenergic precursor (Thomas and Erickson, 2008). *Mitf* (micropthalmia-associated transcription factor) is considered the master regulator of melanocyte gene expression and is necessary for melanoblast specification. Different genes and morphogens are expressed during the formation and migration of the melanocyte precursors to activate expression of *Mitf* and its downstream target genes(Dorsky et al., 2000; Hornyak et al., 2001; Thomas and Erickson, 2008; Curran et al., 2009; Adameyko et al., 2012).

Activation of *Mitf* by Sox10 and Pax3 is important in melanocyte development. *Pax3* and *Mitf* act in parallel on different aspects of melanocyte development, with Pax3 promoting proliferation of progenitor cells and Mitf promoting survival of committed melanoblasts (Hornyak et al., 2001). *Pax3* plays a role in multiple aspects of NCC development including NCC formation, premigratory NCC, and differentiation into glia and melanocytes. Mice with mutations in *Pax3* have defects in NCC-derived tissues, including pigmentation (Epstein et al., 1991). Morpholino-mediated knockdown of *pax3* in zebrafish specifically disrupts xanthophore development, leading to an absence of xanthoblasts (Minchin and Hughes, 2008). Notably, *pax3* morphants display reduced *mitfa* expression, which may indicate a conserved function of *pax3* in its activation, although direct regulation has not been shown. Sox10 is also involved in activation of *Mitf* along with Pax3 (Bondurand et al., 2000; Potterf et al., 2000). Mutations in *Sox10* both in mice and zebrafish result in pigmentation defects (Southard-Smith et al., 1998; Dutton et al., 2001). In zebrafish, the pigmentation defects in $sox10^{-/-}$ embryos can be rescued upon reintroduction of *mitfa*. Furthermore, Sox10 binding sites in the *mitfa* promoter indicate a

29

direct role for Sox10 in the activation of *mitfa* (Elworthy et al., 2003). Mutations in *PAX3* as well as *SOX10* result in Waardenburg syndrome (Hoth et al., 1993; Pingault et al., 2010), confirming a role for these genes in pigmentation. *Foxd3* and *Sox2* are two other genes that also have roles in the activation of *Mitf* and these genes are typically active in neuronal and glial derivatives of NCC. Conditional deletion of *Foxd3* or *Sox2* from NCC results in a switch from glial to melanocyte fate in mice (Adameyko et al., 2012; Nitzan et al., 2013). In zebrafish, mutation of *foxd3* results in disruption of neuronal and cartilage derivatives, but not melanocytes (Stewart et al., 2006). Mechanistic studies in zebrafish revealed that there are Foxd3 binding sites in the *mitfa* promoter region which allow Foxd3 to repress *mitfa* transcription (Curran et al., 2009). *In vitro* evidence demonstrates that Sox2 binds and represses activity at the *Mitf* promoter (Adameyko et al., 2012).

The proper migration of melanoblasts is important in distinguishing the melanocyte lineage from the neuronal/glial lineage and involves expression of Kit, endothelin, and Wnt signaling. Kit is a receptor tyrosine kinase expressed in melanocyte precursors (Keshet et al., 1991) for the Kit ligand (Kitl) and is important for the survival and migration of melanoblasts. In the absence of the Kit receptor or ligand, melanocyte precursors remain in the migration staging area and fail to survive (Wehrle-Haller and Weston, 1995). Mice carrying mutations in *Kit* or *Kitl* show an absence of NCC derived melanocytes (Chabot et al., 1988; Geissler et al., 1988; Huang et al., 1990; Zsebo et al., 1990). Similarly, *kit* mutations in zebrafish result in pigmentation defects and these are accordingly known as the *sparse* mutants (Parichy et al., 1999). Not all zebrafish pigment cells are dependent on *kit* expression, but in those that are, Kit acts cell autonomously to promote melanocyte

30

migration. Parichy *et al*. also showed a role for *kit* in melanocyte survival. Studies in mice have revealed a role for endothelin signaling in melanoblast migration, although these signaling events are also involved in formation of the enteric nervous system and are not unique to the melanocyte lineage. NCC expressing EDNRB will proliferate in the presence of EDN3 and disruptions in endothelin signaling result in Waardenburg Syndrome and/or Hirschsprung Disease. One of the important functions of EDNRB in melanocyte development is activation of the Ras signaling cascade. Signaling through MAPK will lead to proliferation, while signaling through PI3K will provide anti-apoptotic factors. Wnt signaling also functions in melanocyte specification. Overexpression of β-catenin in zebrafish leads to enhanced melanocyte formation and diminished neural and glial cell formation, while inhibition of Wnt results in diminished melanocyte formation (Dorsky et al., 1998). In addition, the zebrafish homolog of *Mitf, nacre*, is directly activated by Wnt signaling (Dorsky et al., 2000).

In summary, expression of *Mitf* is the first step in the gene cascade needed to produce the melanin pigment. Tyr, Tyrp1, and Dct are the major enzymes involved in melanin synthesis. Finally, transporter proteins are needed to transport melanin from the melanocyte to the neighboring keratinocytes (See Sommer, 2011 for review). The specification of melanocytes, and therefore expression of *Mitf,* involves Wnt, endothelin, and Kit signaling. Thus, the production of melanocytes involves genetic interactions and signaling cascades to specify melanoblasts from NCC and guide their migration and differentiation.

DIFFERENTIATION OF CARTILAGE AND BONE

In contrast to the neuronal and pigment lineages which occur in trunk and cranial NCC, a unique feature of cranial NCC is their ability to differentiate into craniofacial cartilage and bone. Endochondral and intramembranous are two methods of ossification in the formation of bone. In endochondral ossification, chondrocytes form an initial cartilaginous template which undergoes hypertrophy and is replaced by osteoblasts and occurs in the long bones of the skeleton and some of the facial bones, such as the ceratohyal of the zebrafish. In intramembranous ossification, an initial condensation of mesenchyme calcifies directly to form the bone such as occurs in the flat bones of the cranium. The mammalian cranial vault consists of two frontal bones, two parietal bones, and one occipital bone and this anatomy is conserved in zebrafish. Sutures maintain separation between the calvarial bones and regulate skull growth. A combination of NCC and paraxial mesoderm form the cranial vault and sutures; the frontal bones are derived from NCC while the remaining calvarial bones form from the mesoderm (Jiang et al., 2002; Yoshida et al., 2008).

A recent study by Kague *et al*. examined craniofacial cartilage and bone elements in the zebrafish using the Cre-lox system to permanently label NCC and identify the origins of the different cartilage elements (Kague et al., 2012). The zebrafish skeleton (as shown in Figure I-6) consists of the viscerocranium, or the more ventral components, and the neurocranium, which lies dorsally. The viscerocranium consists of cartilage elements derived from pharyngeal arches 1-7 and all of these elements are NCC-derived. Meckel's cartilage and the palatoquadrate are derived from PA1 which have homology to jaw

elements in a human skeleton. The elements derived from PA2 have homology with jaw support structures and include the ceratohyal, basihyal, hyosymplectic, and interhyal. In particular, there is homology of the palatoquadrate to the incus and the hyomandibular to the stapes, which are bones of the middle ear. NCC from PA 3-7 form the ceratobranchial cartilage elements. In the neurocranium, the anterior region is derived from NCC while the parachordal plate appears to be of mixed NCC and mesodermal origin. The ethmoid plate and trabecular cartilage have homology with the primary palate and nasal capsule in mammals (Swartz et al., 2011). The use of transgenic labeling and high-resolution imaging also revealed the mode of ossification in the cranioskeletal elements. Many of the cartilage elements of the craniofacial skeleton form by endochondral ossification including the ceratohyal, ceratobranchials, quadrate, and ethmoid. Other elements, such as the jaw including the maxilla, form by intramembranous ossification. A variety of signaling events are involved in the formation of these elements and will be discussed below.
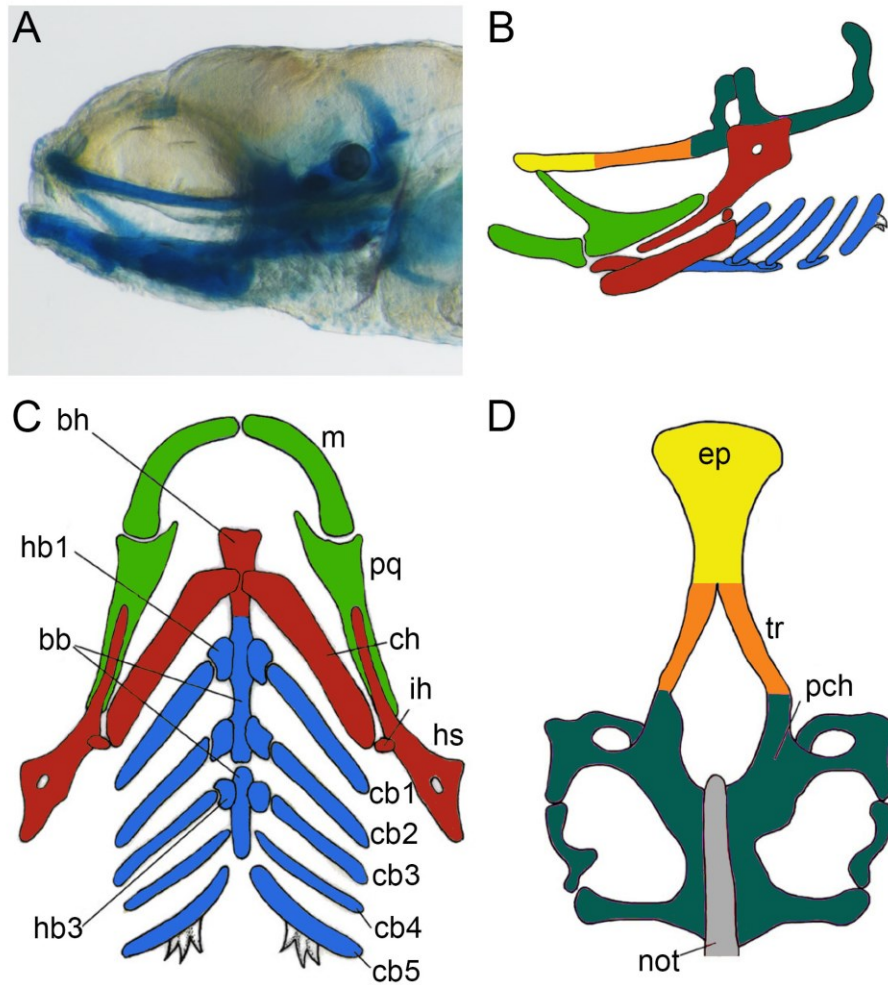
Figure I-6 Zebrafish cartilage anatomy.

A) 5 dpf zebrafish craniofacial cartilage stained with Alcian blue. B) Schematic of 5 dpf cartilage elements as shown in A. C) Cartilage elements of the viscerocranium. Cartilage elements in green are derived from PA1, red from PA2, and blue from PA3-7. D) Cartilage elements of the neurocranium include the ethmoid plate (ep) in yellow, trabeculae (tr) in orange, and the parachordal(pch) in teal. Abbreviations: bb: basibranchial; bh: basihyal cb: ceratobranchial; ch: ceratohyal; hb: hypobranchial; hs: hyosymplectic; ih: interhyal; m: Meckel's cartilage; not: notochord; pq: palatoquadrate. Panels B-D adapted from Kimmel *et al*. (Kimmel et al., 2001).

The commitment of NCC to differentiate into cartilage is marked by expression of *Sox9* (Bi et al., 1999), which is also involved earlier in NCC development (see previous section on NCC migration). Msx2 inhibits Sox9 in the mandibular region to prevent differentiation until cranial NCC migration is complete (Takahashi et al., 2001). Sox9 along with Sox10 will activate expression of the type II collagen, *Col2a1* (Ng et al., 1997). Two other Sox genes, Sox6 and LSox5, are known to coordinate with Sox9 in promoting cartilage development in mice (Lefebvre, 2010), but these genes have not been shown to function in cartilage development in zebrafish. Sox9 will also stimulate expression of *Runx2*, an early marker of bone formation. Runx2 is key in initiating the expression of other late osteogenic markers such as *osterix, osteocalcin, osteopontin*, and *alkaline phosphatase* (ALP) as well as type I collagen (*Col1a1*). Mice carrying a mutation in *Runx2* fail to form any bone and have only cartilaginous skeletons (Komori et al., 1997), demonstrating the essential function of *Runx2* in osteogenesis.

Many signaling pathways and transcription factors have been shown to influence the expression of *Runx2*. *Msx2*, a target of BMP signaling, is important for inducing *Runx2* expression in the frontonasal NCC (Han et al., 2007). Dlx5 was also found to increase expression of *Runx2* by BMP signaling in chick embryos (Holleville et al., 2007). *Runx2* is also negatively regulated. *Twist1* is another gene involved in osteoblast gene expression which inhibits osteoblast differentiation through regulating Runx2 (Yoshida et al., 2005). Knockdown of *twist1a* and *twist1b* leads to increased *runx2b* expression in zebrafish, while overexpression of *twist1a* or *twist1b* had the opposite effect (Yang et al., 2011). This suggests that, as in mice, *twist1* inhibits *runx2* in zebrafish.

35

The BMP, Hh, Fgf, and TGFβ (Transforming Growth Factor β) signaling pathways have all been shown to influence expression of transcription factors related to formation of cartilage and bone. The balance of these signals functions to guide and pattern NCC during migration and later to control chondrocyte differentiation. BMPs, along with endothelins, are important for establishing ventral identity within the PAs to pattern the ventral skeletal elements while Notch/Jagged establishes dorsal identities (Miller et al., 2000; Zuniga et al., 2010; Alexander et al., 2011). Expression of a dominant negative form of the BMP receptor *bmpr1a* showed defects in ventral cartilage elements such as Meckel's, confirming a role in dorsal-ventral patterning (Alexander et al., 2011). In addition to their role in patterning, BMP signals have an important role in differentiation. Bmpr1a and Bmpr1b are both expressed in chondrocyte condensations in mice(Yoon et al., 2005). Skeletal development is severely disrupted in mice carrying mutations in both the BMP receptors *Bmpr1a* and *Bmpr1b*, while a mutation in only one of the receptors has milder phenotypes, suggesting overlapping functions for these receptors. Interestingly, the double mutant embryos severely disrupt the formation of the endochondral skeleton while intramembranous forming bones, such as those of the skull, are less affected (Yoon et al., 2005). Examination of these mice reveal a lack of *Sox9*, *LSox5*, and *Sox6* expression, which are important in the differentiation of cartilage, and demonstrate that BMP signaling is needed for the survival and proliferation of chondrocytes (Yoon et al., 2005).

In addition to BMPs, Hh signaling is important in endochondral bone formation. Specifically, the Indian hedgehog (Ihh) signaling pathway is implicated in chondrocyte proliferation and differentiation. Ihh signaling is important for expression of the secreted

36

factor parathyroid hormone-related peptide (PTHrP), which is known to have a role in formation of hypertrophic chondrocytes during endochondral ossification (St-Jacques et al., 1999). *ihha* and *ihhb* are expressed in hypertrophic chondrocytes of zebrafish, showing a conserved role for these genes in chondrocyte maturation (Avaron et al., 2006). A severe decrease specifically in endochondral bone formation is evident in *ihha* mutant zebrafish, while dermal bone formation is able to proceed, exhibiting the importance of *ihh* in endochondral ossification. Alternatively, mutations in the patched genes, *ptc1* and *ptc2,* lead to increased Hh signaling and show premature bone formation (Hammond and Schulte-Merker, 2009). Consistent with this, *Ihh* mutant mice display rounded skulls, shortened faces, and shortened limbs and tails, with the endochondral skeleton being more severely affected. Differentiation markers *Runx2*, *Col1α, ALP*, and *Ocn* are reduced in *Ihh*$^{-/-}$ embryos and suggest an important role for Ihh in chondrocyte proliferation and osteoblast differentiation. Decreased expression of Bmp2 and Bmp4 in the calvarial bones of *Ihh*$^{-/-}$ embryos also suggest that Ihh functions upstream of these BMP ligands (Lenton et al., 2011). Therefore, the Ihh pathway functions in ossification along with the BMP pathway in endochondral osteogenesis.

BMP interacts with other signaling pathways in chondrogenesis such as Fgfs. Studies in mice have revealed that the Fgf receptor, *Fgfr3*, is involved in the degradation of Bmpr1a (Qi et al., 2014). Fgfr3 activation is associated with negative regulation of chondrocyte proliferation and differentiation (Deng et al., 1996). In contrast to this negative regulation, other Fgfs are involved in stimulating BMP expression. For example, Fgf2 stimulates BMP2 expression in osteoblasts, and this is regulated by Runx2 (Choi et al.,

2005). In zebrafish, inhibition of Fgf using SU5402 results in agenesis of the pharyngeal and neurocranial cartilages. *fgf3* and *fgf8* were shown to be especially important as morpholino knockdown of these genes led to nearly complete absence of cartilage in morphant zebrafish (Walshe and Mason, 2003). The Fgf receptors (Fgfrs) are important in the intramembranous ossification of the calvarial bones. Their functions in development are discussed with respect to craniosynostosis syndromes in the following section.

Along with Fgfs, the TGFβ pathway, which signals through Smad proteins, is another signaling pathway involved in intramembranous cranial bone development. TGFβ ligands bind to type II receptors (TGFβR2) which heterodimerizes with type I receptors to initiate a phosphorylation signaling cascade. TGFβR2 is expressed in the NCC-derived ectomesenchyme and cranial sutures in mice. *Wnt1-Cre* (NCC) conditional inactivation of TGFβR2 in mice results in cardiovascular defects and craniofacial defects including calvarial defects, a small mandible, and cleft palate (Sasaki et al., 2006). Interestingly, *Fgfr2* was downregulated in *Wnt1-Cre; Tgfbr2* mice, indicating Fgf functions downstream of TGFβ. Further study of the *Wnt1-Cre; Tgfbr2* mice showed that *Tgfbr2* functions in proliferation and differentiation, but not migration or survival of NCC (Sasaki et al., 2006). Similarly, zebrafish *tgfb3* is expressed in migratory NCC and neurocranial cartilage. Morpholino knockdown of *tgfb3* results in impaired chondrogenesis, also suggesting a role for TGFβ signaling in cartilage differentiation (Cheah et al., 2010), although not specifically in intramembranous ossification. In support of these *in vivo* studies, *in vitro* studies have shown that *Runx2* responds to both TGFβ1 and BMP2 signals in the formation of osteoblasts (Lee et al., 2000).

In summary, expression of *sox9* indicates an early commitment to the chondrogenic lineage, followed by *runx2*, which is involved in osteogenesis. Pharyngeal arch patterning, such as that by *dlx* genes and *endothelin* signaling, has an important function in generating the correct skeletal elements from each arch. Finally, Runx2 is regulated by multiple signaling pathways in the formation of both endochondral and intramembranous bones including BMP and Ihh. Thus a variety of signals are required for the formation of craniofacial bone and cartilage from NCC.

NCC Development in Neurocristopathies

Alterations in the development of NCC result in a collection of syndromes known as neurocristopathies. Depending on which phase of NCC development is disrupted, different phenotypes may arise. In the following section I present an example of neurocristopathies which arise from deficiencies of NCC formation (Postaxial acrofacial dysostosis), migration (DiGeorge Syndrome), and differentiation (craniosynostosis).

NCC FORMATION: POSTAXIAL ACROFACIAL DYSOSTOSIS

Postaxial Acrofacial Dysostosis (also known as Miller syndrome) is characterized by postaxial limb deformities and craniofacial anomalies including orofacial clefts, micrognathia, and malar hypoplasia. Given the NCC contribution to these structures, Postaxial Acrofacial Dysostosis is classified as a neurocristopathy. Remarkably, mutations in *dihydroorotate dehydrogenase* (*DHODH*) are responsible for Postaxial Acrofacial Dysostosis, an enzyme which is involved in the synthesis of uracil, one of the bases of

RNA (Ng et al., 2010). Given the ubiquitous nature of RNA synthesis, the specific phenotypes arising from *DHODH* mutations are surprising. *Dhodh* is strongly expressed in the pharyngeal arches, forelimbs, hindlimbs, and somites in mouse embryos which is consistent with the tissues affected by Postaxial Acrofacial Dysostosis (Rainger et al., 2012). A DHODH inhibitor, leflunomide, has been used to examine its function during zebrafish development. Leflunomide treatment disrupts the development of NCC derivatives including melanocytes and glia while the development of mesodermal tissues are not disrupted (White et al., 2011). Expression of *foxd3* is severely reduced and expression of migratory NCC markers *sox10* and *crestin* are absent (White et al., 2011). Although further study is necessary to understand the function of DHODH, these results suggest it plays an important and tissue-specific role early in NCC development.

NCC MIGRATION: 22Q11 DELETION SYNDROME

The importance of patterning and signal integration in the development of the pharyngeal arches can be demonstrated by the *Tbx1* mutant, which is a model of DiGeorge syndrome/22q11.2 deletion syndrome (DGS). DGS is characterized by cardiac defects and occasionally mild craniofacial defects, cleft palate, and hypothyroidism. *Tbx1* is expressed in the pharyngeal endoderm, the mesodermal core of the pharyngeal arches, and a region known as the second heart field, which is important for outflow tract development (Garg et al., 2001; Vitelli et al., 2002). Homozygous mutations of *Tbx1* in mice lead to similar features of DGS including cardiac outflow tract abnormalities and abnormal facial structures (Jerome and Papaioannou, 2001). Although not expressed by NCC, *Tbx1*

influences the expression of other genes implicated in NCC migration, as evidenced by the *Tbx1* mice (Xu et al., 2004; Calmont et al., 2009). Loss of *Tbx1* impacts tissue-specific gene expression and alters the environment through which NCC migrate (Vitelli et al., 2002; Calmont et al., 2009). One of the genes which may be indirectly regulated by *tbx1* is *edn1*, as shown by studies in zebrafish (Piotrowski et al., 2003). Zebrafish *tbx1* mutants fail to develop pharyngeal pouches 2-6, confirming a role for *tbx1* function in the endoderm (Piotrowski et al., 2003). Another example of altered gene expression is a change in *Gbx2*, a transcription factor for the guidance molecule *Slit*. Tbx1 controls the expression of *Gbx2* at the time of the fourth PAA specification (Calmont et al., 2009), and *Tbx1*^{-/-} embryos show reduced *Gbx2* expression especially in the fourth pharyngeal arch. Ablation of *Gbx2* in the pharyngeal surface ectoderm (using *Ap2a*-Cre) disrupted cardiac NCC migration and formation of the fourth PAA. *Slit2*, a Robo ligand, was found to be downregulated in both *Tbx1*^{-/-} and *Gbx2*^{-/-} mice. *Robo1*, the receptor expressed on NCC, was also found to be downregulated and its expression pattern more disorganized in mutant mice, showing an alteration in migratory cardiac NCC in *Tbx1*^{-/-} mice (Calmont et al., 2009). These studies demonstrate that alterations in the tissues surrounding NCC can disrupt their normal development. Thus, defective NCC migration in neurocristopathies could be cell autonomous or non-cell autonomous.

NCC DIFFERENTIATION**: C**RANIOSYNOSTOSIS

Disruption of the balance of morphogenic signals can alter craniofacial development. The influence of these morphogens on craniofacial bone development,

particularly the FGFs, is demonstrated by the craniosynostosis syndromes which are defined by the premature fusion of the cranial sutures. Most craniosynostosis syndromes are associated with mutations in the FGF receptors (*FGFR*) -1, -2, and -3 as well as *TWIST* (Saethre-Crouzon syndrome), *MSX2* (Boston-type CS), and *EFNB1* (craniofrontonasal dysplasia). In suture development, osteoblast proliferation, differentiation, apoptosis, and mineralization must be balanced; disruption of any one of these processes can impact suture formation. Fgfrs are receptor tyrosine kinases and activate signaling cascades through PI3K as well as MAPK. Specificity in Fgf signaling is obtained through alternative splicing, tissue-specific expression patterns, and other modifications. For example, alternative splicing of *Fgfr2* is tissue specific with b forms in epithelial cells and c forms in mesenchymal cells (Orr-Urtreger et al., 1993). All *Fgfrs* are expressed in the mesenchyme. *Fgfr1* is expressed in the calvarial mesenchyme and later in osteoblasts, *Fgfr2* is expressed at sites of ossification while *Fgfr3* is expressed at low levels in the sutural osteogenic front (Iseki et al., 1999; Johnson et al., 2000). Homozygous mutations in *Fgfr1* and *Fgfr2* are pregastrulation lethal in mice, however, *Fgfr3*$^{-/-}$ mice are viable and fertile and do not display skull abnormalities (Colvin et al., 1996; Deng et al., 1996). Conditional deletion of *Fgfr2* in osteoblast lineages reveals that *Fgfr2* is required for osteoblast proliferation but not differentiation or survival (Yu et al., 2003).

In addition to the *Fgfrs*, *Twist1* is expressed in the sutural mesenchyme and has a role in differentiation by regulating Runx2 (Yoshida et al., 2005). *Msx2* is regulated by both BMP and TGFβ signaling. Studies of the *Msx2* mouse mutant show that a foramen in the skull vault is due to a defect in differentiation followed by a proliferation defect and

42

not due to a defect in NCC or apoptosis. An enhancement of the defect in differentiation and proliferation, resulting in a larger foramen, was seen in *Twist1*^{+/-}*; Msx2*^{+/-} embryos. Diminished differentiation was demonstrated by reduced expression of *Runx2* and *ALP*. However, *Msx2* expression was not affected in *Twist1*^{+/-} embryos and *Twist1* expression was not affected in *Msx2*^{+/-} embryos, suggesting that these genes function in parallel pathways (Ishii et al., 2003). *Twist1*^{+/-} mice have increased *Fgfr2* expression and activation as well as increased BMP signaling (Connerney et al., 2008). These CS mouse models demonstrate that there are multiple signaling interactions in formation of cranial cartilage and bone, and that *Runx2* plays a key regulatory role in this process.

Altogether, these neurocristopathies show how different alterations of NCC development can result in the distinct phenotypes. Some are likely the result of cell-autonomous functions of the gene involved, such as in Postaxial Acrofacial Dysostosis, while others are the result of alterations in the NCC migratory environment, as in DiGeorge syndrome. Finally, craniosynostosis models have shown morphogens such as BMP and Fgf are critical for the correct timing of differentiation into bone by NCC.

Summary

Development of NCC and NCC-derived tissues requires expression of specific genes at the proper time and in the correct location; failure to do so can result in neurocristopathies, which can be distinguished in part by which stage of NCC development is disrupted (See (Watt and Trainor, 2014)). Neurocristopathies which disrupt NCC formation can lead to severe malformations, and tend to be associated with more ubiquitous

cellular processes. Postaxial Acrofacial Dysostosis is one such example whereby mutations in *DHODH* disrupt uracil synthesis. Disruption of NCC migration may take several forms including a failure of EMT to begin migration, disruptions in cell-cell signaling needed for appropriate migration, which can be either cell-autonomous or non-cell autonomous, as in DiGeorge syndrome. NCC differentiation into various tissue types also requires cell-autonomous and non-cell autonomous signaling interactions. The expression levels and integration of these signals is important in differentiation as demonstrated by craniosynostosis syndromes. Thus, investigating NCC development in vertebrate models is important for providing insight into the pathogenesis of neurocristopathies. Furthermore, an understanding of NCC may aid in the design of therapies to prevent the phenotypes which arise from disruptions of NCC development, such as the craniofacial phenotypes of TCS and Acrofacial dysostosis, Cincinnati type.

Ribosomopathies and Ribosome Biogenesis

Ribosomopathy syndromes, such as TCS and Acrofacial dysostosis, Cincinnati Type, are characterized by disruption of ribosome biogenesis. Ribosome biogenesis, or the process of making a ribosome, is important for cell growth and proliferation as ribosomes perform essential functions in translating messenger RNA (mRNA) into polypeptides in the cell. Ribosomes consist of four rRNAs, over 70 ribosomal proteins (RPs), as well as additional factors (Lafontaine and Tollervey, 2001; Kressler et al., 2010). RNA polymerase I (RNAPI) is responsible for the transcription of the 28S, 18S, and 5.8S rRNAs, a process

which occurs in the nucleolus, while RNA polymerase III (RNAPIII) transcribes the 5S rRNA. A eukaryotic ribosome consists of two subunits - the 40S (small subunit) and the 60S (large subunit) - in which RPs are assembled onto the rRNA in the nucleolus. Once the pre-40S and pre-60S have formed, they are exported to the cytoplasm where the mature ribosome both decodes the mRNA and forms the peptide bonds between amino acids (Lafontaine and Tollervey, 2001). The process of ribosome biogenesis can be divided into several steps: transcription of ribosomal DNA, covalent modifications to the pre-rRNA, processing of the pre-rRNA to form mature rRNA, assembly of the rRNA and ribosomal proteins, and transport of the maturing ribosomes to the cytoplasm (Lafontaine and Tollervey, 2001; Tschochner and Hurt, 2003). Disruption of any of these steps can lead to disorders termed ribosomopathies (See Figure I-7). The process of ribosome biogenesis is described below with an emphasis on transcription of rRNA and the functions of RNAPI and RNAPIII.
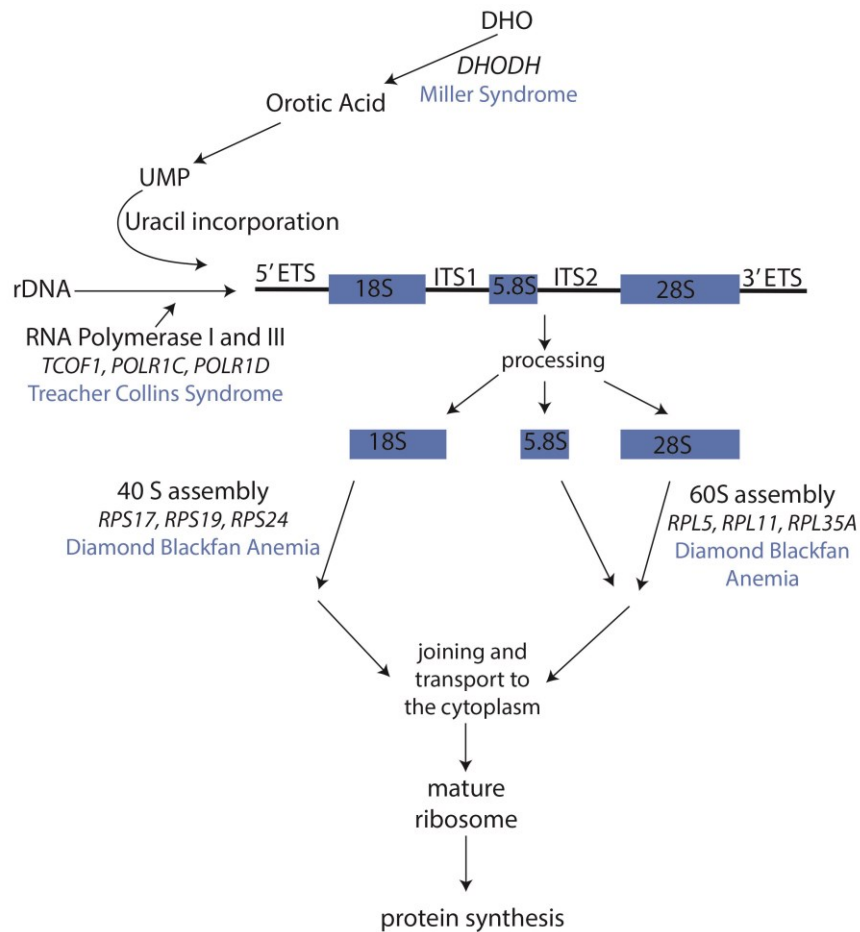
Figure I-7 Schematic of ribosome biogenesis and ribosomopathies.
Ribosome biogenesis requires transcription of the rRNA, processing, assembly of the large and small subunits, and finally export to the cytoplasm. Disruptions of this process result in ribosomopathies, three of which are indicated. Figure from Watt and Trainor (Watt and Trainor, 2014).

The nucleolus is the site of ribosome biogenesis

The nucleolus is the site of three key processes in ribosome biogenesis: pre-rRNA transcription, rRNA processing, and ribosomal ribonucleoprotein assembly (Boulon et al., 2010). Ribosome biogenesis requires the coordination of all the RNA polymerases – RNAPI synthesizes the 25S, 18S, and 5.8S rRNAs, RNAPIII synthesizes the 5S rRNA,

and RNAPII synthesizes the mRNA of the ribosomal proteins. Each of these processes occurs in a particular region of the nucleolus. The nucleolus consists of a granular component, the dense fibrillar center, and the fibrillar center (Figure I-8). rDNA transcription by RNAPI occurs at the periphery of the fibrillar center, while unengaged rDNA transcription machinery, such as UBF (Upstream Binding Factor), can be localized within the fibrillar center. Within the dense fibrillar center, the 47S rRNA undergoes cleavage and early processing events. Proteins involved in this process, such as Nopp140, will localize to the dense fibrillar center. The 5S rRNA and some ribosomal proteins will also localize to the dense fibrillar center for early modifications and assembly. Ribosome assembly then continues in the granular component with the inclusion of more ribosomal proteins and the formation of the pre-40S, or small subunit (SSU), and the pre-60S, or large subunit (LSU). Proteins which lie within the granular component include B23/nucleophosmin, nucleostemin, and Nop52. These LSU and SSU precursors are then exported into the cytoplasm where maturation and assembly is completed and the ribosomes then function in protein synthesis (Reviewed in (James et al., 2014)).
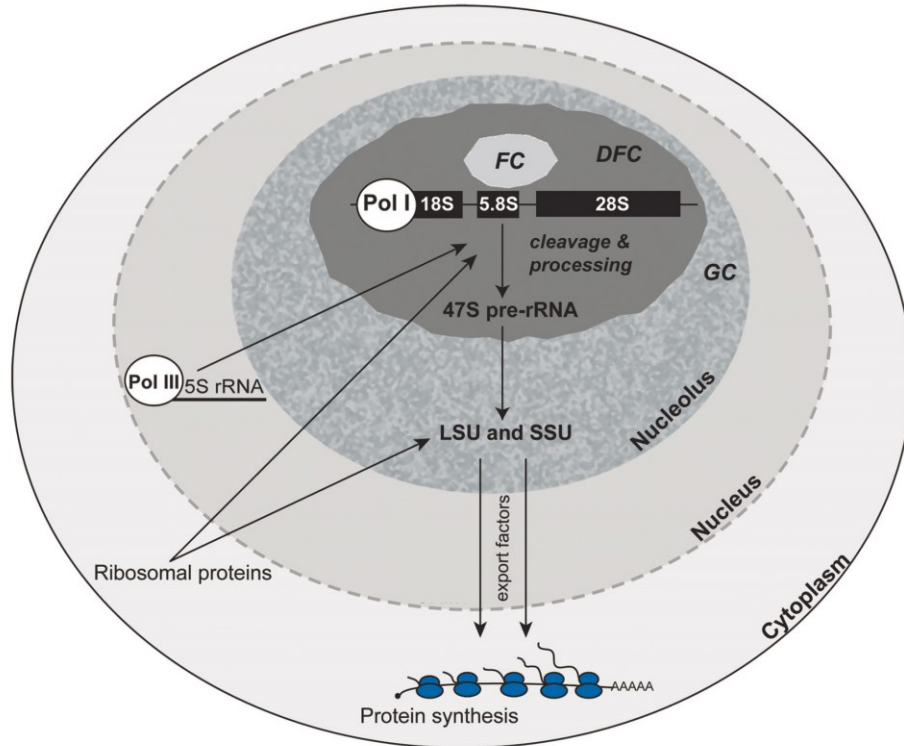
Figure I-8 Structure of the nucleolus and sub-compartments.
    The nucleolus consists of the granular center (GC), the fibrillar center (FC), and the dense fibrillar center (DFC). RNAPI transcription occurs at the periphery of the FC, while RNAPIII transcription of the 5S rRNA occurs in the nucleoplasm. Ribosomal proteins and the 5S rRNA are transported into the DFC to begin ribosome assembly. Ribosome assembly after rRNA processing continues in the GC, and then pre-ribosomes are exported into the cytoplasm. Figure adapted from (James et al., 2014).

RNA Polymerase I

Transcription of the 47S rRNA by RNAPI occurs within the nucleolus and is important to understand as it is one of the rate-limiting steps of ribosome biogenesis (Laferté et al., 2006). In the following section, the structure, function, and regulation of RNAPI will be described.

RNAPI STRUCTURE AND FUNCTION

RNAPI is an enzyme consisting of fourteen subunits and is responsible for the transcription of the 47S rRNA. The structure of eukaryotic RNAPI has been extensively examined in yeast (Engel et al., 2013; Fernandez-Tornero et al., 2013), which revealed a 10-subunit core consisting of A190, A135, AC40, AC19, A12.2, Rpb5, Rpb6, Rpb8, Rpb10, and Rpb12. A190, A135, and A12.2 are unique to RNAPI while AC19 (Polr1d) and AC40 (Polr1c) are shared by RNAPI and RNAPIII. The 5 Rpb subunits are shared amongst RNAPI, II, and III. Two additional subunits, A14 and A43, form a stalk subcomplex while A49 and A34.5 form a TFIIF-like subcomplex (Figure I-9A). Alternative names for these subunits in other species are listed in Table I-1.
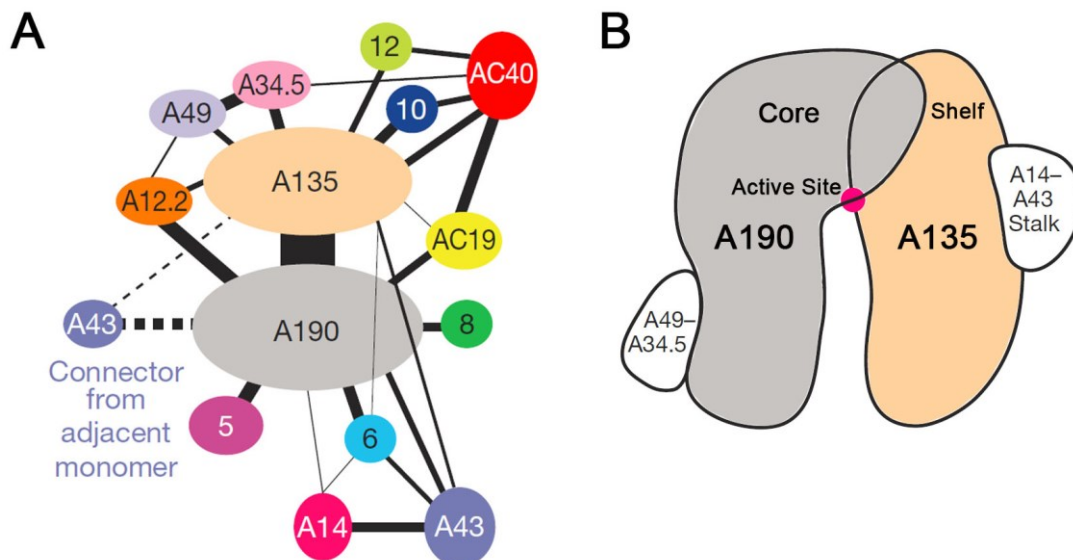
Figure I-9 Schematic of RNA Polymerase I.
A) Diagram of interactions among the 14 subunits of RNA Polymerase I. B) Schematic of the active site of RNA Polymerase I. Adapted from (Engel et al., 2013).

49

Yeast RNAPI subunits	Alternate name	Human RNAPI subunits
A190	Polr1a	hRPA190
A135	Polr1b	hRPA135
AC40	Polr1c	hRPA40
AC19	Polr1d	hRPA19
A12.2	Polr1h	hRPB12
Rpb5	Polr2e	hRPB5
Rpb6	Polr2f	hRPB6
Rpb8	Polr2h	hRPB8
Rpb10	Polr2l	hRPB10
Rpb12	Polr2k	hRPB12
A14		hRPB4
A43	Polr1f	hRPA43
A49	Polr1e	PAF53
A34.5	Polr1g	PAF49 (CAST)

Table I-1 RNAPI subunits in yeast and alternative names.
Alternate names listed in the second column are used in zebrafish.

The different subunits of RNAPI have different functions when it comes to assembly of RNAPI and its interaction with the rDNA. The A14/A43 complex was shown to be important for interacting with Transcription Initiation Factor IA (TIF-IA), which is required for RNAPI transcription (Engel et al., 2013). The A49/A34.5 complex stabilizes A12.2, which forms part of the active site of RNAPI, and is also responsible for making contact with the DNA and mediating RNA cleavage by RNAPI. Together with A12.2, the A190 and A135 subunits are important for forming the catalytic site of the enzyme (Figure I-9B).

TRANSCRIPTION BY RNAPI

The first step in RNAPI transcription is the formation of the pre-initiation complex which consists of, at a minimum, TIF-IA (also known as RRN3 in yeast), Transcription Initiation Factor IB (TIF-IB, known as selectivity factor SL1 in humans), and upstream binding factor (UBF). These proteins interact with each other, RNAPI, and the rDNA prior to transcription. The rDNA sequence is present in tandem repeats with approximately 300 copies present within the human genome (Stults et al., 2008). In humans, the rDNA repeats are located on acrocentric chromosomes. An rDNA repeat (Figure I-10) consists of a transcription start site, the upstream control element (UCE) and the core promoter. This region is followed by the 47S rDNA region which consists of the 5' externally transcribed sequence (5'ETS), 18S rRNA, internally transcribed sequence 1 (ITS1), 5.8S rRNA, internally transcribed sequence 2 (ITS2), 28S rRNA, and the 3'ETS. Finally, there are terminator elements (T) prior to the start of another rDNA repeat.
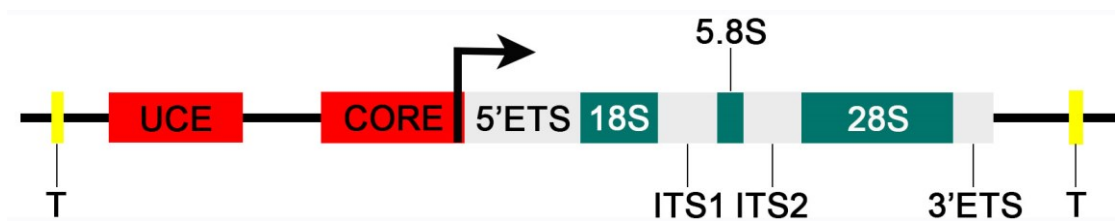
Figure I-10 Structure of an rDNA repeat.
　　　　　The rDNA promoter region consists of the Upstream Control Element (UCE) and the core promoter (CORE), upstream of the transcription start site (arrow). RNAPI will transcribe the 47S rRNA gene which consists of External Transcribed Spacer (ETS) and Internal Transcribed Spacer (ITS) regions along with the 18S, 5.8s, and 28S rRNAs. Following the 47S rRNA gene are the terminator elements (T).

The three main initiation factors will interact with the rDNA in different ways to stimulate rDNA transcription. TIF-IA interacts with RNAPI (Cavanaugh et al., 2002; Beckouet et al., 2008) and binds TIF-IB (Miller et al., 2001). More recent evidence suggests that TIF-IA binds DNA and that this function is required for RNAPI transcription (Stepanchick et al., 2013). TIF-IB binds the UCE and helps confer promoter specificity and is essential for recruiting RNAPI to the transcription start site (Rudloff et al., 1994; Friedrich et al., 2005). TIF-IB also has a role in stabilizing the interaction between UBF and the rDNA promoter (Friedrich et al., 2005). UBF, which is required for transcription initiation (Jantzen et al., 1990), binds throughout the rDNA (O'Sullivan et al., 2002) and interacts with TIF-IB and RNAPI (Hanada et al., 1996; Panov et al., 2006b; Penrod et al., 2015). Together, these interactions help form a stable pre-initiation complex at the rDNA promoter.

Once the pre-initiation complex has formed, RNAPI must escape the promoter and initiate transcription. Phosphorylation of TIF-IA, releasing it from RNAPI, is an important part of this process (Bierhoff et al., 2008), while UBF has a role in stimulating promoter escape (Panov et al., 2006a). After promoter escape and initiation of transcription, the rRNA transcripts are rapidly produced as an estimated 8-10 million transcripts are needed every 24 hours in a mammalian cell to sustain normal levels of ribosome biogenesis (Goodfellow and Zomerdijk, 2013). UBF may also have a role in elongation through remodeling of the rDNA chromatin. Additional factors have been implicated in chromatin remodeling of the rDNA including histone chaperones such as nucleolin (Rickards et al., 2007; Cong et al., 2012) and nucleophosmin (Murano et al., 2008), which help keep rDNA

in a euchromatic state, and topoisomerases such as Topoisomerase IIα, a known component of mammalian RNAPIβ (Panova et al., 2006). The process of termination may occur by different mechanisms in different species. The A12.2 subunit is important for termination because of its ability to cleave RNA (Prescott et al., 2004). In mammals, binding of transcription termination factor TTF-I to the terminator elements causes pausing of RNAPI (Grummt et al., 1986) and then RNAPI dissociates from the rDNA (Jansa and Grummt, 1999). A similar mechanism occurs in yeast, however, another potential mechanism exists. In this mechanism, the pre-rRNA is cleaved by Rnt1, and then the cleavage product is recognized by Rat1 which continues digestion. When Rat1 reaches the elongating RNAPI, the transcription complex becomes unstable and dissociates from the rDNA, resulting in termination (Braglia et al., 2011).

In summary, the process of RNAPI transcription involves the formation of the pre-initiation complex, promoter escape, elongation, and termination. Some of the factors involved in initiation are involved in other steps of the transcription process. How these factors change roles is in part due to alterations in phosphorylation, which then regulate RNAPI transcription.

REGULATION OF RNAPI AND rDNA TRANSCRIPTION

Regulation of transcription by RNAPI is a topic of much interest as rRNA production is crucial for ribosome biogenesis within the cell. Nutrient availability, growth factors, and environmental stressors are all known to affect rRNA transcription by RNAPI. Initiation factors influence rRNA transcription in both a long-term and short-term manner.

Long-term changes, such as the number of active rRNA genes, are determined by the levels of UBF (Sanij et al., 2008). Short-term changes, such as the rate of transcription from each rDNA repeat, are regulated in part by phosphorylation of TIF-IA (Cavanaugh et al., 2002).

The regulation of UBF, both the activity and amount present, is important for the regulation of ribosome biogenesis. Low levels of UBF are associated with diminished rDNA transcription. Phosphorylation of UBF through either the EGF pathway by ERK (Stefanovsky et al., 2001) or IGF pathway by PI3K (Drakas et al., 2004) at different sites can increase rDNA transcription. Alternatively, phosphorylation of UBF through the mTOR pathway increases the interaction between TIF-IB and UBF (Hannan et al., 2003). Notably, UBF is also known to interact with Treacle, one of the proteins that may be altered in TCS (Valdez et al., 2004).

TIF-IA is also regulated by phosphorylation at specific residues, which can be either activating or inhibiting of rDNA transcription. Phosphorylation through the MAPK pathway (Zhao et al., 2003a) leads to increased rDNA transcription whereas hypophosphorylation of TIF-IA through the mTOR pathway upon nutritional stress leads to diminished rRNA transcription (Mayer et al., 2004). Under conditions of oxidative or ribotoxic stress, phosphorylation of TIF-IA by c-jun N-terminal protein kinase 2 (JNK2) disrupts the interaction of TIF-IA with TIF-IB and RNAPI and then directs TIF-IA from the nucleolus into the nucleoplasm (Mayer et al., 2005). Under these conditions, only the activity of TIF-IA is altered, not the levels, making this easily reversible in the cell. Inhibition of TIF-IA is also capable of triggering a stress response which leads to increased levels of the tumor suppressor p53 and p53-dependent apoptosis (Yuan et al., 2005).

Alterations in growth factors, energy levels, and stress therefore regulate both UBF and TIF-IA by phosphorylation to regulate rDNA transcription. Regulation of TIF-IB has not been as thoroughly examined, however, deacetylation of TIF-IB by SIRT1 has been shown to render it inactive (Muth et al., 2001). SIRT1 is a member of the sirtuins, which are deacetylases that have multiple roles in the cell including gene expression and cell survival under stress. Another member of the sirtuin family, SIRT7, will interact with RNAPI and is associated with activation of transcription (Ford et al., 2006). Interestingly, SIRT7 has also been implicated in the regulation of RNAPI during the cell cycle. RNAPI transcription is high during G2 and S phase, low during M phase, and then gradually recovers during G1. This process is in part regulated by phosphorylation of UBF and TIF-IB by cdk/cyclin complexes (Grummt, 2003). SIRT7 interacts specifically with UBF and is important in the resumption of rDNA transcription after mitosis (Grob et al., 2009). Thus, all three factors involved in initiating RNAPI transcription are regulated in different ways under different conditions. A combination of phosphorylation, dephosphorylation, acetylation, and deacetylation regulates these factors and their ability to form the initiation complex under conditions of stress, nutrient depravation, cell cycle progression, or the presence of certain growth factors. As much of the work has been completed in *in vitro* models, it remains to be seen how alterations in these regulations might affect embryonic development.

RNAPIII structure and function

Another key factor in the regulation of ribosome biogenesis is the synthesis of 5S rRNA by RNAPIII, which also has a role in transcribing tRNAs and ncRNAs. RNAPIII is the largest of the polymerases containing seventeen subunits, but also the least studied due to the difficulty in obtaining its crystal structure. Similar to RNAPI, RNAPIII consists of a 10-subunit core containing C160, C128, AC40, AC19, Rpb5, Rpb6, Rpb8, Rpb10, Rpb12, and C11. The subunits unique to RNAPIII are listed in

Table I-2. The exact positions and functions of each subunit of RNAPIII have yet to be identified, but electron cryomicroscopy studies have given insight as to the organization of the enzyme (Fernández-Tornero et al., 2011). Studies of some of the subcomplexes of RNAPIII have revealed various roles in transcription initiation, elongation and termination. Similar to RNAPI, the two largest subunits C160 and C128 form the active center of the enzyme, while C11 has RNA cleavage activity (Chédin et al., 1998). Studies in zebrafish have suggested an interaction between the homologs of the C128 (Polr3b) and C11 (Polr3k) subunits, which is important for pancreas development (Yee et al., 2007). C17 and C25 form a dimer which is involved in initiation of RNAPIII transcription (Jasiak et al., 2006). The C37/C53 dimer is homologous to the A49/A34.5 dimer in RNAPI and has roles in initiation, elongation, and termination (Kassavetis et al., 2010). Finally, the C82/34/31 heterotrimer is involved in nucleic acid binding and transcription initiation (Fernández-Tornero et al., 2011).

Subunit	Alternate names	RNAPI homolog
C160	Polr3a, hRPC160, RPC1	A190
C128	Polr3b hRPC128, RPC2	A135
C11	Polr3k, hRPC11	A12.2
C17	hRPC9	A14
C25	Polr3h, hRPC8	A43
C37	Polr3e, hRPC5	A49
C53	Polr3d, hRPC4	A34.5
C31	Polr3g, hRPC7, RPC32	
C82	Polr3c, hRPC3, RPC62	
C34	Polr3f, hRPC6, RPC39	

Table I-2 Unique subunits of RNAPIII.
Seven of the RNAPIII subunits have RNAPI homologs, while the remaining subunits are unique to RNAPIII.

Transcription initiation is a more complex, variable process for RNAPIII. Unlike RNAPI which only transcribes one gene, RNAPIII transcribes multiple different genes. The specificity for each different gene comes in part through the usage of different promoters to transcribe the RNAs. Type 1 promoters transcribe the 5S rRNA, Type 2 promoters tRNAs, and Type 3 promoters include the U6 snRNA (Figure I-11). The structure of the Type 1 promoter is unique in that it is the only promoter to contain an internal control region (ICR) which contains an intermediate element (IE), C box, and A box. This unique combination allows the transcription initiation factor TFIIIA to bind the 5S rDNA, and TFIIIA does not bind Type 2 or Type 3 promoters. TFIIIA also helps recruit another transcription initiation factor, TFIIIC, to the promoter. Type 2 promoters contain both an A box and a B box, which is bound by TFIIIC. Finally, Type 3 promoters are the only RNAPIII promoter which is external to the gene. These promoters contain a proximal sequence element (PSE) and TATA box. Some genes may also contain a distal sequence

element (DSE) to aid in regulation of transcription initiation at the promoter, although this has only been observed in vertebrates and not in yeast. Type 3 promoters do not require TFIIIA or TFIIIC for transcription initiation but instead, utilize a form of TFIIIB and the small nuclear RNA activating protein complex (SNAPc), which binds the PSE (Schramm and Hernandez, 2002). TFIIIB interacts with RNAPIII and is part of the initiation complex at Type 1 and Type 2 promoters as well. Thus, Type 1 promoters require an initiation complex consisting of TFIIIA, TFIIIB, and TFIIIC while Type 2 promoters utilize TFIIIB and TFIIIC and Type 3 promoters utilize only TFIIIB (Orioli et al., 2012). Once initiated, conformational changes to RNAPIII are hypothesized to aid in the transition to elongation. Termination by RNAPIII is relatively simple and occurs upon encountering a series of T residues; the minimum number of residues is 4 in vertebrates or 5 in yeast (Richard and Manley, 2009).
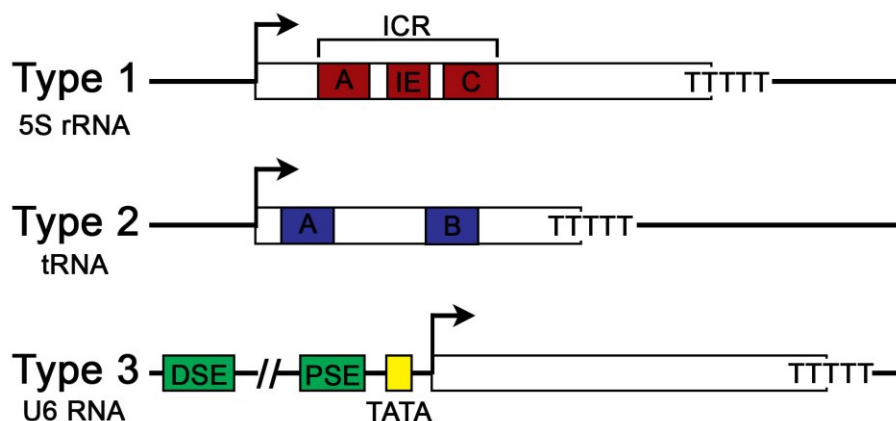
Figure I-11 Three types of promoters are used by RNAPIII to transcribe different RNA products.
Type 1 promoters contain an internal control region (ICR) consisting of an A box (A), an intermediate element (IE), and a C box (C). Type 2 promoters consist of an A box and B box (B). Type 3 promoters may contain a distal sequence element (DSE), and also contain a proximal sequence element (PSE) and a TATA box. Termination of the genes is in part signaled by a run of T residues.

Binding of TFIIIA, TFIIIB, and TFIIIC to initiate RNAPIII transcription is regulated in a similar manner to the factors involved in RNAPI transcription. As TFIIIB is involved in transcription initiation from all of the RNAPIII promoters, much of the regulation of transcription initiation is dependent on modifications of TFIIIB. For example, phosphorylation of TFIIIB by ERK leads to an increase in TFIIIB activity (Felton-Edkins et al., 2003). Expression of c-Myc, a proto-oncogene, will also increase transcription by RNAPIII (Gomez-Roman et al., 2003). Tumor suppressors such as p53 and the retinoblastoma protein (Rb) will diminish RNAPIII activity through modifications or binding of TFIIIB. When hypophosphorylated, Rb will bind TFIIIB and disrupt its interactions with RNAPIII and TFIIIC (Chu et al., 1997; Sutcliffe et al., 2000; Gjidoda and

Henry, 2013). A similar mechanism exists for inhibition by p53, which also binds TFIIIB (Crighton et al., 2003).

In addition to these specific regulators, Maf1 is an important general negative regulator of RNAPIII. The activity of Maf1 is regulated by its level of phosphorylation. Under favorable growth conditions, Maf1 is phosphorylated and is primarily localized within the cytoplasm. In a mammalian model, mTOR localizes to tRNA and 5S rRNA genes through an interaction with TFIIIC. mTOR then functions to phosphorylate Maf1, preventing it from inhibiting RNAPIII transcription (Kantidakis et al., 2010). Under stress conditions such as starvation, replicative stress, or oxidative stress, the nuclear localization signals of Maf1 become dephosphorylated and Maf1 enters the nucleus. It interacts with and ultimately inhibits RNAPIII transcription (Vannini et al., 2010). Thus, under stress conditions, the production of 5S rRNA and tRNAs are reduced while under favorable conditions, phosphorylated Maf1 does not inhibit transcription of RNAPIII genes. Altogether, the regulation of RNAPIII and RNAPI by similar factors including stress and growth conditions helps the cell to maintain appropriate levels of ribosome biogenesis.

Nucleolar Stress and Ribosomopathies

Ribosome biogenesis is a complex process which must be precisely controlled within the cell. Disruptions in ribosome formation may lead to ribosomopathies, while over-production of ribosomes is one hallmark of cancer cells. Alterations in ribosome production can lead to nucleolar stress, which is defined by disruption of the nucleolar

structure. Rubbi & Milner defined nucleolar stress in their studies of nucleoli (Rubbi and Milner, 2003). They found that inhibiting UBF, which blocked RNAPI transcription of rRNAs, disrupted nucleolar structure and ultimately led to p53 activation and cell cycle arrest. This is consistent with the idea that maintaining a balance of rRNAs and ribosomal proteins is important for ribosome biogenesis and cell growth.

P53 RESPONDS TO CELLULAR STRESS

p53 activation is a common response to a number of cellular stresses such as replication and translation stress, DNA damage, and hypoxia, which then acts to suppress proliferation and activate apoptosis (Vazquez et al., 2008). One well-studied mechanism of the p53 response to nucleolar stress involves MDM2, which is required to suppress p53 activation (Ringshausen et al., 2006). Under normal conditions, MDM2 binds p53 and functions to ubiquinate p53, targeting it for degradation by the proteasome (Oliner et al., 1993; Honda et al., 1997; Kubbutat et al., 1997). The balance between ribosomal protein and rRNA synthesis is tightly regulated; if disrupted, this can lead to accumulation of ribosomal proteins, some of which bind MDM2 and prevent its inhibition of p53 (Marechal et al., 1994; Lohrum et al., 2003; Zhang et al., 2003; Dai et al., 2004; Jin et al., 2004; Chen et al., 2007; Donati et al., 2011a). In particular, a complex of RPL5, RPL11, and the 5S rRNA are important in this process (Donati et al., 2013). Bound to MDM2, this complex leads to p53 stabilization. If binding to MDM2 is disrupted, it prevents the p53 response (Jaako et al., 2015).

61

p53 functions as a transcription factor to induce genes involved in cell cycle arrest and apoptosis. One example is *Cdkn1a* (also known as *p21*) which is a cyclin-dependent kinase inhibitor. Activation of p21 inhibits cyclin dependent kinase complexes and results in G1 or G2 arrest (Deng et al., 1995; Abbas and Dutta, 2009). Induction of other genes such as *Bbc3* (also known as *Puma*), *Bax*, and *p53AIP1* by p53 lead to activation of apoptosis. Bbc3 directly binds anti-apoptotic Bcl-2 family proteins, which then displaces Bax and/or Bak proteins enabling them to form pores on the mitochondrial membrane, eventually leading to caspase activation (Yu and Zhang, 2009). Similarly, p53AIP1 will also bind Bcl-2 and lead to cytochrome c release from the mitochondria (Matsuda et al., 2002). Altogether, these transcriptional changes result in activation of the apoptosis pathway through mitochondria (Figure I-12).
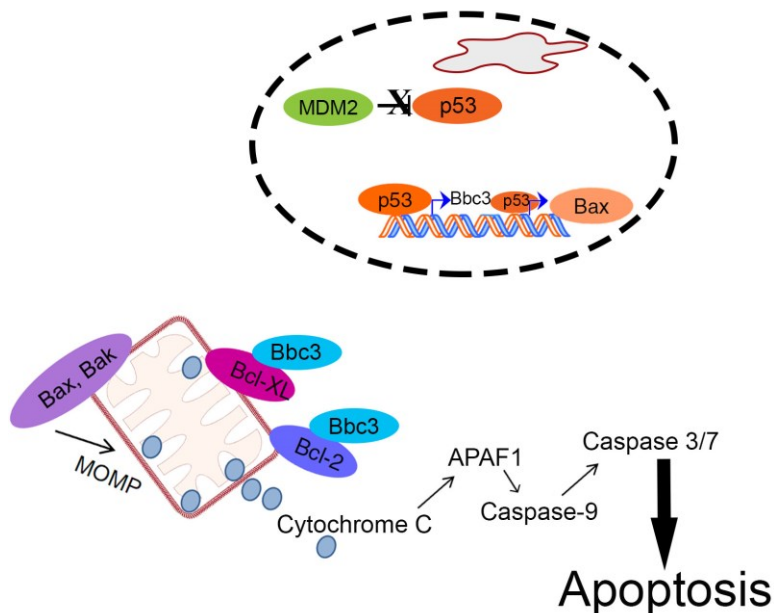
Figure I-12 The apoptotic response is triggered by nucleolar stress.
Disruptions in ribosome biogenesis cause nucleolar stress and RPL5, RPL11, and the 5S rRNA will bind MDM2, preventing its role in p53 degradation. p53 will then act as a transcription factor for target genes including Bbc3 and Bax. Bbc3 will bind Bcl-2 and Bcl-XL which normally function in an anti-apoptotic manner. This allows Bax/Bak to form a pore leading to mitochondrial outer membrane permeabilization (MOMP). Cytochrome c is then released from the mitochondria, leading to a cascade of events eventually resulting in apoptosis. Portions of the figure are adapted from (Nikoletopoulou et al., 2013).

A recent study of MYBB1A, a regulator of p53, showed that the decision between cell cycle arrest and apoptosis may be in part dependent on the type of disruption of rRNA. Disrupting 47S rRNA transcription through depletion of RNAPI transcription factors resulted in apoptosis. However, depletion of rRNA processing factors resulted in cell cycle arrest at G1. MYBB1A functions to acetylate p53 and does so even when rRNA transcription is disrupted, but not when there is a disruption of rRNA processing. The

difference in acetylation may have a role in the differential binding of p53 in eliciting cell cycle arrest versus apoptotic target gene activation (Kumazawa et al., 2015).

Interestingly, activation of the ribosomal protein-Mdm2-p53 pathway may occur in the absence of nucleolar disruption. Mutations in RPS6, which disrupt assembly of the 40S subunit, do not alter nucleolar integrity, but do activate p53 (Fumagalli et al., 2009). Although the mechanisms may not be completely understood, there is a well-established link between ribosome biogenesis, p53 activation, and subsequent cell cycle arrest and apoptosis which underlies multiple ribosomopathies.

RIBOSOMOPATHY: DIAMOND BLACKFAN ANEMIA

Disruptions of ribosome biogenesis underlie the ribosomopathy syndrome Diamond Blackfan anemia (DBA). DBA arises due to mutations in ribosomal proteins including RPS17, RPS19, RPS24, RPL5, RPL11, and RPL35A, (reviewed in (Lipton and Ellis, 2009; Narla and Ebert, 2010), however, the genetic mutation is unknown in about half of DBA patients. These mutations disrupt either 40S or 60S assembly (Figure I-7). The primary characteristics of DBA include anemia, reticulocytopenia, macrocytosis, and a selective decrease or absence of erythroid precursors, while additional features may include thumb abnormalities, craniofacial, and cardiac defects (Lipton and Ellis, 2009). Mutations in RPL5 and RPL11, which function in the aforementioned ribosomal protein-Mdm2-p53 pathway, are associated with cardiac and craniofacial anomalies more often than mutations in the other ribosomal proteins linked to DBA (Gazda et al., 2008). Morpholino knockdown or mutation of *rpl11* in zebrafish results in craniofacial anomalies

64

as well as diminished expression of neurogenic markers, metabolic and hematopoietic defects, consistent with the human DBA phenotype (Danilova et al., 2011) (Chakraborty et al., 2009). In support of a mechanism of nucleolar stress and p53 activation, inhibition of p53 could ameliorate the mutant phenotypes of zebrafish and mice models of DBA carrying mutations in *rpl11* or *Rps19* (Danilova et al., 2008; Chakraborty et al., 2009; Jaako et al., 2011). Given the global nature of ribosome biogenesis, the presence of specific phenotypes in DBA are surprising and represent an interesting area of study. Mutations in ribosomal proteins would be expected to impair growth of all tissues, such as in the Drosophila *minute* mutants (Marygold et al., 2007). However, in humans and vertebrate models, only specific tissues are affected. Even more interesting is that within the ribosomal protein mutations which cause DBA, only some have associations with craniofacial anomalies. One explanation for the tissue-specificity of the phenotype is that the ribosomal proteins may have tissue-specific roles. In support of this idea, differential expression of ribosomal proteins during development has been observed in chick (Kirby et al., 1995) and mice (Kondrashov et al., 2011). The complexities of ribosome biogenesis demonstrated by ribosomopathies are just beginning to be understood in vertebrate models. The future study of these models will be important in developing an understanding of the etiology of tissue specific phenotypes arising from ribosomopathies and their prevention.

Summary

The process of ribosome biogenesis is a highly regulated process and one of the most energy-consuming processes in the cell. The production of rRNAs by RNAPI and RNAPIII in the nucleolus are regulated by similar factors including nutrient availability or cell stressors such as DNA damage. Disruption of ribosome biogenesis often leads to nucleolar stress and activation of a p53 response. This common mechanism underlies different ribosomopathies. However, ribosomopathies have a wide range of phenotypes affecting different tissues (See reviews by (Narla and Ebert, 2010) and (Hannan et al., 2013)). Why there seem to be tissue-specific defects as a result of a disruption in a global process remains a topic of much interest. Many studies of ribosome biogenesis in yeast or human cell lines have provided information on the basic functions of the proteins involved in ribosome biogenesis. However, they have not provided an understanding of the process in the context of development. It is important to understand the function of ribosomal genes and proteins in a developmental context in order to understand the pathogenesis of ribosomopathies.

Research Objectives

Craniofacial anomalies present in a number of syndromes and can range from mild to severe. The current therapies available for improving the quality of life of individuals with craniofacial anomalies are primarily surgically based. Examining the mechanisms underlying the pathogenesis of craniofacial anomalies has the potential to reveal new

therapies for their prevention. In this thesis, I set out to understand the functions of *polr1a, polr1c,* and *polr1d* during embryonic development in order to understand the pathogenesis of TCS and Acrofacial dysostosis, Cincinnati type. In Chapter III, I investigate the impact of mutations in *polr1c* and *polr1d* in NCC development and ribosome biogenesis and the mechanisms underlying TCS. In Chapter IV, I describe the identification of a new syndrome, Acrofacial dysostosis, Cincinnati type, which we named and published in 2015 (Weaver et al., 2015) and investigate the consequences of mutations in *polr1a* in NCC and ribosome biogenesis. These studies provide new information about the function of the RNAPI subunits during embryonic development as well as mechanistic insight into the pathogenesis of two rare congenital syndromes.

II. MATERIALS AND METHODS

Zebrafish

CARE AND MAINTENANCE

Adult zebrafish (*Danio rerio*) were housed and maintained in the Stowers Institute Zebrafish Facility according to IACUC standards (Protocol # 2015-0138). Zebrafish embryos were raised at 28.5°C and staged according to (Kimmel et al., 1995). When necessary, 1-Phenyl-2-thiourea (0.002%) was added to the embryo media to prevent pigment development.

STRAINS

The *polr1a*[hi3639Tg], *polr1c*[hi1124Tg], and *polr1d*[hi2393Tg] zebrafish were generated by an insertional mutagenesis screen (Amsterdam et al., 2004) which used a retroviral construct (Chen et al., 2002) (see Figure II-1A). Theoretically, the viral exonic sequence within the insertion is spliced into the mRNA, and result in a frameshift mutation (Amsterdam, 2003; Amsterdam et al., 2004) (Figure II-1B). In the case of the *polr1a*[hi3639Tg], *polr1c*[hi1124Tg], and *polr1d*[hi2393Tg] zebrafish, the insertion was found to be in the 5'UTR, exon 2, and the first intron, respectively. The location of the mutations in these genes disrupts all of the known splice variants (Figure II-2). Adult *polr1a*[hi3639Tg], *polr1c*[hi1124Tg], and *polr1d*[hi2393Tg] zebrafish were maintained as heterozygotes, which were phenotypically wild-type. Homozygosity of any one of these alleles was found to be embryonic lethal.

The insertional mutant lines were crossed with transgenic reporter lines including Tg(*fli1a:egfp*), referred to as *fli1a:egfp*, and Tg(7.2kb-*sox10:gfp*), referred to as *sox10:gfp*.

fli1a:egfp labels endothelial cells as well as cranial NCC derivatives including the jaw mesenchyme (Lawson and Weinstein, 2002). The *sox10:gfp* transgene contains a fragment 7.2 kb upstream of the *sox10* promoter and drives *gfp* expression in NCC (Hoffman et al., 2007) and was obtained from the Schilling Laboratory. The *tp53*^{M214K} zebrafish line was obtained from the Piotrowski Laboratory and carries a mutation in the DNA binding domain of Tp53 and disrupts its activity (Berghmans et al., 2005). Each of these fish develop normally and survive to adulthood.
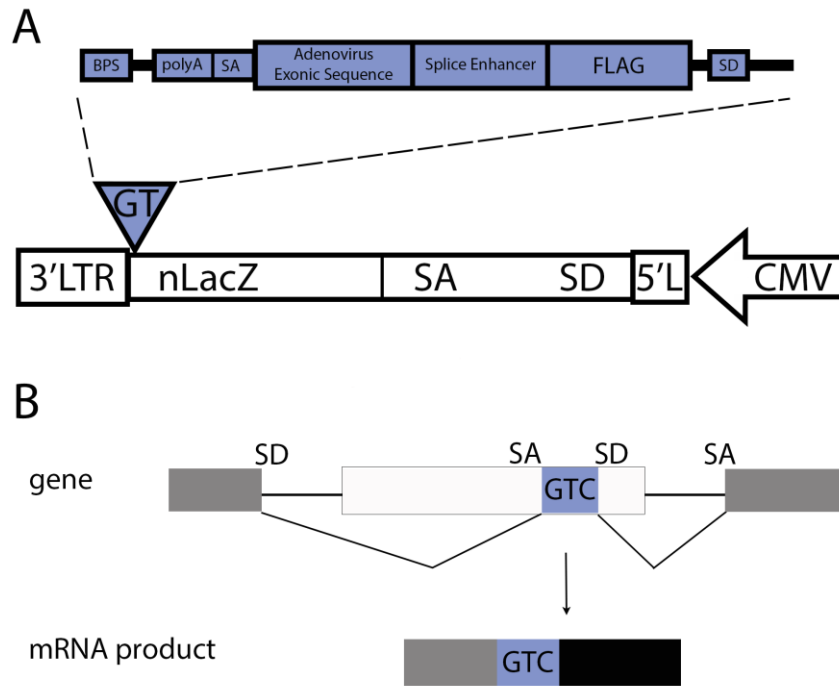
Figure II-1. Theory behind insertional mutagenesis.
A) Structure of the retroviral construct used for insertional mutagenesis. (adapted from Chen et al., 2002) B) Schematic of the consequence of an insertional event. The gene trap construct (GTC) which has inserted into a gene, becomes spliced into the mRNA product, resulting in a frameshift mutation, represented by the black box (adapted from Amsterdam, 2003.) Abbreviations: BPS: branch point sequence; CMV: CMV promoter; GT: gene trap viral vector; 3'LTR: 3' long terminal repeat; 5'L: 5' partial long terminal repeat; SA: splice acceptor; SD: splice donor.
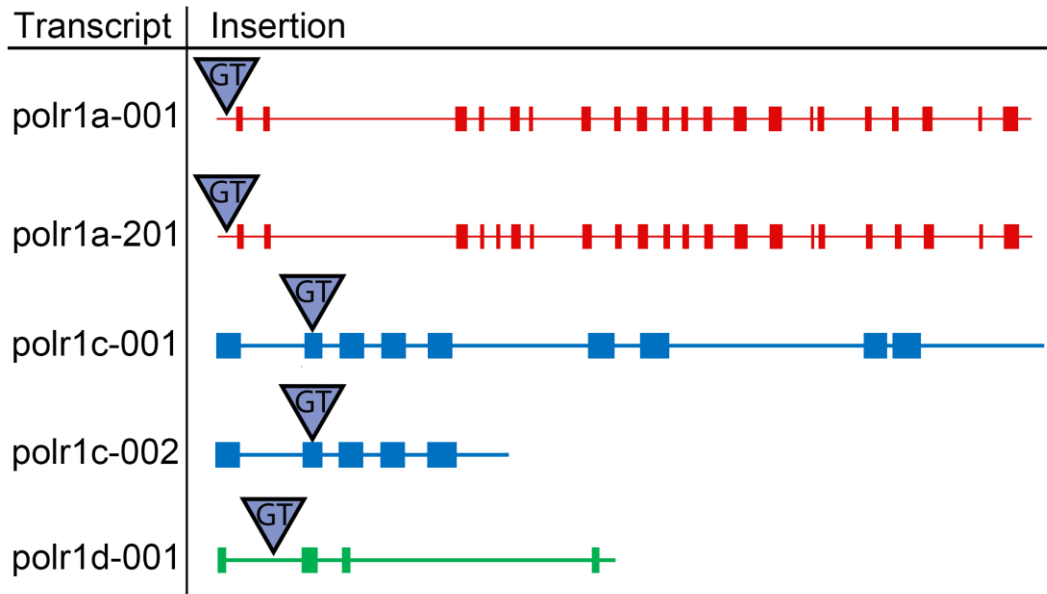
Figure II-2: Schematic of the insertion locations in *polr1a*^hi3639Tg^, *polr1c*^hi1124Tg^, and
polr1d^hi2393Tg^ zebrafish.
Insertion of the gene trap construct (GT) is within the 5'UTR of *polr1a*
(red). The GT is within the second exon of *polr1c* (blue), and within the
first intron of *polr1d* (green).

FIN CLIPS AND GENOTYPING

In order to maintain heterozygous zebrafish colonies of $polr1a^{hi3639Tg}$,

$polr1c^{hi1124Tg}$, $polr1d^{hi2393Tg}$ and $tp53^{M214K}$, adult zebrafish were fin-clipped and genotyped.

Adult zebrafish were anaesthetized in MS-222 prior to fin clips, and a fresh razor blade

was used to remove a small portion of the caudal fin of each fish. The fish were allowed to

recover from anesthesia and then housed individually until genotyping was completed. Fin

clips were placed in lysis buffer (10 mM Tris, 50 mM KCl, 0.03% Tween-20, 0.15% NP-

40) and digested with ProteinaseK (ProK) for 8 hours at 55°C. Following inactivation of

ProK at 94°C, 2μl of the lysis reaction was used for PCR. The presence of wild-type and mutant alleles was detected using the primers listed in Table II-1. Mutant embryos used in experiments were identified by phenotype and confirmed by genotyping.

	Forward Primer (5' → 3')	Reverse Primer (5' → 3')
polr1a mutant	CTCCCAGAACACAGTCACACG	GCTAGCTTGCCAAACCTACAGGT
polr1a wt	CTCCCAGAACACAGTCACACG	GTTTCATCAGCGGAGAACAGG
polr1c mutant	CTATTGCTTTTGTCGCATAAAGCG	GCTAGCTTGCCAAACCTACAGGT
polr1c wt	CTATTGCTTTTGTCGCATAAAGCG	CTCCAGTGTGTTTTCATCTGAAC
polr1d mutant	CAGTCACAACGTGCGACATGC	GCTAGCTTGCCAAACCTACAGGT
polr1d wt	CAGTCACAACGTGCGACATGC	GGTAAACGAGTTGATTTACGCATTG
tp53 mutant	GATAGCCTAGTGCGAGCACACTCTT	AGCTGCATGGGGGGGAA
tp53 wt	GATAGCCTAGTGCGAGCACACTCTT	AGCTGCATGGGGGGGAT

Table II-1: Primers for zebrafish genotyping.

Phenotypic analyses

LIVE EMBRYO IMAGING

Embryos younger than 18 hpf were mounted in 2% methyl cellulose and submerged in E2 media. Older embryos were anaesthetized with MS-222, mounted in 2% methyl cellulose while submerged in E2 media with MS-222, and then imaged with light microscopy.

IN SITU HYBRIDIZATION

Regions of *polr1a, polr1c, and polr1d* were amplified using the primers found in Table II-2. These amplified regions were cloned into the TOPO II vector (Invitrogen). The resulting plasmids were used to generate both sense and anti-sense probes for in situ hybridization. In situ hybridization was completed according to standard protocols. Briefly, embryos were permeabilized with ProK, and hybridized in probes diluted to 2.5ng/μl in hybridization buffer and incubated overnight at 66-68°C. The probe was removed and embryos were washed in maleic acid buffer and blocked for a minimum of 1 hour prior to incubation in AP-Fab (1:5000, Roche). Signal was detected using NBT/BCIP and the development reaction was stopped upon the presence of any visible background signal in the sense probe controls. Embryos were cleared through a glycerol series and imaged with light microscopy in 90% glycerol.

probe	Forward primer (5' → 3')	Reverse primer (5' → 3')
polr1a	CTCCGCTGATGAAACAAGAAA	CAAACGATTAATAGGCCTGTACCTG
polr1c	CAACGTGGATGAAATTCGTG	CACCTTCCTTCCGTTCACAT
polr1d	GGCTGAGCTTGGACAGAAAC	CAGTGTCCACATGCTCACAA

Table II-2: Primers to generate in situ probes.

SKELETAL STAINING

Alcian blue and Alizarin red staining was performed according to Walker and Kimmel (Walker and Kimmel, 2007). Tails were removed after staining for genotyping.

Embryos were further cleared in 75% glycerol for imaging on the light microscope. For flat mounts, embryos were dissected with insect pins and mounted in 75% glycerol.

IMMUNOHISTOCHEMISTRY

Whole-mount immunostaining was completed according to Westerfield, 2000 (The Zebrafish Book) using the primary antibodies listed in Table II-3. Fluorescent secondary antibodies, either Alexa-488 or Alexa-546 (1:500, Invitrogen) were used for detection. TUNEL was performed according to Crump *et al.* (Crump et al., 2004) with slight modifications. Embryos were permeabilized overnight in methanol at -20°C, rehydrated and treated with ProK. Following permeabilization, embryos were incubated for 1 hour on ice followed by 1 hour at 37°C in either the Fluorescein or the TdT/TMR red reaction. Embryos were mounted in 1% agarose and imaged using confocal microscopy.

Primary Antibody	dilution	Host	source
GFP	1:500	Rabbit	Invitrogen
HuC/D	1:200	Mouse, monoclonal	Invitrogen
pHH3	1:2000	Mouse, monoclonal	Millipore
Sox10	1:500	Rabbit, polyclonal	GeneTex
Sox9a	1:500	Rabbit, polyclonal	GeneTex
Zn-8	1:250	Mouse	DSHB

Table II-3: Primary antibodies used in whole-mount immunostaining.

Molecular Methods

WESTERN BLOT

Protein samples of 100 fish/sample were collected at various stages. Embryos less than 3 dpf were deyolked prior to protein extraction in deyolking buffer (55 mM NaCl, 1.8mM KCl, and 1.25 mM NaHCO$_3$). Embryos were homogenized and suspended in sample buffer (100mM Tris, 4% SDS, 10% glycerol, 5% β-mercaptoethanol, protease inhibitors (Sigma)) and used for Western Blotting according to standard protocols (The Zebrafish Book, zfin.org). Primary antibodies used are listed in Table II-4. Blots were incubated with ECL™-Horseradish peroxidase secondary antibodies (1:5000; GE Healthcare), followed by reaction with Amersham ECL™ Prime Western Blotting Detection Reagent (GE Healthcare), according to the manufacturer's instructions. Western blots were developed on autoradiography film (MidSci), and films were scanned and quantified using ImageJ. Alternatively, fluorescent secondary antibodies were used (Alexa-680 anti-mouse and Alexa-800 anti-rabbit, Invitrogen) at a dilution of 1:20,000. Images were taken using the LICOR system and then quantified using ImageJ. Protein levels were normalized to α-tubulin and statistical significance was determined using the Student's T-test.

Antibody	dilution	source
Zfish Tp53	1:500	Anaspec
α-tubulin	1:10000	Sigma
RPS6	1:1000	Santa Cruz Biotechnology
Phospho-RPS6	1:1000	Cell Signaling Technology

Table II-4: Primary antibodies used in Western Blotting.

QUANTITATIVE RT-PCR

RNA was collected from zebrafish embryos using the Qiagen miRNeasy Micro Kit and tested for quality on an Agilent 2100 Bioanalyzer. The Superscript III kit (Invitrogen) was used to synthesize cDNA for qPCR using the random hexamer primers. Primers for the genes investigated are listed in Table II-5. rRNA primer sequences were obtained from Azuma *et al*. (Azuma et al., 2006). Power Sybr (Life Technologies) reaction mix and the ABI 7900HT real time PCR cycler were used to measure cDNA amplification. Five biological replicates were run in technical triplicate for each experiment. No template and no reverse-transcriptase samples were run as negative controls. β-*actin, canx,* and *elf* served as controls for qPCR experiments. Data was analyzed using Biogazelle software and the Mann-Whitney test was used to determine statistical significance.

RNA-SEQ

RNA was collected from zebrafish embryos using the Qiagen miRNeasy Micro Kit and tested for quality on an Agilent 2100 Bioanalyzer. Samples with an RNA integrity (RIN) score greater than 8.0 were used for library construction. RNA-Seq for *polr1c* and

polr1d embryos was conducted at 24 hpf. Three samples with five embryos per sample were collected for both wild-types and mutants. RNA-Seq for *polr1a* embryos was conducted at 15 hpf and 24 hpf. Five samples of five embryos per sample were collected for wild-types and mutants at both time points.

RNA underwent poly(A) selection prior to library construction and sequencing. Amplification and sequencing was completed using the Illumina HiSeq2500 platform. Sequences were aligned to the zebrafish Zv9 genome. For pathway analysis, the input gene sets had a p-value of at least 0.05 and fold change of at least 1.5. SPIA was used to examine top gene sets (Tarca et al., 2009).

gene	Forward primer	Reverse primer
β-actin	ACATCAGGGAGTGATGGTTGGCAT	AGTCACAATACCGTGCTCAATGGG
canx	ACGATACCGCAGAGAATGGAGACA	TCCTGTTTCTGGGAGACCTCCTCA
elf	CTCAAATGGCATGGATGTTGCCCA	GGTCTTGGTTTGCGCACTTTGGTT
18S	CCGCTAGAGGTGAAATTCTTG	CAGCTTTCGAACCATACTCC
5'ETS	CCGGTCTACCTCGAAAGTC	CGAGCAGAGTGGTAGAGGAAG
ITS1	CTCGGAAAACGGTGAACCTG	GTGTTCGTTTCAGGGTCCG
ITS2	CCTAAGCGCAGACCGTCAC	AGCGCTGGCCTCGGAGATC
polr1a	CACCTGGAGAAGAAATCCAAG	GATGTGCTTGACAGGGTCAG
polr1c	GAGCAACGTGGATGAAATTCG	GCCAATCATATCAAACTCCAGTG
polr1d	TGAGCTTGGACAGAAACACG	ATTTTGCTTTCTGATGGGTGTG
tp53	CGAGCCACTGCCATCTATAAG	TGCCCTCCACTCTTATCAAATG

Table II-5: qRT-PCR primers.

POLYSOME PROFILING

150 embryos per sample were collected at 3 dpf and identified by phenotype. Embryos were deyolked and rinsed with ice cold PBS and then dissociated in ice-cold lysis buffer (10mM Tris-HCl, 5 mM MgCl2, 100 mM KCL, 1% TritonX-100, 2 mM DTT, 100ug/ml cycloheximide, 200U/ml RNasin (Promega), and protease inhibitor (Sigma)). Homogenized zebrafish were then centrifuged at 15,000 x g at 4°C for 10 minutes and the supernatant of the zebrafish lysate was kept for analysis. Lysates were loaded onto a 10-50% (w/vol) sucrose gradient prepared in 20 mM HEPES-KOH pH 7.4, 5 mM MgCl$_2$, 100 mM KCl, 2mM DTT, 20 U/mL RNasin (Promega), and 100 µg/mL cycloheximide. The gradients were ultra-centrifuged at 4°C in an SW-41 Ti rotor (Beckman) at 40,000 rpm for 2 hours. To evaluate UV absorbance profiles, each gradient was passed through a UA-6 absorbance reader system (Teledyne ISCO) using a syringe pump (Brandel). The absorbance at 254 nm was recorded using WinDaq data acquisition software (DATAQ INSTRUMENTS) and the profiles were plotted in Microsoft Excel.

Imaging

LIGHT MICROSCOPY

Embryos were mounted and imaged using a Leica MZ16 microscope equipped with a Nikon DS-Ri1 camera and NIS Elements BR 3.2 imaging software. Manual z-stacks were generated for individual embryos and then processed using Helicon Focus6 software to generate a single image.

CONFOCAL MICROSCOPY

Embryos were mounted in 1% agarose and imaged using a Zeiss upright 700 confocal microscope and images were taken and processed using Zen software. Laser settings were determined using mutant embryos, and the same settings were used to image control and mutant embryos.

IMAGE PROCESSING

Additional image processing was completed in Adobe Photoshop for assembly of figures. Any modifications of brightness/contrast were applied to both control and mutant embryos to more clearly present the data.

IMARIS QUANTIFICATION

To quantify regions of interest in confocal images, IMARIS software was used. The surfaces generated from the images used the automated settings. Within the region of interest determined by the surface, the software calculated several measurements including area and volume. Using the Spots tool, cell counts were determined within the region of interest.

III. POLR1C AND POLR1D ZEBRAFISH MODELS OF TREACHER COLLINS SYNDROME

Introduction

Treacher Collins syndrome (TCS), also known as Franceschetti-Klein syndrome or mandibulofacial dysostosis, is a disorder affecting craniofacial development and is estimated to occur at 1:50000 live births. TCS is characterized by downward slanting palpebral fissures, anomalies of the external and middle ear, cleft palate, and hypoplasia of the facial bones, particularly the mandible and zygomatic complex. There is wide phenotypic variation among individuals with TCS and there is no correlation between phenotype and genotype (Altug Teber et al., 2004; Trainor et al., 2008). Mutations in *TCOF1* (Treacher Collins-Franceschetti syndrome 1) account for approximately 80% of TCS cases and are inherited in an autosomal dominant manner (Gladwin et al., 1996; The Treacher Collins Syndrome Collaborative et al., 1996; Edwards et al., 1997; Wise et al., 1997; Marsh et al., 1998; Altug Teber et al., 2004). *TCOF1* encodes the protein Treacle, which localizes to the nucleolus (Marsh et al., 1998; Winokur and Shiang, 1998) where it interacts with Upstream Binding Factor (UBF) to stimulate transcription of ribosomal DNA (rDNA) by RNA Polymerase I (Valdez et al., 2004), establishing a role for ribosome biogenesis in TCS.

More recently, mutations in *POLR1C* and *POLR1D,* which encode subunits of RNA Polymerases I and III (RNAPI and RNAPIII), were identified by whole genome sequencing in a group of individuals with characteristics of TCS, but no mutation in

TCOF1 (Dauwerse et al., 2011). The mutations identified in *POLR1C* suggest autosomal recessive inheritance. Affected individuals carried two separate mutations in *POLR1C*, generally with one allele inherited from an unaffected mother and the other from an unaffected father. The mutations identified in *POLR1D* suggest it can be inherited in either an autosomal dominant or autosomal recessive manner (Dauwerse et al., 2011; Schaefer et al., 2014). Initially, autosomal dominant mutations were identified in *POLR1D* including a premature stop codon, nonsense mutations, and missense mutations occurring within exon 3, with the exception of one mutation in the second intron (Dauwerse et al., 2011). Exon 3 contains the dimerization domain of POLR1D, so these mutations are likely to impede the normal binding and function of the protein. A later study identified a patient with autosomal recessive inheritance, again with the mutation occurring within exon 3 (Schaefer et al., 2014). These studies show that TCS is a genetically heterogeneous syndrome. The variation in penetrance in affected individuals is hypothesized to be due to modifier genes or potentially another mutation at an unlinked locus that is required for the TCS phenotype.

Previous studies to model TCS in mice and zebrafish have examined the role of *Tcof1* during craniofacial development. In mice, mutations in *Tcof1* result in many of the same cranioskeletal anomalies as human TCS such as a small mandible and cleft palate (Dixon et al., 2006). During mouse embryonic development, *Tcof1* is expressed in a broad but dynamic manner throughout development with strong expression in the neuroepithelium at embryonic day (E) 8.5, corresponding to the generation of NCC, as well as in the frontonasal and branchial arch mesenchyme at E9.5 (Dixon et al., 2006). This

expression pattern demonstrates a role for *Tcof1* during NCC formation and migration. *Tcof1*$^{+/-}$ embryos have a decreased population of NCC, and this is due to apoptosis and decreased proliferation in the neuroepithelium (Dixon et al., 2006). In a subsequent study, microarray analysis of *Tcof1*$^{+/-}$ embryos revealed an increase in genes which are associated with p53-dependent transcription; these genes have roles in cell cycle regulation, apoptosis, and DNA repair (Jones et al., 2008). An increase in p53 activity and specific neuroepithelial apoptosis was observed in *Tcof1*$^{+/-}$ mice compared to wild-type siblings (Jones et al., 2008). Furthermore, it was shown that *Tcof1*$^{+/-}$ embryos have diminished production of mature 28S rRNA and it was hypothesized that decreased ribosome biogenesis in NCC underlies the pathogenesis of TCS (Jones et al., 2008). Pharmacological inhibition of p53 using pifithrin-α, as well as genetic inhibition using *p53*$^{+/-}$ mice, reduced neuroepithelial apoptosis and rescued the TCS phenotype in *Tcof1*$^{+/-}$ mice (Jones et al., 2008). Despite this rescue, an increase in ribosome biogenesis was not observed upon p53 inhibition, and further study is necessary to understand the role of ribosome biogenesis in the pathogenesis of TCS. A proposed model of TCS in zebrafish was generated using morpholino injections against a gene which has since been identified as *nolc1* (Weiner et al., 2012). In this model, they found that during early embryonic development, *nolc1* mRNA expression was ubiquitous and at later stages, expression was seen within the pharyngeal arches. Consistent with the *Tcof1*$^{+/-}$ mouse model, hypoplastic skeletons and elevated levels of p21, a downstream target of p53, were observed in *nolc1* morphants but ribosome biogenesis was not investigated.

The role of *Tcof1* in the pathogenesis of TCS has been well studied, however, the function of Polr1c and Polr1d in the TCS phenotype is unknown. It is surprising that mutations in these subunits of RNAPI and RNAPIII would lead to a specific craniofacial phenotype in humans. Studies in yeast have shown that *polr1c* and *polr1d* interact to form a dimer and are essential for growth (Lalo et al., 1993), but these genes have not been investigated in a vertebrate model. In order to understand the role of these genes in craniofacial development, I investigated the function of *polr1c* and *polr1d* in zebrafish.

Results

DYNAMIC EXPRESSION OF POLR1C AND POLR1D

To understand the importance of *polr1c* and *polr1d* in craniofacial development, I first examined the mRNA expression of these genes at various stages of zebrafish embryonic development. Early stages revealed ubiquitous expression as would be expected (Figure III-1). Maternal expression of *polr1c* and *polr1d* is evident at stages <1 hour post fertilization (hpf), and expression is ubiquitous through gastrulation and neural plate formation. Remarkably, a more restricted expression pattern is apparent at 24 hpf, with enriched expression in the eye and brain. At 36 hpf, enriched expression is visible in the pharyngeal arch region, which will eventually give rise to the craniofacial cartilage. Beyond 48 hpf, *polr1c* and *polr1d* are expressed at low levels throughout the embryo. The elevated expression of *polr1*c and *polr1d* in the craniofacial region suggests that higher levels are necessary in these regions for normal development. Thus a disruption of either

polr1c or *polr1d* may have a stronger effect in craniofacial development than in other tissues.
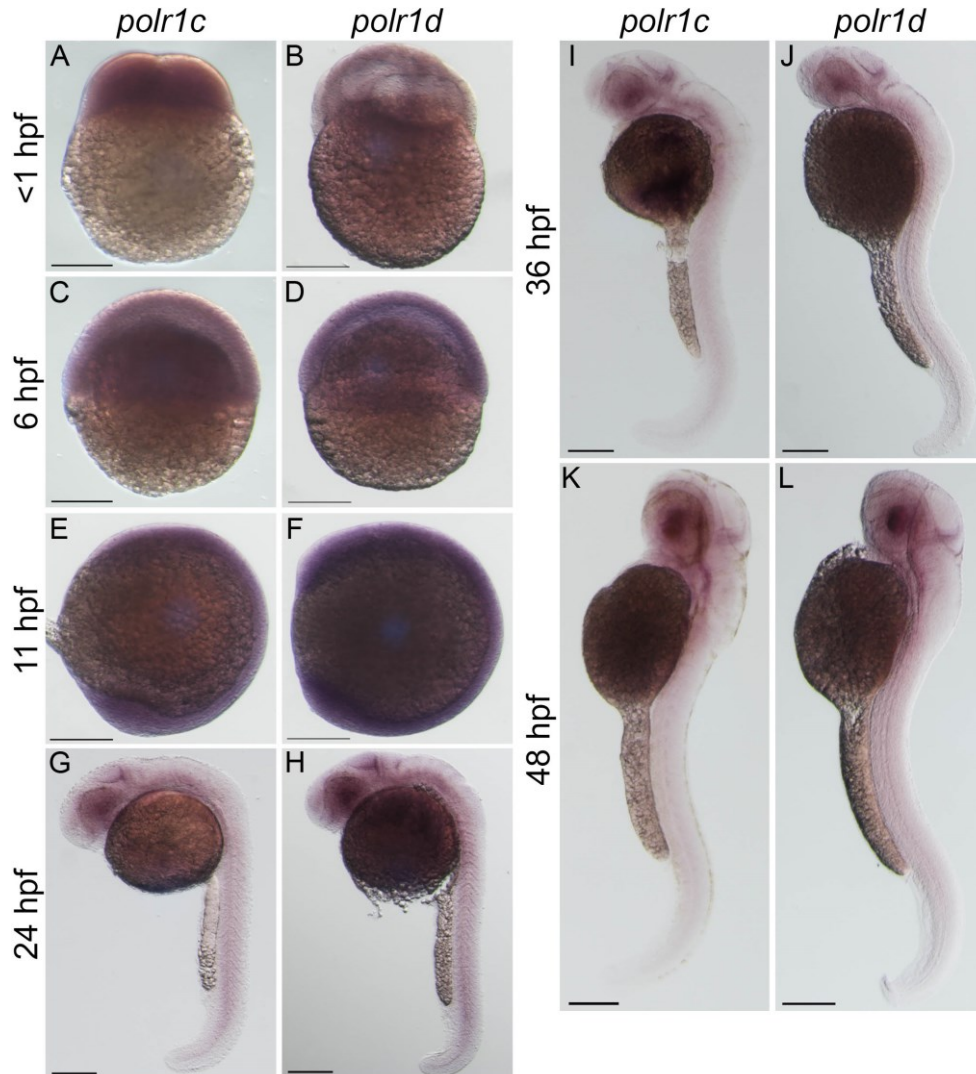
Figure III-1 Expression of *polr1c* and *polr1d* during embryonic development is dynamic.

Both genes show maternal expression at early stages (A,B) and are ubiquitously expressed at 6 hpf (C,D) and 11 hpf (E,F). At 24 hpf, expression becomes enriched in regions such as the eye and midbrain-hindbrain boundary (G,H). Elevated expression can be seen in the pharyngeal arches at 36 hpf (I,J) and then lower levels are observed at stages 48 hpf (K,L) and beyond. Scale bar = 200 μm.

Given the enriched expression of polr1c and polr1d in craniofacial regions, I hypothesized that *polr1c* and *polr1d* are important in craniofacial development. To understand the role of *polr1c* and *polr1d* during embryonic development, I examined two mutant zebrafish: *polr1c*^{hi1124Tg} and *polr1d*^{hi2393Tg}; hereafter referred to as *polr1c*$^-$ and *polr1d*$^-$. These mutant zebrafish were generated by insertional mutagenesis (Amsterdam, 2003; Amsterdam et al., 2004) which severely disrupts the production of mRNA (Figure III-2) resulting in hypomorphic alleles. The mutation in *polr1c* is located in exon 2 while the mutation in *polr1d* is located in the first intron (http://web.mit.edu/hopkins/). The *polr1c* and *polr1d* mutant embryos begin to show a phenotype around 24 hpf (Figure III-3, A-D) and are recognizable by a smaller eye and a disrupted midbrain-hindbrain boundary. Notably, these affected tissues are consistent with areas where *polr1c* and *polr1d* expression is enriched at 24 hpf. Mutant embryos also display varying degrees of what appears to be necrotic tissue in the head. By 5 days post fertilization (dpf), craniofacial anomalies are apparent in *polr1c* and *polr1d* mutants (Figure III-3, E-G). The mutant embryos have a smaller head and eye; however, the body size is generally the same size as control embryos. In addition, these zebrafish have smaller jaws, liver defects, develop pericardial edema, and fail to inflate the swim bladder. *polr1c* and *polr1d* mutant embryos die between 9-10 dpf, likely due to cardiovascular defects.

In order to understand if mutations in *polr1c* and *polr1d* result in similar craniofacial defects as human TCS patients, I examined cartilage and bone using Alcian blue and Alizarin red. Mutant embryos show a clear hypoplasia of the craniofacial cartilage

85

elements at 5 dpf (Figure III-4). While cartilage elements from pharyngeal arches 1 and 2 are present, these elements are smaller and the ceratohyal is reversed in mutant embryos. Consistent with the human TCS phenotype, the jaws of *polr1c* and *polr1d* mutant embryos are smaller (Figure III-4, D-F). The palatoquadrate and Meckel's cartilage are not as elongated in the mutant embryos. Cartilage derived from more posterior arches is more severely affected and ceratobranchials 2-5 show very little Alcian stain (Figure III-4, G-I). In addition, the portions of the neurocranium which are NCC-derived, including the trabeculae and the ethmoid plate (Eberhart et al., 2006), which has homology to the palate (Swartz et al., 2011), are also hypoplastic while the portions which have mesodermal origin are not as severely affected. To determine whether these anomalies arise at earlier stages of development, I also examined the cartilage at 3 dpf by Alcian blue (Figure III-5). At this stage, the cartilage elements are noticeably smaller (Figure III-5 A-C). The ceratohyal is already showing a slight reversal in the mutant embryos (Figure III-5 E,F) and there is the absence of ceratobranchial cartilage elements as well. The cartilage elements of the neurocranium are also smaller, especially the ethmoid plate (Figure III-5 H,I). Altogether, this indicates that cartilage formation is delayed and disrupted in *polr1c* and *polr1d* mutant embryos.
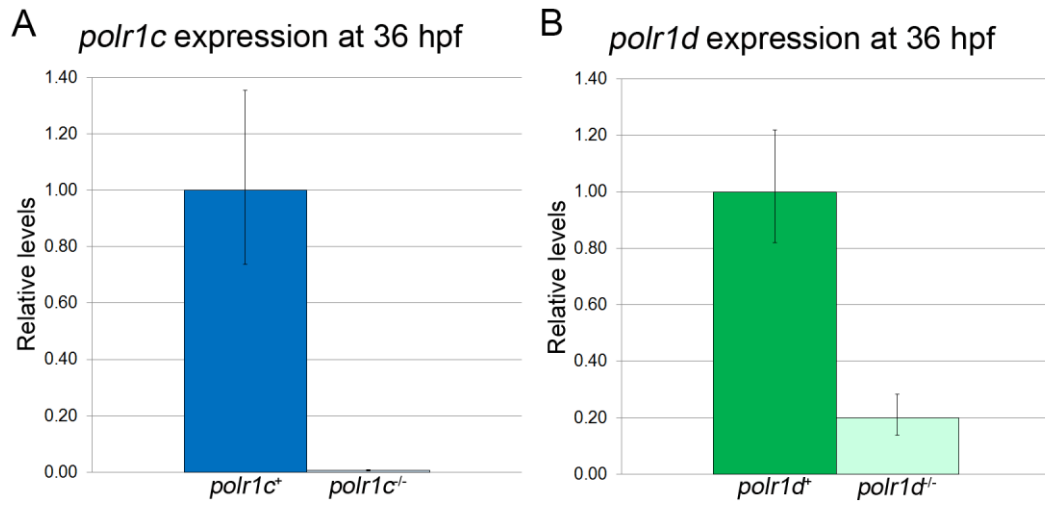
Figure III-2: Quantitative RT-PCR for *polr1c* and *polr1d*.

qPCR data shows significantly reduced expression of *polr1c* (A) and *polr1d* (B) mRNAs in homozygous mutant embryos.
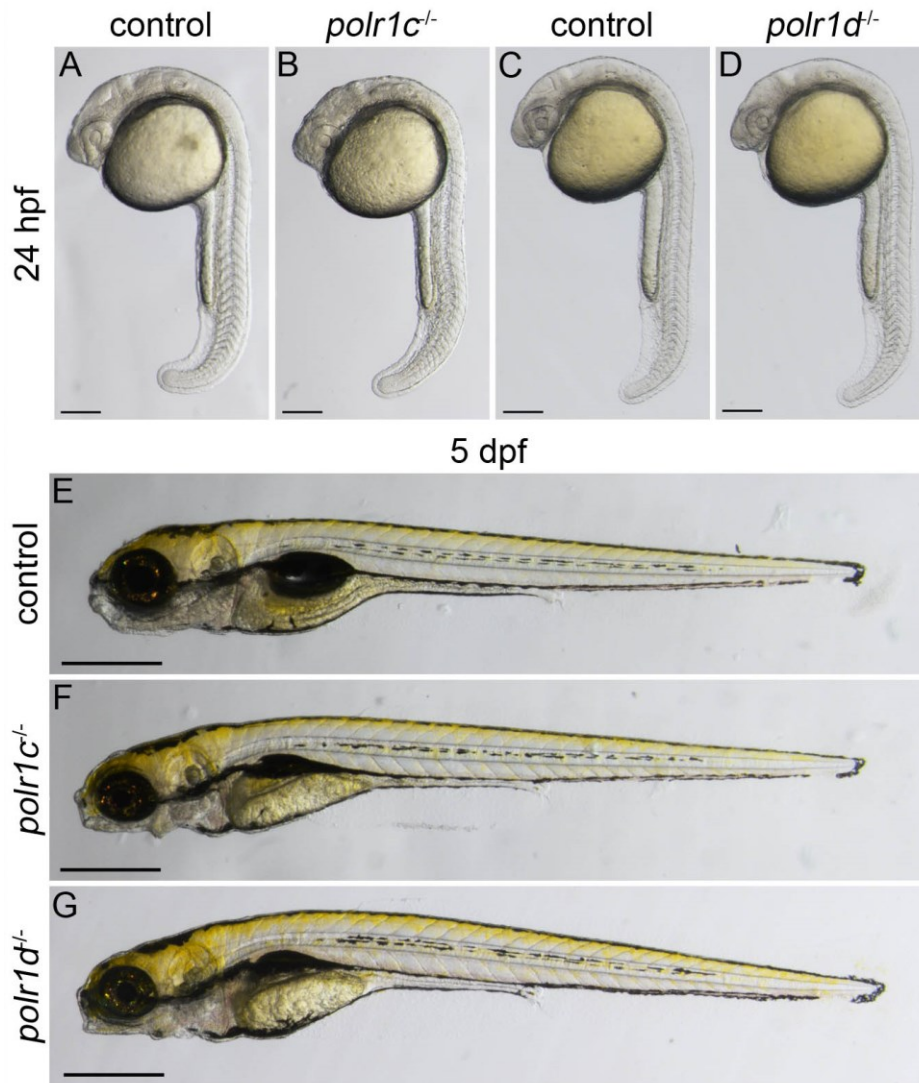
Figure III-3: Live phenotype of *polr1c*$^{-/-}$ and *polr1d*$^{-/-}$ zebrafish.
A-D) At 24 hpf, smaller eyes and disrupted midbrain-hindbrain boundary region is evident in mutant embryos (B,D). E-G) By 5 dpf, mutants are distinguished by the smaller head, abnormal jaw, and failure to inflate the swim bladder (F,G). Scale bar = 200 μm.
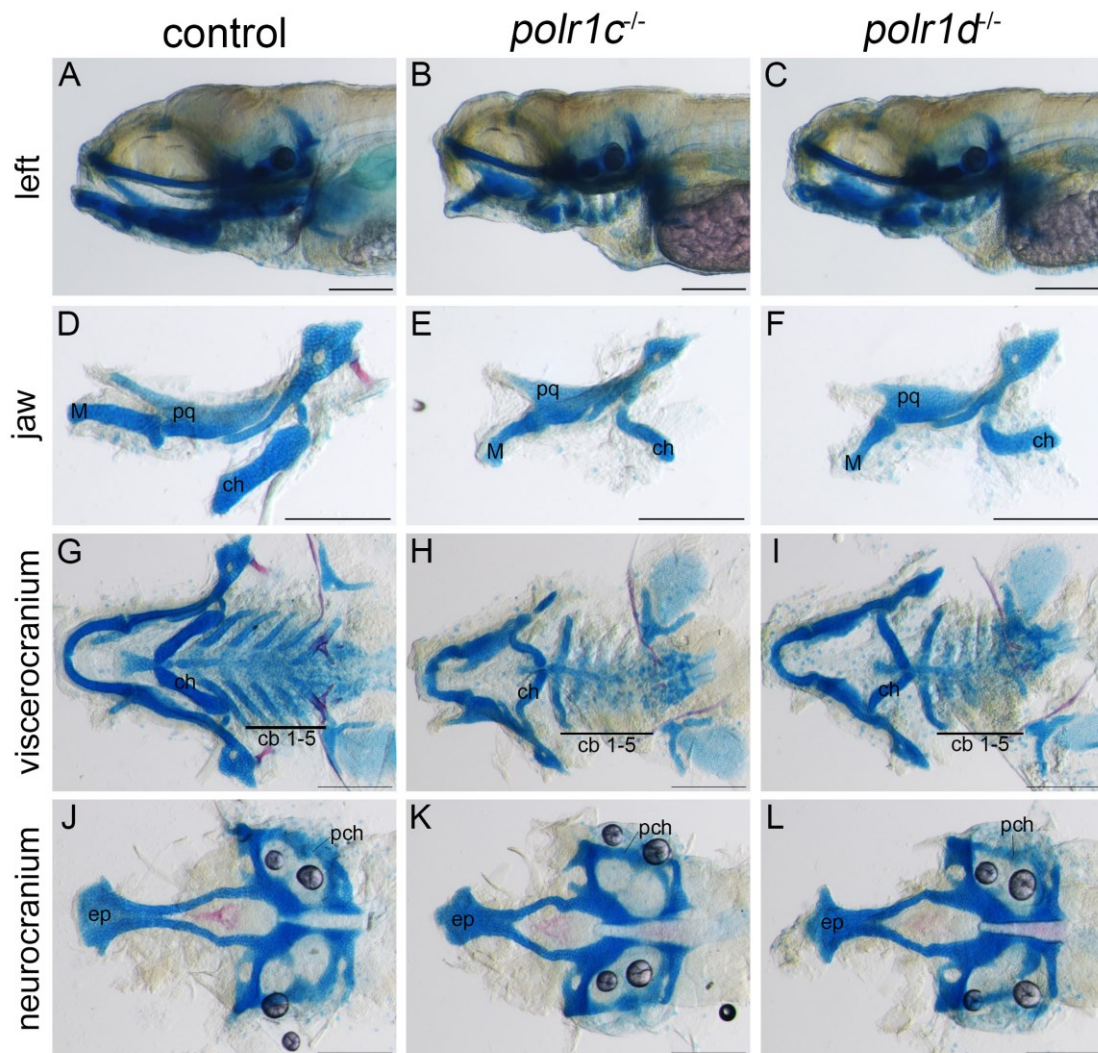
Figure III-4. Skeletal staining reveals hypoplastic cartilage in *polr1c* and *polr1d* mutant embryos.

A-C) Alcian blue and Alizarin red staining at 5 dpf reveals hypoplastic cartilage and bone in *polr1c* and *polr1d* mutant embryos compared to controls. D-F) The jaws of mutant embryos are smaller. G-I) Dissection of the viscerocranium reveals smaller cartilage elements derived from each of the pharyngeal arches in mutant embryos, as well as mispatterning of the ceratohyal. J-L) Dissection of the neurocranium reveals alterations in the NCC-derived portions of the cartilage, including the ethmoid plate. Abbreviations: M - Meckel's cartilage; pq – palatoquadrate; ch – ceratohyal; cb – ceratobranchial; ep – ethmoid plate; pch – parachordal. Scale bar = 200 μm.
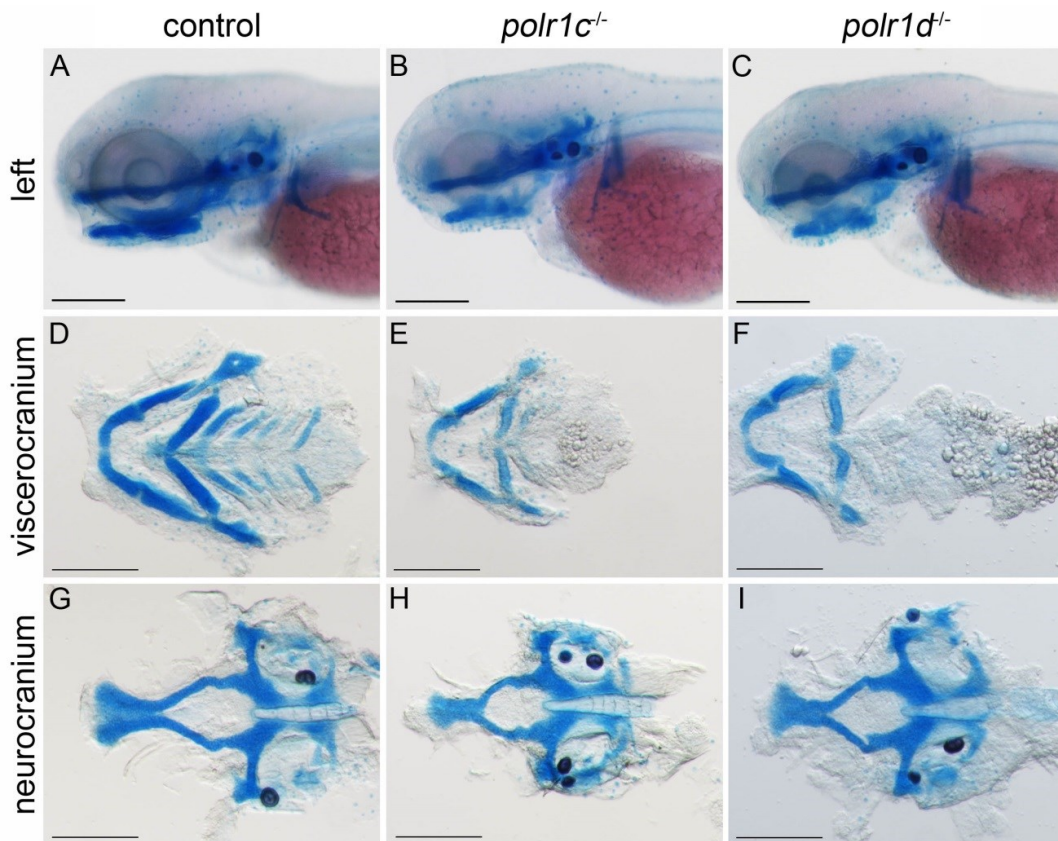
Figure III-5. Cartilage is hypoplastic at 3 dpf in *polr1c* and *polr1d* mutants.
A-C) Alcian blue staining at 3 dpf reveals diminished cartilage formation in *polr1c* and *polr1d* mutant embryos. D-F) The cartilage elements derived from each of the pharyngeal arches are present in control embryos (D), while mutant embryos show hypoplastic elements from arches 1 and 2, and the ceratobranchial cartilage elements derived from arches 3-7 are absent. G-I) In the neurocranium, the NCC-derived cartilage forming the ethmoid plate is hypoplastic in *polr1c* and *polr1d* mutant embryos.

NCC DEVELOPMENT

As the majority of the craniofacial cartilage is NCC-derived, I next investigated whether NCC development was disrupted. The neural plate, labeled by *sox2*, forms in both *polr1c* and *polr1d* mutant embryos (Figure III-6). This suggests that the levels of *polr1c* and *polr1d* present at this stage are sufficient for neural plate formation, which occurs prior to NCC induction. *sox10* and *foxd3* were used to investigate early stages of NCC formation and migration, and do not show a significant reduction in mutant embryos. Expression of *sox10* is found in premigratory NCC at early stages and in migratory NCC as somitogenesis progresses (Dutton et al., 2001). In situ hybridization for *sox10* at 12 hpf reveals similar levels of NCC induction in *polr1c* and *polr1d* mutant embryos compared to control siblings (Figure III-7, A-H). *foxd3* is expressed in premigratory NCC and down-regulated in the migrating cranial NCC (Odenthal and Nüsslein-Volhard, 1998; Kelsh et al., 2000). Correspondingly, the expression of *foxd3* at 14 hpf, when it is expressed within the pre-migratory cranial NCC and the paraxial mesoderm, also did not show significant alteration in the *polr1c* and *polr1d* mutant embryos (Figure III-7, I-P). Thus it seems the early genetic program for NCC formation occurs within *polr1c* and *polr1d* mutant embryos prior to the onset of the mutant phenotype. Another NCC marker, *dlx2,* is expressed in the NCC in the pharyngeal arches (Akimenko et al., 1994), which are precursors to the craniofacial cartilage. At 36 hpf, after the mutant phenotype is evident, the domain of *dlx2* expression showed a slight reduction, which would indicate a smaller population of cells within the pharyngeal arches and is consistent with the hypoplastic craniofacial cartilage in mutant embryos (Figure III-7, Q-X). To determine if the reduced number of NCC within the

91

pharyngeal arches was due to a deficiency of migration, I investigated the pattern of NCC migration using *sox10:gfp* transgenic animals as well as an antibody against Sox10. Using *polr1c; sox10:gfp* and *polr1d; sox10:gfp* transgenic embryos, I found the timing and pattern of NCC migration appeared normal, with NCC migrating in the three typical streams in *polr1c* and *polr1d* mutant embryos (Figure III-8). Therefore the reduced number of NCC was not due to a failure to migrate to the correct location. Immunostaining for Sox10 at 24 hpf did not show a strong difference in expression, however this is at the onset of the mutant phenotype and there may be differences later in development (Figure III-9, A-C). Alternatively, at 24 hpf, some NCC are beginning to become fate-restricted. To investigate if the reduction in the NCC population in the pharyngeal arches at 36 hpf could be due to a reduction specifically within the cartilage precursor population, I investigated the expression of Sox9a. At 24 hpf, *sox9a* is expressed within the cranial mesenchyme which contributes to the formation of the pharyngeal arches and neurocranium as well as within the mesenchyme of the pharyngeal arch primordia (Chiang et al., 2001). Immunostaining for Sox9a at 24 hpf revealed a slight decrease in the domain of expression in the pharyngeal arches of *polr1c* mutants, but no distinguishable difference in *polr1d* mutant embryos (Figure III-9, D-F). Quantification of the volume of pharyngeal arches 1 and 2 stained with Sox9a confirmed this observation, with the volume of *polr1c* embryos tending to be smaller, but not significantly ($p = 0.06$), and the volume of *polr1d* embryos being about the same as controls ($p = 0.88$) (Figure III-9 G, H). Although not significant at 24 hpf, when the mutant phenotype is first distinguishable, this tendency for the arches to be smaller is indicative of presence of smaller arches at 36 hpf (Figure III-7, Q-X).

As NCC development is able to proceed from formation to differentiation, it is unlikely that *polr1c* and *polr1d* are specifically required for the proper genetic programming to occur in NCC. However, the reduced size and altered patterning of the craniofacial cartilage, especially of the ceratohyal and ceratobranchial cartilages, would suggest some alteration of the NCC population or pharyngeal arch patterning. Ceratobranchial cartilage elements fail to form properly in other zebrafish mutants, such as the *tbx1* and *prdm1a* mutants. *tbx1* mutants have a deficiency in formation of the endodermal pouches which results in fusions of the posterior ceratobranchial cartilage elements (Piotrowski and Nüsslein-Volhard, 2000). *prdm1a* mutants fail to form the posterior pharyngeal pouches and fail to develop ceratobranchial cartilage elements by 6 dpf (Birkholz et al., 2009). To rule out the possibility that a difference in pharyngeal arch/pharyngeal pouch patterning was responsible for the phenotype in *polr1c* and *polr1d* embryos, I examined arch structure in the *fli1a:egfp* transgenic zebrafish stained with Zn-8, which can be found in the endodermal pouches (Trevarrow et al., 1990; Warga and Nusslein-Volhard, 1999). This staining revealed no alteration of arch/pouch structure in mutant embryos (Figure III-10, A-C) as the pouches separated each arch. Quantification of the volume of pharyngeal arches 1 and 2 labeled by *fli1a:egfp* (Figure III-10, D-F) revealed that these arches were approximately 20% smaller in mutant embryos, which is consistent with the reduction in the *dlx2* domain observed by in situ and indicative of a reduced number of NCC within the pharyngeal arches. *polr1c$^{-/-}$* embryos averaged a volume of 3.55 x 10^5 μm^3 while control siblings averaged a volume around 4.47 x10^5 μm^3 (p = 0.0088, t-test; Figure III-10, G). Similarly, *polr1d$^{-/-}$* embryos averaged a volume of 2.09 x 10^5 μm^3

while control siblings averaged a volume of 2.49 x 10^5 μm^3 (p = 0.022, Figure III-10, H). Given the proper patterning of the arches, it is possible that development of the ceratobranchial cartilage elements is simply delayed. Alcian blue and Alizarin red staining of *polr1c* and *polr1d* embryos at 9 dpf revealed the presence of all of the cartilage elements (Figure III-11, A-C). However, the size and location of the elements derived from pharyngeal arches 2-7 are smaller in mutant embryos (Figure III-11, E,F) compared to control siblings (Figure III-11 D). The amount of bone formation is also reduced in mutant embryos in both the viscerocranium and neurocranium. The branchiostegal rays and opercles are reduced in the viscerocranium while the parasphenoid shows reduced ossification in the neurocranium. Therefore, as pharyngeal arch/pouch patterning is normal and ceratobranchial cartilages do form by 9 dpf, although severely hypoplastic, it seems likely there is a delay in cartilage development in the mutant embryos. The severe hypoplasia of the ceratobranchial cartilage is also indicative of a reduced number of chondrocytes, as there must be enough present for stacking of the chondrocytes in formation of these cartilage elements. The smaller size of other cartilage elements and the reduction in bone formation also indicate that there are fewer chondrocytes, which is consistent with the earlier finding of a reduced number of NCC populating the pharyngeal arches. Altogether, these results suggest that *polr1c* and *polr1d* are not required for expression of the genes involved in NCC formation, migration, or differentiation. Instead, there appears to be a deficiency in the population of NCC within the pharyngeal arches, which could indicate a role for *polr1c* and *polr1d* in survival or proliferation of NCC.
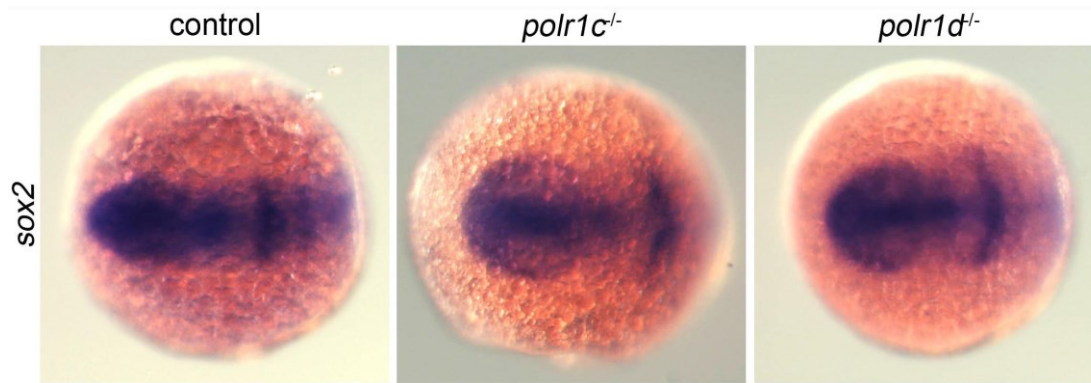
Figure III-6. In situ hybridization for *sox2* at 11 hpf shows neural plate formation. Staining and images by Annita Achilleos.
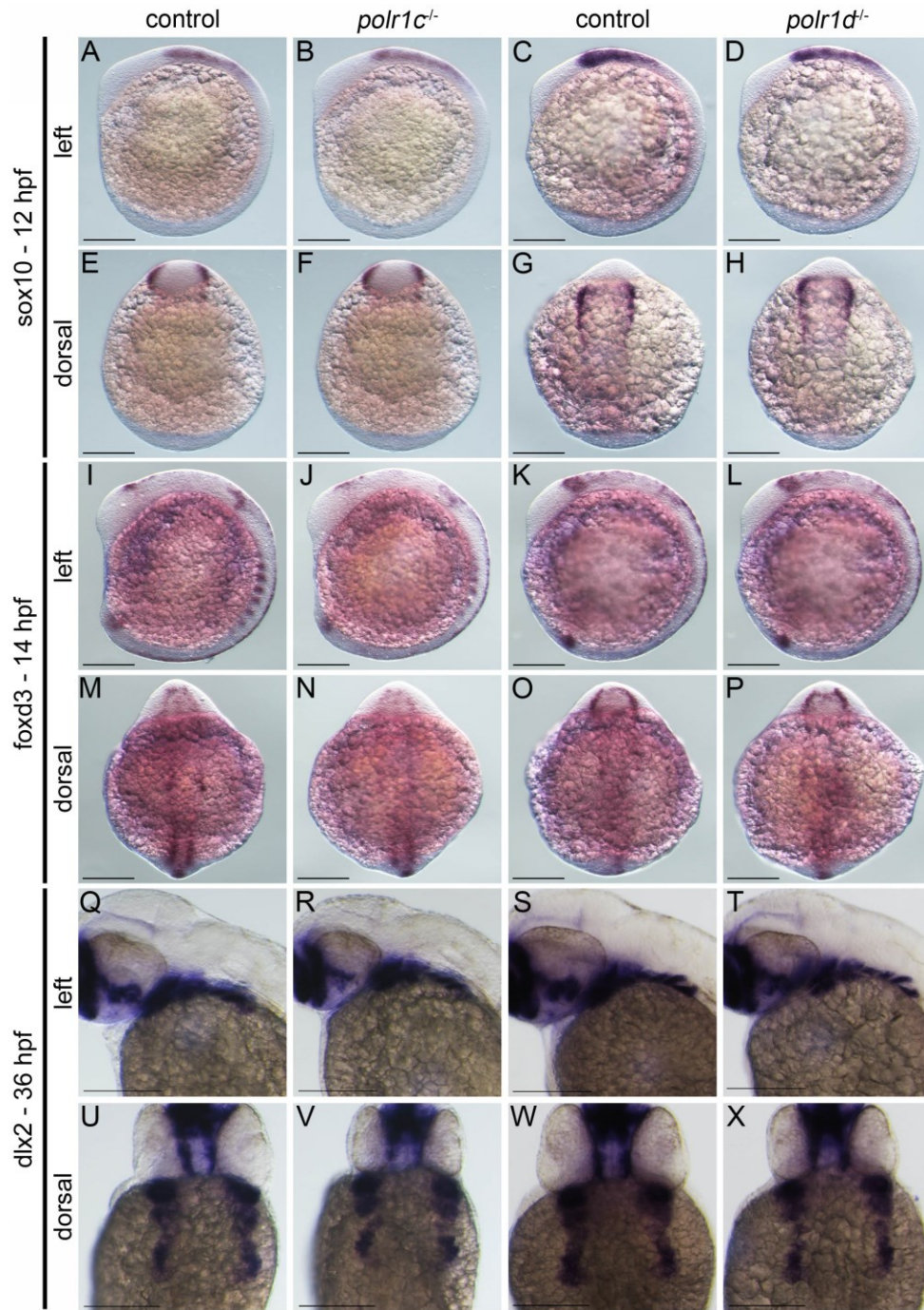
Figure III-7. In situ hybridization for markers of neural crest development.
A-H) *sox10* at 12 hpf shows induction of NCC occurs in mutant embryos.
I-P) *foxd3* at 14 hpf shows similar levels of pre-migratory NCC. Q-X)
dlx2 at 36 hpf shows a slight reduction of the size of the pharyngeal
arches in mutant embryos. Scale bar = 200 μm
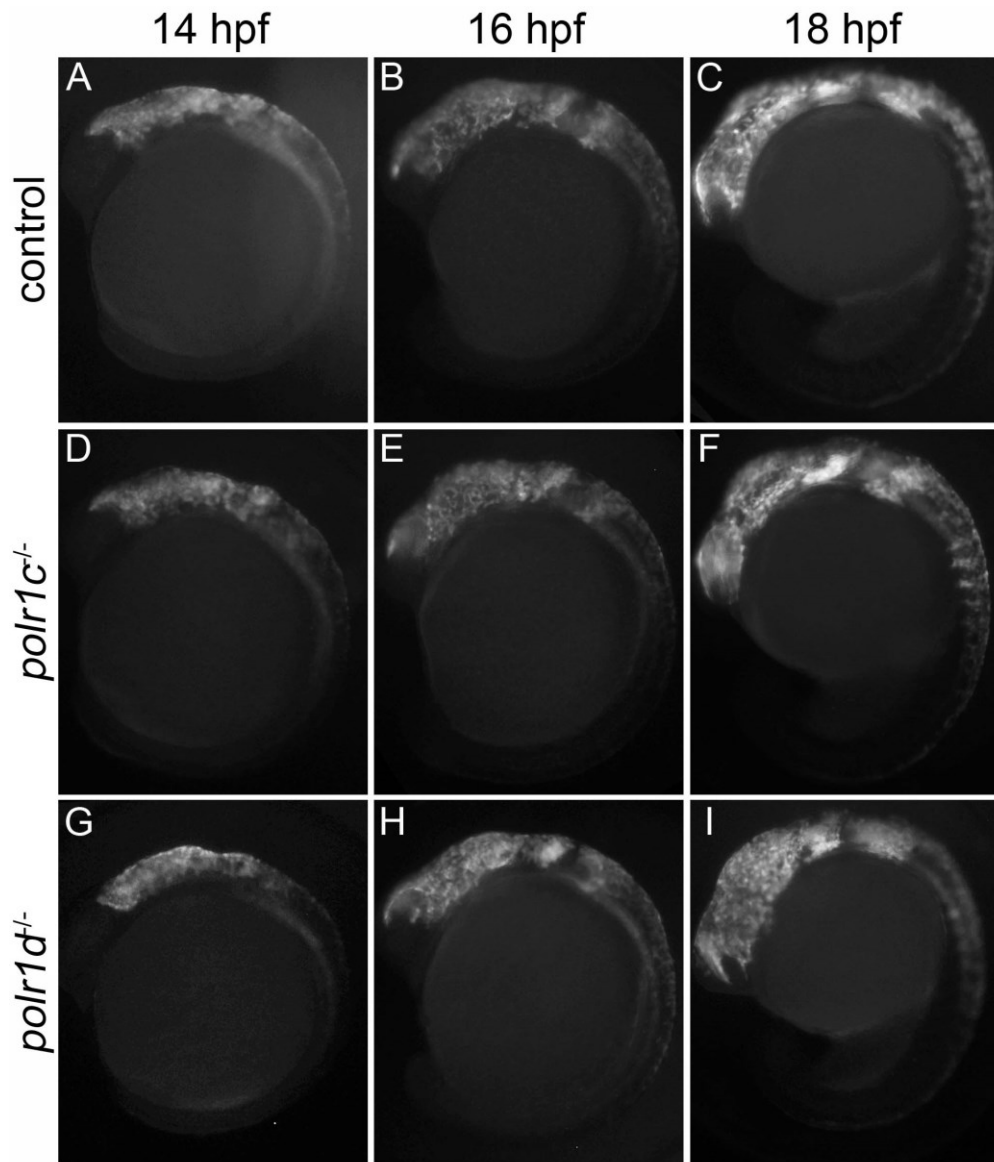
Figure III-8. *sox10:gfp* transgenic zebrafish reveal a normal pattern of NCC migration in *polr1c* and *polr1d* mutant embryos.

Similar levels are observed at 14 hpf (A, D, G), and all three NCC streams are visible at 16 hpf (B, E, H). The migration into the the developing pharyngeal arch region can be observed at 18 hpf (C, F, I).
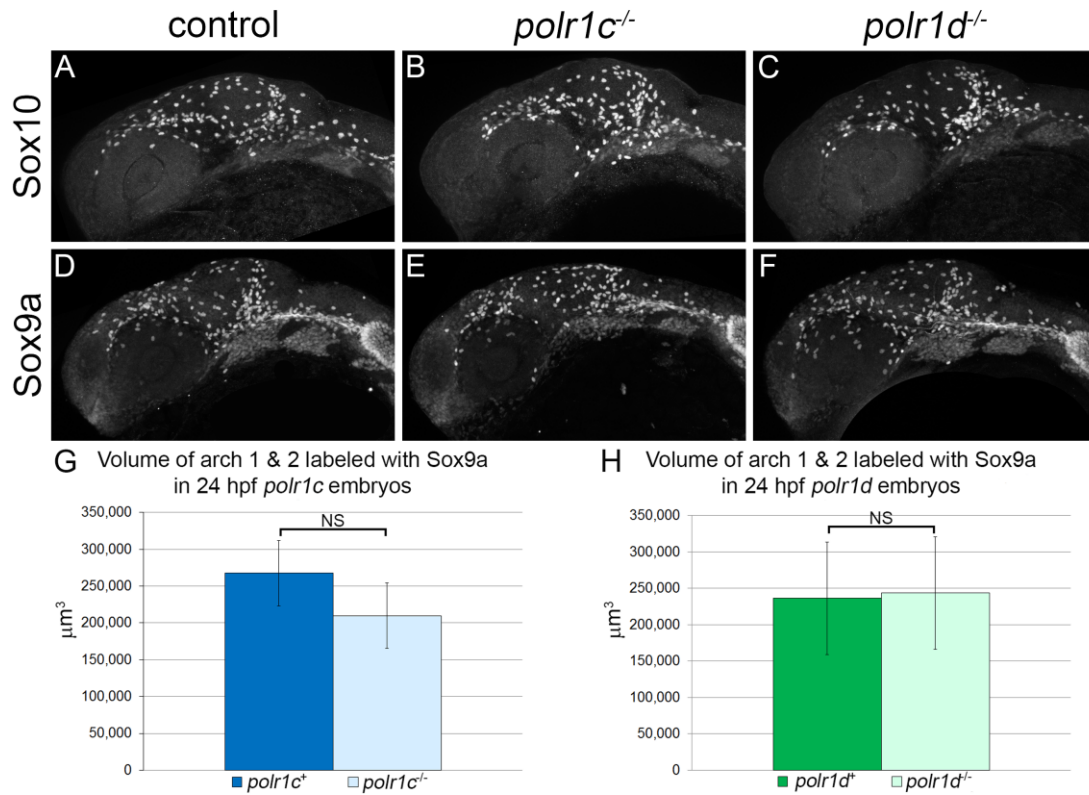
Figure III-9 NCC migration and pharyngeal arch volume at 24 hpf.
A-C) Immunostaining against Sox10 at 24 hpf does not show a significant difference in the amount of migratory NCC in *polr1c* and *polr1d* mutant embryos. D-F) Similarly, immunostaining against Sox9a also shows no significant difference in mutant embryos. G, H) Quantification of arch volume in *polr1c* and *polr1d* mutant embryos confirms no significant difference in Sox9a expression in pharyngeal arches 1 and 2. Error bars represent 95% confidence intervals.
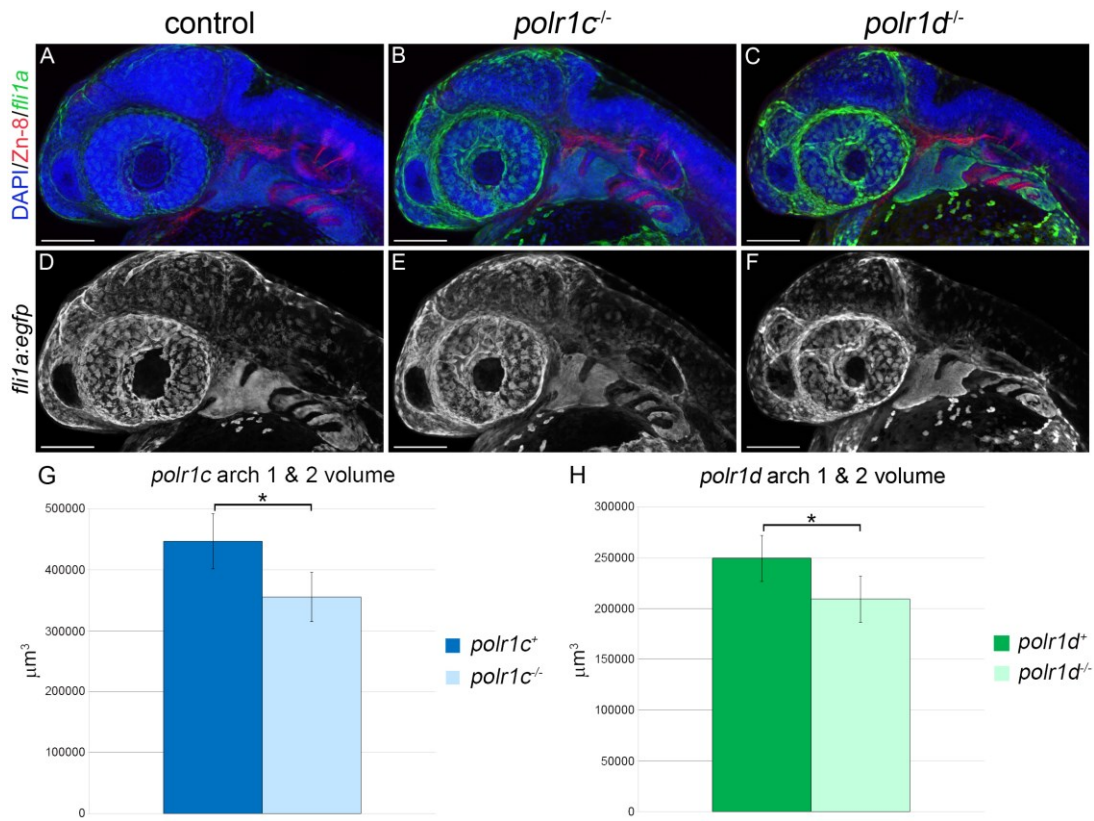
Figure III-10. Pharyngeal arch patterning and volume at 36 hpf.

A-C) Immunostaining *fli1a:egfp* embryos with Zn-8 at 36 hpf reveals proper pharyngeal arch and pharyngeal pouch patterning. Zn-8 (red) can be seen separating the pharyngeal arches marked by *fli1a:egfp*. D-F) *fli1a:egfp* reveals the structure of the arches is slightly smaller. Quantification reveals a reduction in the volume of arch 1 and 2 in *polr1c* (G) and polr1d (H) mutants. Scale bar = 100 µm. * = p < 0.05 and error bars represent 95% confidence intervals.
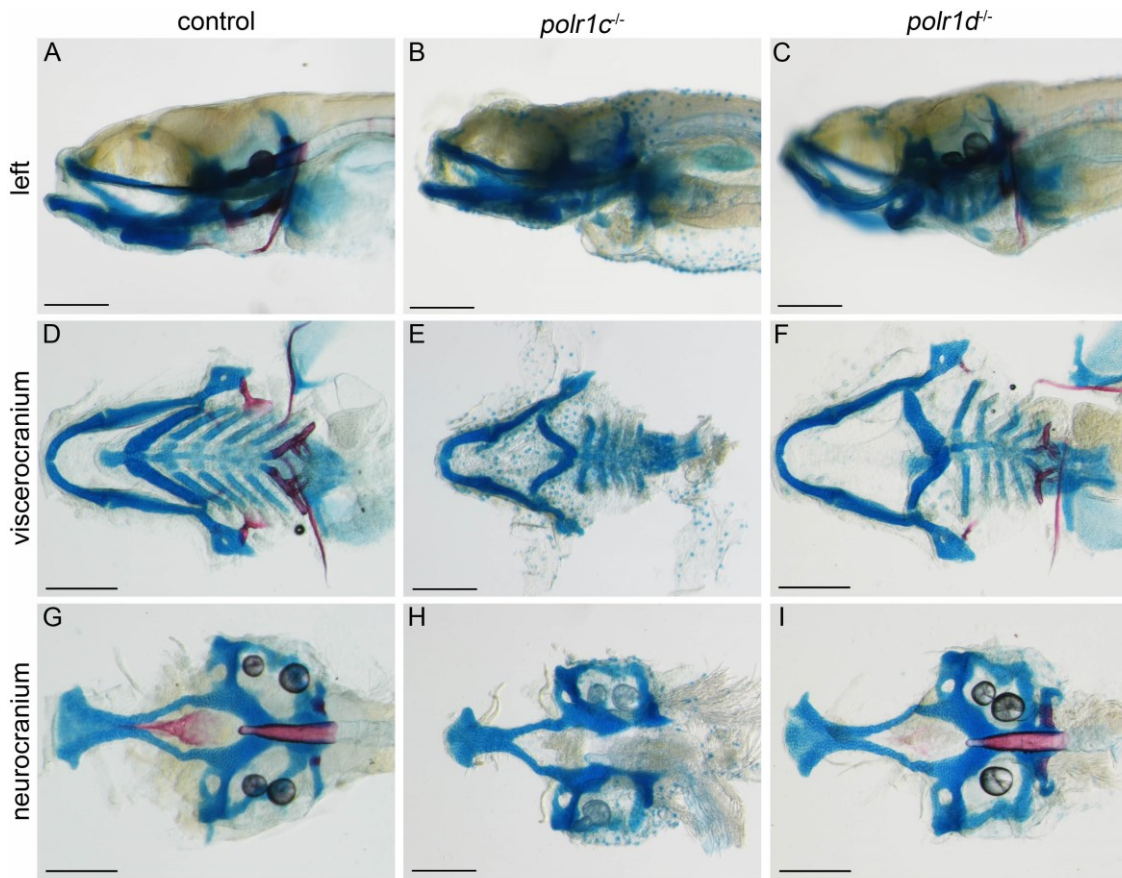
Figure III-11. Alcian blue and Alizarin red staining at 9 dpf reveals diminished cartilage and bone formation in *polr1c* and *polr1d* mutant embryos.
A-C) Deficiencies in the cartilage can be observed in mutant embryos. D-F) Dissection of the viscerocranium reveals mispatterning of the ceratohyal, and hypoplasia of the ceratobranchial cartilages in *polr1c* and *polr1d* mutants. There is also hypoplasia of bone elements including the opercles and pharyngeal teeth. G-H) Dissection of the neurocranium reveals reduced ossification of the parasphenoid in mutant embryos. Scale bar = 200 μm.

CELL SURVIVAL AND PROLIFERATION

Given the smaller pharyngeal arches in *polr1c* and *polr1d* mutant embryos, I next hypothesized that *polr1c* and *polr1d* have roles in NCC survival or proliferation. The importance of NCC survival in TCS has been demonstrated by the *Tcof1* mouse model. In this model, neuroepithelial apoptosis underlies the loss of NCC necessary to form the craniofacial skeleton (Dixon et al., 2006). TUNEL staining on 24 hpf zebrafish embryos revealed increased apoptosis in both *polr1c* and *polr1d* mutant embryos (Figure III-12). Cross sections through the embryos reveal that the majority of cell death is localized to the neural tube (Figure III-12, D-F). To confirm that the migrating and differentiating NCC population was not undergoing apoptosis as well, TUNEL staining was completed in *sox10:gfp* transgenics. This showed no significant co-localization of cell death with expression of *sox10:gfp* at 24 hpf (Figure III-13, A-D), indicating the migratory NCC were not dying at 24 hpf. Additionally, staining was not observed within the developing cartilage at 48 hpf (Figure III-13, E-H) which suggests that the differentiating NCC are not undergoing apoptosis. Together this indicates that neuroepithelial apoptosis at 24 hpf reduces the NCC progenitor population, but the NCC that do survive are able to migrate and differentiate. Therefore, the death of NCC progenitors leads to a smaller number of NCC which migrate to the pharyngeal arches as evidenced by *dlx2* (Figure III-7) and the volume of the arches of *fli1a:egfp* embryos (Figure III-10). The progenitors that do survive are able to migrate normally, as was seen with *sox10:gfp* (Figure III-8), and differentiate into cartilage, indicating that *polr1c* and *polr1d* primarily have a role in the survival of NCC.

Cell death can arise due to multiple stressors, one of which is nucleolar stress. Alterations in ribosome biogenesis, such as might be predicted exist due to mutations in RNAPI subunits, are known to cause nucleolar stress and lead to activation of Tp53 (Rubbi and Milner, 2003). Furthermore, mutations in *Tp53* are able to rescue the phenotype of *Tcof1*^{+/-} mice, suggesting a role for Tp53-dependent cell death in the TCS phenotype (Jones et al., 2008). To determine if cell death observed was Tp53-dependent in *polr1c* and *polr1d* mutant embryos, I examined Tp53 levels by Western blot and quantitative RT-PCR (qPCR). qPCR at 36 hpf showed a significant increase in *tp53* levels in mutant embryos (Figure III-12, G) and Western blot confirmed a strong increase in Tp53 levels in the mutant embryos at 5 dpf (Figure III-12, H). These results suggest that the apoptosis observed is Tp53-dependent, which is consistent with a mechanism of nucleolar stress and activation of Tp53.

In addition to the death of NCC progenitors, I hypothesized that mutations in *polr1c* and *polr1d* might limit the proliferative capacity of the NCC in the pharyngeal arches, contributing to their reduced size. In order to understand how NCC were proliferating, I examined the levels of phospho-histone H3 (pHH3) in *sox10:gfp* transgenic zebrafish. Phosphorylation of histone H3 at Ser 10 occurs during late G2 to M phase and is used as a marker of proliferation (Hendzel et al., 1997). At 24 hpf, the levels of pHH3 staining appeared similar between control and mutant embryos (Figure III-14, A-C). The levels at 36 hpf also appeared to be broadly similar between control and mutant embryos (Figure III-14, D-F). However, to determine if there was a difference in the level of proliferation within the NCC population that will contribute to the craniofacial skeleton, I examined the

102

percentage of pHH3-positive (pHH3+) cells within pharyngeal arches 1 and 2 at 36 hpf. IMARIS software was used to count the number of *sox10:gfp* cells and pHH3+ cells specifically within pharyngeal arches 1 and 2. The percentage of cells was calculated by dividing the number of pHH3+ cells by the number of *sox10:gfp* cells. *polr1c* control embryos had approximately 14% of cells proliferating within arches 1 and 2 while *polr1c* mutant embryos had approximately 6.7%, which was significantly lower (p=0.002, t-test). *polr1d* mutant embryos had a similar, although slightly higher, percentage of cells at 8.4% (Figure III-14, G). This data would suggest that Tp53-dependent cell death of NCC progenitors reduces the NCC population and then the NCC that do survive have reduced proliferation within the pharyngeal arches. Together, this underlies the hypoplasia of skeletal elements in the *polr1c* and *polr1d* mutant embryos and is consistent with the findings of the *Tcof1*^{+/-} mice (Dixon et al., 2006; Jones et al., 2008), indicating a common mechanism for TCS.
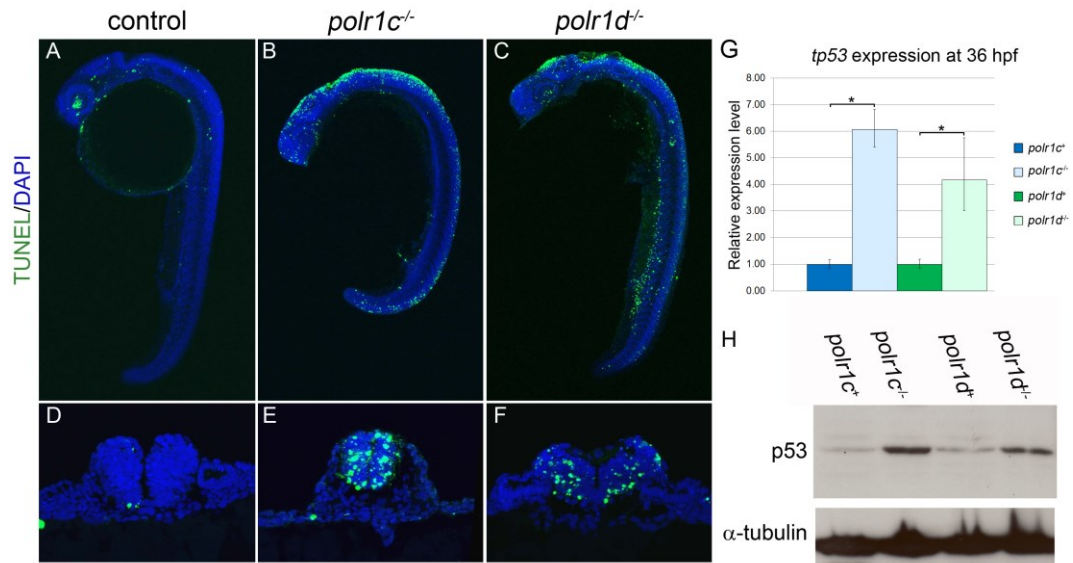
Figure III-12 *polr1c* and *polr1d* mutant embryos display increased neuroepithelial cell death and upregulation of Tp53.

A-C) TUNEL staining at 24 hpf reveals increased neuroepithelial cell death in *polr1c* and *polr1d* mutant embryos. D-E) Cross sections reveal that cell death is largely occuring within the neural tube. G) Western blot reveals increased levels of Tp53 in *polr1c* and *polr1d* mutants. H) qPCR reveals an increase in the level of *tp53* expression in *polr1c* and *polr1d* mutant embryos. * = p < 0.05 and error bars represent 95% confidence intervals. Panels A-F were stained and imaged by Annita Achilleos.
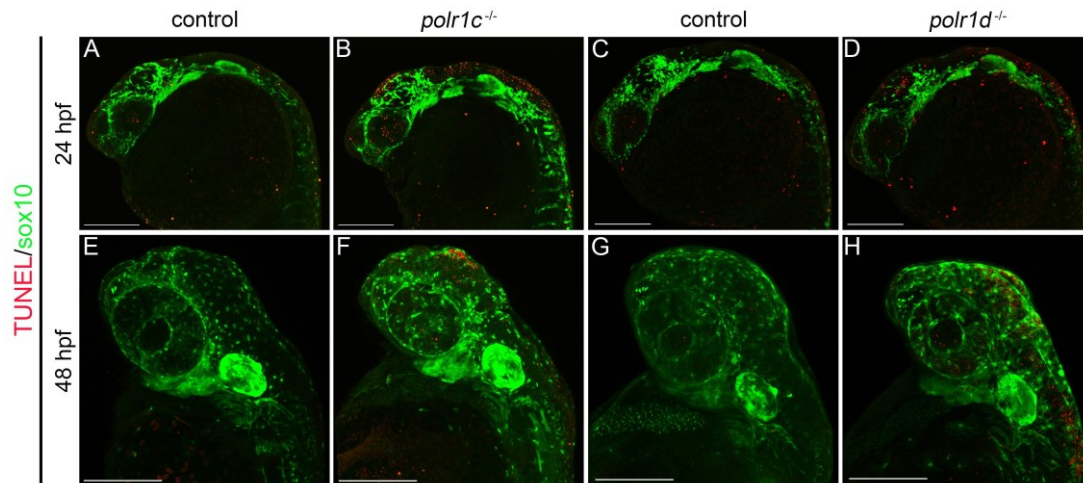
Figure III-13. TUNEL staining in *sox10:gfp* embryos shows increased cell death in mutant embryos which does not co-localize with the migratory NCC population.

A-D) At 24 hpf, increased cell death can be see in the neuroepithelial region of *polr1c*$^{-/-}$ and *polr1d*$^{-/-}$ embryos. E-F) At 48 hpf, increased cell death can be observed in regions of the brain and eye of mutant embryos, but not within the pharyngeal arches. Scale bar = 200 μm.
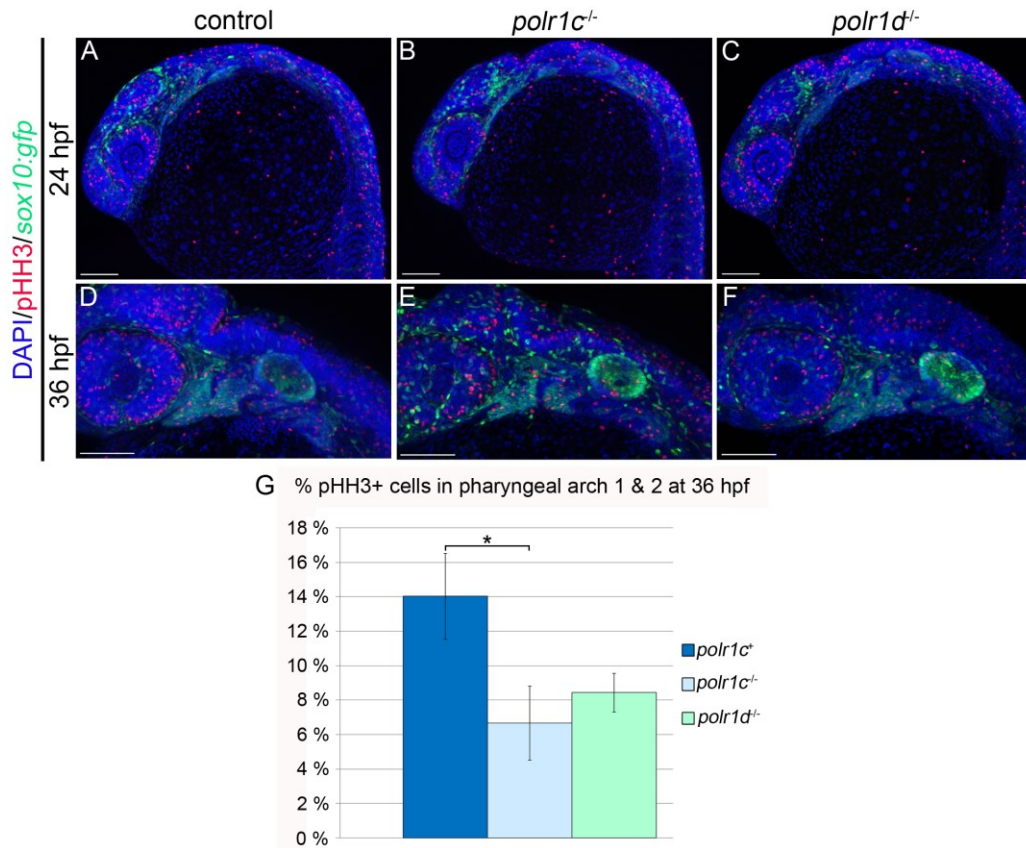
Figure III-14 Analysis of proliferation in *polr1c* and *polr1d* mutant embryos
A-C) Proliferation at 24 hpf in *polr1c* and *polr1d* mutant embryos occurs at similar levels. D-F) Proliferation at 36 hpf in mutant embryos also occurs at broadly similar levels, but there appears to be a difference in the number of pHH3+ cells within pharyngeal arches 1 and 2. G) Quantification revealed a significant decrease in the percentage of pHH3+ cells in pharyngeal arches 1 and 2 in *polr1c* mutant embryos. *polr1d* mutant embryos showed a similar level of proliferation as *polr1c* mutants. Scale bar = 100 μm. * = p < 0.01 and error bars represent 95% confidence intervals.

MUTATIONS IN *POLR1C* AND *POLR1D* ALTER RIBOSOME BIOGENESIS

I next hypothesized that activation of the Tp53 pathway in *polr1c* and *polr1d* mutants may be caused by alterations in ribosome biogenesis, which has been associated with nucleolar stress (Rubbi and Milner, 2003). Polr1c and Polr1d are subunits of RNAPI and RNAPIII which are responsible for the production of rRNA, a rate-limiting step of ribosome biogenesis (Laferté et al., 2006). Mutations in *polr1c* and *polr1d* would likely disrupt the function of RNAPI and RNAPIII and the production of rRNA, so deficient ribosome biogenesis may underlie the Tp53 activation in the *polr1c* and *polr1d* mutant embryos. To determine if the mutations in *polr1c* and *polr1d* altered the function of RNAPI, I investigated the production of the 45S rRNA transcript using qPCR. Regions of this initial transcript, the 5' ETS and ITS2, show a reduction in both *polr1c* and *polr1d* mutant embryos (Figure III-15 A,B). At 36 hpf, the 5'ETS is reduced by 38% in *polr1c* and 32% in *polr1d* mutants while ITS2 is reduced by 23% in *polr1c* mutants and 25% in *polr1d* mutants, relative to the levels expressed by control embryos. Additionally, the levels of the 18S, which recognizes both the region contained within the 45S transcript as well as the fully processed form, also showed diminished levels in mutant embryos. *polr1c* mutant embryos exhibited a 58% reduction in the level of 18S expressed by control embryos while *polr1d* mutant embryos exhibited a 39% reduction compared to controls. Altogether, these results suggest an overall decrease in the level of rRNA produced. As rRNA production is considered a rate-limiting step of ribosome biogenesis and accounts for as much as 60% of transcription in the cell (Warner, 1999), I hypothesized that *polr1c* and *polr1d* mutants would also display deficiencies in ribosome biogenesis. To confirm that the alterations in

rRNA production diminished overall ribosome biogenesis, I examined the polysome profiles of mutant embryos at 3 dpf. The polysome profiles revealed reductions in the size of the 80S and polysome peaks in *polr1c* (Figure III-15 C) and *polr1d* (Figure III-15 D) mutant embryos, but similar 40S and 60S peaks. The sizes of the 40S and 60S peaks indicate that there is not a problem with the incorporation of the mature rRNA into the small and large ribosomal subunits. If 40S or 60S assembly was altered, a difference in the height of the peak would be evident. For example, mutations *nop10,* which functions to modify the 18S rRNA for its assembly into the small subunit, result in a collapse of the 40S peak (Pereboom et al., 2011). The reduced 80S peak height in *polr1c* and *polr1d* mutant embryos indicates a fewer number of mature assembled ribosomes while the shorter, broader polysome peaks would suggest fewer transcripts are being highly translated. Highly transcribed genes have a larger number of ribosomes present on the transcript and thus have higher sedimentations; conversely, if there are few transcripts being highly transcribed, these polysome peaks will be smaller and indicative of less overall transcription. Altogether, the polysome profiling results indicate an overall decrease in ribosome biogenesis in *polr1c* and *polr1d* mutant embryos, consistent with diminished production of the 47S rRNA (Figure III-15 A, B) and reduced proliferation (Figure III-14G). Although the global difference in ribosome biogenesis is not as dramatically altered as rRNA production, this may be due to a stronger difference in specific tissues. It could be that NCC or cranial tissue alone would show a stronger difference in ribosome biogenesis, however this remains to be investigated. Thus, reduced

rRNA transcription and ribosome biogenesis likely results in reduced proliferation and an

increase in p53-dependent apoptosis in *polr1c* and *polr1d* mutant embryos.
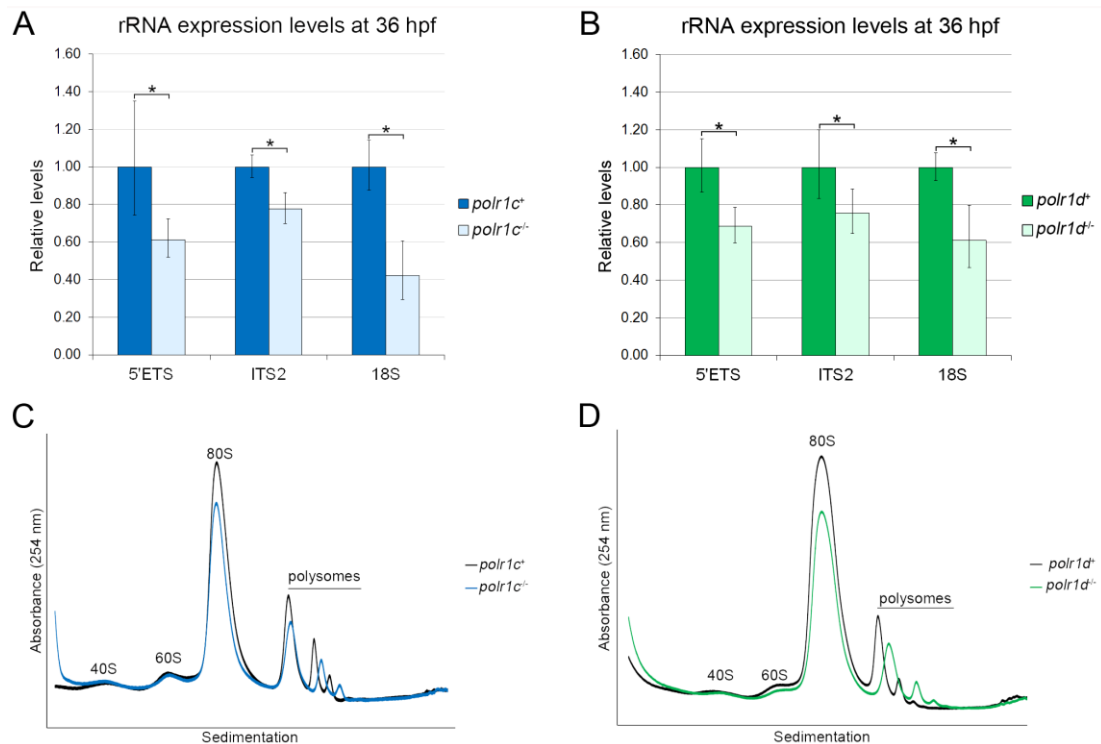
Figure III-15. qPCR and polysome profiling demonstrate diminished ribosome biogenesis in *polr1c* and *polr1d* mutant embryos.

A) qPCR shows reduced transcription of regions of the 45S rRNA transcript. *polr1c* mutants show a 39% reduction in the levels of 5'ETS, 23% reduction in the levels of ITS2 and 58% reduction in the levels of the 18S compared to controls. B) qPCR shows reduced transcription of regions of the 45S rRNA transcript in *polr1d* mutants. Mutants show a 32% reduction in the levels of 5'ETS, 25% reduction in the levels of ITS2 and 39% reduction in the levels of the 18S compared to controls. C,D) Polysome profiling shows a reduction in the 80S peak and polysome peaks in *polr1c* (C) and *polr1d* (D) mutant embryos. Polysome profiling experiments were completed in collaboration with Cynthia Neben and Amy Merrill.

TP53 INHIBITION CAN IMPROVE THE PHENOTYPE OF *POLR1C* AND *POLR1D* MUTANT

EMBRYOS

As the data suggest that Tp53-dependent cell death of NCC progenitors underlies the craniofacial anomalies in *polr1c* and *polr1d* mutants, I hypothesized that genetic inhibition of *tp53* would be able to ameliorate the mutant phenotype. *polr1c* and *polr1d* mutants were crossed to the *tp53*^{M214K} mutant, hereafter referred to as *tp53*⁻, which carries a mutation in the DNA binding domain of Tp53 (Berghmans et al., 2005). TUNEL staining revealed reduced levels of cell death at 24 hpf in both *polr1c*⁻ᐟ⁻; *tp53*⁻ᐟ⁻ and *polr1d*⁻ᐟ⁻;*tp53*⁻ᐟ⁻ embryos (Figure III-16; Figure III-17). Cross sections confirmed a reduction in cell death within the neural tube in embryos with *tp53* inhibition and that the reduction was dosage dependent (Figure III-16, E-H; Figure III-17 E-H). Analysis of the skeletal phenotypes at 5 dpf showed a similar *tp53* dosage-dependent improvement of cartilage formation in *polr1c* and *polr1d* mutant embryos (Figure III-18; data is shown only for *polr1d* for simplicity). Upon removal of one copy of *tp53*, mutant embryos have improved patterning of the jaw (Figure III-18, G) and elements of the viscerocranium including the ceratohyal and ceratobranchial cartilages (Figure III-18, K). Upon removal of both copies of *tp53*, this patterning is improved to a greater degree (Figure III-18, H, L). To examine the differences in cartilage development, *polr1c* and *polr1d* mutant embryos were classified into severe, mild, and wild-type phenotypes (Figure III-19). The severe phenotype mutants have a reversed ceratohyal, mild mutants have a ceratohyal that is either straight or slightly forward, and wild-type phenotype embryos have a ceratohyal in the proper orientation to the same degree as control siblings. Using these classifications, the percentage of embryos

111

displaying a severe phenotype was reduced to 32% of *polr1c^{-/-}; tp53^{+/-}* embryos and 22% of *polr1d^{-/-}; tp53^{+/-}* embryos. Furthermore, 19% of *polr1c* and 24% of *polr1d* mutant embryos showed a wild-type phenotype. Upon inhibition of both copies of *tp53*, the percentage of severe phenotype embryos was reduced to 9.5% of *polr1c^{-/-}; tp53^{-/-}* embryos and 0% in *polr1d^{-/-}; tp53^{-/-}* embryos. The percentages of wild-type phenotype embryos increased to 62% of *polr1c^{-/-}; tp53^{-/-}* embryos and 35% of *polr1d^{-/-}; tp53^{-/-}* embryos, with the remainder of the embryos showing a mild phenotype.

Despite the improvement in formation and patterning, the cartilage elements in *polr1c^{-/-}; tp53^{-/-}* and *polr1d^{-/-}; tp53^{-/-}* embryos remained smaller relative to control siblings. In addition, these embryos still fail to inflate the swim bladder and die around 10 dpf. This would indicate that although the survival of NCC and cartilage patterning is improved in these embryos, this is not sufficient to rescue the viability of mutant embryos and an insufficient NCC population is not necessarily the cause of lethality. One alternative is that the levels of ribosome biogenesis are not improved upon *tp53* inhibition to a level sufficient for survival of the mutant embryos. The deficiency in ribosome biogenesis in other tissues may cause lethality, or other p53-independent pathways may be impacted that are required for survival. As a result, it is important to investigate alternative strategies for rescue which may be able to improve ribosome biogenesis.
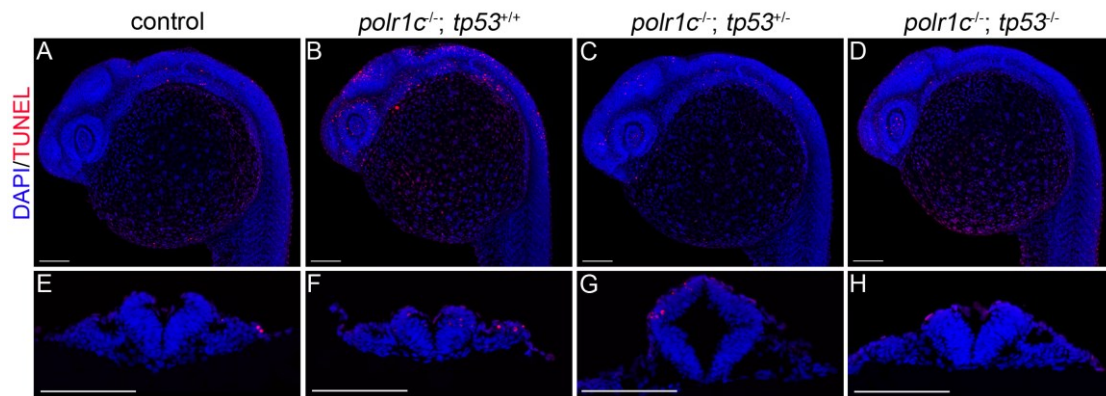
Figure III-16 Analysis of cell death in *polr1c; tp53* embryos.

A-D) TUNEL staining in *polr1c⁻/⁻; tp53* embryos reveals a decrease in cell death depending on the dosage of *tp53*. E-F) Cross sections confirm diminished levels of cell death within and around the neural tube. Scale bars = 100 μm.
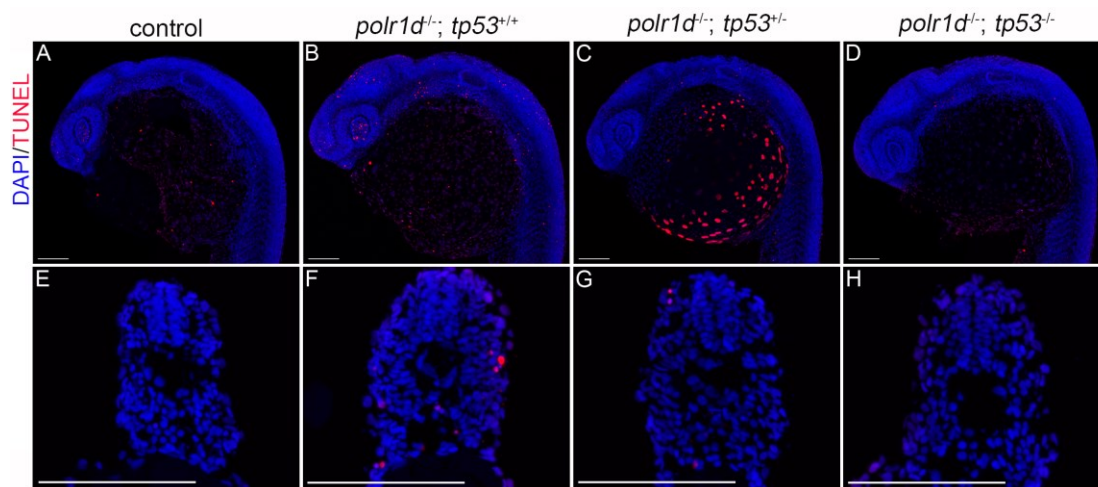
Figure III-17 Analysis of cell death in *polr1d; tp53* embryos.

A-D) TUNEL staining in *polr1d; tp53* embryos reveals a decrease in cell death depending on the dosage of *tp53*. E-F) Cross sections confirm diminished levels of cell death around the neural tube. Scale bars = 100 μm

113
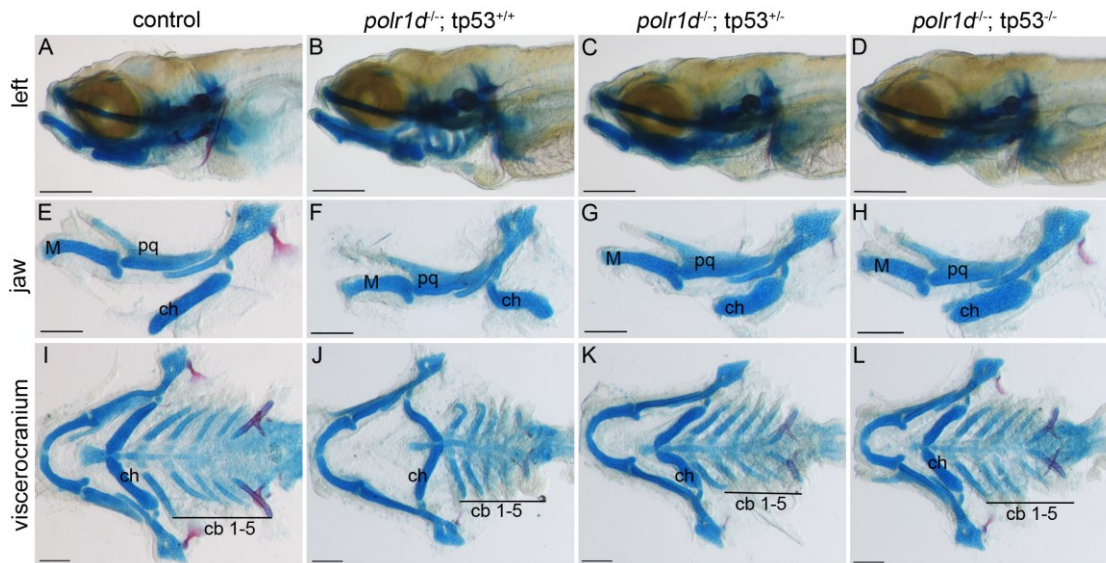
Figure III-18 Skeletal staining shows improved cartilage formation in *polr1d; p53* embryos.

A-D) Alcian blue and Alizarin red staining reveal an improvement in cartilage formation in *polr1d* mutant embryos with increasing inhibition of *tp53*. Improvement is especially noticeable in the jaw (E-H) and the elements of the viscerocranium (I-L). Upon removal of one copy of *tp53*, improved patterning of the ceratohyal is evident (G, K) and a greater improvement is observed upon removal of both copies of *tp53* (H,L). Abbreviations: M - Meckel's cartilage; pq – palatoquadrate; ch – ceratohyal; cb – ceratobranchial. Scale bar = 200 μm.
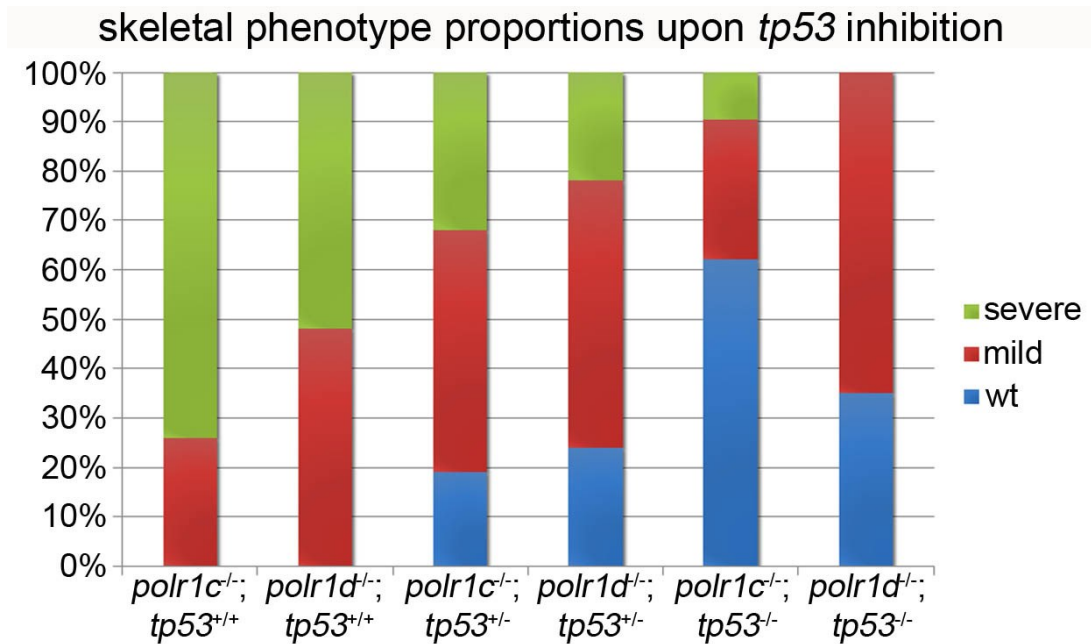
Figure III-19 Quantification of skeletal phenotypes upon *tp53* inhibition.
Percentage of embryos with wild-type (wt, blue), mild (red), and severe (green) phenotypes upon *tp53* inhibition. The percentage of embryos with wild-type appearance upon removal of one copy of *tp53* is around 20% in *polr1c* and *polr1d* embryos. This percentage increases with removal of both copies of *tp53*, with the percentage of severe phenotype accounting for less than 10% of the mutants.

MTOR AS AN ALTERNATIVE PATHWAY FOR RESCUE

If deficient ribosome biogenesis is the cause of the lethality in *polr1c* and *polr1d* mutant embryos, then stimulating ribosome biogenesis may be an alternative to p53 inhibition in the prevention of the mutant phenotype. Improved ribosome biogenesis could also alleviate *tp53* activation and eliminate the need for introducing a tumorigenic mutation for rescue. Hence, I investigated Mammalian target of rapamycin (mTOR) signaling, which has known functions in ribosome biogenesis, as a potential target for rescue. mTOR is a positive regulator of cell growth and proliferation and plays an important role in regulating

many cellular processes which are essential for development including nutrient sensing, cell growth, and apoptosis (Wyllie, 2010). The rapamycin-sensitive complex TORC1, which incorporates mTOR, is of most interest as it is known that growth factors and nutrients signal through this complex, which in turn signals to downstream targets and leads to changes in translation and autophagy. Changes in translation are controlled through regulating phosphorylation of proteins involved in stimulating or inhibiting initiation. mTOR will phosphorylate 4E-BP1, which disrupts the interaction between 4E-BP1 and eIF4E, allowing eIF4E to interact with other components of the translation initiation complex (Powers and Walter, 1999). Activation of mTOR also leads to phosphorylation of multiple proteins by p70S6K, including ones that regulate rRNA transcription by RNAPI (Hannan et al., 2003; Mayer et al., 2004). mTOR regulates RNAPIII, as transcription by RNAPIII is sensitive to rapamycin (Zaragoza et al., 1998; Tsang et al., 2010), and has been shown to stimulate rDNA transcription in different ways. One study in 3T3 cells showed that rDNA transcription required p70S6K activation and that it was regulated through phosphorylation of UBF. The phosphorylation of UBF in its carboxy-terminal domain promotes interaction with SL1(TIF-IB) and stimulation of RNAPI transcription (Hannan et al., 2003). A separate study showed that TIF-IA phosphorylation on specific residues was required for stimulating rDNA transcription (Mayer et al., 2004). Thus, all components of the ribosome biogenesis pathway – rRNA transcription by RNAPI and RNAPIII and ribosomal protein translation by RNA polymerase II – can be affected through mTOR signaling.

In order to determine if there was an alteration in the mTOR pathway, I examined the protein levels of downstream targets of the mTOR pathway, including RPS6. Western blot analysis revealed a decrease in the levels of RPS6 in both *polr1c* and *polr1d* mutant embryos (p = 0.005 and 0.03, respectively; Figure III-20). The levels of phosphorylated RPS6 (pRPS6), the activated form of the protein, were also examined. In *polr1c* and *polr1d* mutant embryos, the levels of pRPS6 were about 20% lower. This difference was not significant in the *polr1d* embryos, but did show a slight difference in *polr1c* embryos (p = 0.035). Finally, as a readout of the overall activity of the protein, I examined the ratio of pRPS6 to RPS6 and found that there was no significant difference between mutant embryos and control siblings. This would indicate that although the total levels of RPS6 tend to be lower in *polr1c* and *polr1d* mutant embryos, the activity of the protein is comparable to their wild-type siblings. Western blot analysis of other mTOR pathway components including p70S6K and 4E-BP1 also showed slight reductions (data not shown), so I anticipated that leucine treatment would be one approach to stimulate ribosome biogenesis through the mTOR pathway.

It is well known that the mTOR pathway is responsive to changes in nutrients, such as leucine. TIF-IA can sense nutrient availability in an mTOR-dependent manner (Mayer et al., 2004), indicating that rDNA transcription may be dependent upon available nutrients. The amino acid L-leucine stimulates protein synthesis through mTOR. Leucyl-tRNA synthetase (LeuRS), which charges the tRNA with leucine, functions to signal leucine availability to mTOR through Rag/Gtr GTPases in mammalian and yeast cells (Bonfils et al., 2012; Han et al., 2012). The Rag GTPases, when in a GTP-bound heterodimeric state,

are known to bind TORC1 and stimulate mTOR signaling (Sancak et al., 2008). mTOR resides in the cytoplasm in a starved state, but upon amino acid stimulation, the Rag-bound Raptor induces recruitment of mTOR to the lysosome membrane, which contains the mTOR activator Rheb (Sancak et al., 2008). Further upstream of this pathway, LeuRS interacts directly with GTP-bound RagD in an amino acid-dependent manner and translocates to the lysosome where mTOR becomes activated (Han et al., 2012).

Leucine has been used as a mechanism to increase activation of mTOR, and subsequently translation, in the ribosomopathy Diamond Blackfan Anemia (DBA). DBA is a ribosomopathy in which 40% of patients have a variety of malformations including craniofacial defects that arise due to mutations in ribosomal protein genes (Cmejlova et al., 2006). Some DBA patients have been successfully treated through L-leucine supplementation (Cmejlova et al., 2006; Pospisilova et al., 2007). More recently, L-leucine treatment rescued the mutant phenotype in mouse and zebrafish DBA models (Jaako et al., 2012; Payne et al., 2012). Treatment of zebrafish embryos injected with *rps14* or *rps19* morpholinos with 100mM L-leucine results in the rescue of craniofacial defects (Payne et al., 2012). Given the rescue of craniofacial defects in these models, I hypothesized that L-leucine treatment could ameliorate the TCS phenotype of the *polr1c* and *polr1d* mutant zebrafish.

To determine the minimum dosage of leucine necessary for rescue, I examined the consequences of L-leucine treatment at concentrations from 1 mM to 100 mM. Concentrations of 100 mM were used previously to rescue the phenotype of DBA in zebrafish, however, I found this concentration to be too high for the viability of wild-type

118

embryos beyond 3 dpf. Treatment with 100 mM L-leucine resulted in early embryonic lethality of nearly all embryos. In subsequent studies, a maximum concentration of 50 mM L-leucine was used. Alcian blue and Alizarin red staining was used to examine any improvement in the craniofacial phenotype in *polr1c* and *polr1d* mutant embryos after L-leucine treatment. These results showed no improvement of the mutant phenotype with 1 mM, 5 mM, or 10 mM of L-leucine added to the embryo media (Figure III-21, D-K; Figure III-22, D-L). Upon treatment with the higher dosage of 50 mM of L-leucine, mutant embryos showed either no improvement of the phenotype (Figure III-21 N; Figure III-22 O) or an even more severe phenotype (Figure III-22 Q). In addition, heterozygous fish which are phenotypically wild-type could also be severely affected by the higher dosage of L-leucine (Figure III-22 P). These results indicate that leucine supplementation is not a viable treatment for the successful prevention of the craniofacial anomalies that result from mutations in *polr1c* and *polr1d*. The higher dosages of leucine used in previous studies to rescue embryonic defects increased embryonic lethality in the *polr1c* and *polr1d* zebrafish. Lower dosages of L-leucine which did not increase lethality were not able to improve the mutant phenotype. This could be due to the way ribosome biogenesis is affected in the *polr1c* and *polr1d* mutants. Since these mutations are in subunits of RNAPI and RNAPIII, they affect the production of rRNA. The mechanism by which L-leucine stimulates mTOR would increase production of rRNA and ribosomal proteins. With decreased function of RNAPI in *polr1c* and *polr1d* mutants, stimulation by mTOR may not be able to sufficiently increase rRNA production, but ribosomal protein synthesis would be increased. As a result, the balance between ribosomal protein and rRNA production undergoes further

119

perturbation. The balance between rRNA and ribosome biogenesis is carefully regulated by the cell and disruptions lead to p53 stabilization (Donati et al., 2011a). Therefore, further altering this balance likely amplified the p53 response and resulted in increased lethality. Consequently, I concluded that other alternate pathways to improve the mutant phenotype need to be investigated.
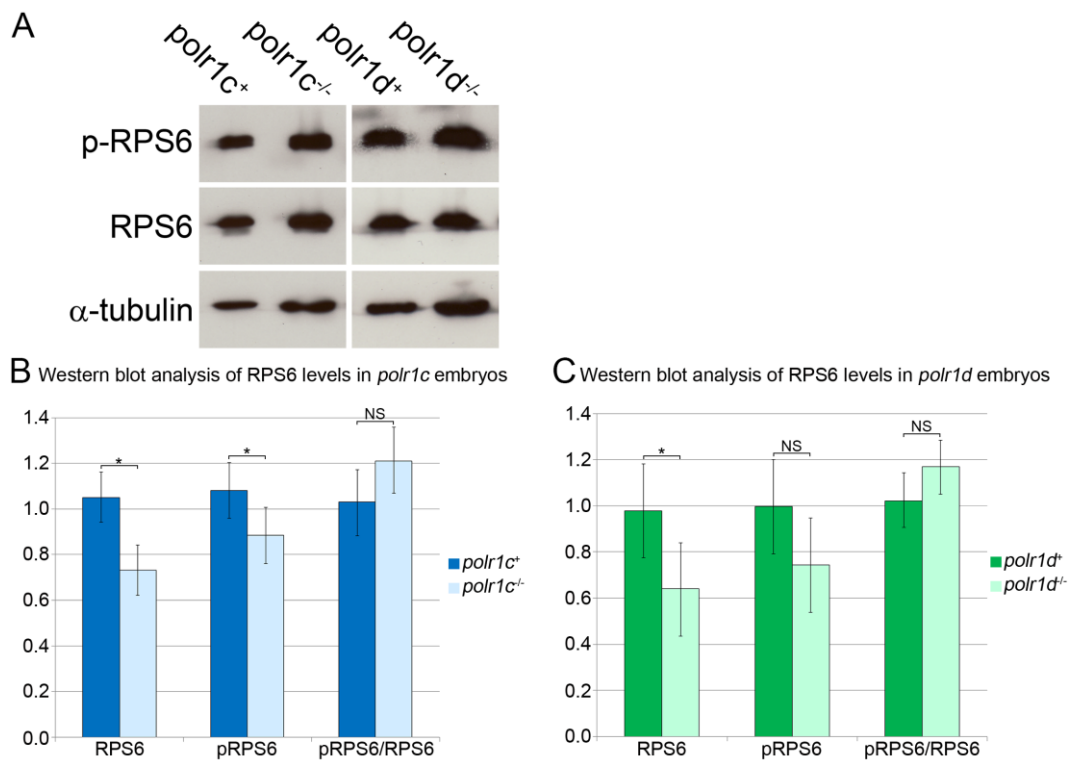
Figure III-20. Western blots for RPS6 and pRPS6 (A). RPS6 levels are quantified for *polr1c* embryos (B) and *polr1d* embryos (C). *p < 0.05 and error bars represent 95% confidence intervals.
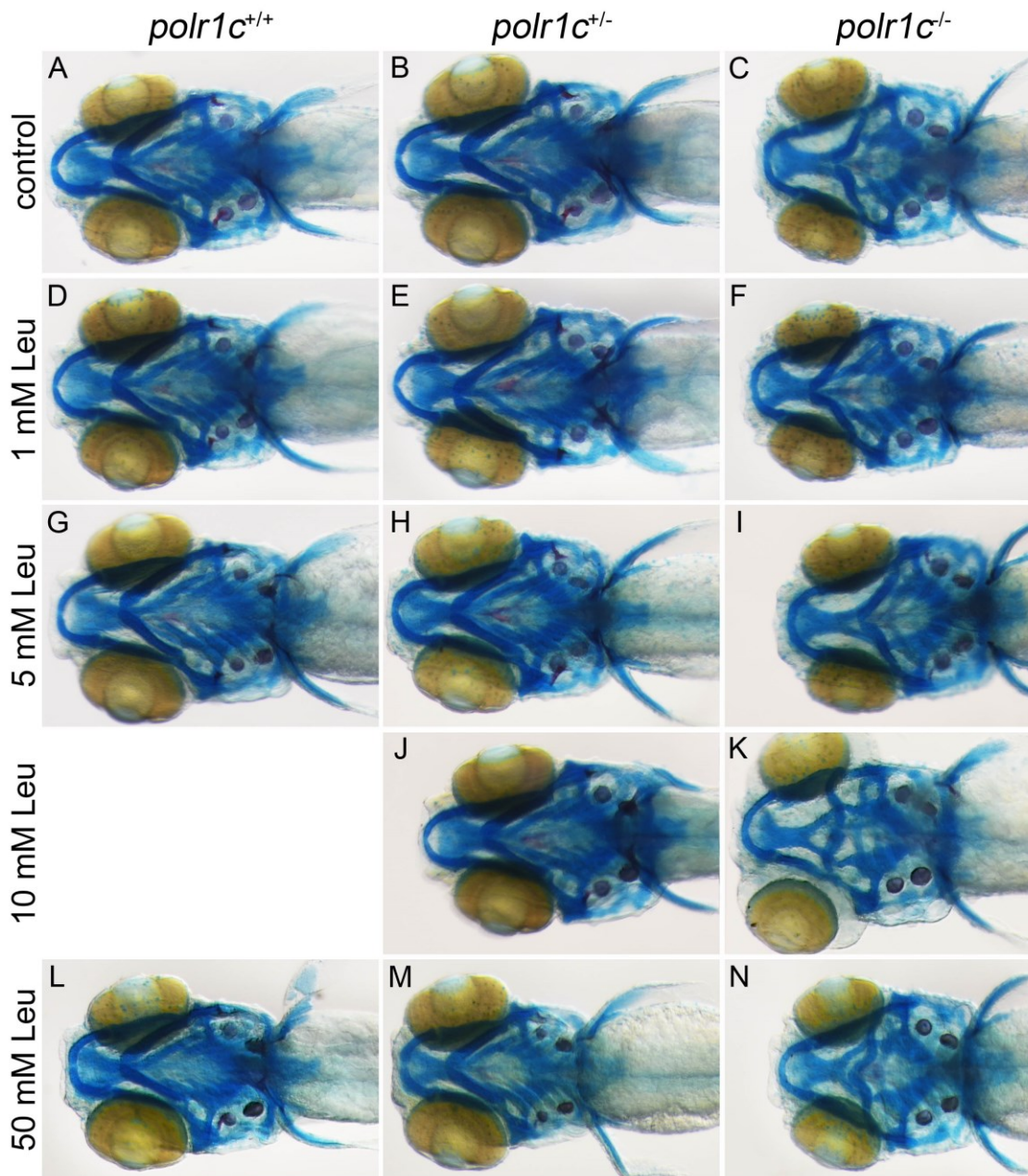
Figure III-21 Alcian blue and Alizarin red staining of 5 dpf *polr1c* embryos after L-leucine treatment reveals no improvement of the mutant phenotype.
A-C) Control embryos raised in E2 media alone show the expected phenotypes. D-F) Embryos raised in E2 media with 1 mM Leu show no improvement. G-I) Embryos raised in E2 media with 5 mM Leu show no improvement. J-K) Embryos raised in E2 media with 10 mM Leu show no improvement. L-N) Embryos raised in E2 media with 50 mM Leu show no improvement.
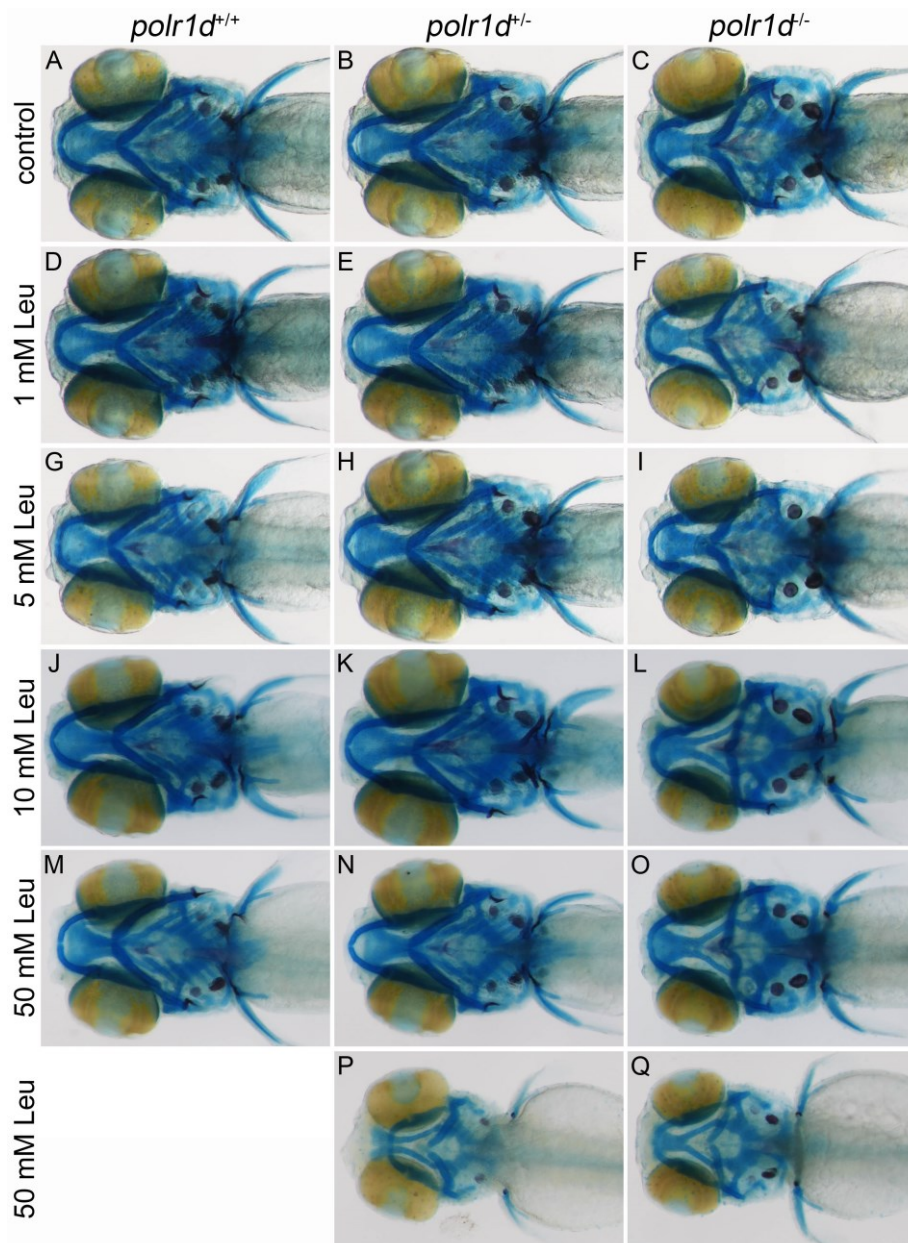
Figure III-22 Alcian blue and Alizarin red staining of 5 dpf *polr1d* embryos after L-leucine treatment reveals no improvement of the mutant phenotype.

A-C) Control embryos raised in E2 media alone show the expected phenotypes. D-F) Embryos raised in E2 media with 1 mM Leu show no improvement. G-I) Embryos raised in E2 media with 5 mM Leu show no improvement. J-L) Embryos raised in E2 media with 10 mM Leu show no improvement. M-O) Embryos raised in E2 media with 50 mM Leu show no improvement, with some embryos showing a worsening phenotype (P, Q).

RNA-Seq Analysis to determine alternative pathways for rescue

In order to further our understanding of the mechanisms underlying the *polr1c* and *polr1d* mutant phenotypes in an unbiased manner, RNA-Seq analysis was performed at 24 hpf. I hypothesized that the pathways altered at the onset of the mutant phenotype could reveal other potential pathways for manipulation that are not tumorigenic like the Tp53 pathway, and more successful than leucine stimulation of the mTOR pathway. Many of the genes showing the greatest changes between wild-type and mutant embryos were those involved in p53 signaling, cell cycle arrest, and apoptosis (Table III-1). *cdkn2b* (ink4b), *cdkn1a* (p21), *ccng1*, *cdkn1ba* (p27), and *rbl2* (p130) are all regulators of the cell cycle. Notably, upregulation of *Ccng1* (cyclin G1), which functions to arrest cells in G1 as a part of the p53 response (Zhao et al., 2003b), was also identified by microarray in the *Tcof1*$^{+/-}$ mice (Jones et al., 2008). Cyclin dependent kinase inhibitors (cdkn) also inhibit progression through the cell cycle, with *cdkn1a* being a main target of p53. Retinoblastoma-like 2 (*rbl2*, also known as p130) is involved in negative regulation of the cell cycle and results in a stall in G1 phase (Helmbold et al., 2009). Genes involved in the apoptotic response include pleckstrin homology-like domain family member A3 (*phlda3*), caspase 8 (*casp8*), bcl2 binding component 3 (*bbc3*, also known as *puma*), and bcl2-associated X protein (*bax*). *phlda3* is a p53 target gene and functions to induce apoptosis through inhibiting Akt, which functions in cell proliferation and survival (Kawase et al., 2009). Interestingly, *casp8* is involved in the extrinsic apoptosis pathway, while *bbc3* and *bax* function to permeabilize the mitochondrial membrane for cytochrome c release in the intrinsic apoptosis pathway. Although increased transcription of *mdm2* was also found, it is unlikely that an increase in

123

mdm2 would be able to overcome the increases in cell cycle arrest and apoptosis genes. Therefore, the primary response in *polr1c* and *polr1d* mutant embryos is one of cell cycle arrest and apoptosis. This is consistent with upregulated genes found in *rps29* mutant zebrafish, a model of DBA, which include *cdkn1b, cdkn2b, phlda3, bbc3*, and *casp8* (Taylor et al., 2012). The commonality of these upregulated genes in the *polr1c, polr1d,* and *rps29* mutants are indicative of a mechanism of an increased p53 response upon disruption of ribosome biogenesis. Other genes which showed a high degree of differential expression in *polr1c* and *polr1d* mutant embryos currently do not have known functions and will be interesting targets to investigate in the future (see Appendix for a listing of genes up and down-regulated). In order to understand how the differentially expressed genes might be involved in the mutant phenotype, KEGG pathway analysis was performed. This analysis revealed both activated and inhibited pathways in *polr1c* and *polr1d* mutants (Table III-2 and Table III-3). Interestingly, the mTOR pathway was up-regulated in *polr1c* mutant embryos, although not significantly. This supports the previous RPS6 data which showed a slight, but not significant, increase in the activity of RPS6. The other up-regulated pathway, MAPK signaling, is typically involved in the process of proliferation and differentiation, but can also be involved in signaling apoptosis. The down-regulated pathways in *polr1c* mutants are consistent with alterations in expression of collagens and laminins, which are involved in extracellular matrix interactions and focal adhesions. The genes down-regulated in the Jak-Stat pathway, including *osmr* and *il11ra*, are consistent with diminished cytokine activity and potentially reduced proliferation. Cell cycle was significantly decreased in *polr1d* mutants, which is congruent with an increase in p53

124

signaling. However, none of the down-regulated pathways showed significant overlap between *polr1c* and *polr1d*. The p53 pathway was the only common pathway significantly upregulated in both *polr1c* and *polr1d* mutant embryos, which confirmed my previous results in which inhibition of p53 was able to improve the mutant phenotype. However, as p53 inhibition was unable to improve the viability of the mutant embryos, it is possible that other mechanisms are involved at later stages of development which are necessary for survival. Alternatively, there may be p53 independent mechanisms which are critical for embryo survival that act at times either prior to 24 hpf or at later stages. RNA-Seq analysis at both earlier and later stages may be able to reveal some of these other potential pathways.

gene	*polr1c* Fold Change	*polr1d* Fold Change
cdkn2b	47.96	15.04
rbl2	11.71	12.01
casp8	10.68	7.75
bbc3	9.57	8.08
mdm2	7.89	8.25
phlda3	7.65	5.89
cdkn1a	6.02	4.20
tp53	5.89	4.79
ccng1	4.88	4.83
cdkn1ba	2.75	2.07
baxa	2.11	2.65

Table III-1. Genes upregulated by RNA-Seq analysis involved in *tp53* signaling. All differences are significant at $p < 0.01$.

Name	# of differentially expressed genes	total perturbation accumulation	p Value	Status
p53 signaling pathway	13	1.185659	0.003499	Activated
MAPK signaling pathway	30	6.071711	0.030131	Activated
mTOR signaling pathway	8	1.24254	0.052998	Activated
ECM-receptor interaction	13	-5.53103	0.000773	Inhibited
Focal adhesion	26	-19.1086	0.005824	Inhibited
Jak-STAT signaling pathway	13	-1.01411	0.033624	Inhibited

Table III-2: KEGG pathway analysis of *polr1c* RNA-Seq data reveals up- and down-regulated pathways.
Analysis was completed in collaboration with Chris Seidel.

Name	# of differentially expressed genes	total perturbation accumulation	p Value	Status
p53 signaling pathway	10	0.695385	0.000169	Activated
MAPK signaling pathway	11	1.633288	0.378988	Activated
Cell cycle	8	-10.7538	0.009492	Inhibited
Jak-STAT signaling pathway	2	0	0.955322	Inhibited

Table III-3 KEGG pathway analysis of *polr1d* RNA-Seq data reveals up and down-regulated pathways.
Analysis was completed in collaboration with Chris Seidel.

Conclusions

In summary, I found *polr1c* and *polr1d* to be important for normal craniofacial development in zebrafish and establish the *polr1c* and *polr1d* mutants as new genetic models for TCS. Given the similarity of the cartilage anomalies with both the human TCS phenotype and the *Tcof1* mouse model, these zebrafish will be useful models to investigate the pathogenesis of TCS.

In these studies, I found *polr1c* and *polr1d* to be dynamically expressed during embryonic development, suggesting that there may be different tissue-specific requirements for these genes and the process of ribosome biogenesis at different stages of development. Ubiquitous expression was observed at early stages, including the stages of NCC formation and early NCC migration. Expression is enriched in cranial regions at stages after 24 hpf, and these regions are disrupted in *polr1c* and *polr1d* mutant embryos, while regions such as the tail develop normally. This observation supports the idea that some tissues require a greater amount of *polr1c* and *polr1d*, and perhaps ribosome biogenesis, for normal development. The mutant embryos show disrupted craniofacial development, particularly of the NCC-derived craniofacial cartilage. This disruption, however, is not due to any alteration in the genetic programming of NCC specification and migration as the proper genes are expressed at the correct time in development at similar levels between wild-type and mutant embryos. Despite the proper programming of NCC in *polr1c* and *polr1d* mutant embryos, there was a significant decrease in the size of the

pharyngeal arches at 36 hpf, which are populated by NCC. This reduction was likely due to an increase in neuroepithelial cell death at 24 hpf, which diminished the NCC progenitor pool and therefore the number of migrating NCC, similar to the *Tcof1*$^{+/-}$ mice (Dixon et al., 2006).

An increase in p53-dependent cell death is a common mechanism among several ribosomopathies including TCS (Jones et al., 2008) and DBA (Chakraborty et al., 2009; Barlow et al., 2010), which is thought to arise from the stress of alterations in ribosome biogenesis. I hypothesized a similar mechanism was involved in the *polr1c* and *polr1d* mutants. Consistent with this, I found diminished production of rRNA and an overall decrease in ribosome biogenesis. Previous studies have shown that an alteration in the balance between ribosomal protein production and rRNA production can result in activation of p53. In one study, it was shown that upon inhibition of Polr1a, the catalytic subunit of RNAPI, ribosomal proteins RPL5 and RPL11 bound MDM2 and led to p53 activation; if both rRNA and RPL5 and RPL11 synthesis was reduced, then p53 activation was not observed (Donati et al., 2011a). This result is consistent with previous studies showing a role for RPL5 and RPL11 in regulating MDM2, which normally functions to polyubiquinate p53, targeting it for degradation (Marechal et al., 1994; Honda et al., 1997; Lohrum et al., 2003; Zhang et al., 2003). In our hypothetical model (Figure III-23), mutations in *polr1c* or *polr1d* disrupt the production of rRNA, which disrupts the balance between rRNA and ribosomal protein synthesis and leads to nucleolar stress. As a result, ribosomal proteins such as RPL5 and RPL11 will bind MDM2, causing it to undergo a conformational change in which it will no longer polyubiquinate p53. As a result, p53

128

becomes active and then leads to cell cycle arrest and apoptosis. Recent studies have revealed an important role for the 5S rRNA in mediating binding of RPL5 and RPL11 to MDM2 (Donati et al., 2013; Sloan et al., 2013). Given this new mechanism for binding, in the future it will be important to evaluate the production of the 5S rRNA by RNAPIII in *polr1c* and *polr1d* mutants to determine if it is involved in mediating the p53 response. Regardless of the precise mechanism, p53 activation is clearly involved in the resulting phenotype of *polr1c* and *polr1d* mutant embryos. This function for p53 is supported by both the RNA-Seq data and the improved phenotype of mutant embryos upon genetic inhibition of *tp53*. The result is also consistent with the *Tcof1*$^{+/-}$ mouse model in which *p53* inhibition rescued the craniofacial defects of the mice (Jones et al., 2008), and indicates a common mechanism for the TCS phenotype across the different genes and species.
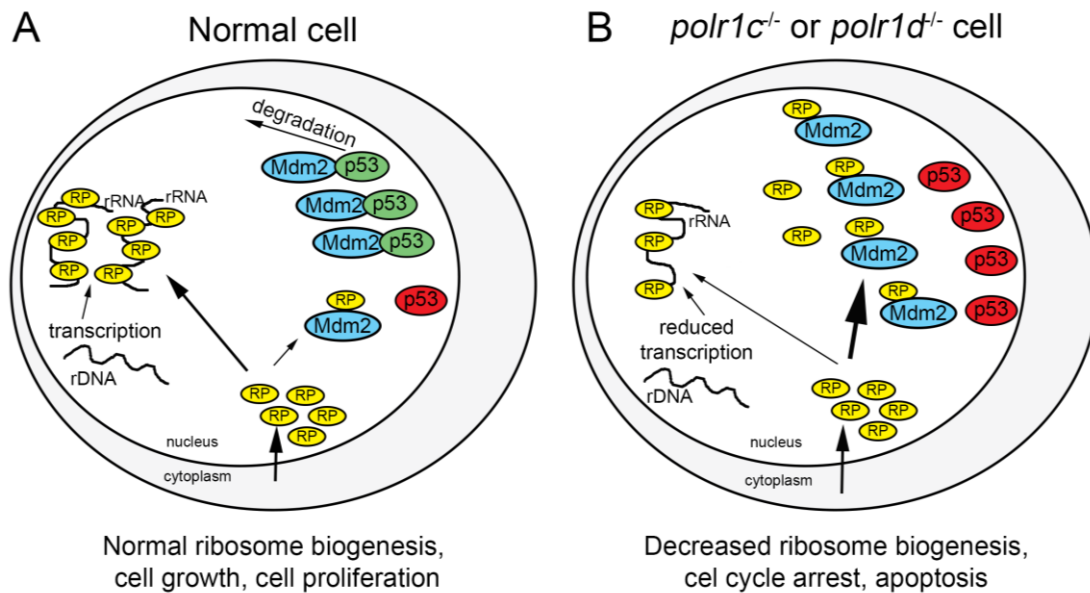
Figure III-23 The cellular mechanism of disrupted ribosome biogenesis and activation of p53 in *polr1c* and *polr1d* mutant embryos.
Ribosomal proteins (RP) from the cytoplasm associate with rRNA to make ribosomes under normal conditions (A). Upon reduction of rRNA synthesis due to mutations in *polr1c* or *polr1d*, fewer RPs associate with rRNA, and more are available to bind Mdm2 (B). This prevents degradation of p53, leading to increased p53 levels and cell cycle arrest and apoptosis in *polr1c* or *polr1d* mutants.

One question that remains is to the specificity of the disruption of ribosome biogenesis and subsequent activation of p53 and apoptosis within the cranial NCC. Craniofacial cartilage is particularly affected in humans with TCS, as well as the zebrafish and mouse models of TCS. However, the *polr1c* and *polr1d* mutant zebrafish do have phenotypes outside of the craniofacial skeleton including cardiac and liver defects. A recent study indicates that mutations in *POLR1D* may result in phenotypes outside of the craniofacial skeleton in humans as well (Giampietro et al., 2015). In these affected

130

individuals, there were phenotypes characteristic of Klipel-Feil syndrome, including a short neck and fusion of cervical vertebrae, in addition to craniofacial anomalies. One of the affected individuals also presented with Sprengel deformity and rib segmentation anomalies. These anomalies would suggest some role for *POLR1D* in the development of mesodermal structures in addition to cranial NCC-derived structures.

It will be important to investigate the function of *polr1c* and *polr1d* in all of the different tissue types in order to understand the role these genes may have in other regions of the body. It is currently unknown if Polr1c and Polr1d have functions outside of RNAPI and RNAPIII, and proteomics studies will be useful in identifying new potential binding partners. With the increase in whole genome sequencing to find new mutations in human patients, this could further our understanding of the full spectrum of phenotypes arising from mutations in the same gene and potentially identify new functions for POLR1C and POLR1D.

IV.   A ZEBRAFISH MODEL OF ACROFACIAL DYSOSTOSIS, CINCINNATI TYPE

Introduction

The cause of many craniofacial anomalies is unknown and approaches such as whole exome sequencing and whole genome sequencing are being used to identify new mutations. Whole exome sequencing involves sequencing the known protein coding genes in the human genome, thus only sequencing exons of genes and not the introns. Alternatively, whole genome sequencing covers both introns and exons and can identify mutations that would not be found by whole exome sequencing. Whole genome sequencing was used to identify mutations in *POLR1D* in Treacher Collins syndrome (TCS) patients who did not have mutations in *TCOF1* and subsequently mutations in *POLR1C* were also identified (Dauwerse et al., 2011). However, there are some patients diagnosed with TCS who do not have mutations in *TCOF1*, *POLR1C*, or *POLR1D* (Cesaretti et al., 2011). A recent study used whole exome sequencing to identify the mutations present in an individual with features of TCS but lacking a mutation in any of the known genes (Weaver et al., 2015). This led to the identification of mutations in *POLR1A* in association with a new syndrome, Acrofacial dysostosis, Cincinnati Type. So far, three individuals have been identified with mutations in *POLR1A* and their phenotypes and mutations are described below.

Individual 1 was identified with multiple craniofacial anomalies prior to birth, and both parents were healthy and unaffected. At birth, Individual 1 displayed severe

micrognathia, downward slanting palpebral fissures, lower eyelid clefts, and midfacial hypoplasia, which are features characteristic of TCS (Figure IV-1 A). In addition, Individual 1 had bilateral anotia and conductive hearing loss. At 18 months of age, these features were still present after multiple reconstructive surgeries (Figure IV-1B,C). A computed-tomography (CT) scan revealed severe hypoplasia of multiple skeletal elements, including the zygomatic arches and maxillary bones, and agenesis of the mandibular rami (Figure IV-1 D). In addition, X-rays revealed short, bowed femurs (Figure IV-1 F) which are not part of the TCS phenotype. Based on the features of mandibulofacial dysostosis characteristic of TCS, *TCOF1* sequencing was performed but did not detect any pathogenic variants. Whole-exome sequencing was subsequently revealed a G to C point mutation in *POLR1A*. This results in an amino acid change from Glu to Gln at position 593, which is within the active site of POLR1A.

After identification of *POLR1A* as a candidate gene, 48 other individuals with a diagnosis of mandibulofacial dysostosis but no known mutation underwent Sanger sequencing for *POLR1A*. Two additional individuals were identified with mutations in *POLR1A*. Individual 2 was identified to carry a frameshift mutation in *POLR1A*, inherited from her mildly affected father, which is predicted to be pathogenic. The mutation occurs at amino acid position 1217 (of 1666), within one of the cleft domains of POLR1A. Individual 2 displayed craniofacial anomalies including downward slanting palpebral fissures, upper and lower eyelid clefts, hypoplastic zygomatic arches and maxilla, and choanal atresia (Figure IV-2 A-C). CT scans confirmed a moderate hypoplasia of the

midface, including the zygomatic arches (Figure IV-2 B), as well as choanal atresia (Figure IV-2 C). Microcephaly was also present in Individual 2.

Individual 3 was identified with a missense variant in *POLR1A*, in which a G to T transition results in an amino acid change from valine to phenylalanine at position 1299. The variant is predicted to be pathogenic. While mildly affected, Individual 3 displays some craniofacial anomalies including downward slanting palpebral fissures, micrognathia, low-set ears, and a dysplastic helix of the left ear (Figure IV-2 D, E). Examination of the limbs of Individual 3 revealed short, broad fingers and toes (Figure IV-2 F).
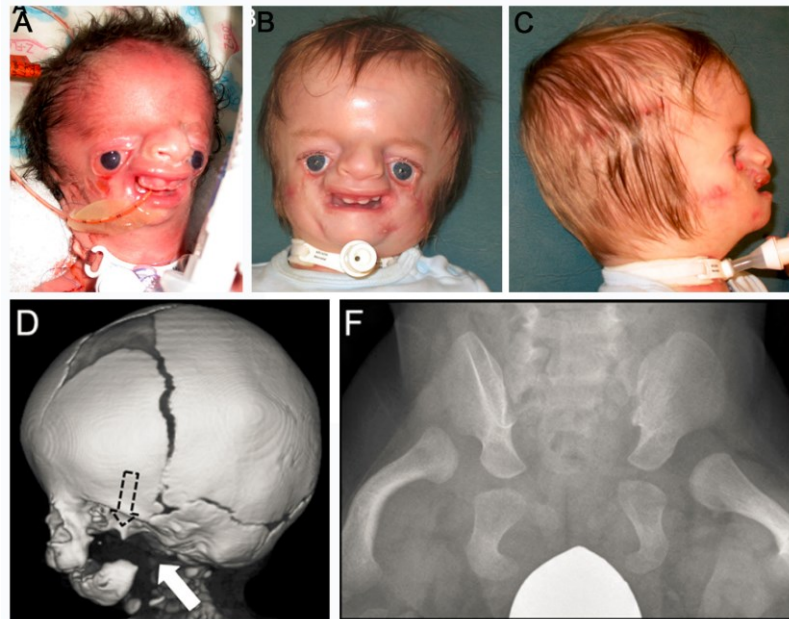
Figure IV-1 Affected individual 1 displays multiple craniofacial anomalies.
A) Individual 1 at birth showing severe craniofacial anomalies. B,C) Individual 1 at 18 months after reconstructive surgeries. D) 3D CT image showing severe hypoplasia of the zygomatic and maxillae (dashed arrow) as well as retrognathia (white arrow). F) X-ray showing hip dysplasia and bowed femurs. Figure adapted from Weaver, Watt, *et al.,* 2015.
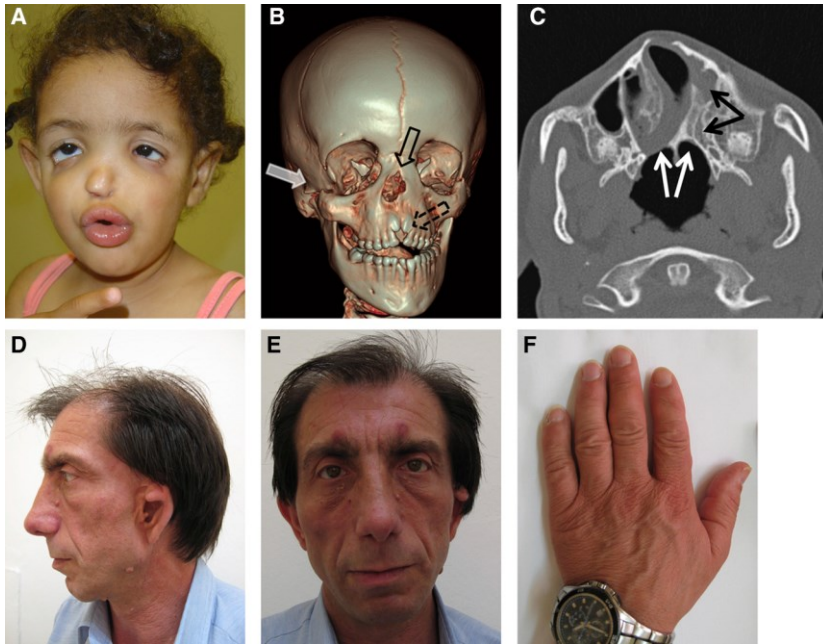
Figure IV-2 Phenotypes of Individuals 2 and 3.
A) Individual 2 displays several craniofacial anomalies including downward slanting palpebral fissures and clefts in the upper and lower eyelids. B) CT scan of Individual 2 shows hypoplasia of the zygomatic arch (white arrow), absent nasal bones (open arrow) and hypoplasia of the midline alveolar process (dashed arrow). C) CT image confirms bilateral choanal atresia (white arrows) as well as hypoplasia of the left ethmoid and maxillary sinus (black arrows). D,E) Individual 3 shows a mild craniofacial phneotype including micrognathia, anomalies of the ear, and malar hypoplasia. F) Individual 3 also displays short, broad fingers. Figure is from Weaver, Watt, *et al.,* 2015.

Facial dysostosis syndromes, which account for a proportion of congenital skeletal disorders, can be broadly characterized into mandibulofacial dysostoses and acrofacial dysostoses (Trainor and Andrews, 2013). TCS is a well characterized example of mandibulofacial dysostosis in which derivatives of the first and second pharyngeal arches fail to develop properly. Acrofacial dysostoses can be characterized by similar disruptions of craniofacial development with the addition of defects in limb development. As two of

the three individuals with mutations in *POLR1A* have both craniofacial and limb anomalies, the syndrome was therefore characterized as acrofacial dysostosis, distinct from TCS. The syndrome was named Acrofacial dysostosis, Cincinnati Type to reflect the location of where the first individual was diagnosed and sequenced. Interestingly, all three individuals identified carry mutations in *POLR1A*, which is the largest subunit of RNAPI. Also known as A190, this subunit contains the active site of the enzyme complex (Engel et al., 2013). RNAPI plays a key role in regulating ribosome biogenesis through the synthesis of rRNA (Laferté et al., 2006). Given the similarities in the craniofacial phenotypes to TCS, it is likely that *POLR1A* has an important role in craniofacial development. In order to understand the function of *POLR1A* in the etiology and pathogenesis of acrofacial dysostosis, we investigated the role of *polr1a* during zebrafish embryogenesis and craniofacial development.

Results

EXPRESSION OF *POLR1A*

To understand the spatiotemporal requirements for *polr1a* during zebrafish embryonic development, we examined the mRNA expression of *polr1a* by in situ hybridization. This revealed a surprisingly dynamic pattern of *polr1a* activity (Figure IV-3). *polr1a* is expressed as early as the 2-cell stage which is indicative of maternal contribution and *polr1a* continues to be ubiquitously expressed at 12 hours post fertilization (hpf) (Figure IV-3 A-F). As early as 18 hpf the expression of *polr1a* becomes more specific with elevated levels in the developing eye and brain (Figure IV-3 G), and by

24 hpf *polr1a* expression is strongly enriched in regions of the brain, eyes, and otic vesicle as well as in the somites (Figure IV-3 I). Beyond 36 hpf, *polr1a* is maintained broadly at low levels throughout the embryos but with elevated levels remaining at the midbrain-hindbrain boundary and the lens of the eye (Figure IV-3 K). At 48 hpf expression begins in the liver (Figure IV-3M). By 72 hpf, expression in the cranial regions is reduced, however, expression persists within the liver (Figure IV-3 O). These dynamic patterns of expression reveal that *polr1a* is initially highly expressed in the cranial regions during the stages of NCC formation and migration. At later stages, other tissues exhibit elevated levels of *polr1a* expression. It is therefore possible that *polr1a* is required at different levels in different tissues during development, which would help to explain why only some tissues are affected in humans with *POLR1A* mutations.
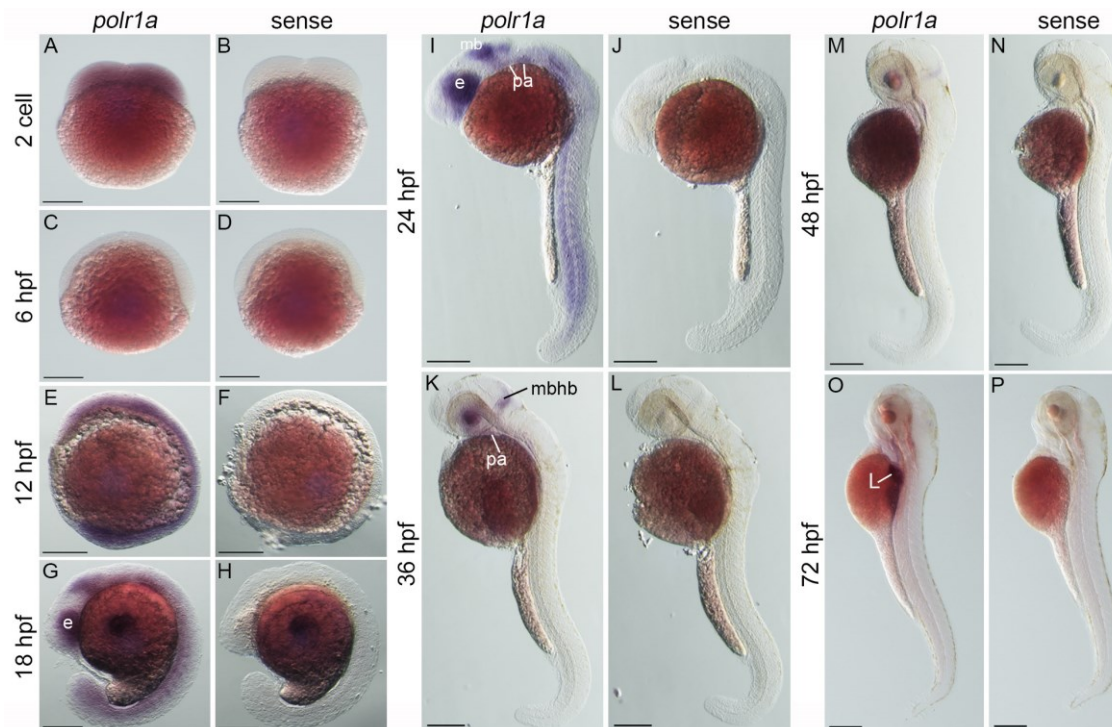
Figure IV-3 In situ hybridization reveals the expression of *polr1a* during zebrafish embryonic development.

Expression is evident at the 2 cell stage (A), is downregulated at 6 hpf (C), and ubiquitous at 12 hpf (E). Restricted expression is evident at 18 hpf (G), with enriched expression in the eye and regions of the brain. There is enrichment in these same regions at 24 hpf (I). At 36 hpf and 48 hpf, expression becomes reduced in the cranial regions (K, M). At 72 hpf, there is an increase in expression within the liver (O). Sense probe controls show no signal at any of the stages examined (B, D, F, H, J, L, N, P). Abbreviations: e – eye; mb – midbrain; pa – pharyngeal arches; mbhb – midbrain-hindbrain boundary; L – liver. Scale bar = 200 μm. Figure adapted from Weaver, Watt, *et al.,* 2015.

PHENOTYPE OF *POLR1A* MUTANT ZEBRAFISH

To better understand the function of *polr1a* during embryonic development, I examined zebrafish with an insertional mutation (Amsterdam et al., 1999; Amsterdam et al., 2004) in the 5'UTR of *polr1a*, *polr1a*[hi3639Tg]. This insertional mutation disrupts the

transcription of *polr1a* (Figure IV-4), resulting in a severe hypomorphic phenotype in *polr1a*^{hi2639Tg/hi3639Tg} embryos. Homozygous *polr1a* mutant embryos exhibit a phenotype which is evident from 15 hpf onwards (Figure IV-5). At 15 hpf, mutants are identifiable by smaller, misshapen eyes and tissue with a necrotic appearance in the cranial region (Figure IV-5 A,B). By 24 hpf, the craniofacial phenotype is well pronounced, including a smaller head and abnormalities of the eye, brain, and somites (Figure IV-5 C,D). These more strongly affected tissues in the mutant embryos are consistent with the regions of enriched *polr1a* expression. A granulated cell pattern could be observed in the head and the end of the tail which is indicative of extensive cell death. The phenotype becomes more pronounced and severe by 36 - 48 hpf, with the head being proportionally smaller in size together with a reduction in the amount of pigmentation (Figure IV-5 E, F). At 3 days post fertilization (dpf), *polr1a* embryos are smaller overall (Figure IV-5 I, J) and appear to lack the developing pharyngeal cartilage (arrows, Figure IV-5 G, H). By 4 dpf, mutant embryos remain smaller in size and exhibit a severe lack of the cranial skeleton and jaw, smaller eyes, abnormal pigmentation, and defects in heart, ear and pectoral fin development (Figure IV-5 I, J). The majority of mutant embryos die by 4 - 5 dpf, likely due to cardiovascular defects.

In order to examine the pharyngeal skeleton in mutant embryos, Alcian blue staining was performed. This revealed that *polr1a*^{hi3639Tg/hi3639Tg} zebrafish have almost no NCC-derived cartilage at 5 dpf (Figure IV-6 A-D), which is consistent with the observation of jaw agenesis in live embryos. Small portions of cartilage were able to form in mutant embryos including portions of the trabeculae (red arrows) and what may be a portion of

140

Meckel's cartilage (black arrows). Mesoderm-derived cartilage elements were also reduced in size in the *polr1a* mutant embryos. The pectoral fins were present (green arrows), but much smaller, in mutant embryos which is consistent with the limb phenotype observed in humans. Further analysis of limb phenotypes and the axial skeleton could not be performed due to the early lethality of the *polr1a* mutant embryos.
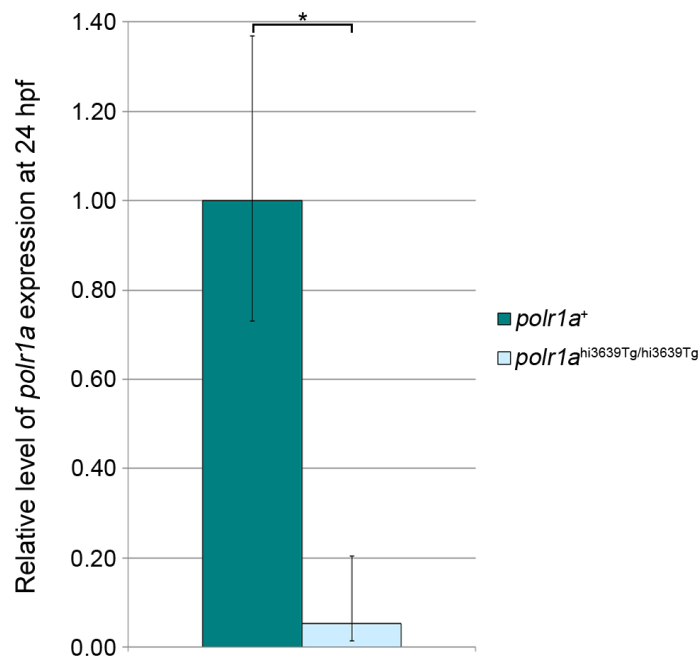
Figure IV-4 qRT-PCR reveals a significant decrease in the level of *polr1a* expression in *polr1a* mutant embryos at 24 hpf.
* p = 0.0095, error bars represent 95% confidence intervals. Figure is from Weaver, Watt, *et al.*, 2015.
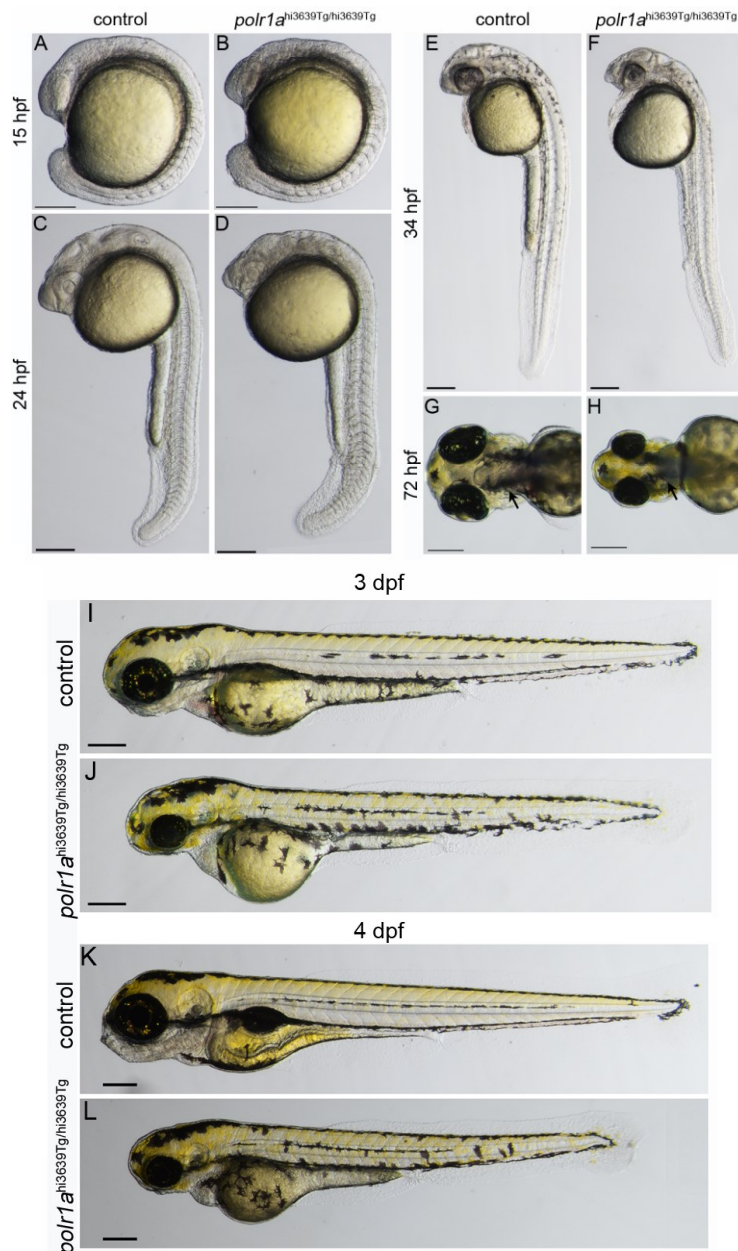
Figure IV-5 Live phenotype of *polr1a* mutant embryos.

A,B) At 15 hpf, *polr1a* mutant embryos are distinguished by increased death in the cranial region. C,D) At 24 hpf, a smaller head and eye are evident, and this difference persists at 34 hpf (E, F). By 3 dpf, *polr1a* mutants are smaller in size (I,J), and appear to lack jaw structures (arrows G, H). By 4 dpf (K,L), mutant embryos are smaller, lack jaw structures and develop cardiac edema. Scale bar = 200 μm. Figure is from Weaver, Watt, *et al.*, 2015.
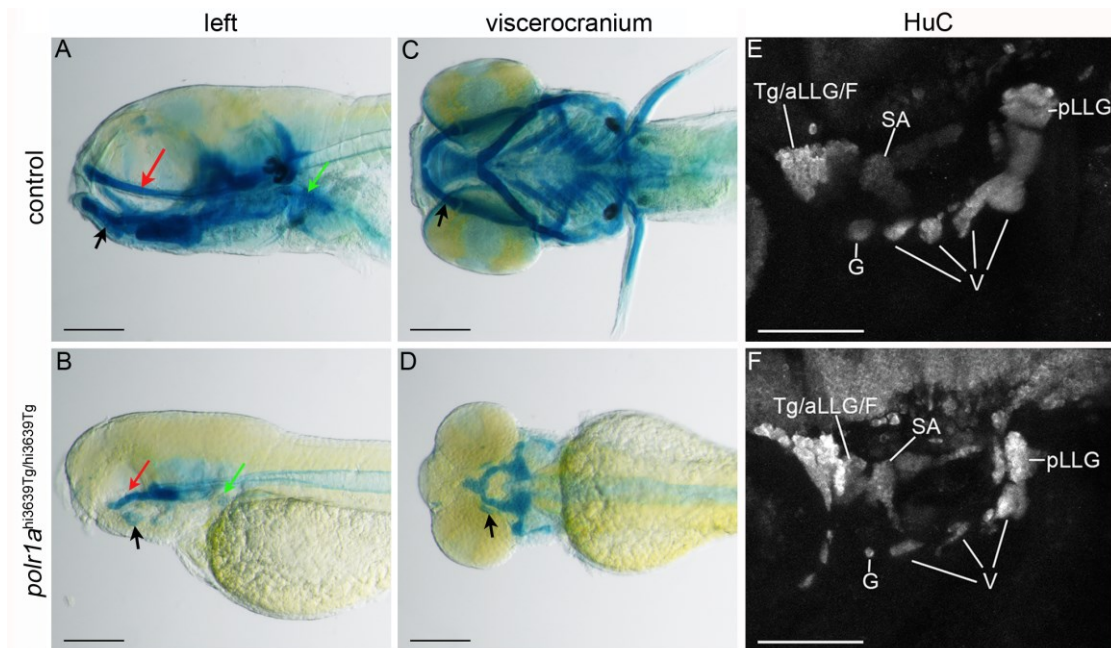
Figure IV-6 Cranial NCC derivatives are hypoplastic in *polr1a* mutant embryos.
A-D) Alcian blue staining reveals a severe loss of cartilage formation in *polr1a* mutant embryos. Regions of the neurocranim, such as the trabeculae (red arrows), are present. Regions of the viscerocranium are more severely affected, with only a remnant of what may be Meckel'scartilage (black arrows) present. In addition, the pectoral fin cartilage (green arrows) is much smaller in mutant embryos. Scale bars = 200 µm. E,F) HuC immunostaining reveals reduced cranial ganglia formation in *polr1a* mutants. Scale bars = 100 µm. Abbreviations: Tg/aLLG/F trigeminal/anterior lateral line/facial ganglion complex; SA statoacoustic ganglion; pLLg posterior lateral line ganglion; G glossopharyngeal ganglion; V vagal ganglia. Figure is from Weaver, Watt, *et al*., 2015.

NEURAL CREST CELL DEVELOPMENT

As much of the craniofacial skeleton is derived from NCC, I hypothesized that NCC development would be reduced or disrupted in *polr1a* mutant embryos. Analysis of NCC development through in situ hybridization revealed that a NCC precursors form and migrate properly early in development (Figure IV-7). At 12 hpf, *sox2* expression reveals

143

that the neural plate has formed in both wild-type and mutant embryos (Figure IV-7 A-D). At the same time, *sox10* staining reveals the appearance of the early migratory NCC to similar levels in control and mutant embryos (Figure IV-7 E-H). These results suggest that early NCC programming and formation occurs in *polr1a* mutant embryos prior to the onset of the mutant phenotype. Alterations in NCC are recognizable concomitant with the appearance of the mutant phenotype. At 17 hpf, there is a reduction in *sox10*-positive migratory NCC, especially in the population migrating towards pharyngeal arch 1. This reduction is also present at 24 hpf (see Figure IV-12 A,B). Consistent with a reduction in *sox10*-positive NCC, immunostaining for HuC revealed a hypoplasia of the cranial ganglia (Figure IV-6 E, F), which is derived in part from the *sox10*-expressing NCC (Culbertson et al., 2011). In addition to the reduction in *sox10* expression, there was a striking reduction of the cartilage precursor population labeled by *sox9a* in *polr1a^{hi3639Tg/hi3639Tg}* embryos (Figure IV-7 M-P). The population of cells within pharyngeal arch 1 and 2 is particularly reduced. Furthermore, *dlx2a* expression, which is a marker of NCC in the pharyngeal arches (Akimenko et al., 1994), shows that arches are smaller and reduced in number in mutants compared to controls (Figure IV-7 Q-T). Only 4 arches are visible in mutant embryos while there are 5 arches present in controls. This loss of *sox9a* cartilage precursors in combination with a reduced population of NCC within the pharyngeal arches could explain the resulting loss of much of the craniofacial cartilage in *polr1a* mutants.

To determine if the NCC were not migrating properly to populate the pharyngeal arches, I analyzed NCC migration using time-lapse confocal microscopy of *sox10:gfp* transgenic zebrafish. By examining NCC migration from approximately 15 hpf until 20

hpf, it was found that the NCC migrate in the proper pattern towards the pharyngeal arches of *polr1a* mutant embryos (Figure IV-8). The population of *sox10:gfp* cells was reduced in the *polr1a* mutant embryos, which is consistent with the reduction in *sox10* labeled cells observed by in situ (Figure IV-7 I-L). This study indicates that the reduction in NCC within the pharyngeal arches is not due to improper migration, but rather a deficiency in the NCC population itself. Altogether, these results suggest that a reduction in the number of migratory NCC that populate the pharyngeal arches underlie the defects in cranioskeletal and neuronal development observed in mutant embryos.
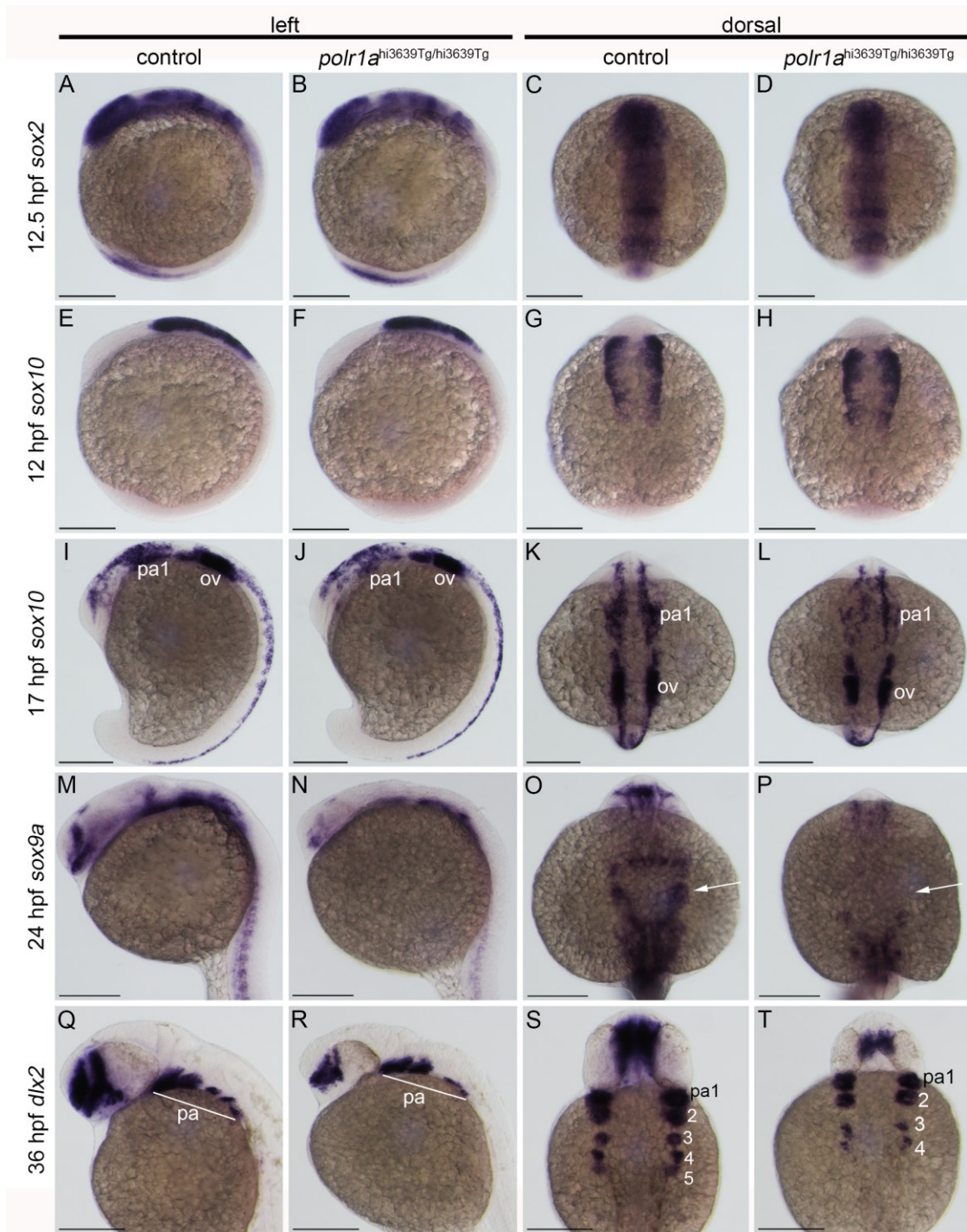
Figure IV-7 In situ hybridization for markers of NCC development in *polr1a* mutant embryos.
(Legend continues on next page)

A-D) *sox2* at 12 hpf shows normal neural plate formation in mutant embryos. E-H) *sox10* at 12 hpf shows that NCC induction occurs at relatively normal levels in mutant embryos. I-L) At 17 hpf, soon after the onset of athe onset of a visible mutant phenotype, a reduction can be seen in the level of *sox10* in pharyngeal arch 1 (pa1) of mutant embryos, indicating a reduced migratory NCC population. (ov = otic vesicle) M-P) At 24 hpf, the population of cartilage precursors labeled by *sox9a* shows a strong reduction throughout mutant embryos, especially in the pharyngeal arches (arrows). Q-T) *dlx2a* at 36 hpf shows a reduced population of NCC in the pharyngeal arches (pa) as well as a reduced number of pa in mutant embryos. Scale bar = 200 μm. Figure from Weaver, Watt, *et al.*, 2015.
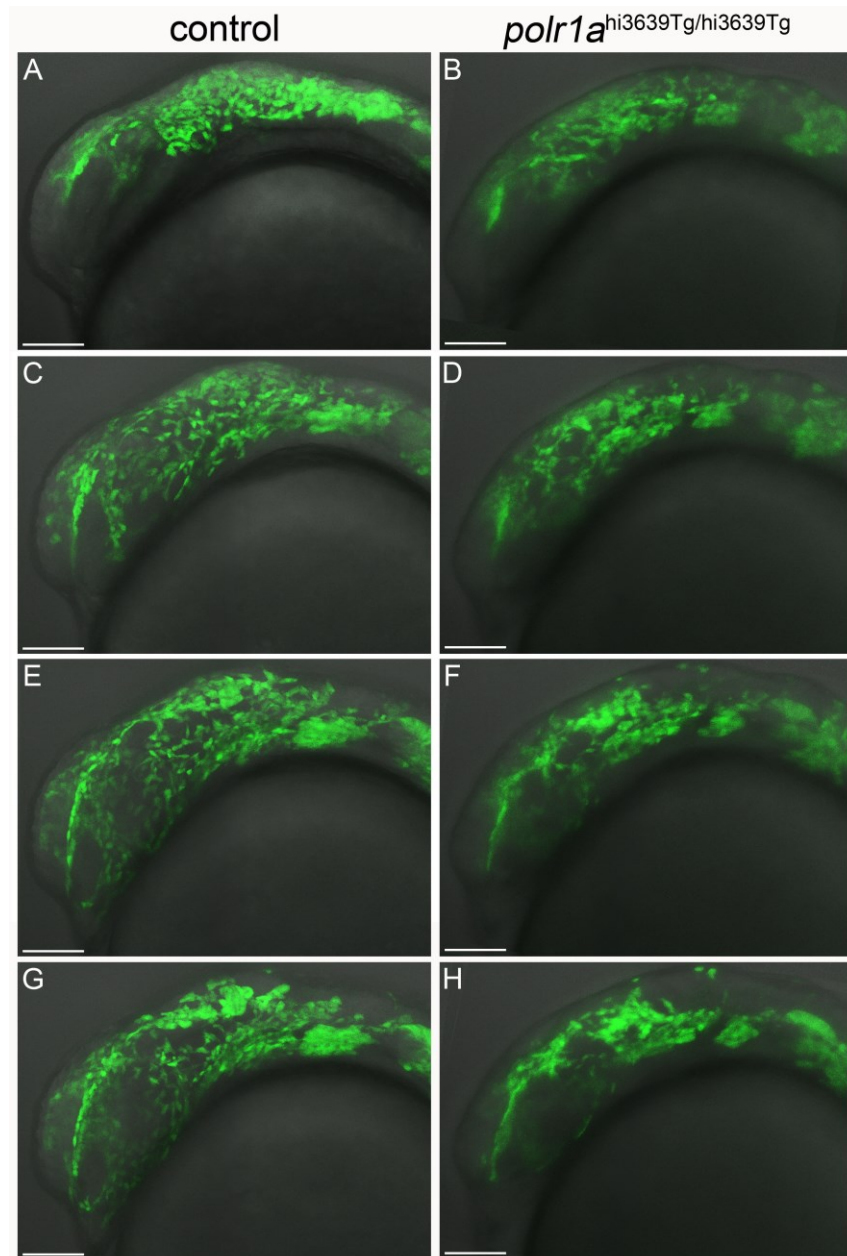
Figure IV-8 Time-lapse microscopy reveals NCC migration in *sox10:gfp* embryos from approximately 15 hpf – 20 hpf.

The migration pattern of *polr1a* mutant embryos (B, D, F, H) occurs properly relative to controls (A, C, E, G). However, the overall *sox10:gfp* population is reduced in *polr1a* mutant embryos. Experiment performed in collaboration with Joaquin Navajas-Acedo. Scale bars = 100 μm.

CELL DEATH AND PROLIFERATION

As *polr1a* mutants displayed a reduced population of NCC, I next hypothesized that this reduction could be the result of an increase in cell death. Prior to the onset of the mutant phenotype, increased cell death is observed throughout *polr1a* mutant embryos at 14 hpf (Figure IV-9 C, D). Extensive TUNEL staining is not evident in the migratory NCC labeled with *sox10:gfp*, indicating that death within the migratory NCC is not the primary cause for the reduced NCC population. At 24 hpf, TUNEL staining showed an increase in cell death in *polr1a*[hi3639Tg/hi3639Tg] embryos especially along the neuroepithelium (Figure IV-10 A, B). Cross-sections through the neural tube revealed cell death in the dorsal portion, where NCC progenitors are located (Figure IV-10 C-F). These embryos were also immunostained for Sox10, and there was not significant co-localization with the TUNEL stain. This suggests that the reduction in NCC number is mainly due to a reduction of the NCC progenitor pool, and not cell death within the migratory NCC population. In vitro studies of human cancer cells have demonstrated that silencing *POLR1A* leads to increased apoptosis through both p53 dependent and independent mechanisms (Donati et al., 2011a; Donati et al., 2011b). To determine if cell death was p53-dependent, I examined p53 levels by qPCR and Western blot. Transcript levels of *tp53* showed a greater than 4-fold increase in mutant embryos at 24 hpf, while the protein levels showed a 1.2 fold increase at 4 dpf (Figure IV-11).

In addition to an increase in cell death, I hypothesized that an alteration in proliferation could also have a role in the reduced number of NCC observed in mutant embryos. To assess proliferation, I examined the amount of phospho-histone H3 (pHH3)

in control and mutant embryos. At 24 hpf, there was an overall decrease in the level of pHH3 staining in *polr1a* mutant embryos (Figure IV-12 A-D). Co-staining with Sox10 revealed that this decrease was not restricted to migratory NCC. In fact, the regions with the most obvious reductions were in the eye, the neural tube, and within the pharyngeal arches. Cross sections through the neural tube confirmed a diminished number of pHH3+ cells within the neural tube of *polr1a* mutant embryos. This, in combination with the increased neuroepithelial cell death, suggests that an alteration in both the ability of NCC progenitors to survive and proliferate underlies the reduced NCC population in *polr1a* mutant embryos.
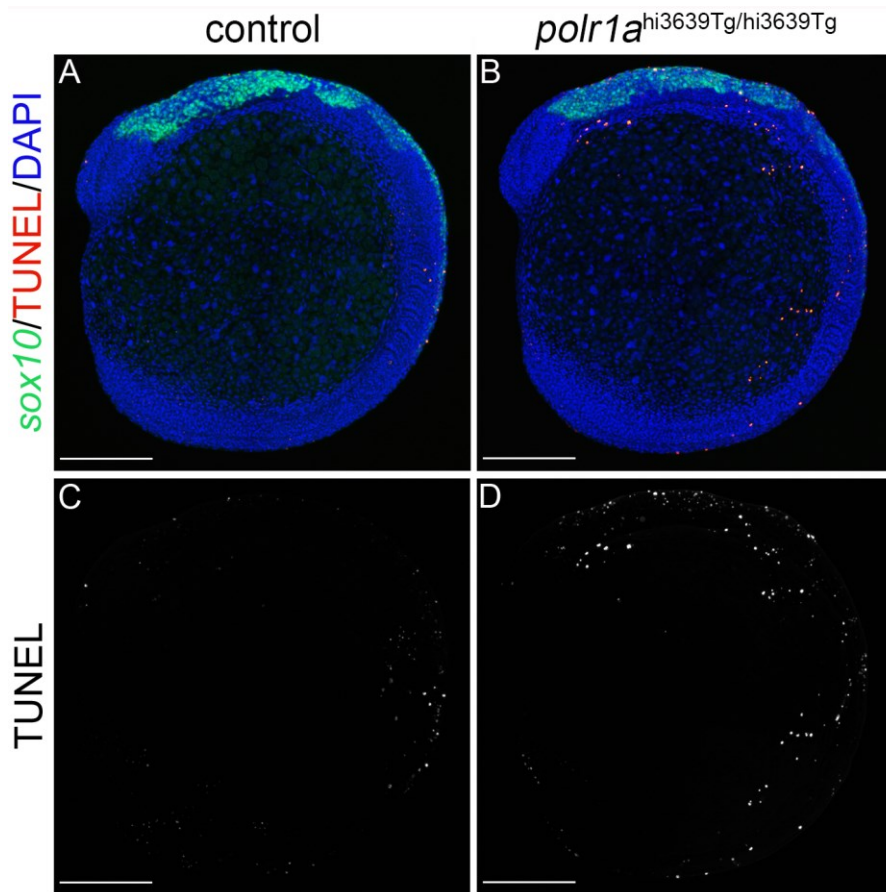
Figure IV-9 TUNEL staining at 14 hpf reveals increased cell death in *polr1a* mutant
embryos.
A,B) TUNEL staining within *sox10:gfp* embryos shows cell death
occuring within multiple regions of *polr1a*^{hi3639Tg/hi3639Tg} embryos and not
solely within the migratory NCC population. C,D) TUNEL stain alone is
increased in *polr1a* mutant embryos. Scale bar = 100 μm. Figure adapted
from Weaver, Watt *et al*., 2015.
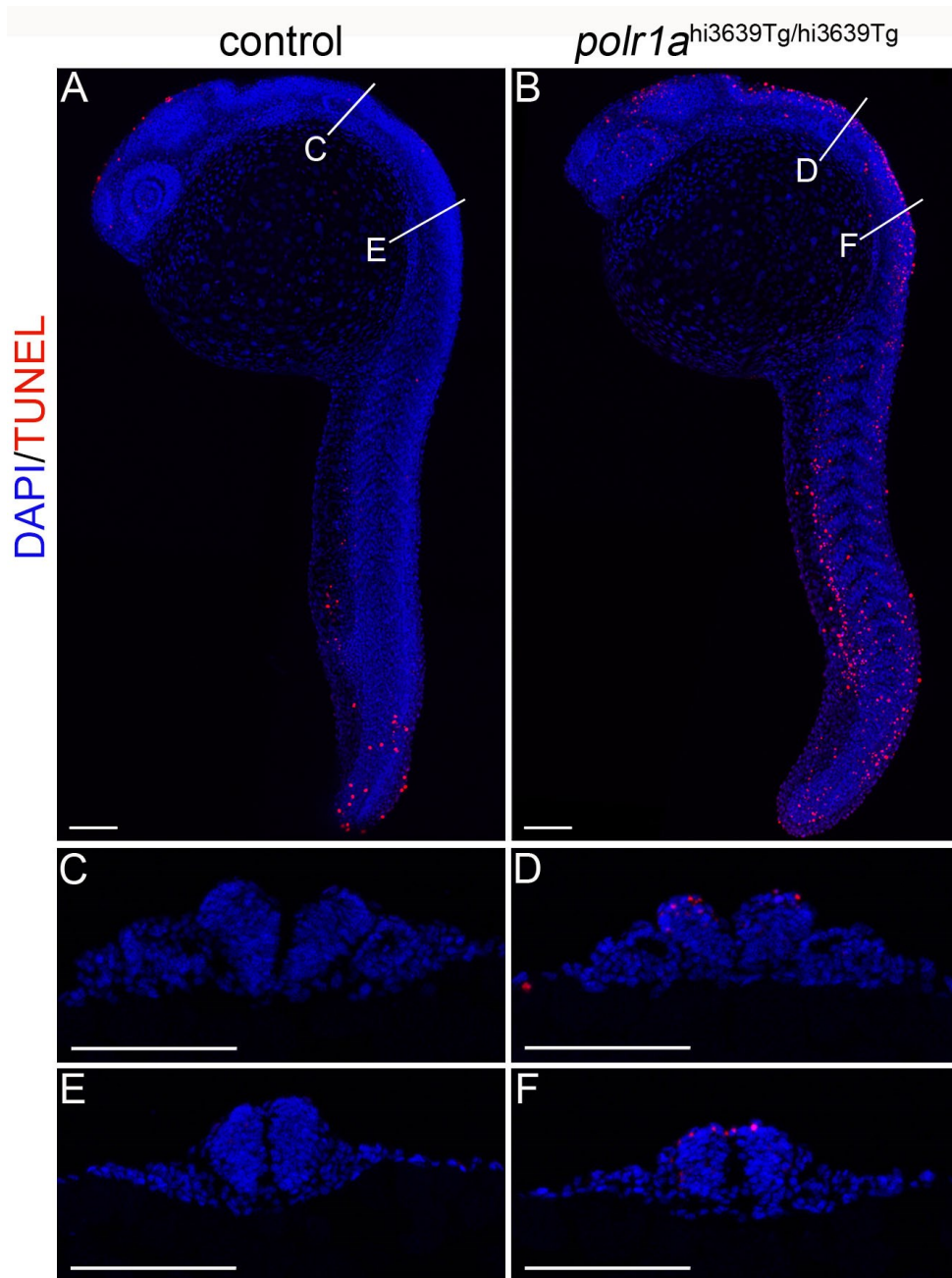
Figure IV-10 TUNEL staining at 24 hpf shows increased neuroepithelial cell death in *polr1a* mutant embryos (A,B).
C-F) Cross-sections through the neural tube confirm increased levels of cell death within the dorsal portion of the neural tube (D,F), which is the NCC-progenitor domain. Scale bar = 100 μm. Figure adapted from Weaver, Watt et al., 2015.
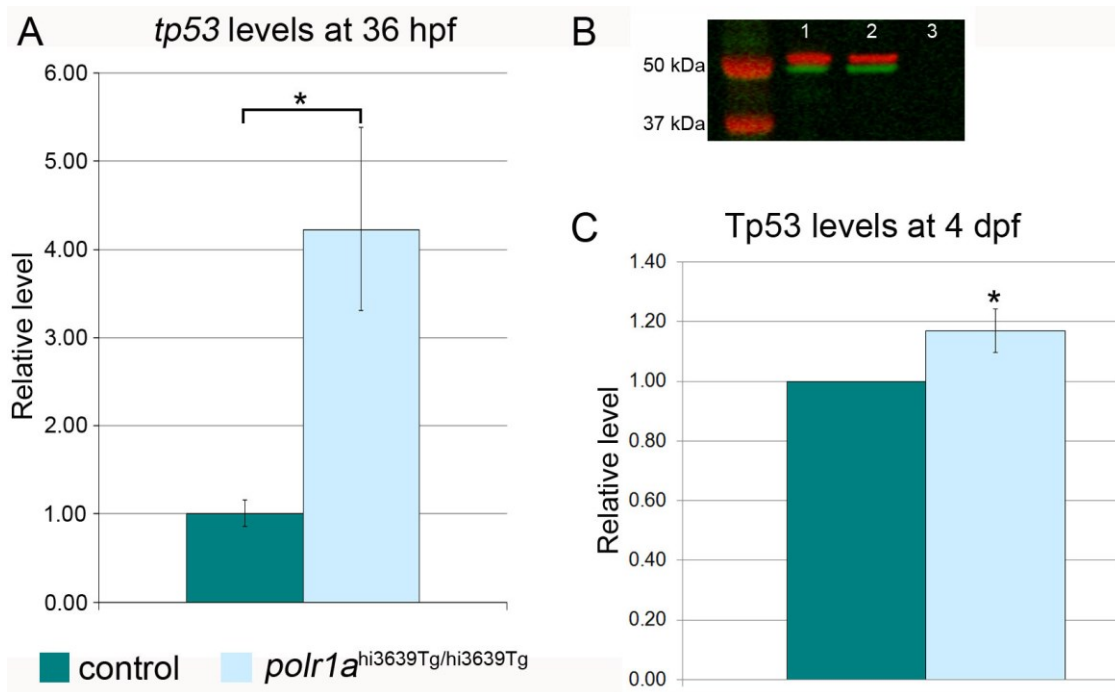
Figure IV-11 Quantification of Tp53 in *polr1a* mutant embryos.
A) qPCR for *tp53* at 24 hpf reveals a significant increase in expression in polr1a mutant embryos. B) Western blot analysis for Tp53 at 4 dpf. Red signal is α-tubulin, green signal is Tp53. Lane 1 is control embryos, lane 2 is *polr1a*^{hi3639Tg/hi3639Tg} embryos, and lane 3 is the negative control. C) Quantification of the Western blot normalized to α-tubulin reveals a significant increase in the levels of Tp53 in polr1a mutant embryos. * p < 0.01. Error bars represent 95% confidence intervals. Figure adapted from Weaver, Watt, *et al.,* 2015.
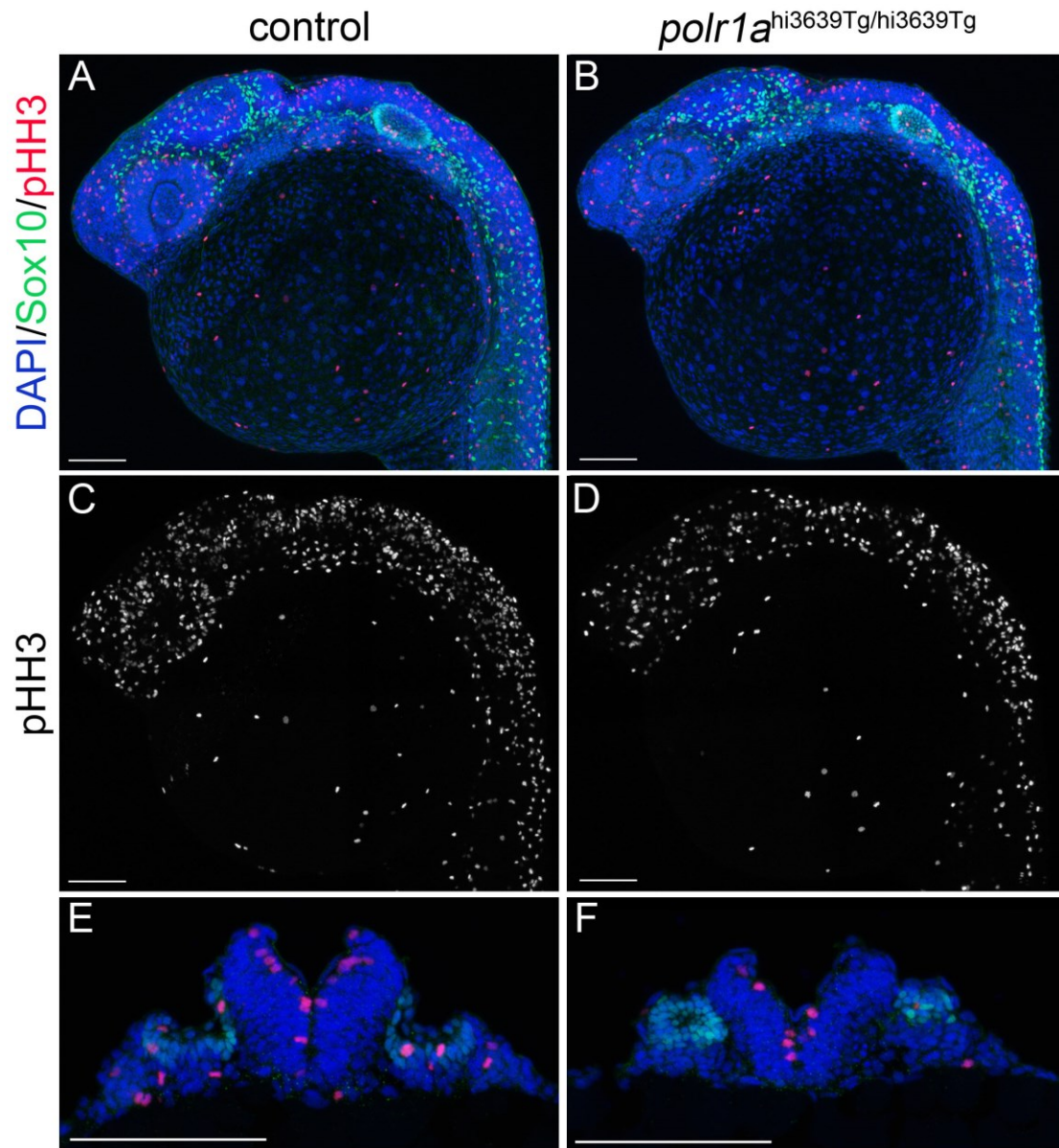
Figure IV-12 pHH3 staining reveals diminished proliferation in *polr1a*^{hi3639Tg/hi3639Tg} embryos.

A,B) Immunostaining for Sox10 and pHH3 revealed a diminished population of NCC and reduced proliferation. C,D) The diminished proliferation is evident in regions around the eye and neural tube. E,F) Cross-sections through the neural tube confirm that there are fewer pHH3+ cells within the neural tube of *polr1a* mutant embryos. Scale bar = 100 μm.

RNAPI function is essential for the transcription of the majority of rRNAs. As Polr1a contains the catalytic site of the enzyme (Engel et al., 2013), mutations in this subunit would be predicted to severely disrupt rRNA production and therefore ribosome biogenesis. I therefore hypothesized that alterations in proliferation and cell survival could be the result of altered ribosome biogenesis in *polr1a* mutant embryos. It has previously been shown that alterations in ribosome biogenesis can lead to p53 activation in multiple ribosomopathy syndromes (Jones et al., 2008; McGowan et al., 2008; Barlow et al., 2010; Pereboom et al., 2011). I hypothesized that mutations in *polr1a* would disrupt rRNA transcription, leading to nucleolar stress and activation of Tp53 (Rubbi and Milner, 2003). The levels of rRNA transcription were determined using quantitative RT-PCR (qPCR) in 24 hpf embryos, with primers designed against regions of the initial, unprocessed transcript (47S). All three regions of the unprocessed transcript showed a significant reduction (p < 0.01) in *polr1a*$^{hi3639Tg/hi3639Tg}$ embryos to less than half of the levels of transcript production in wild-type controls (Figure IV-13 A). In *polr1a* mutant embryos, the 5'ETS was reduced by 73%, ITS1 by 77%, and ITS2 by 59% relative to control levels. The 18S transcript, which includes both the stable processed form as well as the unprocessed 47S, was reduced in *polr1a*$^{hi3639Tg/hi3639Tg}$ embryos, although this result was not statistically significant. These results indicate that the 47S rRNA production is reduced in *polr1a* mutant embryos. As 47S rRNA production is considered a rate-limiting step for ribosome biogenesis, we next examined the consequences of a *polr1a* mutation on ribosome biogenesis by polysome profiling. The polysome profiles of *polr1a* mutant embryos show a strong decrease in all

of the peaks – 40S, 60S, 80S, and polysomes – which is an indication of an overall decrease in ribosome biogenesis. Altogether, these results are consistent with a mechanism of diminished rRNA production and ribosome biogenesis leading to nucleolar stress and activation of Tp53, resulting in cell death of NCC precursors within the neuroepithelium.
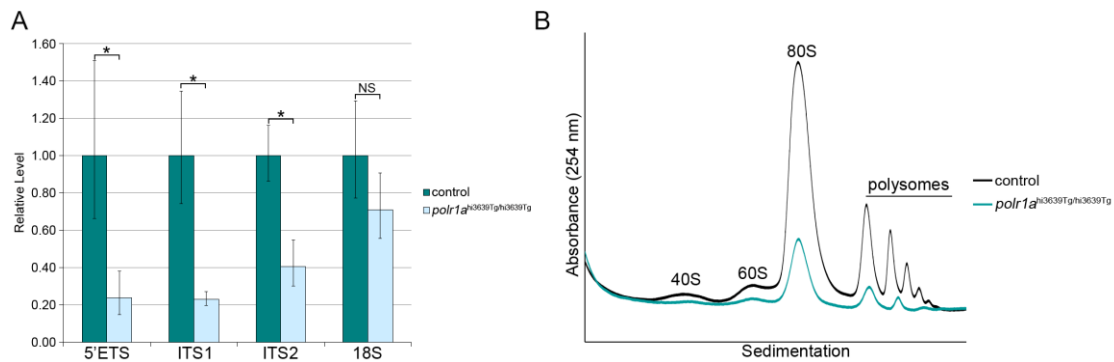
Figure IV-13 Analysis of rRNA and ribosome biogenesis in *polr1a* mutant embryos.
A) qPCR for regions of the 47S transcript reveal diminished production of rRNA in polr1a mutant embryos. The 5'ETS, ITS1, and ITS2 regions all showed significant decreases in rRNA levels in polr1a mutant embryos * $p < 0.01$. The 18S transcript was reduced, but not significantly ($p = 0.095$). Error bars represent 95% confidence intervals. Figure adapted from Weaver, Watt, et al., 2015. B) Polysome profiling reveals a strong difference in the overall level of ribosome biogenesis in polr1a mutant embryos. 40S, 60S, 80S, and plysome peaks all show a reduction. Experiment performed in collaboration with Cynthia Neben and Amy Merrill.

RNA-S<small>EQ</small> A<small>NALYSIS OF POLR</small>1<small>A MUTANT EMBRYOS</small>

To determine if there were alterations outside of p53 signaling involved in the *polr1a* mutant phenotype, RNA-Seq analysis was performed. Two stages were examined: 15 hpf, at the onset of the mutant phenotype, and 24 hpf, when the phenotype and p53-dependent cell death within the neuroepithelium are established. Consistent with the up-regulation of *tp53*, genes involved in p53 signaling, cell cycle, and apoptosis were increased in *polr1a* mutant embryos at both 15 hpf and 24 hpf (Table IV-1). A detailed list of the differentially expressed genes can be found in the Appendix. In order to understand the pathways that may be affected in the *polr1a* mutants, KEGG pathway analysis was performed. Pathways with significant changes included p53 signaling and cell cycle at 15 hpf (Table IV-2).

The upregulation of several cyclin dependent kinase inhibitors (cdkns) including *cdkn2b* (ink4a), *cdkn1a* (p21), *cdkn1ba* (p27), along with retinoblastoma-like 2 (*rbl2*) and cyclin G1 (*ccng1*) was consistent with a decrease in cell cycle progression, similar to what was found in *polr1c* and *polr1d* mutant embryos. In addition, several genes were upregulated that have functions in apoptosis including *casp8, phlda3, bbc3, baxa*, and *tp53inp*. These all corresponded to the genes upregulated in *polr1c* and *polr1d* mutants, with the exception of *tp53inp1*. The Tp53inp1 protein binds Bcl2 to release Bax and eventually leads to cytochrome c release from the mitochondria (Matsuda et al., 2002). At 24 hpf, p53 signaling and cell cycle were significantly altered as well, with the addition of alterations in Notch signaling (Table IV-3).

157

gene	15 hpf Fold Change	24 hpf Fold Change
cdkn2b	185.4	335.3
rbl2	38.9	19.2
mdm2	25.3	22.3
casp8	18.1	18.5
bbc3	17.4	18.1
phlda3	16.3	21.2
cdkn1a	8.5	17.5
tp53inp1	8.0	2.9
ccng1	4.4	7.2
baxa	3.9	3.1
cdkn1ba	3.8	2.9
tp53	3.7	6.5

Table IV-1 List of genes with up-regulation in *polr1a* mutant embryos involved in p53 signaling and cell cycle regulation.
All p-values are significant with at least p < 0.01.

Name	# differentially expressed genes	perturbation accumulation	p-value
p53 signaling pathway	20	-7.31764	9.60E-08
Cell cycle	28	-10.9737	1.72E-06

Table IV-2 KEGG pathway analysis of 15 hpf *polr1a* embryos

Name	# differentially expressed genes	perturbation accumulation	p-value
p53 signaling pathway	19	-3.47237	2.38E-05
Cell cycle	24	-10.5521	1.27E-03
Notch signaling pathway	12	-8.69548	9.15E-03

Table IV-3 KEGG pathway analysis of 24 hpf *polr1a* embryos

An alteration in Notch signaling is interesting since this signaling pathway has many functions during embryogenesis, including craniofacial, neuronal, and brain development. There are two ligands for the Notch receptor, Jagged and Delta. Signaling activated by either of these ligands leads to cleavage of the Notch receptor, releasing the Notch intracellular domain (NICD). The NICD then bind co-factors within the nucleus to activate its target genes (see Figure IV-14). Some of the co-factors include RBPJs, which are down-regulated in *polr1a* mutant embryos (Table IV-4). Interestingly, inhibitors of Notch are also down-regulated including *ctbp1* and *dvl1b*, although not to the same extent as some of the Notch activators, indicating an overall decrease in Notch signaling. The levels of some downstream target genes, which are considered a readout of the overall activity of Notch signaling, are decreased in the *polr1a* mutants. Down-regulation of Notch targets *her15.1*, *her12,* and *her4*, but not *her9* were found. In addition, down-regulation of all of the delta ligands – *dla, dlb, dlc, dld* – were observed, but there was not a consistent down-regulation of jagged ligands. Levels of *jag1a* were decreased while there was a slight increase in *jag1b*. However, as *her9* expression is induced by Jag1-Notch signaling and *her9* expression was only slightly increased (fold change = 1.36), this would indicate that Jag-Notch signaling is not significantly altered. This is particularly interesting since *jag1b* is known to play a role in craniofacial development in zebrafish. In particular, *jag1b* confers dorsal identities within the pharyngeal arches (Zuniga et al., 2010). This would indicate that the proper signals are in place for development of the craniofacial skeleton in the *polr1a* mutants, but that the reduction in the NCC population is too extensive to generate the cartilage elements. Delta-Notch signaling is more significantly affected, as

many genes in this pathway were down-regulated in the *polr1a* mutant embryos. There are several potential consequences for alterations in these genes. *notch1a, notch1b,* and *notch3* are all expressed in the hindbrain and *notch1a* and *notch3* have been shown to be required for rhombomere boundary maintenance (Qiu et al., 2009). It would be interesting to investigate whether there is any alteration of rhombomere structure in *polr1a* mutant embryos. In addition, Delta-Notch signaling has important roles in neuronal development. Mutations in *dla* result in a decrease of trunk NCC derivatives and an increase in Rohon-Beard neuron formation (Cornell and Eisen, 2000). A downstream target of Delta-Notch signaling, *her4* (an ortholog of mammalian *Hes5*), has roles in neuronal development within the trigeminal ganglia outgrowth (So et al., 2009) and the inner ear (Radosevic et al., 2014). Given the hypoplastic cranial ganglia in the *polr1a* mutants (Figure IV-6 E,F), an alteration in neural development is likely. Further examination of the Notch signaling genes and neuronal development in *polr1a* mutants will be investigated in the future.
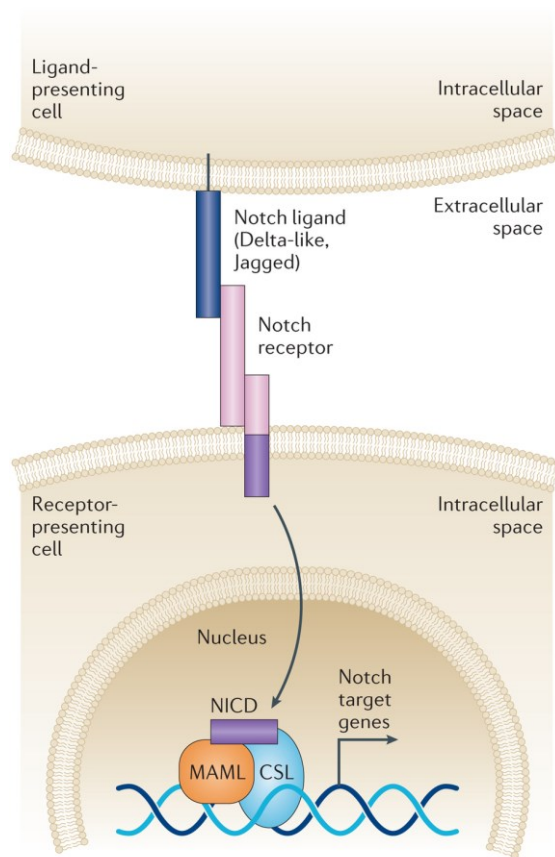
Figure IV-14 Diagram of Notch signaling .

The Notch ligands Delta and Jagged interact with the Notch receptor. The Notch intracellular domain (NICD) is cleaved and then binds to co-factors within the nucleus to activate target gene expression. CSL is also known as RBPJ. From (Andersson and Lendahl, 2014).

gene	fold change	p-value
her4.2	-3.25	1.57E-04
dld	-2.70	9.66E-51
dla	-2.63	7.52E-48
her4.1	-2.55	8.20E-05
rbpjb	-2.13	4.98E-12
jag1a	-2.10	3.68E-15
her15.1	-1.93	1.95E-05
her12	-1.83	1.59E-04
notch1a	-1.77	1.93E-09
dvl1b	-1.74	1.55E-03
ctbp1	-1.73	5.05E-20
dlb	-1.68	2.37E-13
dlc	-1.63	2.69E-14
notch3	-1.62	4.85E-11
notch1b	-1.57	1.97E-10
jag1b	1.63	3.25E-08

Table IV-4 Notch signaling pathway genes are altered in 24 hpf *polr1a* mutant embryos.

Conclusions

In summary, I analyzed the function of *polr1a* during zebrafish embryogenesis which revealed the importance of *polr1a* for craniofacial development, in support of the human acrofacial dysostosis phenotype. I found dynamic expression of *polr1a* during zebrafish embryonic development. At early stages, *polr1a* is ubiquitously expressed, later it becomes enriched in the eye, brain, and cranial regions, and at even later stages it is expressed in the liver. This dynamic pattern would suggest that *polr1a* is needed at different levels in certain tissues at different times during development. The presence of specific phenotypes in human patients with Acrofacial Dysostosis, Cincinnati Type, namely the

cr- anioskeletal and limb, would also suggest that *POLR1A* may have tissue-specific requirements.

Consistent with the pattern of *polr1a* expression, *polr1a*[hi3639Tg/hi3639Tg] embryos display a number of craniofacial defects, smaller size, an underdeveloped liver, and cardiac edema by 4 dpf. One striking feature was the apparent lack of a jaw, which was confirmed by staining with Alcian blue. By 5 dpf, *polr1a* mutant embryos have formed very little cartilage. This severe hypoplasia of the jaw is reminiscent of the phenotype of Individual 1 with Acrofacial dysostosis, Cincinnati Type. In addition to severe hypoplasia of the craniofacial cartilage, *polr1a* mutant embryos also displayed hypoplasia of the cranial ganglia; both of these tissues have a NCC contribution. Analysis of NCC development by in situ hybridization revealed that early stages of NCC formation occur normally in *polr1a* mutant embryos. However, correlating with the onset of the mutant phenotype, alterations in NCC development were apparent. There was reduced expression of *sox10* and *sox9a* labeled NCC, which contribute to neuronal (Culbertson et al., 2011) and cartilage (Yan et al., 2002) lineages, respectively. By 36 hpf, alterations in the pharyngeal arches were visible in the mutant embryos and the domain of *dlx2a* expression revealed the arches were smaller and reduced in number. This also suggests a decrease in NCC number in the *polr1a* mutant embryos. Time-lapse analysis of NCC migration showed that, while reduced in number, the NCC migrate in the proper pattern in *polr1a* mutant embryos. Together, the expression of NCC markers and the proper migration of NCC suggest that *polr1a* is not necessary for proper genetic programming of NCC, but is important in the survival and/or proliferation of the NCC population. I hypothesized that the reduction in NCC would be

163

due to p53-dependent cell death, and increased cell death was found at both 14 hpf and 24 hpf along with increased levels of *tp53*. Interestingly, the majority of the cell death occurred within the neuroepithelium and not within the migratory NCC population which was labeled with Sox10. This suggests that a loss of NCC progenitors underlies the reductions in the *sox10* and *sox9a* populations, and ultimately the skeletal and neuronal defects observed in *polr1a* mutants. As alterations in ribosome biogenesis are known to activate p53 signaling (Azuma et al., 2006; Chakraborty et al., 2009; Donati et al., 2011a) and Polr1a contains the catalytic site of RNAPI which synthesizes rRNA (Engel et al., 2013), we examined the levels of rRNA production. Multiple regions of the initial 47S rRNA transcript showed a significant reduction in *polr1a* mutant embryos ranging from ~60-80% reduction relative to control siblings. Given this strong reduction, and that 47S production is considered a rate-limiting step in ribosome biogenesis (Laferté et al., 2006), I hypothesized that there would be a subsequent alteration in ribosome biogenesis. Polysome profiling confirmed this alteration, with *polr1a* mutants showing a strong decrease in the 40S, 60S, 80S, and polysome peaks. The alteration in every peak indicates that the overall level of ribosome biogenesis is diminished, and that the decrease is not due to any specific alteration in either small or large subunit assembly. Given the decrease in ribosome biogenesis, it is not surprising that a reduction in proliferation, shown by pHH3, was observed in *polr1a* mutants. Altogether, the data suggests a similar mechanism to that of *polr1c* and *polr1d* mutant embryos in the pathogenesis of TCS. That is, diminished levels of rRNA production lead to stress and accumulation of p53, resulting in cell cycle arrest and apoptosis (Figure IV-15).
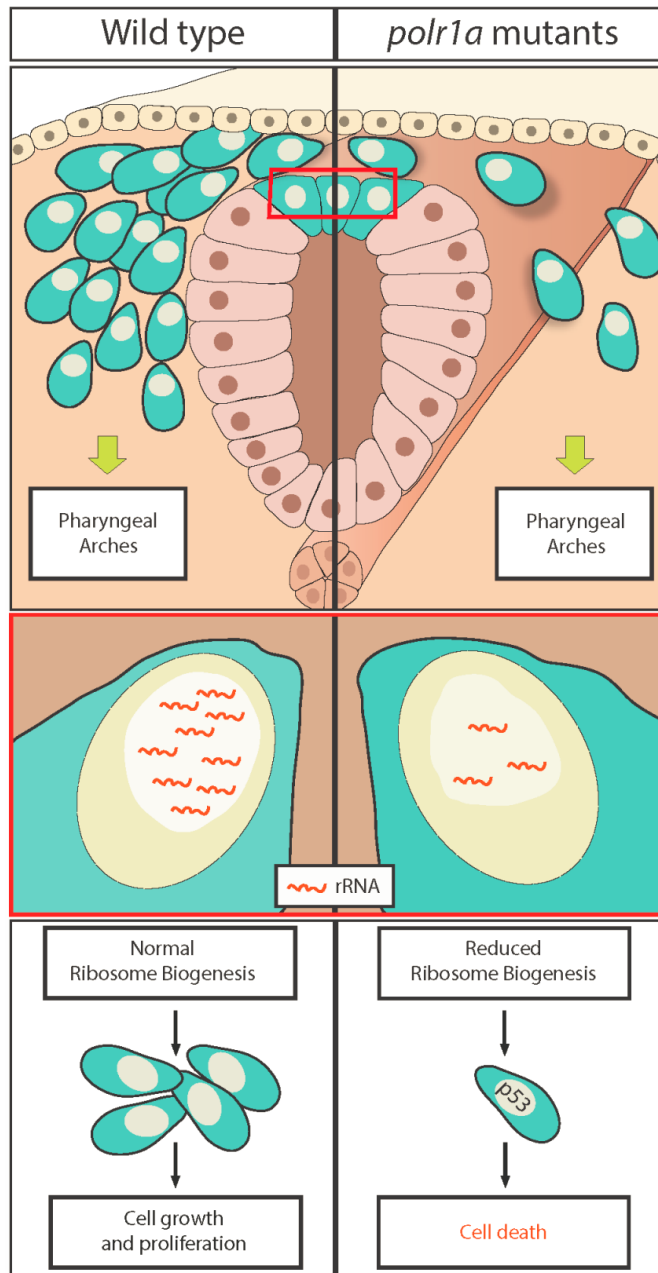
Figure IV-15 Mechanism of the *polr1a* mutant phenotype.
Cells, particularly those within the neuroepithelium, have reduced production of rRNA and ribosome biogenesis, leading to stress and activation of p53, resulting in cell death. This cell death particularly affects the NCC progenitor population and reduces the number of NCC that migrate to the pharyngeal arches. Figure from Weaver, Watt, *et al.,* 2015.

Given the similarity of mechanism between *polr1a*, *polr1c*, and *polr1d* mutant embryos, studies are currently underway to examine if genetic inhibition of *tp53* is able to improve the *polr1a* mutant phenotype.

Remarkably, mutations in *POLR1C* and *POLR1D* which are known to cause TCS, have craniofacial anomalies but not limb phenotypes. Thus, despite the common functions of *polr1a, polr1c,* and *polr1d,* there may be different threshold requirements for each of these genes. RNA-Seq analysis of the three mutants revealed a common alteration in p53 signaling. One intriguing difference was the alteration in the Notch signaling pathway only in *polr1a* mutant embryos at 24 hpf. While alterations in the Notch pathway genes have not yet been validated, it represents an interesting pathway potentially involved in the *polr1a* mutant phenotype. Notch signaling has roles in the development of many different tissue types, including cardiac, neuronal, vascular, and cartilage. It remains to be seen if alterations in this pathway could have a role in the limb phenotype associated with mutations in *POLR1A*. In order to understand the differences in phenotype between patients with *POLR1A* mutations and those with *POLR1C* or *POLR1D* mutations, the functions of each individual RNAPI subunit will require further study.

In summary, we have identified mutations in POLR1A in association with Acrofacial dysostosis, Cincinnati type and developed a zebrafish model of the syndrome. These zebrafish studies reveal that *polr1a* functions specifically in NCC and craniofacial development. In addition, we have shown that the loss of *polr1a* results in diminished ribosome biogenesis, p53-dependent neuroepithelial apoptosis, a loss of NCC, and

consequently craniofacial anomalies. This mechanism underlies the etiology and pathogenesis of Acrofacial dysostosis, Cincinnati Type.

V.   DISCUSSION

Craniofacial anomalies account for approximately one third of all congenital birth defects. These anomalies are typically classified according to the extent of disruption to the craniofacial skeleton, which arises from NCC. Understanding normal NCC development and identifying the perturbations that occur in a disease state are important in understanding the pathogenesis of individual anomalies. Ultimately, this will aid in the design of new therapies for preventing craniofacial syndromes.

In this thesis, I examined zebrafish models of TCS and Acrofacial dysostosis, Cincinnati type in an effort to understand the pathogenesis of these syndromes. TCS is a mandibulofacial dysostosis which is characterized by hypoplasia of the mandible and zygomatic complex in addition to downward slanting palpebral fissures and anomalies of the external and middle ear, although the phenotype and penetrance is variable. Autosomal dominant mutations in *TCOF1* account for the majority of individuals diagnosed with TCS. *TCOF1* encodes a nucleolar phosphoprotein known as Treacle, which has roles in rRNA transcription and processing. A mouse model of *Tcof1* haploinsufficiency demonstrated that the cranioskeletal anomalies arise from p53 dependent apoptosis within NCC progenitors and deficient NCC proliferation. *Tcof1* haploinsufficiency disrupts ribosome biogenesis, leading to nucleolar stress and activation of p53. Therefore, TCS is classified as both a ribosomopathy and neurocristopathy.

Consistent with the classification of TCS as a ribosomopathy, two other genes involved in ribosome biogenesis were identified to cause TCS – *POLR1C* and *POLR1D*

(Dauwerse et al., 2011). These genes encode subunits of RNAPI and RNAPIII and are important for rDNA transcription. Interestingly, the mutations identified in *POLR1C* are autosomal recessive while both autosomal recessive and autosomal dominant mutations have been identified in *POLR1D* (Dauwerse et al., 2011; Schaefer et al., 2014). However, *TCOF1, POLR1C*, and *POLR1D* do not account for all cases of TCS, so other genes remain to be identified. Other syndromes also have mandibulofacial dysostosis as a primary characteristic and identifying the genetic mutations assist in the diagnosis of these syndromes. One example is Acrofacial dysostosis, Cincinnati type in which the craniofacial phenotype has extensive overlap with TCS, but the addition of limb phenotypes makes it a distinct syndrome. In an effort to diagnose these patients with craniofacial anomalies similar to TCS, sequencing was performed for *TCOF1*, *POLR1C,* and *POLR1D* and no mutations were located in these genes. Whole exome sequencing identified a mutation in *POLR1A* as the likely causative mutation and, to date, three individuals with *POLR1A* mutations have been identified. POLR1A is a subunit of RNAPI and is critical for rRNA synthesis. Phenotypes arising from mutations in *POLR1A* were confirmed through my studies in zebrafish *polr1a* mutants which showed diminished rRNA production and disrupted craniofacial development and therefore suggest a role for *polr1a* in craniofacial morphogenesis (Weaver et al., 2015).

The functions of *Polr1a*, *Polr1c*, and *Polr1d* in craniofacial development are not well understood. I therefore characterized the role of these genes during zebrafish development to gain an understanding of how RNAPI subunits function in the developing craniofacial skeleton. I found that *polr1a, polr1c*, and *polr1d* are dynamically expressed

during embryonic development in very similar patterns, including enriched expression in the cranial region at 24 hpf. Mutations in *polr1a*, *polr1c*, and *polr1d* result in craniofacial anomalies, with mutations in *polr1a* producing the most severe phenotype. This is consistent with Polr1a having a more important role in RNAPI, as it contains the active site of the enzyme, in contrast to Polr1c and Polr1d which localize to the periphery of RNAPI and RNAPIII. I also show that reduced rRNA production and ribosome biogenesis underlie p53-dependent apoptosis of NCC progenitors and a diminished NCC population in these models. Remarkably, the mechanism of action for *polr1a, polr1c*, and *polr1d* is very similar and is also consistent with that previously reported for *Tcof1* in mice. The existence of a common mechanism for TCS and Acrofacial dysostosis, Cincinnati type is exciting for the development of therapies, as one therapy may be applicable to many syndromes. In this chapter I discuss the possibilities for tissue specificity arising from mutations in *polr1a, polr1c,* and *polr1d*, the mechanism of action involving p53, and speculate on the future of research in this area.

Tissue Specificity in Ribosome Biogenesis

The phenotypes of *polr1a, polr1c*, and *polr1d* mutant embryos suggests that there are tissue specific effects of mutations in RNAPI. The global nature of ribosome biogenesis and requirement for rRNA makes it surprising that alterations in this process elicit tissue specific effects. Specificity may be mediated through threshold requirements, ribosome composition, RNAPI composition, RNAPI regulation, or any combination of these. How

these tissue specific effects are facilitated during embryonic development remains an area of active research, and below I present several possibilities.

TISSUE-SPECIFIC THRESHOLDS FOR RIBOSOME BIOGENESIS

One attractive hypothesis that arises from my studies is that there may be tissue specific requirements for ribosome biogenesis. The similarly dynamic expression of *polr1a*, *polr1c*, and *polr1d* is indicative of higher levels of these genes being expressed in different tissues during development. This would suggest that these tissues have a higher requirement for RNAPI and thus ribosome biogenesis. *polr1a*, *polr1c*, and *polr1d* all show ubiquitous expression at 12 hpf, when the neural plate has formed and the NCC are beginning to migrate. During NCC migration, the expression of these RNAPI genes changes such that certain tissues express higher levels. By 24 hpf, expression levels of *polr1a, polr1c,* and *polr1d* are higher in areas such as the eye, midbrain hindbrain boundary, and the developing pharyngeal arches. At 36 hpf, elevated expression within the pharyngeal arches remains (See Figures III-1 and IV-3). These areas of enriched expression are congruent with the tissues affected by mutations in *polr1a, polr1c,* and *polr1d*. Interestingly, another RNAPI subunit, *polr1b*, shows enriched expression in gut and craniofacial tissues (Stuckenholz et al., 2009). These areas of higher expression correspond to rapidly proliferating tissues, including the neural plate and pharyngeal arches, where NCC are born and migrate. This suggests that NCC development has a high threshold requirement for ribosome biogenesis.

In addition to *polr1c* and *polr1d*, expression of *Tcof1*, also suggests a higher threshold for ribosome biogenesis in craniofacial tissues in the etiology of TCS. Treacle functions to stimulate rDNA transcription by RNAPI through interactions with Upstream Binding Factor (UBF) and also has functions in rRNA modification (Valdez et al., 2004; Gonzales et al., 2005). *Tcof1* is broadly expressed with elevated activity in the neuroepithelium at E8.5 and the pharyngeal arches and frontonasal process at E9.5 indicating a tissue-specific role in craniofacial development, consistent with the TCS phenotype. Similarly, the gene *nolc1*, a nucleolar phosphoprotein which interacts with RNAPI (Chen et al., 1999), has been used to model TCS in zebrafish. Expression of *nolc1* is enriched within the pharyngeal arches at 26 hpf (Weiner et al., 2012), which corresponds to the areas of stronger expression of *polr1a, polr1c,* and *polr1d* and suggests a role for increased ribosome biogenesis in the developing pharyngeal arches.

Further evidence for tissue-specific levels of ribosome biogenesis comes from analyses of genes involved in rRNA processing. Wdr43 is a component of the small subunit processome which functions in the formation of the 40S subunit and the maturation of the 18S rRNA. *wdr43* is expressed ubiquitously during early zebrafish development, but at later stages shows tissue-specific expression in the neuroepithelium and pharyngeal arches. It is worth noting that these are the same regions where *Tcof1* is highly expressed. Mutations in *wdr43* in zebrafish result in tissue specific phenotypes including disrupted development of craniofacial cartilages (Zhao et al., 2014). Similarly, zebrafish *bap28* has homology to yeast Utp10, which functions in rDNA transcription and in the small subunit processome. Expression of *bap28* at 24 hpf reveals elevated levels in the eye, brain, and

172

pharyngeal arch region, and the disrupted craniofacial development in *bap28* mutants support a need for higher levels of ribosome biogenesis within these tissues (Azuma et al., 2006). The *bap28* mutation disrupted development of neuronal precursors, however, the development of NCC was not investigated. Given the similarity in appearance to *polr1a* mutant embryos at 24 hpf, it seems highly likely that NCC development would be affected in *bap28* mutant embryos. Another example comes from examination of *nol11,* a nucleolar protein implicated in North American Indian childhood cirrhosis. In Xenopus, *nol11* is strongly expressed within the neural tube and pharyngeal arches and knock down of *nol11* resulted in reduced craniofacial cartilage formation (Griffin et al., 2015). Altogether, these examples illustrate the importance of normal ribosome biogenesis for proper craniofacial development and suggest that cranial NCC have a high threshold for ribosome biogenesis.

Disrupting ribosome biogenesis in different ways – either in rRNA transcription, processing, or RP synthesis – often results in a disruption of craniofacial development. Highly proliferative tissues, such as cranial NCC, may have a greater need for ribosome biogenesis. Therefore, the different ribosome biogenesis co-factors and RNAPI subunits are highly expressed within the same cranial regions to produce enough ribosomes for the growth and proliferation. Mutations in *polr1a*, *polr1c*, and *polr1d* all lead to perturbations of NCC development and cranioskeletal anomalies. Mutations in *polr1a* lead to especially severe hypoplasia of cartilage, more so than mutations in *polr1c* and *polr1d* (compare Figure III-4 and Figure IV-6). While all of the cartilage elements are present, although smaller, in *polr1c* and *polr1d* mutant embryos, *polr1a* mutant embryos fail to form the majority of the craniofacial cartilage. This difference in the phenotypes can be explained

173

as a result of the degree to which ribosome biogenesis is affected. The phenotypes of *polr1c* and *polr1d* mutants are very similar, as would be predicted by their function as a heterodimer, and ribosome biogenesis is diminished slightly as evidenced by polysome profiling (Figure III-15). In contrast, *polr1a* mutants exhibit a more severe reduction in the level of ribosome biogenesis, as demonstrated by reduced 40S, 60S, 80S, and polysome peaks (Figure IV-13). This more severe reduction in ribosome biogenesis can explain the greater reduction of NCC in these mutants (Figure IV-7). *polr1a* mutant embryos have lost the majority of *sox9* expression in the pharyngeal arches at 24 hpf, which results in the absence of craniofacial cartilage development at 5 dpf. Numerous other examples across multiple organisms, including *Tcof1* mutant mice, *nolc1* and *wdr43* mutant zebrafish, and *nol11* mutant frogs, show disrupted cranioskeletal development upon impeded ribosome biogenesis.

Mutations in ribosomal proteins, such as those that occur in Diamond-Blackfan anemia (DBA), display variable phenotypes. DBA is characterized by disruptions of the erythroid precursor population with the addition of other craniofacial and digit anomalies in some individuals. The majority of DBA cases are caused by mutations in RPs, components of either the 40S or 60S subunits (Narla and Ebert, 2010). Interestingly, mutations in *RPL5* and *RPL11* are more frequently associated with craniofacial phenotypes (Gazda et al., 2008). Mouse and zebrafish models of DBA have also shown specific phenotypes affecting erythroid and craniofacial development (Danilova et al., 2008; Danilova et al., 2011; Jaako et al., 2011), which is consistent with the idea that NCC and other highly proliferative tissues require a high level of ribosome biogenesis.

The extent of NCC loss and craniofacial cartilage anomalies varies among the different models and may reflect the extent to which ribosome biogenesis is disrupted. Other affected tissues may not require the same level of ribosome biogenesis. However, not all ribosomopathies exhibit the same phenotypes, which raises questions concerning tissue specific threshold requirements for ribosome biogenesis. For example, if cranial NCC have a high threshold for ribosome biogenesis, alterations in this process would be expected to impact their development and thus all ribosomopathies would have craniofacial phenotypes. As ribosomopathies exist which do not have a known alteration in NCC development or a craniofacial phenotype, this suggests that there may be more to regulating ribosome biogenesis than mere levels.

TISSUE SPECIFICITY IN RIBOSOME FUNCTION

Another explanation for tissue-specific phenotypes which arise due to altered ribosome biogenesis is tissue-specific functions for ribosomes. Work from the Barna Lab has suggested that ribosomes may have tissue-specific functions. In a mouse containing a mutation in *Rpl38*, tissue specific homeotic transformations were observed in the head and axial skeleton. These axial skeleton patterning defects were found to be the result of altered Hox gene expression. The mutation in *Rpl38* did not affect global protein synthesis, but did specifically impact translation of *Hox* genes, suggesting a specific role for Rpl38 in these tissues (Kondrashov et al., 2011). Furthermore, investigation of the expression levels of 72 ribosomal proteins in different tissues revealed a surprising level of differential expression (Kondrashov et al., 2011). The differential expression of some ribosomal

proteins is due to their extra-ribosomal functions, such as RPL5 and RPL11 which can mediate the p53 response. Another intriguing interpretation is that the composition of the ribosome may differ in different tissue types, with some ribosomal proteins being critical for ribosome function only in certain tissues. These studies have raised the fascinating possibility that ribosome function may be more heterogeneous than once thought, and that the regulation of ribosomal protein modifications or perhaps even the composition of the ribosome may be altered in a tissue specific manner to provide the necessary level of activity.

Tissue specificity in RNAPI composition. An attractive extrapolation of these studies is that there may be alternative regulation of RNAPI for rRNA synthesis. An example of cell-type specific rRNA synthesis comes from the malaria parasite Plasmodium. This organism has two different genes that encode the small subunit rRNA and these are expressed at different times during its lifecycle. (Gunderson et al., 1987). While different rRNA genes are not known to exist in zebrafish, the modification and regulation of RNAPI subunits could confer tissue specific activity. Co-factors for RNAPI and RNAPIII transcription are known to be regulated by multiple signals within the cell to coordinate the transcription of rRNA with the need for ribosome biogenesis. These include the mTOR, MAPK, IGF, and EGF pathways (Stefanovsky et al., 2001; Hannan et al., 2003{Mayer, 2004 #114; Zhao et al., 2003a; Drakas et al., 2004; Mayer et al., 2004). Different factors, such as *Tcof1*, may have tissue-specific functions and therefore only regulate ribosome biogenesis in some tissues. It is not known whether there are modifications of the RNAPI/III subunits

themselves, such as phosphorylations or acetylations, which could add another level of regulation.

Polr1c and Polr1d form a dimer that is located on the periphery of RNAPI and RNAPIII and therefore would be in a location to interact with or be modified by other proteins. There may be tissue-specific interactions which lead to the TCS phenotype. Finding co-factors that could interact with Polr1c and Polr1d in a tissue specific manner remains to be investigated. Polr1a contains the active site of RNAPI and is located more centrally (Engel et al., 2013; Fernandez-Tornero et al., 2013), making it less likely to interact with proteins or cofactors external to RNAPI. The expression of *polr1a*, *polr1c*, and *polr1d* all revealed areas of enriched expression in specific tissues, however, there are some differences in the expression of *polr1a* compared to *polr1c* and *polr1d*. The differences in expression could indicate functions for these proteins outside of RNAPI/III which have yet to be identified, or that the composition of RNAPI/III could also vary. Studies of RNAPI and RNAPIII structure have been conducted in yeast (Fernández-Tornero et al., 2011; Engel et al., 2013; Fernandez-Tornero et al., 2013), but the structure in vertebrates has not been characterized. Interestingly, the *polr1a* and *polr1c* genes have two protein coding transcripts in zebrafish (see Figure II-2), so it is possible that the proteins resulting from these transcripts have different functions. These alternate transcripts may be incorporated into RNAPI in a tissue specific manner, or they may have roles outside of RNAPI. Further examination of RNAPI function in vertebrates is needed to understand how the structure and function of RNAPI might change in distinct tissues or if RNAPI/III subunits have alternate tasks during embryogenesis.

177

LINEAGE SPECIFIC REGULATION OF RIBOSOME BIOGENESIS

Another layer of regulation of ribosome biogenesis and rRNA transcription comes from lineage-specific sensitivity to alterations in ribosome biogenesis during embryonic development. Regulation of rRNA transcription in a tissue-specific manner is one possible explanation for phenotypes arising from alterations in this seemingly ubiquitous process. An interesting example comes from studies in the *Drosophila* ovarian germline stem cell lineage. CG18316, referred to as *udd*, localizes to nucleoli and co-immunoprecipitation identified an association with proteins homologous to TAF1B and TAF1C, which are components of SL1 and required for initiation of RNAPI transcription. Expression of *udd* is generally higher in germline stem cells and mutations in *udd* reduced rRNA transcription and also affected the expression of proteins that regulate cell fate decisions (Zhang et al., 2014). Altogether, these studies indicate that altering rRNA transcription can affect cell-fate decisions of a specific lineage as well as affecting decisions of growth and proliferation.

TCS provides another example of lineage-specific regulation of rRNA transcription. Treacle, while widely expressed during embryogenesis, displays tissue-specific elevated expression in regions important in NCC development. Treacle localizes to the nucleolus (Marsh et al., 1998; Winokur and Shiang, 1998) where it interacts with Upstream Binding Factor (UBF) to stimulate transcription of rDNA by RNAPI (Valdez et al., 2004). Mutations in *TCOF1* show variable phenotypes and penetrance, and this lack of genotype-phenotype correlation is indicative of potential modifier genes of the TCS phenotype (Trainor et al., 2008). How mutations in *POLR1C* and *POLR1D* also result in

178

the tissue-specific phenotypes of TCS is less understood, but is likely mediated through their regulation.

Numerous ribosomopathies have skeletal anomalies as a part of the phenotype, including Postaxial acrofacial dysostosis, Acrofacial dysostosis, Cincinnati type, TCS, and DBA (Trainor and Merrill, 2014). In fact, a number of ribosomopathies with disruption of RNAPI affect similar tissues, including craniofacial tissues (reviewed in (Hannan et al., 2013)). Alterations in craniofacial development are indicative of a specific disruption of NCC, and suggests that there is something about the NCC and craniofacial cartilage progenitors that are particularly sensitive to changes in ribosome biogenesis. It may be that the bone and cartilage lineage has specific requirements for high levels of active rDNA, and obstruction of ribosome biogenesis then results in the inability of these tissues to develop properly. Therefore, another possibility for tissue-specific phenotypes observed in *polr1a, polr1c,* and *polr1d* mutants may be due to differential control of ribosome biogenesis in the cartilage/bone lineage. For example, *Runx2*, a gene involved in osteoblast differentiation, represses activity at the rDNA promoter in mammalian cells through association with UBF, a component of the RNAPI regulator complex (Young et al., 2007). Mutations in *RUNX2* may cause cleidocranial dysplasia, which is characterized in part by skeletal anomalies and decreased bone density (Otto et al., 2002). Further evidence for lineage specific disruption of ribosome biogenesis in bone and cartilage comes from a mouse model of Bent Bone Dysplasia Syndrome (BBDS). BBDS is characterized by skeletal dysplasia including bent long bones, poor mineralization of the skull and other craniofacial anomalies and is caused by mutations in *FGFR2* (Merrill et al., 2012). Further

study of the nature of FGFR2 mutations in BBDS revealed that FGFR2 functions to activate rDNA transcription. FGFR2 and FGF2 interact with UBF at the rDNA promoter, stimulating production of rRNA. This blocks the repression of rDNA transcription by Runx2, which is necessary in osteoblast differentiation, resulting in altered bone development (Neben et al., 2014). Thus a link can be established between ribosome biogenesis and bone formation. Further studies are needed to understand any role that Polr1a, Polr1c, and Polr1d might have specifically in bone and cartilage development and the levels of active rDNA in various tissues in the embryo.

Mechanisms in the prevention of craniofacial anomalies

In my studies of *polr1a, polr1c,* and *polr1d,* I found that mutations in these genes diminish rRNA production, which leads to *tp53* activation and neuroepithelial cell death, reducing the NCC progenitor population and resulting in craniofacial defects. Thus the mechanism by which craniofacial phenotypes arise in these models appears to revolve around Tp53 (p53) activity. Disrupted ribosome biogenesis leading to p53 activation and cell death is a common mechanism among many ribosomopathies, but not all. The role of p53 in the phenotypes of ribosomopathies such as TCS and Acrofacial dysostosis, Cincinnati type will be discussed in the following section. In addition, I consider contributions form p53-independent pathways in the phenotype of these syndromes

Tp53 DEPENDENT APOPTOSIS IS A UNIFYING MECHANISM UNDERLYING TCS AND

ACROFACIAL DYSOSTOSIS, CINCINNATI TYPE

The craniofacial phenotypes present in *polr1a, polr1c*, and *polr1d* mutant embryos are a result of alterations in the NCC population. These alterations are two-fold: first, a reduction in the NCC progenitor pool as a result of neuroepithelial apoptosis (See Figure III-12 and Figure IV-9), and second, reduced proliferation of NCC within the pharyngeal arches (See Figure III-14 and Figure IV-11). While disruptions in ribosome biogenesis are known to lead to nucleolar stress and activate Tp53, the specific disruption of NCC in these models is curious. One possibility is that NCC death indicates that they require higher rates of ribosome biogenesis. A recent study showed that when the rate of ribosome biogenesis is high, cells are more likely to undergo apoptosis in the event of a disruption in ribosome biogenesis. If there is a lower rate of ribosome biogenesis, then cells will undergo cell cycle arrest in response to disruption of ribosome biogenesis (Scala et al., 2015). However, this study was completed in cell lines, so it remains to be seen if the same is true in the developing embryo. If the rate of ribosome biogenesis varies among different embryonic tissues and is higher within NCC, then this would help explain why the NCC progenitor population specifically undergoes cell death in TCS and Acrofacial Dysostosis, Cincinnati type.

The phenotypes of *polr1c* and *polr1d* mutant embryos can be improved greatly upon *tp53* inhibition (Figure III-18), indicating that much of the phenotype arises as a failure of NCC progenitors to survive. The degree of rescue is variable, indicating that the reduction in NCC proliferation may also function in diminished cartilage development.

181

RNA-Seq data revealed a similar activation of the p53 response in *polr1a* mutant embryos. Studies are currently underway to determine if a similar improvement in cartilage development can be observed in *polr1a* mutant embryos with inhibition of *tp53*. Preliminary results suggest there is some improvement in cartilage formation, revealing a consistent mechanism with *polr1c* and *polr1d.*

These studies are consistent with the mechanism underlying TCS in mouse models. *Tcof1*$^{+/-}$ embryos have a reduced population of NCC, which is due to apoptosis and decreased proliferation in the neuroepithelium (Dixon et al., 2006). Microarray analysis of *Tcof1*$^{+/-}$ embryos revealed an increase in genes which are associated with p53-dependent transcription; these genes have roles in cell cycle regulation, apoptosis, and DNA repair (Jones et al., 2008). An increase in p53 activity and specific neuroepithelial apoptosis is observed in *Tcof1*$^{+/-}$ mice. Furthermore, *Tcof1*$^{+/-}$ embryos have diminished production of mature 28S rRNA and it was hypothesized that perturbations of ribosome biogenesis in NCC underlies the pathogenesis of TCS (Jones et al., 2008). Pharmacological inhibition of p53 using pifithrin-α, as well as genetic inhibition using *p53*$^{+/-}$ mice, reduced neuroepithelial apoptosis and rescued the TCS phenotype in *Tcof1*$^{+/-}$ mice (Jones et al., 2008). In contrast to what was observed in the *polr1c* and *polr1d* zebrafish, *Tcof1*$^{+/-}$ mice are viable to adulthood upon inactivation of *tp53*.

Other ribosomopathies show a similar mechanism of alterations in ribosome biogenesis and Tp53 activation. These include both zebrafish and mouse models of 5q-syndrome, DBA, and dyskeratosis congenita. Dyskeratosis congenita (DC) is a genetically heterogeneous ribosomopathy primarily characterized by bone marrow failure and

182

defective telomere maintenance. A zebrafish model of DC carries a mutation in *nop10*, which results in 18S rRNA processing defects and activation of the p53 pathway. Upon *p53* inhibition, there was improvement in formation of the hematopoietic stem cell population (Pereboom et al., 2011). Similarly, both *wrd43* and *nol11* phenotypes can also be improved upon *tp53* inhibition (Zhao et al., 2014; Griffin et al., 2015). An overlapping feature of 5q- syndrome and DBA is macrocytic anemia, and interestingly, both syndromes have been linked to mutations in ribosomal protein genes. A mouse model of 5q- syndrome carrying a mutation in *Rps14* is rescued upon *p53* inhibition (Barlow et al., 2010). In addition, zebrafish models of DBA have shown improvement upon p53 inhibition. *rpl11* morphant zebrafish show reduced cell death and improved craniofacial development upon co-injection of *p53* morpholino, but hematopoiesis was not investigated (Chakraborty et al., 2009). A separate study showed improved hematopoiesis in *rpl11* mutant zebrafish injected with *p53* morpholino (Danilova et al., 2011). Mutations in other ribosomal protein genes in mice and zebrafish including *Rps6, Rps19/rps19*, and *rps29* have shown upregulation of p53 with improved phenotypes upon its inhibition (Danilova et al., 2008; McGowan et al., 2008; Taylor et al., 2012). Additionally, mutations in nucleostemin, a protein which localizes to the nucleolus and regulates p53 activity, result in loss of 5.8S rRNA processing and p53 activation (Essers et al., 2014). Collectively, all of these studies provide strong evidence for activation of the p53 pathway upon perturbation of ribosome biogenesis, regardless of where in ribosome production the disruption occurs.

Nucleolar stress, or disruption of nucleolar structure, occurs upon alterations in ribosome biogenesis (Rubbi and Milner, 2003). It has been hypothesized that nucleolar

stress is a primary mechanism by which p53 is activated in ribosomopathies. However, in human cancer cell lines, inhibition of POLR1A led to p53 activation without altering nucleolar structure (Donati et al., 2011a). Interestingly, if both rRNA and ribosomal protein production are diminished, p53 activation does not occur. These studies indicate that the balance between rRNA synthesis and ribosomal protein synthesis is carefully regulated in the cell, and disrupting the balance activates the p53 response.

The major regulator of p53 activation in response to altered ribosome biogenesis is Mdm2. Mdm2 regulates p53 stability, targets it for proteasomal degradation, and is required to suppress p53 activity and function (Haupt et al., 1997; Kubbutat et al., 1997; Ringshausen et al., 2006). Ribosomal proteins can bind to Mdm2 and prevent its interaction with p53, and recently it was found that RPL5 and RPL11 are specifically required along with the 5S rRNA to inhibit Mdm2 and allow for p53 stabilization (Donati et al., 2013; Sloan et al., 2013). Thus, if rRNA production by RNAPI is diminished, there is an excess of ribosomal proteins, of which Rpl5 and Rpl11 will bind the 5S rRNA and Mdm2, leading to activation of p53. The presence of the 5S rRNA as a part of the complex to induce p53 is curious, since p53 activation is observed in *polr1c* and *polr1d* mutant embryos. Polr1c and Polr1d are subunits of both RNAPI and RNAPIII which are involved in transcribing all of the rRNAs, however it remains to be understood how an alteration in 5S rRNA might impact p53 activation in the *polr1c* and *polr1d* zebrafish. 5S rRNA production was not examined in my studies, so the level to which it may or may not be reduced remains to be resolved. It is possible that the milder phenotype in *polr1c* and *polr1d* mutant embryos compared to *polr1a* mutants is in part due to the disruption of 5S rRNA production. If the

mutations in *polr1c* and *polr1d* diminish transcription of the 5S rRNA and the 47S rRNA, then reduced levels of 5S rRNA would diminish the binding of RPL5 and RPL11 to Mdm2 and blunt the p53 response. As mutations in *polr1a* only reduce the levels of 47S rRNA, there is no abrogation of the p53 response by this mechanism, and more cell death is observed in these embryos. However, this explanation does not preclude the possibility that the more severe phenotypes observed in *polr1a* mutant embryos are a result of the critical function of Polr1a in the catalytic site of RNAPI. In fact, this explanation is also more likely because there is a greater reduction in rRNA production in *polr1a* mutants as are the alterations in ribosome biogenesis (compare Figure IV-12 to Figure III-15).

In summary, mutations in *polr1a, polr1c*, and *polr1d* disrupt ribosome biogenesis which in turn activates the p53 response and results in cell death within the NCC progenitor population. Inhibiting the function of Mdm2 is the primary path through which disruptions of ribosome biogenesis produce enhanced p53 activity. This has been demonstrated by numerous animal models of ribosomopathies in which inhibition of p53 is capable of ameliorating defects caused by mutations in ribosome related genes (Danilova et al., 2008; McGowan et al., 2008; Chakraborty et al., 2009; Danilova et al., 2011; Pereboom et al., 2011; Taylor et al., 2012; Zhao et al., 2014; Griffin et al., 2015). Some phenotypes can be completely prevented by p53 inhibition, as in the *Tcof1* model of TCS (Jones et al., 2008), but most fail to completely rescue the phenotypes. This could be due to i) the failure to rescue defects in ribosome biogenesis necessary for proper growth and proliferation (as in (Griffin et al., 2015) and/or ii) the role of p53-independent pathways in the phenotype that remain to be investigated.

185

TP53-INDEPENDENT DEFECTS ARISE FROM DISRUPTED RIBOSOME BIOGENESIS

tp53 inhibition is not sufficient to completely rescue the phenotype and viability of *polr1a, polr1c*, and *polr1d* mutant embryos, indicating that there may be additional p53 independent causes for the observed phenotypes. While the levels of ribosome biogenesis may simply not be enough for normal development in these models, other studies indicate that it is important to consider alternate pathways. First, despite the complete rescue and viability of *Tcof1*$^{+/-}$ mice upon *Tp53* inhibition, an increase in ribosome biogenesis was not observed (Jones et al., 2008). Therefore in this rescued TCS model, the level of ribosome biogenesis was enough, provided the cells survived. However, this does not seem to be the case in *polr1a, polr1c*, or *polr1d* mutant embryos. In these embryos it is likely that the disruption of RNAPI function and ribosome biogenesis in the cells to be circumvented by p53 inhibition, although the level of ribosome biogenesis in double homozygous mutant embryos has not been determined. Second, not all disruptions in ribosome biogenesis can be improved by p53 inhibition (see below). This could indicate that disruptions in ribosome biogenesis can be mediated either with or without p53.

Several studies have implicated p53-independent mechanisms in ribosomopathies outside of the ribosomal protein-Mdm2-p53 pathway which include the response to DNA damage, the mTOR pathway, and autophagy. A role for Treacle was recently implicated in the DNA damage response. Two separate studies identified interactions between Treacle and NBS1, which is a protein involved in recruitment of ATM to sites of double-strand breaks (Ciccia et al., 2014; Larsen et al., 2014). These studies suggest a mechanism whereby Treacle and NBS1 interact at the rDNA promoter as well as along the rDNA to

inhibit rRNA transcription upon DNA damage. The mechanism by which rRNA transcription is repressed remains to be investigated; however, Ciccia *et al*. identified subunits of RNAPI as a part of the Treacle complexes, including POLR1A, POLR1B, and POLR1E. This indicates that there could be direct regulation of RNAPI upon DNA damage or that these subunits function in the DNA damage response separately from their association with RNAPI. Moreover, this indicates a possible role for DNA damage in the *polr1a, polr1c*, and *polr1d* phenotypes. If mutations in these genes alter RNAPI such that Treacle-NBS1 binding is hindered upon DNA damage, the necessary inhibition of rRNA during repair may not occur. This could then lead to proliferation of genomically unstable cells, which then undergo apoptosis. In the embryo, DNA damage may arise from the rapid proliferation necessary for development. In support of this, the neuroepithelium in mouse embryos, which is a rapidly proliferating tissue, has a naturally higher level of reactive oxygen species (ROS), and excessive ROS can be associated with DNA damage (Sakai et al., 2016). Furthermore, examination of mouse embryonic fibroblasts show that there is delayed DNA damage repair in *Tcof1*$^{+/-}$ fibroblasts, confirming the previously reported interaction of Treacle with sites of DNA damage. Thus, in the *Tcof1*$^{+/-}$ embryos, the neuroepithelium has a reduced capacity to respond to the effects of ROS such as DNA damage, and neuroepithelial apoptosis is induced by oxidative stress. Importantly, reducing oxidative stress by *in utero* treatment with the antioxidant N-acetyl-cystein (NAC) improves the phenotype of *Tcof1*$^{+/-}$ embryos such that a greater percentage of embryos display mild phenotypes (Sakai et al., 2016). However, a complete rescue of the phenotype such that embryos survive to adulthood was not observed upon NAC treatment, which is

187

in contrast to the rescue upon genetic inhibition of *tp53*. This could indicate that there are multiple triggers of the p53 response underlying the pathogenesis of TCS: i) the response to oxidative stress and DNA damage and ii) the response to disrupted ribosome biogenesis. The increased sensitivity to ROS and impaired response to DNA damage could then contribute to some of the increased cell death in the *polr1c* and *polr1d* mutant zebrafish in the absence of high levels of 5S rRNA that is involved in the ribosome-Mdm2-p53 response. In addition to ROS, there may be an alternate mechanism for DNA damage in mutant zebrafish. Less efficient transcription of the rDNA by RNAPI occurs in *polr1a*, *polr1c,* and *polr1d* mutants as 47S rRNA transcription is reduced, but not eliminated, in these embryos. In an effort to increase the availability of rRNA, the cell could potentially increase the number of active rDNA repeats. However, if too many rDNA repeats are active this could lead to genome instability, as a certain amount of silent rDNA repeats are needed for sister chromatid cohesion (Ide et al., 2010). DNA damage may then be induced in these mutants and lead to cell cycle arrest and apoptosis, demonstrating another link between ribosome biogenesis and DNA damage. Further examination of DNA damage in the *polr1a, polr1c,* and *polr1d* zebrafish is necessary to determine if it similarly functions in the pathogenesis of these mutations or if there are other mechanisms mediating apoptosis.

The mTOR pathway, which regulates cell growth and proliferation through phosphorylation events impacting all three RNA Polymerases, has been associated with the treatment of DBA. Mutations in ribosomal proteins result in diminished ribosome biogenesis, and stimulation of ribosome biogenesis through the mTOR pathway is an attractive alternative to p53 inhibition in the development of therapies for prevention. In

DBA, treatment with L-leucine can ameliorate macrocytic anemia in human patients as well as the phenotypes of zebrafish and mouse models of the syndrome (Cmejlova et al., 2006; Pospisilova et al., 2007; Jaako et al., 2012; Payne et al., 2012). L-leucine functions through Leucyl-tRNA synthetase to activate mTOR signaling and stimulate protein synthesis (Bonfils et al., 2012; Han et al., 2012). mTOR activation also leads to phosphorylation of factors involved in initiating rRNA transcription (Hannan et al., 2003; Mayer et al., 2004), thus stimulating both rRNA synthesis and increased translation of ribosomal proteins. Investigation of this pathway in the *polr1c* and *polr1d* mutants revealed a slight reduction in mTOR pathway component RPS6 (Figure III-20), however, stimulation of mTOR through L-leucine treatment exacerbated the mutant phenotype (Figure III-22). This is likely due to the increased disruption in the rRNA/ribosomal protein balance. The mutations in *polr1c* and *polr1d* reduce the function of RNAPI, and so, hypothetically, stimulation of RNAPI by mTOR is not able to increase rRNA transcription in coordination with ribosomal protein synthesis. Consequently, stimulation of mTOR signaling to improve ribosome biogenesis is not a viable therapy for all ribosomopathies and the pathogenesis must be understood in order to develop viable therapies for their prevention.

Another p53-independent pathway implicated in ribosome biogenesis is autophagy, demonstrated by the *titania* mutant zebrafish. Autophagy is a mechanism used by the cell to promote intracellular recycling of organelles and often occurs under starvation conditions. The *titania* mutation was identified in the gene *pwp2h*, which is involved in 18S rRNA maturation as a part of the small subunit processome. Mutations in *pwp2h* result

189

in craniofacial and intestine defects and also result in increased autophagy as well as increased p53 (Boglev et al., 2013). Notably, the phenotypes arising from mutations in *pwp2h* were not prevented by p53 inhibition and neither was autophagy (Boglev et al., 2013). This indicates that the autophagy response is independent of p53 and that alterations in ribosome biogenesis can somehow stimulate autophagy.

In other ribosomopathies, such as the zebrafish model of Shwachmam-Bodian-Diamond syndrome (SBDS), p53-independent phenotypes are also present, but the underlying mechanisms are not well understood. In a zebrafish model of SBDS, morpholino knockdown of the *sbds* gene results in pancreatic and craniofacial defects as well as an absence of neutrophils, which are consistent with the human phenotype (Provost et al., 2012). Disruptions in subunit assembly induce the ribosome defects associated with SBDS. Co-injection of *p53* morpholino in *sbds* morphants could improve the gross morphology of the embryos but not the cranioskeletal, pancreatic, or neutrophil phenotypes, suggesting a p53-independent pathway is involved in the mutant phenotype. The improvement upon *p53* inhibition could be due to the nature of morpholino injections which can also induce cell death (Robu et al., 2007), and a genetic model for *sbds* would reveal more about the role of p53. Two other genes investigated in this study were identified by microarray, *rpl3* and *pes*. *rpl3* and *pes* mutants have similar phenotypes to *sbds* morphants and also fail to show improvement of pancreas development upon p53 inhibition (Provost et al., 2012).

A recent study has implicated a p53-independent role for Rpl3 in cell cycle arrest and apoptosis. In human cells, RPL3 overexpression leads to increased levels of p21, also

known as Cdkn1a, an inhibitor of the cell cycle (Russo et al., 2013). This increase required a complex of RPL3, Sp1 (a regulator of p21), and nucleophosmin (a nucleolar protein) and the level of RPL3 overexpression governs whether cell cycle arrest or apoptosis is activated (Russo et al., 2013). p53-independent functions on ribosome biogenesis and cell proliferation have also been observed for another ribosomal protein, RPL11. Again in human cell lines, over expression of RPL11 reduced c-Myc activity at the promoters of c-Myc target genes (Dai et al., 2007). c-Myc, an oncogene, has multiple functions in ribosome biogenesis as it is involved in the regulation of RNAPI, II, and III. Of particular interest, c-Myc will increase rRNA transcription and proliferation (Dai et al., 2007). It would be fascinating to learn whether these p53-independent functions for RPL3 and RPL11 might be tissue-specific. Further study of these interactions in vertebrate models may illuminate whether extra-ribosomal functions occur only in certain tissues during development.

In summary, events outside of p53 activation have roles in ribosome biogenesis and ribosomopathies. In TCS, there may be a role for DNA damage, although this remains to be investigated in the RNAPI mutants. Autophagy is one mechanism by which altered ribosome biogenesis can lead to cell cycle arrest and apoptosis independent of p53, as demonstrated by the *titania* mutants. Stimulation of the mTOR pathway by L-leucine can increase rRNA transcription and translation and is capable of improving the phenotype of DBA and potentially other ribosomal protein mutants. Finally, extra-ribosomal functions of ribosomal proteins may also play a p53-independent role in mediating cell proliferation. Examination of p53-independent pathways in other ribosome biogenesis mutants will

potentially uncover tissue-specific functions of these pathways and aid in our understanding of their pathogenesis.

General Conclusions and Future Directions

In this thesis, I examined the roles of RNAPI subunits Polr1a, Polr1c, and Polr1d in zebrafish craniofacial development. In my examination of *polr1a*, *polr1c* and *polr1d*, I found spatiotemporally dynamic expression during zebrafish embryogenesis, suggesting tissue specific levels or functions for these genes. Curiously, there were differences between the expression of *polr1a* and *polr1c* and *polr1d* which could indicate functions for these genes outside of RNAPI that contribute to tissue specificity. In support of tissue specific functions for these RNAPI subunits, mutations in *polr1a, polr1c*, and *polr1d* result in specific phenotypes of the craniofacial skeleton, which is derived primarily from cranial NCC. Increased levels of *tp53*, neuroepithelial cell death, and reduced proliferation of NCC underlies the cranioskeletal anomalies in these models. Activation of p53 likely occurs due to nucleolar stress, as reduced rRNA synthesis perturbs ribosome biogenesis. These findings establish a common mechanism for TCS, regardless of the mutation. Importantly, I establish the first genetic models of *polr1c* and *polr1d* to examine their function in the pathogenesis of TCS. Furthermore, my studies established *polr1a* zebrafish as a model for a newly identified ribosomopathy, Acrofacial dysostosis, Cincinnati type. *polr1a* mutant embryos exhibit a similar phenotype to models of TCS, indicating a common mechanism underlying disruptions of RNAPI function. Questions remain concerning the tissue specificity of the phenotypes arising from mutations in *polr1a, polr1c*, and *polr1d* and will

192

be an area of future research. Additionally, a central role for *tp53* in the *polr1a, polr1c*, and *polr1d* mutant phenotypes was identified; however, additional pathways need to be investigated for the prevention of ribosomopathies and neurocristopathies such as TCS and Acrofacial dysostosis, Cincinnati type. Future directions in the examination of these models are discussed below.

TISSUE SPECIFICITY OF RNAPI FUNCTION

The phenotypes of *polr1a, polr1c*, and *polr1d* mutant embryos suggest that tissue specificity exists in RNAPI transcription, however, how this specificity is obtained remains under investigation. The first question to address is how much of the phenotype is specific to NCC and whether Acrofacial dysostosis, Cincinnati type and TCS are primarily neurocristopathies or ribosomopathies. While NCC are critical for the generation of the craniofacial skeleton, they must interact with endoderm, mesoderm, and ectoderm during their development. It is currently unknown whether the expression of RNAPI subunits Polr1a, Polr1c, and Polr1d is absolutely required in each of these tissue types. In order to address the tissue-specific requirements for these genes, the Trainor lab is currently generating mice with conditional deletions of each of these genes. *Polr1c* conditional mutant embryos have been generated in the lab and reveal similar disruption of craniofacial development to *polr1c* mutant zebrafish after temporal removal of Polr1c from E8.5. In support of a critical role for Polr1c in NCC, *Wnt1-Cre* conditional deletion of *Polr1c* phenocopies the whole-organism removal at E8.5 (unpublished data, Annita Achilleos). A conditional allele of Polr1d has not yet been generated, but mutations in *Polr1d* are pre-

implantation lethal, demonstrating a requirement for Polr1d in early embryonic development (unpublished data, Annita Achilleos). We are currently in the process of generating the *Polr1a* conditional mouse mutant in the lab using CRISPR technology, and anticipate that *Polr1a* will be required for early embryonic development, similar to *Polr1c* and *Polr1d*.

The generation of mouse models will also aid in our understanding of RNAPI regulation in different tissues and at different times. How *polr1a, polr1c,* and *polr1d* function in a tissue specific manner is unknown. It could be due to different requirements for ribosome biogenesis, ribosome composition, RNAPI composition, or the regulation of RNAPI. Mice are advantageous for these questions because of the greater amount of tissue available in the embryo as well as a better library of available antibodies. Dissection of different tissues for use in proteomics studies could also aid in identification of tissue specific factors interacting with Polr1a, Polr1c, and Polr1d.

In addition to specific functions of Polr1a, Polr1c, and Polr1d, mutations in RNAPI subunits could differentially alter levels of rRNA and ribosome biogenesis in certain lineages. In order to investigate this, tissue-specific fluorescent reporters in combination with flow cytometry will be used to isolate a cell population of interest. For example, *sox10:gfp* zebrafish can be used to examine NCC. In sorted NCC, 47S rRNA levels will be examined to understand if NCC specifically exhibit high levels of rRNA transcription. Using *sox10:gfp* bred into the background of *polr1a, polr1c,* and *polr1d* mutant embryos, I can determine if rRNA synthesis levels are more greatly reduced specifically in NCC. Once the conditional mice are generated, I can also take advantage of available fluorescent

194

reporters and perform similar experiments to see if there is greater importance of rRNA synthesis in NCC and if this is conserved from zebrafish to mammals.

Another question arising from the RNAPI mutants is if protein synthesis, as a readout of ribosome function, is altered in either a global or tissue-specific manner. If global protein synthesis is reduced in mutant embryos, this would indicate a globally important role for Polr1a, Polr1c, or Polr1d. However, if global protein synthesis is not significantly different between mutant and wild-type embryos, this could indicate a tissue-specific difference. Isolating particular tissues for examination could then confirm if there is, for example, a NCC specific attenuation of protein synthesis, similar to what was shown in *Rpl38* mutants (Kondrashov et al., 2011).

ALTERNATIVE PATHWAYS FOR THE PREVENTION OF CRANIOFACIAL ANOMALIES

Activation of p53 is central to the mechanism which underlies the TCS phenotype, as well as Acrofacial dysostosis, Cincinnati type, and many other ribosomopathies previously mentioned. The phenotypes of *polr1c* and *polr1d* embryos were improved upon inhibition of *tp53*, and studies currently underway suggest a slight improvement in cartilage formation *in polr1a* mutant embryos upon *tp53* inhibition. It will be important to determine whether ribosome biogenesis is also improved on the *tp53* mutant background. *p53* inhibition fails to completely rescue *polr1c* and *polr1d* embryos, as these embryos still die at approximately 10 dpf. This could be due to either a failure to rescue ribosome biogenesis to a functional level for survival, or indicate important p53-independent functions.

To examine potential genes that may function in the phenotypes of the *polr1a*, *polr1c*, and *polr1d* embryos, RNA-Seq was performed. As expected, genes involved in the p53 pathway were significantly upregulated in all three mutants (Table III-I, Table IV-I). Indeed, KEGG pathway analysis revealed a significant change in p53 signaling and this was the only pathway in common among *polr1a, polr1c*, and the *polr1d* results. While this fails to identify new therapeutic avenues that would be applicable to all three mutants, it does confirm the role of p53. Interestingly, MAPK was an activated pathway in *polr1c* mutants, which has multiple roles in the cell related to proliferation or alternatively to responses to DNA damage or oxidative stress. Phosphorylation events by MAPK lead to increased rDNA transcription by RNAPI and increased tRNA synthesis by RNAPIII (Felton-Edkins et al., 2003; Zhao et al., 2003a). This could indicate a compensatory mechanism by which *polr1c* mutants are attempting to increase rRNA production despite reduced functionality of RNAPI. Alternatively, it will be interesting to learn if DNA damage or oxidative stress has a role in the *polr1c* phenotype as Treacle was recently implicated in the DNA damage response. The genes altered in the MAPK pathway will need to be validated by qPCR and in situ hybridization to determine if upregulation of the pathway occurs in a tissue-specific manner in *polr1c* mutant embryos. Another interesting finding coming from the RNA-Seq data was the downregulation of Notch signaling in 24 hpf *polr1a* mutant embryos. Similar validation experiments will be performed and it will be interesting to learn how Notch signaling may be related to ribosome biogenesis or an independent function of Polr1a. Further analysis of these pathways may reveal new insights about the roles of RNAPI genes in zebrafish development.

196

While the RNA-Seq results confirm the importance of the p53 pathway in the phenotype of the *polr1a, polr1c*, and *polr1d* mutant embryos, another common therapeutic target was not identified. Identification of other targets will be important for the treatment of TCS and Acrofacial dysostosis, Cincinnati type due to the tumorigenic effects of p53 inhibition. Current methods for improving defects associated with craniofacial anomalies are primarily surgical (Trainor and Andrews, 2013). Mechanisms to improve craniofacial development during the critical time frame of NCC development have the potential to improve the quality of life in individuals with TCS and other neurocristopathies. Therefore, to identify mechanisms beyond p53 inhibition, a chemical screen could be performed. Zebrafish are an excellent model for such a screen because of the quantity of embryos generated from a single breeding pair and the ability to rapidly identify phenotypes. Using mutants with *sox10:gfp,* the formation of cartilage can be visualized directly with fluorescence microscopy and analyzed for rescue. The generation of mouse models in the lab will complement these studies as any chemical identified to rescue or improve cartilage formation in zebrafish can next be tested on a mammalian model.

In conclusion, the *polr1a, polr1c,* and *polr1d* zebrafish will serve as useful models to understand the pathogenesis of Acrofacial dysostosis, Cincinnati type and TCS. These models indicate that there may be tissue specific regulation of ribosome biogenesis, adding to the body of work which suggests ribosome biogenesis is not as ubiquitous as initially perceived. Further examination of these zebrafish models and the generation of conditional mouse mutants has the potential to uncover previously unknown functions and interactions of Polr1a, Polr1c, and Polr1d that will facilitate an understanding of the pathogenesis of

TCS and Acrofacial dysostosis, Cincinnati type. Finally, these models will aid in the identification of new treatments that have the potential to improve the quality of life in individuals with facial dysostoses.

VI. REFERENCES

Abbas, T. and Dutta, A. (2009) 'p21 in cancer: intricate networks and multiple activities', *Nat Rev Cancer* 9(6): 400-414.

Abu-Issa, R., Smyth, G., Smoak, I., Yamamura, K.-i. and Meyers, E. N. (2002) 'Fgf8 is required for pharyngeal arch and cardiovascular development in the mouse', *Development* 129(19): 4613-4625.

Adameyko, I., Lallemend, F., Furlan, A., Zinin, N., Aranda, S., Kitambi, S. S., Blanchart, A., Favaro, R., Nicolis, S., Lübke, M. et al. (2012) 'Sox2 and Mitf cross-regulatory interactions consolidate progenitor and melanocyte lineages in the cranial neural crest', *Development* 139(2): 397-410.

Akimenko, M., Ekker, M., Wegner, J., Lin, W. and Westerfield, M. (1994) 'Combinatorial expression of three zebrafish genes related to distal- less: part of a homeobox gene code for the head', *The Journal of Neuroscience* 14(6): 3475-3486.

Alexander, C., Zuniga, E., Blitz, I. L., Wada, N., Le Pabic, P., Javidan, Y., Zhang, T., Cho, K. W., Crump, J. G. and Schilling, T. F. (2011) 'Combinatorial roles for BMPs and Endothelin 1 in patterning the dorsal-ventral axis of the craniofacial skeleton', *Development* 138(23): 5135-5146.

Altug Teber, O., Gillessen-Kaesbach, G., Fischer, S., Bohringer, S., Albrecht, B., Albert, A., Arslan-Kirchner, M., Haan, E., Hagedorn-Greiwe, M., Hammans, C. et al. (2004) 'Genotyping in 46 patients with tentative diagnosis of Treacher Collins syndrome revealed unexpected phenotypic variation', *Eur J Hum Genet* 12(11): 879-890.
Amsterdam, A. (2003) 'Insertional mutagenesis in zebrafish', *Developmental Dynamics* 228(3): 523-534.

Amsterdam, A., Burgess, S., Golling, G., Chen, W., Sun, Z., Townsend, K., Farrington, S., Haldi, M. and Hopkins, N. (1999) 'A large-scale insertional mutagenesis screen in zebrafish', *Genes & Development* 13(20): 2713-2724.

Amsterdam, A., Nissen, R. M., Sun, Z., Swindell, E. C., Farrington, S. and Hopkins, N. (2004) 'Identification of 315 genes essential for early zebrafish development', *Proceedings of the National Academy of Sciences of the United States of America* 101(35): 12792-12797.

Andermann, P., Ungos, J. and Raible, D. W. (2002) 'Neurogenin1 Defines Zebrafish Cranial Sensory Ganglia Precursors', *Developmental Biology* 251(1): 45-58.

Andersson, E. R. and Lendahl, U. (2014) 'Therapeutic modulation of Notch signalling - are we there yet?', *Nat Rev Drug Discov* 13(5): 357-378.

Aoki, Y., Saint-Germain, N., Gyda, M., Magner-Fink, E., Lee, Y.-H., Credidio, C. and Saint-Jeannet, J.-P. (2003) 'Sox10 regulates the development of neural crest-derived melanocytes in Xenopus', *Developmental Biology* 259(1): 19-33.

Araya, C., Ward, L. C., Girdler, G. C. and Miranda, M. (2015) 'Coordinating cell and tissue behavior during zebrafish neural tube morphogenesis', *Developmental Dynamics*: n/a-n/a.

Avaron, F., Hoffman, L., Guay, D. and Akimenko, M. A. (2006) 'Characterization of two new zebrafish members of the hedgehog family: Atypical expression of a zebrafish indian hedgehog gene in skeletal elements of both endochondral and dermal origins', *Developmental Dynamics* 235(2): 478-489.

Azuma, M., Toyama, R., Laver, E. and Dawid, I. B. (2006) 'Perturbation of rRNA Synthesis in the bap28 Mutation Leads to Apoptosis Mediated by p53 in the Zebrafish Central Nervous System', *Journal of Biological Chemistry* 281(19): 13309-13316.

Barlow, J. L., Drynan, L. F., Hewett, D. R., Holmes, L. R., Lorenzo-Abalde, S., Lane, A. L., Jolin, H. E., Pannell, R., Middleton, A. J., Wong, S. H. et al. (2010) 'A p53-dependent mechanism underlies macrocytic anemia in a mouse model of human 5q- syndrome', *Nat Med* 16(1): 59-66.

Barrallo-Gimeno, A., Holzschuh, J., Driever, W. and Knapik, E. W. (2004) 'Neural crest survival and differentiation in zebrafish depends on mont blanc/tfap2a gene function', *Development* 131(7): 1463-1477.

Beckouet, F., Labarre-Mariotte, S., Albert, B., Imazawa, Y., Werner, M., Gadal, O., Nogi, Y. and Thuriaux, P. (2008) 'Two RNA Polymerase I Subunits Control the Binding and Release of Rrn3 during Transcription', *Molecular and Cellular Biology* 28(5): 1596-1605.

Begbie, J., Brunet, J. F., Rubenstein, J. L. and Graham, A. (1999) 'Induction of the epibranchial placodes', *Development* 126(5): 895-902.

Begemann, G., Schilling, T. F., Rauch, G.-J., Geisler, R. and Ingham, P. W. (2001) 'The zebrafish neckless mutation reveals a requirement for raldh2 in mesodermal signals that pattern the hindbrain', *Development* 128(16): 3081-3094.

Berghmans, S., Murphey, R. D., Wienholds, E., Neuberg, D., Kutok, J. L., Fletcher, C. D. M., Morris, J. P., Liu, T. X., Schulte-Merker, S., Kanki, J. P. et al. (2005) 'tp53 mutant zebrafish develop malignant peripheral nerve sheath tumors', *Proceedings of the National Academy of Sciences of the United States of America* 102(2): 407-412.

Berndt, J. D. and Halloran, M. C. (2006) 'Semaphorin 3d promotes cell proliferation and neural crest cell development downstream of TCF in the zebrafish hindbrain', *Development* 133(20): 3983-3992.

Betancur, P., Bronner-Fraser, M. and Sauka-Spengler, T. (2010) 'Assembling Neural Crest Regulatory Circuits into a Gene Regulatory Network', *Annual Review of Cell and Developmental Biology* 26(1): 581-603.

Bi, W., Deng, J. M., Zhang, Z., Behringer, R. R. and de Crombrugghe, B. (1999) 'Sox9 is required for cartilage formation', *Nat Genet* 22(1): 85-89.

Bi, W., Huang, W., Whitworth, D. J., Deng, J. M., Zhang, Z., Behringer, R. R. and de Crombrugghe, B. (2001) 'Haploinsufficiency of Sox9 results in defective cartilage primordia and premature skeletal mineralization', *Proceedings of the National Academy of Sciences* 98(12): 6698-6703.

Bierhoff, H., Dundr, M., Michels, A. A. and Grummt, I. (2008) 'Phosphorylation by Casein Kinase 2 Facilitates rRNA Gene Transcription by Promoting Dissociation of TIF-IA from Elongating RNA Polymerase I', *Molecular and Cellular Biology* 28(16): 4988-4998.

Birkholz, D. A., Killian, E. C. O., George, K. M. and Artinger, K. B. (2009) 'Prdm1a is necessary for posterior pharyngeal arch development in zebrafish', *Developmental Dynamics* 238(10): 2575-2587.

Blanco, M. J., Barrallo-Gimeno, A., Acloque, H., Reyes, A. E., Tada, M., Allende, M. L., Mayor, R. and Nieto, M. A. (2007) 'Snail1a and Snail1b cooperate in the anterior migration of the axial mesendoderm in the zebrafish embryo', *Development* 134(22): 4073-4081.

Boglev, Y., Badrock, A. P., Trotter, A. J., Du, Q., Richardson, E. J., Parslow, A. C., Markmiller, S. J., Hall, N. E., de Jong-Curtain, T. A., Ng, A. Y. et al. (2013) 'Autophagy Induction Is a Tor- and Tp53-Independent Cell Survival Response in a Zebrafish Model of Disrupted Ribosome Biogenesis', *PLoS Genet* 9(2): e1003279.

Bondurand, N., Kobetz, A., Pingault, V., Lemort, N., Encha-Razavi, F., Couly, G., Goerich, D. E., Wegner, M., Abitbol, M. and Goossens, M. (1998) 'Expression of the SOX10 gene during human development', *FEBS Letters* 432(3): 168-172.

Bondurand, N., Natarajan, D., Barlow, A., Thapar, N. and Pachnis, V. (2006) 'Maintenance of mammalian enteric nervous system progenitors by SOX10 and endothelin 3 signalling', *Development* 133(10): 2075-2086.

Bondurand, N., Pingault, V., Goerich, D. E., Lemort, N., Sock, E., Caignec, C. L., Wegner, M. and Goossens, M. (2000) 'Interaction among SOX10, PAX3 and MITF, three genes altered in Waardenburg syndrome', *Human Molecular Genetics* 9(13): 1907-1917.

Bonfils, G., Jaquenoud, M., Bontron, S., Ostrowicz, C., Ungermann, C. and De Virgilio, C. (2012) 'Leucyl-tRNA Synthetase Controls TORC1 via the EGO Complex', *Molecular Cell* 46(1): 105-110.

Boulon, S., Westman, B. J., Hutten, S., Boisvert, F.-M. and Lamond, A. I. (2010) 'The Nucleolus under Stress', *Molecular Cell* 40(2): 216-227.

Braglia, P., Kawauchi, J. and Proudfoot, N. J. (2011) 'Co-transcriptional RNA cleavage provides a failsafe termination mechanism for yeast RNA polymerase I', *Nucleic Acids Research* 39(4): 1439-1448.

Brodeur, G. M., Minturn, J. E., Ho, R., Simpson, A. M., Iyer, R., Varela, C. R., Light, J. E., Kolla, V. and Evans, A. E. (2009) 'Trk Receptor Expression and Inhibition in Neuroblastomas', *Clinical Cancer Research* 15(10): 3244-3250.

Bronner-Fraser, M. (1994) 'Neural crest cell formation and migration in the developing embryo', *The FASEB Journal* 8(10): 699-706.

Calmont, A., Ivins, S., Van Bueren, K. L., Papangeli, I., Kyriakopoulou, V., Andrews, W. D., Martin, J. F., Moon, A. M., Illingworth, E. A., Basson, M. A. et al. (2009) 'Tbx1 controls cardiac neural crest cell migration during arch artery development by regulating Gbx2 expression in the pharyngeal ectoderm', *Development* 136(18): 3173-3183.

Cano, A., Perez-Moreno, M. A., Rodrigo, I., Locascio, A., Blanco, M. J., del Barrio, M. G., Portillo, F. and Nieto, M. A. (2000) 'The transcription factor Snail controls epithelial-mesenchymal transitions by repressing E-cadherin expression', *Nat Cell Biol* 2(2): 76-83.

Cavanaugh, A. H., Hirschler-Laszkiewicz, I., Hu, Q., Dundr, M., Smink, T., Misteli, T. and Rothblum, L. I. (2002) 'Rrn3 Phosphorylation Is a Regulatory Checkpoint for Ribosome Biogenesis', *Journal of Biological Chemistry* 277(30): 27423-27432.

Cesaretti, C., Gentilin, B., Bianchi, V., Melloni, G., Bonaguro, M., Rossi, C., Meazzini, C., Brusati, R. and Lalatta, F. (2011) 'Occurrence of complete arhinia in two siblings with a clinical picture of Treacher Collins syndrome negative for TCOF1, POLR1D and POLR1C mutations', *Clinical dysmorphology* 20(4): 229-231 10.1097/MCD.0b013e3283491725.

Chabot, B., Stephenson, D. A., Chapman, V. M., Besmer, P. and Bernstein, A. (1988) 'The proto-oncogene c-kit encoding a transmembrane tyrosine kinase receptor maps to the mouse W locus', *Nature* 335(6185): 88-89.

Chakraborty, A., Uechi, T., Higa, S., Torihara, H. and Kenmochi, N. (2009) 'Loss of Ribosomal Protein L11 Affects Zebrafish Embryonic Development through a p53-Dependent Apoptotic Response', *PLoS ONE* 4(1): e4152.

Cheah, F. S. H., Winkler, C., Jabs, E. W. and Chong, S. S. (2010) 'tgfβ3 regulation of chondrogenesis and osteogenesis in zebrafish is mediated through formation and survival of a subpopulation of the cranial neural crest', *Mechanisms of Development* 127(7–8): 329-344.

Chédin, S., Riva, M., Schultz, P., Sentenac, A. and Carles, C. (1998) 'The RNA cleavage activity of RNA polymerase III is mediated by an essential TFIIS-like subunit and is important for transcription termination', *Genes & Development* 12(24): 3857-3871.

Chen, D., Zhang, Z., Li, M., Wang, W., Li, Y., Rayburn, E. R., Hill, D. L., Wang, H. and Zhang, R. (2007) 'Ribosomal protein S7 as a novel modulator of p53-MDM2 interaction: binding to MDM2, stabilization of p53 protein, and activation of p53 function', *Oncogene* 26(35): 5029-5037.

Chen, H.-K., Pai, C.-Y., Huang, J.-Y. and Yeh, N.-H. (1999) 'Human Nopp140, Which Interacts with RNA Polymerase I: Implications for rRNA Gene Transcription and Nucleolar Structural Organization', *Molecular and Cellular Biology* 19(12): 8536-8546.

Chen, W., Burgess, S., Golling, G., Amsterdam, A. and Hopkins, N. (2002) 'High-Throughput Selection of Retrovirus Producer Cell Lines Leads to Markedly Improved Efficiency of Germ Line-Transmissible Insertions in Zebra Fish', *Journal of Virology* 76(5): 2192-2198.

Cheng, Y.-C., Cheung, M., Abu-Elmagd, M. M., Orme, A. and Scotting, P. J. (2000) 'Chick Sox10, a transcription factor expressed in both early neural crest cells and central nervous system', *Developmental Brain Research* 121(2): 233-241.

Cheung, M., Chaboissier, M.-C., Mynett, A., Hirst, E., Schedl, A. and Briscoe, J. (2005) 'The Transcriptional Control of Trunk Neural Crest Induction, Survival, and Delamination', *Developmental cell* 8(2): 179-192.

Chiang, E. F. L., Pai, C.-I., Wyatt, M., Yan, Y.-L., Postlethwait, J. and Chung, B.-c. (2001) 'Two Sox9 Genes on Duplicated Zebrafish Chromosomes: Expression of Similar Transcription Activators in Distinct Sites', *Developmental Biology* 231(1): 149-163.

Choi, K.-Y., Kim, H.-J., Lee, M.-H., Kwon, T.-G., Nah, H.-D., Furuichi, T., Komori, T., Nam, S.-H., Kim, Y.-J., Kim, H.-J. et al. (2005) 'Runx2 regulates FGF2-induced Bmp2 expression during cranial bone development', *Developmental Dynamics* 233(1): 115-121.

203

Chu, W.-M., Wang, Z., Roeder, R. G. and Schmid, C. W. (1997) 'RNA Polymerase III Transcription Repressed by Rb through Its Interactions with TFIIIB and TFIIIC2', *Journal of Biological Chemistry* 272(23): 14755-14761.

Ciccia, A., Huang, J.-W., Izhar, L., Sowa, M. E., Harper, J. W. and Elledge, S. J. (2014) 'Treacher Collins syndrome TCOF1 protein cooperates with NBS1 in the DNA damage response', *Proceedings of the National Academy of Sciences* 111(52): 18631-18636.

Clay, M. R. and Halloran, M. C. (2014) 'Cadherin 6 promotes neural crest cell detachment via F-actin regulation and influences active Rho distribution during epithelial-to-mesenchymal transition', *Development* 141(12): 2506-2515.

Cmejlova, J., Dolezalova, L., Pospisilova, D., Petrtylova, K., Petrak, J. and Cmejla, R. (2006) 'Translational efficiency in patients with Diamond-Blackfan anemia', *Haematologica* 91(11): 1456-1464.

Colvin, J. S., Bohne, B. A., Harding, G. W., McEwen, D. G. and Ornitz, D. M. (1996) 'Skeletal overgrowth and deafness in mice lacking fibroblast growth factor receptor 3', *Nat Genet* 12(4): 390-397.

Cong, R., Das, S., Ugrinova, I., Kumar, S., Mongelard, F., Wong, J. and Bouvet, P. (2012) 'Interaction of nucleolin with ribosomal RNA genes and its role in RNA polymerase I transcription', *Nucleic Acids Research* 40(19): 9441-9454.

Connerney, J., Andreeva, V., Leshem, Y., Mercado, M. A., Dowell, K., Yang, X., Lindner, V., Friesel, R. E. and Spicer, D. B. (2008) 'Twist1 homodimers enhance FGF responsiveness of the cranial sutures and promote suture closure', *Developmental Biology* 318(2): 323-334.

Cordero, D. R., Brugmann, S., Chu, Y., Bajpai, R., Jame, M. and Helms, J. A. (2011) 'Cranial neural crest cells on the move: Their roles in craniofacial development', *American Journal of Medical Genetics Part A* 155(2): 270-279.

Cornell, R. A. and Eisen, J. S. (2000) 'Delta signaling mediates segregation of neural crest and spinal sensory neurons from zebrafish lateral neural plate', *Development* 127(13): 2873-2882.

Crighton, D., Woiwode, A., Zhang, C., Mandavia, N., Morton, J. P., Warnock, L. J., Milner, J., White, R. J. and Johnson, D. L. (2003) *p53 represses RNA polymerase III transcription by targeting TBP and inhibiting promoter occupancy by TFIIIB*.

Crump, J. G., Swartz, M. E. and Kimmel, C. B. (2004) 'An Integrin-Dependent Role of Pouch Endoderm in Hyoid Cartilage Development', *PLoS Biol* 2(9): e244.

Culbertson, M. D., Lewis, Z. R. and Nechiporuk, A. V. (2011) 'Chondrogenic and Gliogenic Subpopulations of Neural Crest Play Distinct Roles during the Assembly of Epibranchial Ganglia', *PLoS ONE* 6(9): e24443.

Curran, K., Raible, D. W. and Lister, J. A. (2009) 'Foxd3 controls melanophore specification in the zebrafish neural crest by regulation of Mitf', *Developmental Biology* 332(2): 408-417.

D'Amico-Martel, A. and Noden, D. M. (1983) 'Contributions of placodal and neural crest cells to avian cranial peripheral ganglia', *American Journal of Anatomy* 166(4): 445-468.

Dai, M.-S., Arnold, H., Sun, X.-X., Sears, R. and Lu, H. (2007) 'Inhibition of c-Myc activity by ribosomal protein L11', *EMBO J* 26(14): 3332-3345.

Dai, M.-S., Zeng, S. X., Jin, Y., Sun, X.-X., David, L. and Lu, H. (2004) 'Ribosomal Protein L23 Activates p53 by Inhibiting MDM2 Function in Response to Ribosomal Perturbation but Not to Translation Inhibition', *Molecular and Cellular Biology* 24(17): 7654-7668.

Danilova, N., Sakamoto, K. M. and Lin, S. (2008) 'Ribosomal protein S19 deficiency in zebrafish leads to developmental abnormalities and defective erythropoiesis through activation of p53 protein family', *Blood* 112(13): 5228-5237.

Danilova, N., Sakamoto, K. M. and Lin, S. (2011) 'Ribosomal protein L11 mutation in zebrafish leads to haematopoietic and metabolic defects', *British Journal of Haematology* 152(2): 217-228.

Dauwerse, J. G., Dixon, J., Seland, S., Ruivenkamp, C. A. L., van Haeringen, A., Hoefsloot, L. H., Peters, D. J. M., Boers, A. C.-d., Daumer-Haas, C., Maiwald, R. et al. (2011) 'Mutations in genes encoding subunits of RNA polymerases I and III cause Treacher Collins syndrome', *Nat Genet* 43(1): 20-22.

Davy, A., Aubin, J. and Soriano, P. (2004) 'Ephrin-B1 forward and reverse signaling are required during mouse development', *Genes & Development* 18(5): 572-583.

Davy, A., Bush, J. O. and Soriano, P. (2006) 'Inhibition of Gap Junction Communication at Ectopic Eph/ephrin Boundaries Underlies Craniofrontonasal Syndrome', *PLoS Biol* 4(10): e315.

Deng, C., Wynshaw-Boris, A., Zhou, F., Kuo, A. and Leder, P. (1996) 'Fibroblast Growth Factor Receptor 3 Is a Negative Regulator of Bone Growth', *Cell* 84(6): 911-921.

Deng, C., Zhang, P., Wade Harper, J., Elledge, S. J. and Leder, P. (1995) 'Mice Lacking p21CIP1/WAF1 undergo normal development, but are defective in G1 checkpoint control', *Cell* 82(4): 675-684.

Depew, M. J., Simpson, C. A., Morasso, M. and Rubenstein, J. L. R. (2005) 'Reassessing the Dlx code: the genetic regulation of branchial arch skeletal pattern and development', *Journal of Anatomy* 207(5): 501-561.

Deschamps, J. and van Nes, J. (2005) 'Developmental regulation of the Hox genes during axial morphogenesis in the mouse', *Development* 132(13): 2931-2942.

Dixon, J., Jones, N. C., Sandell, L. L., Jayasinghe, S. M., Crane, J., Rey, J.-P., Dixon, M. J. and Trainor, P. A. (2006) 'Tcof1/Treacle Is Required for Neural Crest Cell Formation and Proliferation Deficiencies That Cause Craniofacial Abnormalities', *Proceedings of the National Academy of Sciences of the United States of America* 103(36): 13403-13408.

Donati, G., Bertoni, S., Brighenti, E., Vici, M., Trere, D., Volarevic, S., Montanaro, L. and Derenzini, M. (2011a) 'The balance between rRNA and ribosomal protein synthesis up- and downregulates the tumour suppressor p53 in mammalian cells', *Oncogene* 30(29): 3274-3288.

Donati, G., Brighenti, E., Vici, M., Mazzini, G., Treré, D., Montanaro, L. and Derenzini, M. (2011b) 'Selective inhibition of rRNA transcription downregulates E2F-1: a new p53-independent mechanism linking cell growth to cell proliferation', *Journal of Cell Science* 124(17): 3017-3028.

Donati, G., Peddigari, S., Mercer, Carol A. and Thomas, G. (2013) '5S Ribosomal RNA Is an Essential Component of a Nascent Ribosomal Precursor Complex that Regulates the Hdm2-p53 Checkpoint', *Cell Reports* 4(1): 87-98.

Doray, B., Salomon, R., Amiel, J., Pelet, A., Touraine, R. L., Billaud, M., Attié, T., Bachy, B., Munnich, A. and Lyonnet, S. (1998) 'Mutation of the RET ligand, neurtutin, supports multigenic inheritance in Hirschsprung disease', *Human Molecular Genetics* 7(9): 1449-52.

Dorsky, R. I., Moon, R. T. and Raible, D. W. (1998) 'Control of neural crest cell fate by the Wnt signalling pathway', *Nature* 396(6709): 370-373.

Dorsky, R. I., Raible, D. W. and Moon, R. T. (2000) 'Direct regulation of nacre, a zebrafish MITF homolog required for pigment cell formation, by the Wnt pathway', *Genes & Development* 14(2): 158-162.

Dottori, M., Gross, M. K., Labosky, P. and Goulding, M. (2001) 'The winged-helix transcription factor Foxd3 suppresses interneuron differentiation and promotes neural crest cell fate', *Development* 128(21): 4127-4138.

Drakas, R., Tu, X. and Baserga, R. (2004) 'Control of cell size through phosphorylation of upstream binding factor 1 by nuclear phosphatidylinositol 3-kinase', *Proceedings of the National Academy of Sciences of the United States of America* 101(25): 9272-9276.

Dubreuil, V., Ramanantsoa, N., Trochet, D., Vaubourg, V., Amiel, J., Gallego, J., Brunet, J.-F. and Goridis, C. (2008) 'A human mutation in Phox2b causes lack of CO2 chemosensitivity, fatal central apnea, and specific loss of parafacial neurons', *Proceedings of the National Academy of Sciences* 105(3): 1067-1072.

Dupé, V. and Pellerin, I. (2009) 'Retinoic acid receptors exhibit cell-autonomous functions in cranial neural crest cells', *Developmental Dynamics* 238(10): 2701-2711.

Dutton, K. A., Pauliny, A., Lopes, S. S., Elworthy, S., Carney, T. J., Rauch, J., Geisler, R., Haffter, P. and Kelsh, R. N. (2001) 'Zebrafish colourless encodes sox10 and specifies non-ectomesenchymal neural crest fates', *Development* 128(21): 4113-4125.

Eberhart, J. K., Swartz, M. E., Crump, J. G. and Kimmel, C. B. (2006) 'Early Hedgehog signaling from neural to oral epithelium organizes anterior craniofacial development', *Development* 133(6): 1069-1077.

Edwards, S. J., Gladwin, A. J. and Dixon, M. J. (1997) 'The Mutational Spectrum in Treacher Collins Syndrome Reveals a Predominance of Mutations That Create a Premature-Termination Codon', *American Journal of Medical Genetics* 60: 515-524.

Elworthy, S., Lister, J. A., Carney, T. J., Raible, D. W. and Kelsh, R. N. (2003) 'Transcriptional regulation of mitfa accounts for the sox10 requirement in zebrafish melanophore development', *Development* 130(12): 2809-2818.

Elworthy, S., Pinto, J. P., Pettifer, A., Cancela, M. L. and Kelsh, R. N. (2005) 'Phox2b function in the enteric nervous system is conserved in zebrafish and is sox10-dependent', *Mechanisms of Development* 122(5): 659-669.

Engel, C., Sainsbury, S., Cheung, A. C., Kostrewa, D. and Cramer, P. (2013) 'RNA polymerase I structure and transcription regulation', *Nature* 502(7473): 650-655.

Epstein, D. J., Vekemans, M. and Gros, P. (1991) 'splotch (Sp2H), a mutation affecting development of the mouse neural tube, shows a deletion within the paired homeodomain of Pax-3', *Cell* 67(4): 767-774.

Essers, P. B., Pereboom, T. C., Goos, Y. J., Paridaen, J. T. and MacInnes, A. W. (2014) 'A comparative study of nucleostemin family members in zebrafish reveals specific roles in ribosome biogenesis', *Developmental Biology* 385(2): 304-315.

Felton-Edkins, Z. A., Fairley, J. A., Graham, E. L., Johnston, I. M., White, R. J. and Scott, P. H. (2003) *The mitogen‑activated protein (MAP) kinase ERK induces tRNA synthesis by phosphorylating TFIIIB*.

Fernández-Tornero, C., Böttcher, B., Rashid, U. J. and Müller, C. W. (2011) 'Analyzing RNA polymerase III by electron cryomicroscopy', *RNA Biology* 8(5): 760-765.

Fernandez-Tornero, C., Moreno-Morcillo, M., Rashid, U. J., Taylor, N. M. I., Ruiz, F. M., Gruene, T., Legrand, P., Steuerwald, U. and Muller, C. W. (2013) 'Crystal structure of the 14-subunit RNA polymerase I', *Nature* 502(7473): 644-649.

Ford, E., Voit, R., Liszt, G., Magin, C., Grummt, I. and Guarente, L. (2006) 'Mammalian Sir2 homolog SIRT7 is an activator of RNA polymerase I transcription', *Genes & Development* 20(9): 1075-1080.

Friedrich, J. K., Panov, K. I., Cabart, P., Russell, J. and Zomerdijk, J. C. B. M. (2005) 'TBP-TAF Complex SL1 Directs RNA Polymerase I Pre-initiation Complex Formation and Stabilizes Upstream Binding Factor at the rDNA Promoter', *Journal of Biological Chemistry* 280(33): 29551-29558.

Frisdal, A. and Trainor, P. A. (2014) 'Development and evolution of the pharyngeal apparatus', *Wiley Interdisciplinary Reviews: Developmental Biology* 3(6): 403-418.

Fumagalli, S., Di Cara, A., Neb-Gulati, A., Natt, F., Schwemberger, S., Hall, J., Babcock, G. F., Bernardi, R., Pandolfi, P. P. and Thomas, G. (2009) 'Absence of nucleolar disruption after impairment of 40S ribosome biogenesis reveals an rpL11-translation-dependent mechanism of p53 induction', *Nat Cell Biol* 11(4): 501-508.

Fürthauer, M., Van Celst, J., Thisse, C. and Thisse, B. (2004) 'Fgf signalling controls the dorsoventral patterning of the zebrafish embryo', *Development* 131(12): 2853-2864.

Gammill, L. S., Gonzalez, C. and Bronner-Fraser, M. (2007) 'Neuropilin 2/semaphorin 3F signaling is essential for cranial neural crest migration and trigeminal ganglion condensation', *Developmental Neurobiology* 67(1): 47-56.

Garg, V., Yamagishi, C., Hu, T., Kathiriya, I. S., Yamagishi, H. and Srivastava, D. (2001) 'Tbx1, a DiGeorge Syndrome Candidate Gene, Is Regulated by Sonic Hedgehog during Pharyngeal Arch Development', *Developmental Biology* 235(1): 62-73.

Garnett, A. T., Square, T. A. and Medeiros, D. M. (2012) 'BMP, Wnt and FGF signals are integrated through evolutionarily conserved enhancers to achieve robust expression of Pax3 and Zic genes at the zebrafish neural plate border', *Development* 139(22): 4220-4231.

Gazda, H. T., Sheen, M. R., Vlachos, A., Choesmel, V., O'Donohue, M.-F., Schneider, H., Darras, N., Hasman, C., Sieff, C. A., Newburger, P. E. et al. (2008) 'Ribosomal Protein L5 and L11 Mutations Are Associated with Cleft Palate and Abnormal Thumbs in Diamond-Blackfan Anemia Patients', *American journal of human genetics* 83(6): 769-780.

Geissler, E. N., Ryan, M. A. and Housman, D. E. (1988) 'The dominant-white spotting (W) locus of the mouse encodes the c-kit proto-oncogene', *Cell* 55(1): 185-192.

Giampietro, P. F., Armstrong, L., Stoddard, A., Blank, R. D., Livingston, J., Raggio, C. L., Rasmussen, K., Pickart, M., Lorier, R., Turner, A. et al. (2015) 'Whole exome sequencing identifies a POLRID mutation segregating in a father and two daughters with findings of Klippel–Feil and Treacher Collins syndromes', *American Journal of Medical Genetics Part A* 167(1): 95-102.

Gilbert, S. F. (2010) *Developmental Biology*, 9th Edition, Sunderland, MA, USA: Sinauer Associates, Inc.

Gjidoda, A. and Henry, R. W. (2013) 'RNA polymerase III repression by the Retinoblastoma tumor suppressor protein', *Biochimica et biophysica acta* 1829(3-4): 385-392.

Gladwin, A. J., Dixon, J., Loftus, S. K., Edwards, S., Wasmuth, J. J., Hennekam, R. C. M. and Dixon, M. J. (1996) 'Treacher Collins Syndrome may Result from Insertions, Deletions or Splicing Mutations, Which Introduce a Termination Codon into the Gene', *Human Molecular Genetics* 5(10): 1533-1538.

Gomez-Roman, N., Grandori, C., Eisenman, R. N. and White, R. J. (2003) 'Direct activation of RNA polymerase III transcription by c-Myc', *Nature* 421(6920): 290-294.

Gonzales, B., Henning, D., So, R. B., Dixon, J., Dixon, M. J. and Valdez, B. C. (2005) 'The Treacher Collins syndrome (TCOF1) gene product is involved in pre-rRNA methylation', *Human Molecular Genetics* 14(14): 2035-2043.

Goodfellow, S. and Zomerdijk, J. B. M. (2013) Basic Mechanisms in RNA Polymerase I Transcription of the Ribosomal RNA Genes. in T. K. Kundu (ed.) *Epigenetics: Development and Disease*, vol. 61: Springer Netherlands.

Griffin, J. N., Sondalle, S. B., del Viso, F., Baserga, S. J. and Khokha, M. K. (2015) 'The Ribosome Biogenesis Factor Nol11 Is Required for Optimal rDNA Transcription and Craniofacial Development in *Xenopus*, *PLoS Genet* 11(3): e1005018.

Grob, A., Roussel, P., Wright, J. E., McStay, B., Hernandez-Verdun, D. and Sirri, V. (2009) 'Involvement of SIRT7 in resumption of rDNA transcription at the exit from mitosis', *Journal of Cell Science* 122(4): 489-498.

Grummt, I. (2003) 'Life on a planet of its own: regulation of RNA polymerase I transcription in the nucleolus', *Genes & Development* 17(14): 1691-1702.

Grummt, I., Rosenbauer, H., Niedermeyer, I., Maier, U. and Öhrlein, A. (1986) 'A repeated 18 bp sequence motif in the mouse rDNA spacer mediates binding of a nuclear factor and transcription termination', *Cell* 45(6): 837-846.

Guillemot, F., Lo, L.-C., Johnson, J. E., Auerbach, A., Anderson, D. J. and Joyner, A. L. (1993) 'Mammalian achaete-scute homolog 1 is required for the early development of olfactory and autonomic neurons', *Cell* 75(3): 463-476.

Gunderson, J. H., Sogin, M. L., Wollett, G., Hollingdale, M., Cruz, V. F. D. L., Waters, A. P. and McCutchan, T. F. (1987) 'Structurally Distinct, Stage-Specific Ribosomes Occur in Plasmodium', *Science* 238(4829): 933-937.

Guo, S., Brush, J., Teraoka, H., Goddard, A., Wilson, S. W., Mullins, M. C. and Rosenthal, A. (1999) 'Development of Noradrenergic Neurons in the Zebrafish Hindbrain Requires BMP, FGF8, and the Homeodomain Protein Soulless/Phox2a', *Neuron* 24(3): 555-566.

Hall, B. K. (2000) 'The neural crest as a fourth germ layer and vertebrates as quadroblastic not triploblastic', *Evolution & Development* 2(1): 3-5.

Hammond, C. L. and Schulte-Merker, S. (2009) 'Two populations of endochondral osteoblasts with differential sensitivity to Hedgehog signalling', *Development* 136(23): 3991-4000.

Han, J., Ishii, M., Bringas Jr, P., Maas, R. L., Maxson Jr, R. E. and Chai, Y. (2007) 'Concerted action of Msx1 and Msx2 in regulating cranial neural crest cell differentiation during frontal bone development', *Mechanisms of Development* 124(9–10): 729-745.

Han, Jung M., Jeong, Seung J., Park, Min C., Kim, G., Kwon, Nam H., Kim, Hoi K., Ha, Sang H., Ryu, Sung H. and Kim, S. (2012) 'Leucyl-tRNA Synthetase Is an Intracellular Leucine Sensor for the mTORC1-Signaling Pathway', *Cell* 149(2): 410-424.

Hanada, K., Song, C. Z., Yamamoto, K., Yano, K., Maeda, Y., Yamaguchi, K. and Muramatsu, M. (1996) 'RNA polymerase I associated factor 53 binds to the nucleolar transcription factor UBF and functions in specific rDNA transcription', *The EMBO Journal* 15(9): 2217-2226.

Hannan, K. M., Brandenburger, Y., Jenkins, A., Sharkey, K., Cavanaugh, A., Rothblum, L., Moss, T., Poortinga, G., McArthur, G. A., Pearson, R. B. et al. (2003) 'mTOR-Dependent Regulation of Ribosomal Gene Transcription Requires S6K1 and Is Mediated by Phosphorylation of the Carboxy-Terminal Activation Domain of the Nucleolar Transcription Factor UBF†', *Molecular and Cellular Biology* 23(23): 8862-8877.

Hannan, K. M., Sanij, E., Rothblum, L. I., Hannan, R. D. and Pearson, R. B. (2013) 'Dysregulation of RNA polymerase I transcription during disease', *Biochimica et Biophysica Acta (BBA) - Gene Regulatory Mechanisms* 1829(3–4): 342-360.

Hari, L., Miescher, I., Shakhova, O., Suter, U., Chin, L., Taketo, M., Richardson, W. D., Kessaris, N. and Sommer, L. (2012) 'Temporal control of neural crest lineage generation by Wnt/β-catenin signaling', *Development* 139(12): 2107-2117.

Haupt, Y., Maya, R., Kazaz, A. and Oren, M. (1997) 'Mdm2 promotes the rapid degradation of p53', *Nature* 387(6630): 296-299.

Haworth, K. E., Healy, C., Morgan, P. and Sharpe, P. T. (2004) 'Regionalisation of early head ectoderm is regulated by endoderm and prepatterns the orofacial epithelium', *Development* 131(19): 4797-4806.

Haworth, K. E., Wilson, J. M., Grevellec, A., Cobourne, M. T., Healy, C., Helms, J. A., Sharpe, P. T. and Tucker, A. S. (2007) 'Sonic hedgehog in the pharyngeal endoderm controls arch pattern via regulation of Fgf8 in head ectoderm', *Developmental Biology* 303(1): 244-258.

Helmbold, H., Komm, N., Deppert, W. and Bohn, W. (2009) 'Rb2/p130 is the dominating pocket protein in the p53-p21 DNA damage response pathway leading to senescence', *Oncogene* 28(39): 3456-3467.

Hendzel, M. J., Wei, Y., Mancini, M. A., Van Hooser, A., Ranalli, T., Brinkley, B. R., Bazett-Jones, D. P. and Allis, C. D. (1997) 'Mitosis-specific phosphorylation of histone H3 initiates primarily within pericentromeric heterochromatin during G2 and spreads in an ordered fashion coincident with mitotic chromosome condensation', *Chromosoma* 106(6): 348-360.

Hoffman, T. L., Javier, A. L., Campeau, S. A., Knight, R. D. and Schilling, T. F. (2007) 'Tfap2 transcription factors in zebrafish neural crest development and ectodermal

evolution', *Journal of Experimental Zoology Part B: Molecular and Developmental Evolution* 308B(5): 679-691.

Holleville, N., Matéos, S., Bontoux, M., Bollerot, K. and Monsoro-Burq, A. H. (2007) 'Dlx5 drives Runx2 expression and osteogenic differentiation in developing cranial suture mesenchyme', *Developmental Biology* 304(2): 860-874.

Holzschuh, J., Wada, N., Wada, C., Schaffer, A., Javidan, Y., Tallafuß, A., Bally-Cuif, L. and Schilling, T. F. (2005) 'Requirements for endoderm and BMP signaling in sensory neurogenesis in zebrafish', *Development* 132(16): 3731-3742.

Honda, R., Tanaka, H. and Yasuda, H. (1997) 'Oncoprotein MDM2 is a ubiquitin ligase E3 for tumor suppressor p53', *FEBS Letters* 420(1): 25-27.

Honoré, S. M., Aybar, M. J. and Mayor, R. (2003) 'Sox10 is required for the early development of the prospective neural crest in Xenopus embryos', *Developmental Biology* 260(1): 79-96.

Hornyak, T. J., Hayes, D. J., Chiu, L.-Y. and Ziff, E. B. (2001) 'Transcription factors in melanocyte development: distinct roles for Pax-3 and Mitf', *Mechanisms of Development* 101(1–2): 47-59.

Hoth, C. F., Milunsky, A., Lipsky, N., Sheffer, R., Clarren, S. K. and Baldwin, C. T. (1993) 'Mutations in the paired domain of the human PAX3 gene cause Klein-Waardenburg syndrome (WS-III) as well as Waardenburg syndrome type I (WS-I)', *American journal of human genetics* 52(3): 455-62.

Huang, E., Nocka, K., Beier, D. R., Chu, T.-Y., Buck, J., Lahm, H.-W., Wellner, D., Leder, P. and Besmer, P. (1990) 'The hematopoietic growth factor KL is encoded by the SI locus and is the ligand of the c-kit receptor, the gene product of the W locus', *Cell* 63(1): 225-233.

Hunter, M. P. and Prince, V. E. (2002) 'Zebrafish Hox Paralogue Group 2 Genes Function Redundantly as Selector Genes to Pattern the Second Pharyngeal Arch', *Developmental Biology* 247(2): 367-389.

Ide, S., Miyazaki, T., Maki, H. and Kobayashi, T. (2010) 'Abundance of Ribosomal RNA Gene Copies Maintains Genome Integrity', *Science* 327(5966): 693-696.
Iseki, S., Wilkie, A. O. and Morriss-Kay, G. M. (1999) 'Fgfr1 and Fgfr2 have distinct differentiation- and proliferation-related roles in the developing mouse skull vault', *Development* 126(24): 5611-5620.

Ishii, M., Merrill, A. E., Chan, Y.-S., Gitelman, I., Rice, D. P. C., Sucov, H. M. and Maxson, R. E. (2003) 'Msx2 and Twist cooperatively control the development of the neural crest-derived skeletogenic mesenchyme of the murine skull vault', *Development* 130(24): 6131-6142.

Jaako, P., Debnath, S., Olsson, K., Bryder, D., Flygare, J. and Karlsson, S. (2012) 'Dietary L-leucine improves the anemia in a mouse model for Diamond-Blackfan anemia', *Blood* 120(11): 2225-2228.

Jaako, P., Debnath, S., Olsson, K., Zhang, Y., Flygare, J., Lindstrom, M. S., Bryder, D. and Karlsson, S. (2015) 'Disruption of the 5S RNP-Mdm2 interaction significantly improves the erythroid defect in a mouse model for Diamond-Blackfan anemia', *Leukemia*.

Jaako, P., Flygare, J., Olsson, K., Quere, R., Ehinger, M., Henson, A., Ellis, S., Schambach, A., Baum, C., Richter, J. et al. (2011) 'Mice with ribosomal protein S19 deficiency develop bone marrow failure and symptoms like patients with Diamond-Blackfan anemia', *Blood* 118(23): 6087-6096.

James, A., Wang, Y., Raje, H., Rosby, R. and DiMario, P. (2014) 'Nucleolar stress with and without p53', *Nucleus* 5(5): 402-426.

Jansa, P. and Grummt, I. (1999) 'Mechanism of transcription termination: PTRF interacts with the largest subunit of RNA polymerase I and dissociates paused transcription complexes from yeast and mouse', *Molecular and General Genetics MGG* 262(3): 508-514.

Jantzen, H.-M., Admon, A., Bell, S. P. and Tjian, R. (1990) 'Nucleolar transcription factor hUBF contains a DNA-binding motif with homology to HMG proteins', *Nature* 344(6269): 830-836.

Jasiak, A. J., Armache, K.-J., Martens, B., Jansen, R.-P. and Cramer, P. (2006) 'Structural Biology of RNA Polymerase III: Subcomplex C17/25 X-Ray Structure and 11 Subunit Enzyme Model', *Molecular Cell* 23(1): 71-81.

Jerome, L. A. and Papaioannou, V. E. (2001) 'DiGeorge syndrome phenotype in mice mutant for the T-box gene, Tbx1', *Nat Genet* 27(3): 286-291.

Jiang, R., Lan, Y., Norton, C. R., Sundberg, J. P. and Gridley, T. (1998) 'The slug gene is not essential for mesoderm or neural crest development in mice', *Developmental Biology* 198(2): 277-285.

Jiang, X., Iseki, S., Maxson, R. E., Sucov, H. M. and Morriss-Kay, G. M. (2002) 'Tissue Origins and Interactions in the Mammalian Skull Vault', *Developmental Biology* 241(1): 106-116.

Jin, A., Itahana, K., O'Keefe, K. and Zhang, Y. (2004) 'Inhibition of HDM2 and Activation of p53 by Ribosomal Protein L23', *Molecular and Cellular Biology* 24(17): 7669-7680.

Johnson, D., Iseki, S., Wilkie, A. O. M. and Morriss-Kay, G. M. (2000) 'Expression patterns of Twist and Fgfr1, -2 and -3 in the developing mouse coronal suture suggest a key role for Twist in suture initiation and biogenesis', *Mechanisms of Development* 91(1–2): 341-345.

Jones, N. C., Lynn, M. L., Gaudenz, K., Sakai, D., Aoto, K., Rey, J.-P., Glynn, E. F., Ellington, L., Du, C., Dixon, J. et al. (2008) 'Prevention of the neurocristopathy Treacher Collins syndrome through inhibition of p53 function', *Nat Med* 14(2): 125-133.

Kague, E., Gallagher, M., Burke, S., Parsons, M., Franz-Odendaal, T. and Fisher, S. (2012) 'Skeletogenic Fate of Zebrafish Cranial and Trunk Neural Crest', *PLoS ONE* 7(11): e47394.

Kantidakis, T., Ramsbottom, B. A., Birch, J. L., Dowding, S. N. and White, R. J. (2010) 'mTOR associates with TFIIIC, is found at tRNA and 5S rRNA genes, and targets their repressor Maf1', *Proceedings of the National Academy of Sciences* 107(26): 11823-11828.

Kassavetis, G. A., Prakash, P. and Shim, E. (2010) 'The C53/C37 Subcomplex of RNA Polymerase III Lies Near the Active Site and Participates in Promoter Opening', *Journal of Biological Chemistry* 285(4): 2695-2706.

Kawase, T., Ohki, R., Shibata, T., Tsutsumi, S., Kamimura, N., Inazawa, J., Ohta, T., Ichikawa, H., Aburatani, H., Tashiro, F. et al. (2009) 'PH Domain-Only Protein PHLDA3 Is a p53-Regulated Repressor of Akt', *Cell* 136(3): 535-550.

Kelsh, R. N. (2006) 'Sorting out Sox10 functions in neural crest development', *BioEssays* 28(8): 788-798.

Kelsh, R. N., Dutton, K., Medlin, J. and Eisen, J. S. (2000) 'Expression of zebrafish fkd6 in neural crest-derived glia', *Mechanisms of Development* 93(1–2): 161-164.

Keshet, E., Lyman, S. D., Williams, D. E., Anderson, D. M., Jenkins, N. A., Copeland, N. G. and Parada, L. F. (1991) 'Embryonic RNA expression patterns of the *c-kit* receptor and its cognate ligan suggest multiple functional roles in mouse development', *EMBO J* 10(9): 2425-2435.

Kessel, M. and Gruss, P. (1991) 'Homeotic transformations of murine vertebrae and concomitant alteration of Hox codes induced by retinoic acid', *Cell* 67(1): 89-104.

Kimmel, C. B., Ballard, W. W., Kimmel, S. R., Ullmann, B. and Schilling, T. F. (1995) 'Stages of embryonic development of the zebrafish', *Developmental Dynamics* 203(3): 253-310.

Kimmel, C. B., Miller, C. T. and Moens, C. B. (2001) 'Specification and Morphogenesis of the Zebrafish Larval Head Skeleton', *Developmental Biology* 233(2): 239-257.

Kimmel, C. B., Ullmann, B., Walker, M., Miller, C. T. and Crump, J. G. (2003) 'Endothelin 1-mediated regulation of pharyngeal bone development in zebrafish', *Development* 130(7): 1339-1351.

Kirby, M. L., Cheng, G. H., Stadt, H. and Hunter, G. (1995) 'Differential Expression of the L10 Ribosomal Protein during Heart Development', *Biochemical and Biophysical Research Communications* 212(2): 461-465.

Klymkowsky, M. W., Rossi, C. C. and Artinger, K. B. (2010) 'Mechanisms driving neural crest induction and migration in the zebrafish and Xenopus laevis', *Cell Adhesion & Migration* 4(4): 595-608.

Knecht, A. K. and Bronner-Fraser, M. (2002) 'Induction of the neural crest: a multigene process', *Nat Rev Genet* 3(6): 453-461.

Komori, T., Yagi, H., Nomura, S., Yamaguchi, A., Sasaki, K., Deguchi, K., Shimizu, Y., Bronson, R. T., Gao, Y. H., Inada, M. et al. (1997) 'Targeted Disruption of Cbfa1 Results in a Complete Lack of Bone Formation owing to Maturational Arrest of Osteoblasts', *Cell* 89(5): 755-764.

Kondrashov, N., Pusic, A., Stumpf, C. R., Shimizu, K., Hsieh, Andrew C., Xue, S., Ishijima, J., Shiroishi, T. and Barna, M. (2011) 'Ribosome-Mediated Specificity in Hox mRNA Translation and Vertebrate Tissue Patterning', *Cell* 145(3): 383-397.

Kontges, G. and Lumsden, A. (1996) 'Rhombencephalic neural crest segmentation is preserved throughout craniofacial ontogeny', *Development* 122(10): 3229-3242.

Kopinke, D., Sasine, J., Swift, J., Stephens, W. Z. and Piotrowski, T. (2006) 'Retinoic acid is required for endodermal pouch morphogenesis and not for pharyngeal endoderm specification', *Developmental Dynamics* 235(10): 2695-2709.

Kressler, D., Hurt, E. and Baβler, J. (2010) 'Driving ribosome assembly', *Biochimica et Biophysica Acta (BBA) - Molecular Cell Research* 1803(6): 673-683.

Kubbutat, M. H. G., Jones, S. N. and Vousden, K. H. (1997) 'Regulation of p53 stability by Mdm2', *Nature* 387(6630): 299-303.

Kubota, Y. and Ito, K. (2000) 'Chemotactic migration of mesencephalic neural crest cells in the mouse', *Developmental Dynamics* 217(2): 170-179.

Kuhlbrodt, K., Herbarth, B., Sock, E., Hermans-Borgmeyer, I. and Wegner, M. (1998) 'Sox10, a Novel Transcriptional Modulator in Glial Cells', *The Journal of Neuroscience* 18(1): 237-250.

Kumazawa, T., Nishimura, K., Katagiri, N., Hashimoto, S., Hayashi, Y. and Kimura, K. (2015) 'Gradual reduction in rRNA transcription triggers p53 acetylation and apoptosis via MYBBP1A', *Scientific Reports* 5: 10854.

LaBonne, C. and Bronner-Fraser, M. (1998) 'Neural crest induction in Xenopus: evidence for a two-signal model', *Development* 125(13): 2403-2414.

LaBonne, C. and Bronner-Fraser, M. (1999) 'Molecular Mechanisms of Neural Crest Formation', *Annual Review of Cell and Developmental Biology* 15(1): 81-112.

Labosky, P. A. and Kaestner, K. H. (1998) 'The winged helix transcription factor Hfh2 is expressed in neural crest and spinal cord during mouse development', *Mechanisms of Development* 76(1–2): 185-190.

Laferté, A., Favry, E., Sentenac, A., Riva, M., Carles, C. and Chédin, S. (2006) 'The transcriptional activity of RNA polymerase I is a key determinant for the level of all ribosome components', *Genes & Development* 20(15): 2030-2040.

Lafontaine, D. L. J. and Tollervey, D. (2001) 'The function and synthesis of ribosomes', *Nat Rev Mol Cell Biol* 2(7): 514-520.

Lalo, D., Carles, C., Sentenac, A. and Thuriaux, P. (1993) 'Interactions between three common subunits of yeast RNA polymerases I and III', *Proceedings of the National Academy of Sciences* 90(12): 5524-5528.

Larsen, D. H., Hari, F., Clapperton, J. A., Gwerder, M., Gutsche, K., Altmeyer, M., Jungmichel, S., Toledo, L. I., Fink, D., Rask, M.-B. et al. (2014) 'The NBS1–Treacle complex controls ribosomal RNA transcription in response to DNA damage', *Nat Cell Biol* 16(8): 792-803.

Lawson, N. D. and Weinstein, B. M. (2002) 'In Vivo Imaging of Embryonic Vascular Development Using Transgenic Zebrafish', *Developmental Biology* 248(2): 307-318.

216

Le Douarin, N. M. and Kalcheim, C. (1999) *The Neural Crest*, Cambridge, United Kingdom: Cambridge University Press.

Lee, H.-Y., Kléber, M., Hari, L., Brault, V., Suter, U., Taketo, M. M., Kemler, R. and Sommer, L. (2004) 'Instructive Role of Wnt/ß-Catenin in Sensory Fate Specification in Neural Crest Stem Cells', *Science* 303(5660): 1020-1023.

Lee, K.-S., Kim, H.-J., Li, Q.-L., Chi, X.-Z., Ueta, C., Komori, T., Wozney, J. M., Kim, E.-G., Choi, J.-Y., Ryoo, H.-M. et al. (2000) 'Runx2 Is a Common Target of Transforming Growth Factor β1 and Bone Morphogenetic Protein 2, and Cooperation between Runx2 and Smad5 Induces Osteoblast-Specific Gene Expression in the Pluripotent Mesenchymal Precursor Cell Line C2C12', *Molecular and Cellular Biology* 20(23): 8783-8792.

Lefebvre, V. (2010) 'The SoxD transcription factors – Sox5, Sox6, and Sox13 – are key cell fate modulators', *The International Journal of Biochemistry & Cell Biology* 42(3): 429-432.

Lenton, K., James, A. W., Manu, A., Brugmann, S. A., Birker, D., Nelson, E. R., Leucht, P., Helms, J. A. and Longaker, M. T. (2011) 'Indian hedgehog positively regulates calvarial ossification and modulates bone morphogenetic protein signaling', *genesis* 49(10): 784-796.

Lewis, J. L., Bonner, J., Modrell, M., Ragland, J. W., Moon, R. T., Dorsky, R. I. and Raible, D. W. (2004) 'Reiterated Wnt signaling during zebrafish neural crest development', *Development* 131(6): 1299-1308.

Lipton, J. M. and Ellis, S. R. (2009) 'Diamond-Blackfan Anemia: Diagnosis, Treatment, and Molecular Pathogenesis', *Hematol Oncol Clin North Am* 23(2): 261-282.

Lister, J. A., Cooper, C., Nguyen, K., Modrell, M., Grant, K. and Raible, D. W. (2006) 'Zebrafish Foxd3 is required for development of a subset of neural crest derivatives', *Developmental Biology* 290(1): 92-104.

Lo, L., Morin, X., Brunet, J.-F. and Anderson, D. J. (1999) 'Specification of Neurotransmitter Identity by Phox2 Proteins in Neural Crest Stem Cells', *Neuron* 22(4): 693-705.

Lohnes, D., Mark, M., Mendelsohn, C., Dolle, P., Dierich, A., Gorry, P., Gansmuller, A. and Chambon, P. (1994) 'Function of the retinoic acid receptors (RARs) during development (I). Craniofacial and skeletal abnormalities in RAR double mutants', *Development* 120(10): 2723-2748.

Lohrum, M. A. E., Ludwig, R. L., Kubbutat, M. H. G., Hanlon, M. and Vousden, K. H. (2003) 'Regulation of HDM2 activity by the ribosomal protein L11', *Cancer Cell* 3(6): 577-587.

Lowery, L. A. and Sive, H. (2004) 'Strategies of vertebrate neurulation and a re-evaluation of teleost neural tube formation', *Mechanisms of Development* 121(10): 1189-1197.

Lucas, M. E., Müller, F., Rüdiger, R., Henion, P. D. and Rohrer, H. (2006) 'The bHLH transcription factor hand2 is essential for noradrenergic differentiation of sympathetic neurons', *Development* 133(20): 4015-4024.

Lumsden, A., Sprawson, N. and Graham, A. (1991) 'Segmental origin and migration of neural crest cells in the hindbrain region of the chick embryo', *Development* 113(4): 1281-1291.

Macatee, T. L., Hammond, B. P., Arenkiel, B. R., Francis, L., Frank, D. U. and Moon, A. M. (2003) 'Ablation of specific expression domains reveals discrete functions of ectoderm- and endoderm-derived FGF8 during cardiovascular and pharyngeal development', *Development* 130(25): 6361-6374.

Maden, C. H., Gomes, J., Schwarz, Q., Davidson, K., Tinker, A. and Ruhrberg, C. (2012) 'NRP1 and NRP2 cooperate to regulate gangliogenesis, axon guidance and target innervation in the sympathetic nervous system', *Developmental Biology* 369(2): 277-285.

Marchant, L., Linker, C., Ruiz, P., Guerrero, N. and Mayor, R. (1998) 'The inductive properties of mesoderm suggest that the neural crest cells are specified by a BMP gradient', *Developmental Biology* 198(2): 319-329.

Marechal, V., Elenbaas, B., Piette, J., Nicolas, J. C. and Levine, A. J. (1994) 'The ribosomal L5 protein is associated with mdm-2 and mdm-2-p53 complexes', *Molecular and Cellular Biology* 14(11): 7414-7420.

Mark, M., Ghyselinck, N. B. and Chambon, P. (2004) 'Retinoic acid signalling in the development of branchial arches', *Current Opinion in Genetics & Development* 14(5): 591-598.

Marsh, K. L., Dixon, J. and Dixon, M. J. (1998) 'Mutations in the Treacher Collins Syndrome Gene Lead to Mislocalization of the Nucleolar Protein Treacle', *Human Molecular Genetics* 7(11): 1795-1800.

Marygold, S. J., Roote, J., Reuter, G., Lambertsson, A., Ashburner, M., Millburn, G. H., Harrison, P. M., Yu, Z., Kenmochi, N., Kaufman, T. C. et al. (2007) 'The ribosomal protein genes and Minute loci of *Drosophila melanogaster*', *Genome Biology* 8: R216.

Matsuda, K., Yoshida, K., Taya, Y., Nakamura, K., Nakamura, Y. and Arakawa, H. (2002) 'p53AIP1 Regulates the Mitochondrial Apoptotic Pathway', *Cancer Research* 62(10): 2883-2889.

Mayer, C., Bierhoff, H. and Grummt, I. (2005) 'The nucleolus as a stress sensor: JNK2 inactivates the transcription factor TIF-IA and down-regulates rRNA synthesis', *Genes & Development* 19(8): 933-941.

Mayer, C., Zhao, J., Yuan, X. and Grummt, I. (2004) 'mTOR-dependent activation of the transcription factor TIF-IA links rRNA synthesis to nutrient availability', *Genes & Development* 18(4): 423-434.

Mayor, R. and Aybar, M. (2001) 'Induction and development of neural crest in *Xenopus laevis*', *Cell and Tissue Research* 305(2): 203-209.

McGowan, K. A., Li, J. Z., Park, C. Y., Beaudry, V., Tabor, H. K., Sabnis, A. J., Zhang, W., Fuchs, H., de Angelis, M. H., Myers, R. M. et al. (2008) 'Ribosomal mutations cause p53-mediated dark skin and pleiotropic effects', *Nat Genet* 40(8): 963-970.

Medeiros, D. M. and Crump, J. G. (2012) 'New perspectives on pharyngeal dorsoventral patterning in development and evolution of the vertebrate jaw', *Developmental Biology* 371(2): 121-135.

Merrill, Amy E., Sarukhanov, A., Krejci, P., Idoni, B., Camacho, N., Estrada, Kristine D., Lyons, Karen M., Deixler, H., Robinson, H., Chitayat, D. et al. (2012) 'Bent Bone Dysplasia-FGFR2 type, a Distinct Skeletal Disorder, Has Deficient Canonical FGF Signaling', *The American Journal of Human Genetics* 90(3): 550-557.

Miller, C. T., Schilling, T. F., Lee, K., Parker, J. and Kimmel, C. B. (2000) 'sucker encodes a zebrafish Endothelin-1 required for ventral pharyngeal arch development', *Development* 127(17): 3815-3828.

Miller, C. T., Yelon, D., Stainier, D. Y. R. and Kimmel, C. B. (2003) 'Two endothelin 1 effectors, hand2 and bapx1, pattern ventral pharyngeal cartilage and the jaw joint', *Development* 130(7): 1353-1365.

Miller, G., Panov, K. I., Friedrich, J. K., Trinkle-Mulcahy, L., Lamond, A. I. and Zomerdijk, J. C. B. M. (2001) *hRRN3 is essential in the SL1-mediated recruitment of RNA Polymerase I to rRNA gene promoters*.

Minchin, J. E. N. and Hughes, S. M. (2008) 'Sequential actions of Pax3 and Pax7 drive xanthophore development in zebrafish neural crest', *Developmental Biology* 317(2): 508-522.

Minoux, M., Antonarakis, G. S., Kmita, M., Duboule, D. and Rijli, F. M. (2009) 'Rostral and caudal pharyngeal arches share a common neural crest ground pattern', *Development* 136(4): 637-645.

Minoux, M. and Rijli, F. M. (2010) 'Molecular mechanisms of cranial neural crest cell migration and patterning in craniofacial development', *Development* 137(16): 2605-2621.

Mori-Akiyama, Y., Akiyama, H., Rowitch, D. H. and de Crombrugghe, B. (2003) 'Sox9 is required for determination of the chondrogenic cell lineage in the cranial neural crest', *Proceedings of the National Academy of Sciences* 100(16): 9360-9365.

Morikawa, Y., Zehir, A., Maska, E., Deng, C., Schneider, M. D., Mishina, Y. and Cserjesi, P. (2009) 'BMP signaling regulates sympathetic nervous system development through Smad4-dependent and -independent pathways', *Development* 136(21): 3575-3584.

Murano, K., Okuwaki, M., Hisaoka, M. and Nagata, K. (2008) 'Transcription Regulation of the rRNA Gene by a Multifunctional Nucleolar Protein, B23/Nucleophosmin, through Its Histone Chaperone Activity', *Molecular and Cellular Biology* 28(10): 3114-3126.

Muth, V., Nadaud, S., Grummt, I. and Voit, R. (2001) *Acetylation of TAFI68, a subunit of TIF-IB/SL1, activates RNA polymerase I transcription*.

Nair, S., Li, W., Cornell, R. and Schilling, T. F. (2007) 'Requirements for Endothelin type-A receptors and Endothelin-1 signaling in the facial ectoderm for the patterning of skeletogenic neural crest cells in zebrafish', *Development* 134(2): 335-345.

Narla, A. and Ebert, B. L. (2010) 'Ribosomopathies: human disorders of ribosome dysfunction', *Blood* 115(16): 3196-3205.

Neben, C. L., Idoni, B., Salva, J. E., Tuzon, C. T., Rice, J. C., Krakow, D. and Merrill, A. E. (2014) 'Bent bone dysplasia syndrome reveals nucleolar activity for FGFR2 in ribosomal DNA transcription', *Human Molecular Genetics*.

Nechiporuk, A., Linbo, T., Poss, K. D. and Raible, D. W. (2007) 'Specification of epibranchial placodes in zebrafish', *Development* 134(3): 611-623.

Nechiporuk, A., Linbo, T. and Raible, D. W. (2005) 'Endoderm-derived Fgf3 is necessary and sufficient for inducing neurogenesis in the epibranchial placodes in zebrafish', *Development* 132(16): 3717-3730.

Ng, L.-J., Wheatley, S., Muscat, G. E. O., Conway-Campbell, J., Bowles, J., Wright, E., Bell, D. M., Tam, P. P. L., Cheah, K. S. E. and Koopman, P. (1997) 'SOX9 Binds DNA,

Activates Transcription, and Coexpresses with Type II Collagen during Chondrogenesis in the Mouse', *Developmental Biology* 183(1): 108-121.

Ng, S. B., Buckingham, K. J., Lee, C., Bigham, A. W., Tabor, H. K., Dent, K. M., Huff, C. D., Shannon, P. T., Jabs, E. W., Nickerson, D. A. et al. (2010) 'Exome sequencing identifies the cause of a mendelian disorder', *Nat Genet* 42(1): 30-35.

Nguyen, V. H., Schmid, B., Trout, J., Connors, S. A., Ekker, M. and Mullins, M. C. (1998) 'Ventral and Lateral Regions of the Zebrafish Gastrula, Including the Neural Crest Progenitors, Are Established by abmp2b/swirlPathway of Genes', *Developmental Biology* 199(1): 93-110.

Nikoletopoulou, V., Markaki, M., Palikaras, K. and Tavernarakis, N. (2013) 'Crosstalk between apoptosis, necrosis and autophagy', *Biochimica et Biophysica Acta (BBA) - Molecular Cell Research* 1833(12): 3448-3459.

Nitzan, E., Krispin, S., Pfaltzgraff, E. R., Klar, A., Labosky, P. A. and Kalcheim, C. (2013) 'A dynamic code of dorsal neural tube genes regulates the segregation between neurogenic and melanogenic neural crest cells', *Development* 140(11): 2269-2279.

O'Sullivan, A. C., Sullivan, G. J. and McStay, B. (2002) 'UBF Binding In Vivo Is Not Restricted to Regulatory Sequences within the Vertebrate Ribosomal DNA Repeat', *Molecular and Cellular Biology* 22(2): 657-658.

Odenthal, J. and Nüsslein-Volhard, C. (1998) '*fork head* domain genes in zebrafish', *Dev Genes Evol* 208: 245-248.

Olesnicky Killian, E. C., Birkholz, D. A. and Artinger, K. B. (2009) 'A role for chemokine signaling in neural crest cell migration and craniofacial development', *Developmental Biology* 333(1): 161-172.

Oliner, J. D., Pietenpol, J. A., Thiagalingam, S., Gyuris, J., Kinzler, K. W. and Vogelstein, B. (1993) 'Oncoprotein MDM2 conceals the activation domain of tumour suppressor p53', *Nature* 362(6423): 857-860.

Orioli, A., Pascali, C., Pagano, A., Teichmann, M. and Dieci, G. (2012) 'RNA polymerase III transcription control elements: Themes and variations', *Gene* 493(2): 185-194.

Orr-Urtreger, A., Bedford, M. T., Burakova, T., Arman, E., Zimmer, Y., Yayon, A., Givol, D. and Lonai, P. (1993) 'Developmental Localization of the Splicing Alternatives of Fibroblast Growth Factor Receptor-2 (FGFR2)', *Developmental Biology* 158(2): 475-486.

Otto, F., Kanegane, H. and Mundlos, S. (2002) 'Mutations in the RUNX2 gene in patients with cleidocranial dysplasia', *Human Mutation* 19(3): 209-216.

Panov, K. I., Friedrich, J. K., Russell, J. and Zomerdijk, J. C. B. M. (2006a) 'UBF activates RNA polymerase I transcription by stimulating promoter escape', *EMBO J* 25(14): 3310-3322.

Panov, K. I., Panova, T. B., Gadal, O., Nishiyama, K., Saito, T., Russell, J. and Zomerdijk, J. C. B. M. (2006b) 'RNA Polymerase I-Specific Subunit CAST/hPAF49 Has a Role in the Activation of Transcription by Upstream Binding Factor', *Molecular and Cellular Biology* 26(14): 5436-5448.

Panova, T. B., Panov, K. I., Russell, J. and Zomerdijk, J. C. B. M. (2006) 'Casein Kinase 2 Associates with Initiation-Competent RNA Polymerase I and Has Multiple Roles in Ribosomal DNA Transcription', *Molecular and Cellular Biology* 26(16): 5957-5968.

Parichy, D. M., Rawls, J. F., Pratt, S. J., Whitfield, T. T. and Johnson, S. L. (1999) 'Zebrafish sparse corresponds to an orthologue of c-kit and is required for the morphogenesis of a subpopulation of melanocytes, but is not essential for hematopoiesis or primordial germ cell development', *Development* 126(15): 3425-3436.

Pattyn, A., Morin, X., Cremer, H., Goridis, C. and Brunet, J.-F. (1999) 'The homeobox gene Phox2b is essential for the development of autonomic neural crest derivatives', *Nature* 399(6734): 366-370.

Pattyn, A., Morin, X., Cremer, H., Goridis, C. and Brunet, J. F. (1997) 'Expression and interactions of the two closely related homeobox genes Phox2a and Phox2b during neurogenesis', *Development* 124(20): 4065-4075.

Pavan, W. J. and Raible, D. W. (2012) 'Specification of neural crest into sensory neuron and melanocyte lineages', *Developmental Biology* 366(1): 55-63.

Payne, E. M., Virgilio, M., Narla, A., Sun, H., Levine, M., Paw, B. H., Berliner, N., Look, A. T., Ebert, B. L. and Khanna-Gupta, A. (2012) 'L-leucine improves the anemia and developmental defects associated with Diamond-Blackfan anemia and del(5q) MDS by activating the mTOR pathway', *Blood* 120(11): 2214-2224.

Penrod, Y., Rothblum, K., Cavanaugh, A. and Rothblum, L. I. (2015) 'Regulation of the association of the PAF53/PAF49 heterodimer with RNA polymerase I', *Gene* 556(1): 61-67.

Pereboom, T. C., van Weele, L. J., Bondt, A. and MacInnes, A. W. (2011) 'A zebrafish model of dyskeratosis congenita reveals hematopoietic stem cell formation failure resulting from ribosomal protein-mediated p53 stabilization', *Blood* 118(20): 5458-5465.

Pingault, V., Ente, D., Dastot-Le Moal, F., Goossens, M., Marlin, S. and Bondurand, N. (2010) 'Review and update of mutations causing Waardenburg syndrome', *Human Mutation* 31(4): 391-406.

Piotrowski, T., Ahn, D.-g., Schilling, T. F., Nair, S., Ruvinsky, I., Geisler, R., Rauch, G.-J., Haffter, P., Zon, L. I., Zhou, Y. et al. (2003) 'The zebrafish van gogh mutation disrupts tbx1, which is involved in the DiGeorge deletion syndrome in humans', *Development* 130(20): 5043-5052.

Piotrowski, T. and Nüsslein-Volhard, C. (2000) 'The Endoderm Plays an Important Role in Patterning the Segmented Pharyngeal Region in Zebrafish (Danio rerio)', *Developmental Biology* 225(2): 339-356.

Pospisilova, D., Cmejlova, J., Hak, J., Adam, T. and Cmejla, R. (2007) 'Successful treatment of a Diamond-Blackfan anemia patient with amino acid leucine', *Haematologica* 92(5): e66-e67.

Potterf, S. B., Furumura, M., Dunn, K. J., Arnheiter, H. and Pavan, W. J. (2000) 'Transcription factor hierarchy in Waardenburg syndrome: regulation of MITF expression by SOX10 and PAX3', *Human Genetics* 107(1): 1-6.

Powers, T. and Walter, P. (1999) 'Regulation of Ribosome Biogenesis by the Rapamycin-sensitive TOR-signaling Pathway in Saccharomyces cerevisiae', *Molecular Biology of the Cell* 10(4): 987-1000.

Prescott, E. M., Osheim, Y. N., Jones, H. S., Alen, C. M., Roan, J. G., Reeder, R. H., Beyer, A. L. and Proudfoot, N. J. (2004) 'Transcriptional termination by RNA polymerase I requires the small subunit Rpa12p', *Proceedings of the National Academy of Sciences of the United States of America* 101(16): 6068-6073.

Prince, V. E., Joly, L., Ekker, M. and Ho, R. K. (1998) 'Zebrafish hox genes: genomic organization and modified colinear expression patterns in the trunk', *Development* 125(3): 407-420.

Provost, E., Wehner, K. A., Zhong, X., Ashar, F., Nguyen, E., Green, R., Parsons, M. J. and Leach, S. D. (2012) 'Ribosomal biogenesis genes play an essential and p53-independent role in zebrafish pancreas development', *Development* 139(17): 3232-3241.

Qi, H., Jin, M., Duan, Y., Du, X., Zhang, Y., Ren, F., Wang, Y., Tian, Q., Wang, X., Wang, Q. et al. (2014) 'FGFR3 induces degradation of BMP type I receptor to regulate skeletal development', *Biochimica et Biophysica Acta (BBA) - Molecular Cell Research* 1843(7): 1237-1247.

Qiu, X., Lim, C.-H., Ho, S.-K., Lee, K.-H. and Jiang, Y.-J. (2009) 'Temporal Notch activation through Notch1a and Notch3 is required for maintaining zebrafish rhombomere boundaries', *Development Genes and Evolution* 219(7): 339-351.

Radosevic, M., Fargas, L. and Alsina, B. (2014) 'The Role of <italic>her4</italic> in Inner Ear Development and Its Relationship with Proneural Genes and Notch Signalling', *PLoS ONE* 9(10): e109860.

Ragland, J. W. and Raible, D. W. (2004) 'Signals derived from the underlying mesoderm are dispensable for zebrafish neural crest induction', *Developmental Biology* 276(1): 16-30.

Raible, D. W. and Eisen, J. S. (1994) 'Restriction of neural crest cell fate in the trunk of the embryonic zebrafish', *Development* 120(3): 495-503.

Raible, D. W., Wood, A., Hodsdon, W., Henion, P. D., Weston, J. A. and Eisen, J. S. (1992) 'Segregation and early dispersal of neural crest cells in the embryonic zebrafish', *Developmental Dynamics* 195(1): 29-42.

Rainger, J., Bengani, H., Campbell, L., Anderson, E., Sokhi, K., Lam, W., Riess, A., Ansari, M., Smithson, S., Lees, M. et al. (2012) 'Miller (Genée–Wiedemann) syndrome represents a clinically and biochemically distinct subgroup of postaxial acrofacial dysostosis associated with partial deficiency of DHODH', *Human Molecular Genetics* 21(18): 3969-3983.

Richard, P. and Manley, J. L. (2009) 'Transcription termination by nuclear RNA polymerases', *Genes & Development* 23(11): 1247-1269.

Rickards, B., Flint, S. J., Cole, M. D. and LeRoy, G. (2007) 'Nucleolin Is Required for RNA Polymerase I Transcription In Vivo', *Molecular and Cellular Biology* 27(3): 937-948.

Ringshausen, I., O'Shea, C. C., Finch, A. J., Swigart, L. B. and Evan, G. I. (2006) 'Mdm2 is critically and continuously required to suppress lethal p53 activity in vivo', *Cancer Cell* 10(6): 501-514.

Robu, M. E., Larson, J. D., Nasevicius, A., Beiraghi, S., Brenner, C., Farber, S. A. and Ekker, S. C. (2007) 'p53 Activation by Knockdown Technologies', *PLoS Genet* 3(5): e78.

Rogers, C. D., Jayasena, C. S., Nie, S. and Bronner, M. E. (2012) 'Neural crest specification: tissues, signals, and transcription factors', *Wiley Interdisciplinary Reviews: Developmental Biology* 1(1): 52-68.

Rubbi, C. P. and Milner, J. (2003) 'Disruption of the nucleolus mediates stabilization of p53 in response to DNA damage and other stresses', *EMBO J* 22(22): 6068-6077.

Rudloff, U., Eberhard, D., Tora, L., Stunnenberg, H. and Grummt, I. (1994) 'TBP-associated factors interact with DNA and govern species specificity of RNA polymerase I transcription', *The EMBO Journal* 13(11): 2611-2616.

Russo, A., Esposito, D., Catillo, M., Pietropaolo, C., Crescenzi, E. and Russo, G. (2013) 'Human rpL3 induces G_1/S arrest or apoptosis by modulating p21waf1/cip1 levels in a p53-independent manner', *Cell Cycle* 12(1): 76-87.

Sakai, D., Dixon, J., Achilleos, A., Dixon, M. and Trainor, P. A. (2016) 'Prevention of Treacher Collins syndrome craniofacial anomalies in mouse models via maternal antioxidant supplementation', *Nat Commun*.

Sancak, Y., Peterson, T. R., Shaul, Y. D., Lindquist, R. A., Thoreen, C. C., Bar-Peled, L. and Sabatini, D. M. (2008) 'The Rag GTPases Bind Raptor and Mediate Amino Acid Signaling to mTORC1', *Science* 320(5882): 1496-1501.

Sánchez-Martín, M., Pérez-Losada, J., Rodríguez-García, A., González-Sánchez, B., Korf, B. R., Kuster, W., Moss, C., Spritz, R. A. and Sánchez-García, I. (2003) 'Deletion of the SLUG (SNAI2) gene results in human piebaldism', *American Journal of Medical Genetics Part A* 122A(2): 125-132.

Sanij, E., Poortinga, G., Sharkey, K., Hung, S., Holloway, T. P., Quin, J., Robb, E., Wong, L. H., Thomas, W. G., Stefanovsky, V. et al. (2008) 'UBF levels determine the number of active ribosomal RNA genes in mammals', *The Journal of Cell Biology* 183(7): 1259-1274.

Sasaki, T., Ito, Y., Bringas, P., Chou, S., Urata, M. M., Slavkin, H. and Chai, Y. (2006) 'TGFβ-mediated FGF signaling is crucial for regulating cranial neural crest cell proliferation during frontal bone development', *Development* 133(2): 371-381.

Sato, T., Kurihara, Y., Asai, R., Kawamura, Y., Tonami, K., Uchijima, Y., Heude, E., Ekker, M., Levi, G. and Kurihara, H. (2008) 'An endothelin-1 switch specifies maxillomandibular identity', *Proceedings of the National Academy of Sciences* 105(48): 18806-18811.

Scala, F., Brighenti, E., Govoni, M., Imbrogno, E., Fornari, F., Trere, D., Montanaro, L. and Derenzini, M. (2015) 'Direct relationship between the level of p53 stabilization induced by rRNA synthesis-inhibiting drugs and the cell ribosome biogenesis rate', *Oncogene*.

Schaefer, E., Collet, C., Genevieve, D., Vincent, M., Lohmann, D. R., Sanchez, E., Bolender, C., Eliot, M.-M., Nurnberg, G., Passos-Bueno, M.-R. et al. (2014) 'Autosomal

225

recessive POLR1D mutation with decrease of TCOF1 mRNA is responsible for Treacher Collins syndrome', *Genet Med* 16(9): 720-724.

Schier, A. F. and Talbot, W. S. (2001) 'Nodal signaling and the zebrafish organizer', *Int. J. Dev. Biol* 45: 289-297.

Schilling, T. F. and Kimmel, C. B. (1994) 'Segment and cell type lineage restrictions during pharyngeal arch development in the zebrafish embryo', *Development* 120(3): 483-494.

Schilling, T. F., Prince, V. and Ingham, P. W. (2001) 'Plasticity in Zebrafish hox Expression in the Hindbrain and Cranial Neural Crest', *Developmental Biology* 231(1): 201-216.

Schneider, C., Wicht, H., Enderich, J., Wegner, M. and Rohrer, H. (1999) 'Bone Morphogenetic Proteins Are Required In Vivo for the Generation of Sympathetic Neurons', *Neuron* 24(4): 861-870.

Schramm, L. and Hernandez, N. (2002) 'Recruitment of RNA polymerase III to its target promoters', *Genes & Development* 16(20): 2593-2620.

Schumacher, J. A., Hashiguchi, M., Nguyen, V. H. and Mullins, M. C. (2011) 'An Intermediate Level of BMP Signaling Directly Specifies Cranial Neural Crest Progenitor Cells in Zebrafish', *PLoS ONE* 6(11): e27403.

Shen, L., Pichel, J. G., Mayeli, T., Sariola, H., Lu, B. and Westphal, H. (2002) 'Gdnf Haploinsufficiency Causes Hirschsprung-Like Intestinal Obstruction and Early-Onset Lethality in Mice', *The American Journal of Human Genetics* 70(2): 435-447.

Shiau, C. E., Lwigale, P. Y., Das, R. M., Wilson, S. A. and Bronner-Fraser, M. (2008) 'Robo2-Slit1 dependent cell-cell interactions mediate assembly of the trigeminal ganglion', *Nat Neurosci* 11(3): 269-276.

Sloan, Katherine E., Bohnsack, Markus T. and Watkins, Nicholas J. (2013) 'The 5S RNP Couples p53 Homeostasis to Ribosome Biogenesis and Nucleolar Stress', *Cell Reports* 5(1): 237-247.

Smith, A., Robinson, V., Patel, K. and Wilkinson, D. G. (1997) 'The EphA4 and EphB1 receptor tyrosine kinases and ephrin-B2 ligand regulate targeted migration of branchial neural crest cells', *Current biology : CB* 7(8): 561-570.

So, J.-H., Chun, H.-S., Bae, Y.-K., Kim, H.-S., Park, Y.-M., Huh, T.-L., Chitnis, A. B., Kim, C.-H. and Yeo, S.-Y. (2009) 'Her4 is necessary for establishing peripheral projections of the trigeminal ganglia in zebrafish', *Biochemical and Biophysical Research Communications* 379(1): 22-26.

Solomon, K. S., Kudoh, T., Dawid, I. B. and Fritz, A. (2003) 'Zebrafish foxi1 mediates otic placode formation and jaw development', *Development* 130(5): 929-940.

Sommer, L., Shah, N., Rao, M. and Anderson, D. J. (1995) 'The cellular function of MASH1 in autonomic neurogenesis', *Neuron* 15(6): 1245-1258.

Southard-Smith, E. M., Kos, L. and Pavan, W. J. (1998) 'SOX10 mutation disrupts neural crest development in Dom Hirschsprung mouse model', *Nat Genet* 18(1): 60-64.

Spokony, R. F., Aoki, Y., Saint-Germain, N., Magner-Fink, E. and Saint-Jeannet, J.-P. (2002) 'The transcription factor Sox9 is required for cranial neural crest development in Xenopus', *Development* 129(2): 421-432.

St-Jacques, B., Hammerschmidt, M. and McMahon, A. P. (1999) 'Indian hedgehog signaling regulates proliferation and differentiation of chondrocytes and is essential for bone formation', *Genes & Development* 13(16): 2072-2086.

Stanke, M., Junghans, D., Geissen, M., Goridis, C., Ernsberger, U. and Rohrer, H. (1999) 'The Phox2 homeodomain proteins are sufficient to promote the development of sympathetic neurons', *Development* 126(18): 4087-4094.

Stark, M. R., Sechrist, J., Bronner-Fraser, M. and Marcelle, C. (1997) 'Neural tube-ectoderm interactions are required for trigeminal placode formation', *Development* 124(21): 4287-4295.

Stefanovsky, V. Y., Pelletier, G., Hannan, R., Gagnon-Kugler, T., Rothblum, L. I. and Moss, T. (2001) 'An Immediate Response of Ribosomal Transcription to Growth Factor Stimulation in Mammals Is Mediated by ERK Phosphorylation of UBF', *Molecular Cell* 8(5): 1063-1073.

Stepanchick, A., Zhi, H., Cavanaugh, A. H., Rothblum, K., Schneider, D. A. and Rothblum, L. I. (2013) 'DNA Binding by the Ribosomal DNA Transcription Factor Rrn3 Is Essential for Ribosomal DNA Transcription', *Journal of Biological Chemistry* 288(13): 9135-9144.

Steventon, B., Mayor, R. and Streit, A. (2014) 'Neural crest and placode interaction during the development of the cranial sensory system', *Developmental Biology* 389(1): 28-38.

Stewart, R. A., Arduini, B. L., Berghmans, S., George, R. E., Kanki, J. P., Henion, P. D. and Look, A. T. (2006) 'Zebrafish foxd3 is selectively required for neural crest specification, migration and survival', *Developmental Biology* 292(1): 174-188.

Stock, D. W., Ellies, D. L., Zhao, Z., Ekker, M., Ruddle, F. H. and Weiss, K. M. (1996) 'The evolution of the vertebrate Dlx gene family', *Proceedings of the National Academy of Sciences* 93(20): 10858-10863.

Streit, A., Berliner, A. J., Papanayotou, C., Sirulnik, A. and Stern, C. D. (2000) 'Initiation of neural induction by FGF signalling before gastrulation', *Nature* 406(6791): 74-78.

Stuckenholz, C., Lu, L., Thakur, P., Kaminski, N. and Bahary, N. (2009) 'FACS-Assisted Microarray Profiling Implicates Novel Genes and Pathways in Zebrafish Gastrointestinal Tract Development', *Gastroenterology* 137(4): 1321-1332.

Stults, D. M., Killen, M. W., Pierce, H. H. and Pierce, A. J. (2008) 'Genomic architecture and inheritance of human ribosomal RNA gene clusters', *Genome Research* 18(1): 13-18.

Sutcliffe, J. E., Brown, T. R. P., Allison, S. J., Scott, P. H. and White, R. J. (2000) 'Retinoblastoma Protein Disrupts Interactions Required for RNA Polymerase III Transcription', *Molecular and Cellular Biology* 20(24): 9192-9202.

Swartz, M. E., Sheehan-Rooney, K., Dixon, M. J. and Eberhart, J. K. (2011) 'Examination of a palatogenic gene program in zebrafish', *Developmental Dynamics* 240(9): 2204-2220. Takahashi, K., Nuckolls, G. H., Takahashi, I., Nonaka, K., Nagata, M., Ikura, T., Slavkin, H. C. and Shum, L. (2001) 'Msx2 is a repressor of chondrogenic differentiation in migratory cranial neural crest cells†', *Developmental Dynamics* 222(2): 252-262.

Talbot, J. C., Johnson, S. L. and Kimmel, C. B. (2010) 'hand2 and Dlx genes specify dorsal, intermediate and ventral domains within zebrafish pharyngeal arches', *Development* 137(15): 2507-2517.

Taneyhill, L. A., Coles, E. G. and Bronner-Fraser, M. (2007) 'Snail2 directly represses cadherin6B during epithelial-to-mesenchymal transitions of the neural crest', *Development* 134(8): 1481-1490.

Tarca, A. L., Draghici, S., Khatri, P., Hassan, S. S., Mittal, P., Kim, J.-s., Kim, C. J., Kusanovic, J. P. and Romero, R. (2009) 'A novel signaling pathway impact analysis', *Bioinformatics* 25(1): 75-82.

Taylor, A. M., Humphries, J. M., White, R. M., Murphey, R. D., Burns, C. E. and Zon, L. I. (2012) 'Hematopoietic defects in rps29 mutant zebrafish depend upon p53 activation', *Experimental Hematology* 40(3): 228-237.e5.

The Treacher Collins Syndrome Collaborative, G., Dixon, J., Edwards, S. J., Gladwin, A. J., Dixon, M. J., Loftus, S. K., Bonner, C. A., Koprivnikar, K. and Wasmuth, J. J. (1996)

'Positional cloning of a gene involved in the pathogenesis of Treacher Collins syndrome', *Nat Genet* 12(2): 130-136.

Theveneau, E., Steventon, B., Scarpa, E., Garcia, S., Trepat, X., Streit, A. and Mayor, R. (2013) 'Chase-and-run between adjacent cell populations promotes directional collective migration', *Nat Cell Biol* 15(7): 763-772.

Thisse, B., Pflumio, S., Fürthauer, M., Loppin, B., Heyer, V., Degrave, A., Woehl, R., Lux, A., Steffan, T., Charbonnier, X. Q. et al. (2001) 'Expression of the zebrafish genome during embryogenesis', *ZFIN Direct Data Submission (http://zfin.org)*.

Thisse, C., Thisse, B. and Postlethwait, J. H. (1995) 'Expression ofsnail2,a Second Member of the Zebrafish Snail Family, in Cephalic Mesendoderm and Presumptive Neural Crest of Wild-Type andspadetailMutant Embryos', *Developmental Biology* 172(1): 86-99.

Thisse, C., Thisse, B., Schilling, T. F. and Postlethwait, J. H. (1993) 'Structure of the zebrafish snail1 gene and its expression in wild-type, spadetail and no tail mutant embryos', *Development* 119(4): 1203-1215.

Thomas, A. J. and Erickson, C. A. (2008) 'The making of a melanocyte: the specification of melanoblasts from the neural crest', *Pigment Cell & Melanoma Research* 21(6): 598-610.

Thomas, A. J. and Erickson, C. A. (2009) 'FOXD3 regulates the lineage switch between neural crest-derived glial cells and pigment cells by repressing MITF through a non-canonical mechanism', *Development* 136(11): 1849-1858.

Trainor, P. and Krumlauf, R. (2000a) 'Plasticity in mouse neural crest cells reveals a new patterning role for cranial mesoderm', *Nat Cell Biol* 2(2): 96-102.

Trainor, P. A. and Andrews, B. T. (2013) 'Facial dysostoses: Etiology, pathogenesis and management', *American Journal of Medical Genetics Part C: Seminars in Medical Genetics* 163(4): 283-294.

Trainor, P. A., Dixon, J. and Dixon, M. J. (2008) 'Treacher Collins syndrome: etiology, pathogenesis and prevention', *Eur J Hum Genet* 17(3): 275-283.

Trainor, P. A. and Krumlauf, R. (2000b) 'Patterning the cranial neural crest: Hinbrain segmentation and hox gene plasticity', *Nat Rev Neurosci* 1(2): 116-124.

Trainor, P. A. and Krumlauf, R. (2001) 'Hox genes, neural crest cells and branchial arch patterning', *Current Opinion in Cell Biology* 13(6): 698-705.

Trainor, P. A. and Merrill, A. E. (2014) 'Ribosome biogenesis in skeletal development and the pathogenesis of skeletal disorders', *Biochimica et Biophysica Acta (BBA) - Molecular Basis of Disease* 1842(6): 769-778.

Trevarrow, B., Marks, D. L. and Kimmel, C. B. (1990) 'Organization of hindbrain segments in the zebrafish embryo', *Neuron* 4(5): 669-679.

Trumpp, A., Depew, M. J., Rubenstein, J. L. R., Bishop, J. M. and Martin, G. R. (1999) 'Cre-mediated gene inactivation demonstrates that FGF8 is required for cell survival and patterning of the first branchial arch', *Genes & Development* 13(23): 3136-3148.

Tsang, C. K., Liu, H. and Zheng, X. F. S. (2010) 'mTOR binds to the promoters of RNA polymerase I- and III-transcribed genes', *Cell Cycle* 9(5): 953-957.

Tsarovina, K., Pattyn, A., Stubbusch, J., Müller, F., van der Wees, J., Schneider, C., Brunet, J.-F. and Rohrer, H. (2004) 'Essential role of Gata transcription factors in sympathetic neuron development', *Development* 131(19): 4775-4786.

Tschochner, H. and Hurt, E. (2003) 'Pre-ribosomes on the road from the nucleolus to the cytoplasm', *Trends in Cell Biology* 13(5): 255-263.

Tucker, A. S., Yamada, G., Grigoriou, M., Pachnis, V. and Sharpe, P. T. (1999) 'Fgf-8 determines rostral-caudal polarity in the first branchial arch', *Development* 126(1): 51-61.

Valdez, B. C., Henning, D., So, R. B., Dixon, J. and Dixon, M. J. (2004) 'The Treacher Collins syndrome (TCOF1) gene product is involved in ribosomal DNA gene transcription by interacting with upstream binding factor', *Proceedings of the National Academy of Sciences of the United States of America* 101(29): 10709-10714.

Vannini, A., Ringel, R., Kusser, A. G., Berninghausen, O., Kassavetis, G. A. and Cramer, P. (2010) 'Molecular Basis of RNA Polymerase III Transcription Repression by Maf1', *Cell* 143(1): 59-70.

Vazquez, A., Bond, E. E., Levine, A. J. and Bond, G. L. (2008) 'The genetics of the p53 pathway, apoptosis and cancer therapy', *Nat Rev Drug Discov* 7(12): 979-987.

Villanueva, S., Glavic, A., Ruiz, P. and Mayor, R. (2002) 'Posteriorization by FGF, Wnt, and Retinoic Acid Is Required for Neural Crest Induction', *Developmental Biology* 241(2): 289-301.

Vitelli, F., Morishima, M., Taddei, I., Lindsay, E. A. and Baldini, A. (2002) 'Tbx1 mutation causes multiple cardiovascular defects and disrupts neural crest and cranial nerve migratory pathways', *Human Molecular Genetics* 11(8): 915-922.

Wagner, T., Wirth, J., Meyer, J., Zabel, B., Held, M., Zimmer, J., Pasantes, J., Bricarelli, F. D., Keutel, J., Hustert, E. et al. (1994) 'Autosomal sex reversal and campomelic dysplasia are caused by mutations in and around the SRY-related gene SOX9', *Cell* 79(6): 1111-1120.

Walker, M. and Kimmel, C. (2007) 'A two-color acid-free cartilage and bone stain for zebrafish larvae', *Biotechnic & Histochemistry* 82(1): 23-28.

Walker, M. B., Miller, C. T., Swartz, M. E., Eberhart, J. K. and Kimmel, C. B. (2007) 'phospholipase C, beta 3 is required for Endothelin1 regulation of pharyngeal arch patterning in zebrafish', *Developmental Biology* 304(1): 194-207.

Walshe, J. and Mason, I. (2003) 'Fgf signalling is required for formation of cartilage in the head', *Developmental Biology* 264(2): 522-536.

Wang, W.-D., Melville, D. B., Montero-Balaguer, M., Hatzopoulos, A. K. and Knapik, E. W. (2011) 'Tfap2a and Foxd3 regulate early steps in the development of the neural crest progenitor population', *Developmental Biology* 360(1): 173-185.

Warga, R. M. and Nusslein-Volhard, C. (1999) 'Origin and development of the zebrafish endoderm', *Development* 126(4): 827-838.

Warner, J. R. (1999) 'The economics of ribosome biosynthesis in yeast', *Trends in Biochemical Sciences* 24(11): 437-440.

Watt, K. E. N. and Trainor, P. A. (2014) Chapter 17 - Neurocristopathies: The Etiology and Pathogenesis of Disorders Arising from Defects in Neural Crest Cell Development. in P. A. Trainor (ed.) *Neural Crest Cells*. Boston: Academic Press.

Weaver, K. N., Watt, Kristin E. N., Hufnagel, Robert B., Navajas Acedo, J., Linscott, Luke L., Sund, Kristen L., Bender, Patricia L., König, R., Lourenco, Charles M., Hehr, U. et al. (2015) 'Acrofacial Dysostosis, Cincinnati Type, a Mandibulofacial Dysostosis Syndrome with Limb Anomalies, Is Caused by POLR1A Dysfunction', *The American Journal of Human Genetics* 96(5): 765-774.

Wehrle-Haller, B. and Weston, J. A. (1995) 'Soluble and cell-bound forms of steel factor activity play distinct roles in melanocyte precursor dispersal and survival on the lateral neural crest migration pathway', *Development* 121(3): 731-742.

Weiner, A. M. J., Scampoli, N. L. and Calcaterra, N. B. (2012) 'Fishing the Molecular Bases of Treacher Collins Syndrome', *PLoS ONE* 7(1): e29574.

White, R. M., Cech, J., Ratanasirintrawoot, S., Lin, C. Y., Rahl, P. B., Burke, C. J., Langdon, E., Tomlinson, M. L., Mosher, J., Kaufman, C. et al. (2011) 'DHODH modulates transcriptional elongation in the neural crest and melanoma', *Nature* 471(7339): 518-522.

Wilson, J. and Tucker, A. S. (2004) 'Fgf and Bmp signals repress the expression of Bapx1 in the mandibular mesenchyme and control the position of the developing jaw joint', *Developmental Biology* 266(1): 138-150.

Winokur, S. T. and Shiang, R. (1998) 'The Treacher Collins Syndrome (TCOF1) Gene Product, Treacle, is Targeted to the Nucleolus by Signals in Its C-Terminus', *Human Molecular Genetics* 7(12): 1947-1952.

Wise, C. A., Chiang, L. C., Paznekas, W. A., Sharma, M., Musy, M. M., Ashley, J. A., Lovett, M. and Jabs, E. W. (1997) 'TCOF1 gene encodes a putative nucleolar phosphoprotein that exhibits mutations in Treacher Collins Syndrome throughout its coding region', *Proceedings of the National Academy of Sciences* 94(7): 3110-3115.

Wyllie, A. (2010) '"Where, O Death, Is Thy Sting?" A Brief Review of Apoptosis Biology', *Molecular Neurobiology* 42(1): 4-9.

Xu, H., Morishima, M., Wylie, J. N., Schwartz, R. J., Bruneau, B. G., Lindsay, E. A. and Baldini, A. (2004) 'Tbx1 has a dual role in the morphogenesis of the cardiac outflow tract', *Development* 131(13): 3217-3227.

Yamagata, M. and Noda, M. (1998) 'The winged-helix transcription factor CWH-3 is expressed in developing neural crest cells', *Neuroscience Letters* 249(1): 33-36.

Yan, Y.-L., Miller, C. T., Nissen, R., Singer, A., Liu, D., Kirn, A., Draper, B., Willoughby, J., Morcos, P. A., Amsterdam, A. et al. (2002) 'A zebrafish sox9 gene required for cartilage morphogenesis', *Development* 129(21): 5065-5079.

Yan, Y.-L., Willoughby, J., Liu, D., Crump, J. G., Wilson, C., Miller, C. T., Singer, A., Kimmel, C., Westerfield, M. and Postlethwait, J. H. (2005) 'A pair of Sox: distinct and overlapping functions of zebrafish sox9 co-orthologs in craniofacial and pectoral fin development', *Development* 132(5): 1069-1083.

Yang, D.-C., Tsai, C.-C., Liao, Y.-F., Fu, H.-C., Tsay, H.-J., Huang, T.-F., Chen, Y.-H. and Hung, S.-C. (2011) *'Twist* Controls Skeletal Development and Dorsoventral Patterning by Regulating *Runx2* in Zebrafish', *PLoS ONE* 6(11): e27324.

Yee, N. S., Gong, W., Huang, Y., Lorent, K., Dolan, A. C., Maraia, R. J. and Pack, M. (2007) 'Mutation of RNA Pol III Subunit *rpc2/polr3b* Leads to Deficiency of Subunit Rpc11 and Disrupts Zebrafish Digestive Development', *PLoS Biol* 5(11): e312.

Yoon, B. S., Ovchinnikov, D. A., Yoshii, I., Mishina, Y., Behringer, R. R. and Lyons, K. M. (2005) 'Bmpr1a and Bmpr1b have overlapping functions and are essential for chondrogenesis in vivo', *Proceedings of the National Academy of Sciences of the United States of America* 102(14): 5062-5067.

Yoshida, T., Phylactou, L. A., Uney, J. B., Ishikawa, I., Eto, K. and Iseki, S. (2005) 'Twist is required for establishment of the mouse coronal suture', *Journal of Anatomy* 206(5): 437-444.

Yoshida, T., Vivatbutsiri, P., Morriss-Kay, G., Saga, Y. and Iseki, S. (2008) 'Cell lineage in mammalian craniofacial mesenchyme', *Mechanisms of Development* 125(9–10): 797-808.

Young, D. W., Hassan, M. Q., Pratap, J., Galindo, M., Zaidi, S. K., Lee, S.-h., Yang, X., Xie, R., Javed, A., Underwood, J. M. et al. (2007) 'Mitotic occupancy and lineage-specific transcriptional control of rRNA genes by Runx2', *Nature* 445(7126): 442-446.

Yu, H.-H. and Moens, C. B. (2005) 'Semaphorin signaling guides cranial neural crest cell migration in zebrafish', *Developmental Biology* 280(2): 373-385.
Yu, J. and Zhang, L. (2009) 'PUMA, a potent killer with or without p53', *Oncogene* 27(S1): S71-S83.

Yu, K., Xu, J., Liu, Z., Sosic, D., Shao, J., Olson, E. N., Towler, D. A. and Ornitz, D. M. (2003) 'Conditional inactivation of FGF receptor 2 reveals an essential role for FGF signaling in the regulation of osteoblast function and bone growth', *Development* 130(13): 3063-3074.

Yuan, X., Zhou, Y., Casanova, E., Chai, M., Kiss, E., Gröne, H.-J., Schütz, G. and Grummt, I. (2005) 'Genetic Inactivation of the Transcription Factor TIF-IA Leads to Nucleolar Disruption, Cell Cycle Arrest, and p53-Mediated Apoptosis', *Molecular Cell* 19(1): 77-87.

Zaragoza, D., Ghavidel, A., Heitman, J. and Schultz, M. C. (1998) 'Rapamycin Induces the G0 Program of Transcriptional Repression in Yeast by Interfering with the TOR Signaling Pathway', *Molecular and Cellular Biology* 18(8): 4463-4470.

Zhang, Q., Shalaby, N. A. and Buszczak, M. (2014) 'Changes in rRNA Transcription Influence Proliferation and Cell Fate Within a Stem Cell Lineage', *Science* 343(6168): 298-301.

Zhang, Y., Wolf, G. W., Bhat, K., Jin, A., Allio, T., Burkhart, W. A. and Xiong, Y. (2003) 'Ribosomal Protein L11 Negatively Regulates Oncoprotein MDM2 and Mediates a p53-

Dependent Ribosomal-Stress Checkpoint Pathway', *Molecular and Cellular Biology* 23(23): 8902-8912.

Zhao, C., Andreeva, V., Gibert, Y., LaBonty, M., Lattanzi, V., Prabhudesai, S., Zhou, Y., Zon, L., McCann, K. L., Baserga, S. et al. (2014) 'Tissue Specific Roles for the Ribosome Biogenesis Factor Wdr43 in Zebrafish Development', *PLoS Genet* 10(1): e1004074.

Zhao, J., Yuan, X., Frödin, M. and Grummt, I. (2003a) 'ERK-Dependent Phosphorylation of the Transcription Initiation Factor TIF-IA Is Required for RNA Polymerase I Transcription and Cell Growth', *Molecular Cell* 11(2): 405-413.

Zhao, L., Samuels, T., Winckler, S., Korgaonkar, C., Tompkins, V., Horne, M. C. and Quelle, D. E. (2003b) 'Cyclin G1 Has Growth Inhibitory Activity Linked to the ARF-Mdm2-p53 and pRb Tumor Suppressor Pathways1 1 D.E.Q. from the American Cancer Society (RSG-98-254-04-MGO) and NIH (RO1 CA90367), and by a grant from the NIH to M.C.H. (RO1 GM56900)', *Molecular Cancer Research* 1(3): 195-206.

Zsebo, K. M., Williams, D. A., Geissler, E. N., Broudy, V. C., Martin, F. H., Atkins, H. L., Hsu, R.-Y., Birkett, N. C., Okino, K. H., Murdock, D. C. et al. (1990) 'Stem cell factor is encoded at the SI locus of the mouse and is the ligand for the c-kit tyrosine kinase receptor', *Cell* 63(1): 213-224.

Zuniga, E., Stellabotte, F. and Crump, J. G. (2010) 'Jagged-Notch signaling ensures dorsal skeletal identity in the vertebrate face', *Development* 137: 1843-1852.

APPENDICES

Appendix A: *polr1*c and *polr1d* RNA-Seq Data

UPREGULATED GENES

The following list of genes was found to be upregulated in both *polr1c* and *polr1d* mutant embryos. All values are significant at p < 0.01. FC = fold change

gene	polr1c FC	polr1d FC	id	description
CDKN2B	47.96	15.04	ENSDARG00000037262	cyclin-dependent kinase inhibitor 2B (p15, inhibits CDK4)
rspo1	45.72	26.23	ENSDARG00000039957	R-spondin homolog (Xenopus laevis)
ms4a17a.2	13.27	31.01	ENSDARG00000093546	membrane-spanning 4-domains, subfamily A, member 17a.2
rnf14	12.92	7.22	ENSDARG00000078683	ring finger protein 14
rbl2	11.71	12.01	ENSDARG00000045636	retinoblastoma-like 2 (p130)
ghrh	11.50	18.96	ENSDARG00000069481	growth hormone releasing hormone
casp8	10.68	7.75	ENSDARG00000058325	caspase 8, apoptosis-related cysteine peptidase
cx36.7	9.97	5.54	ENSDARG00000017927	connexin 36.7
bbc3	9.57	8.08	ENSDARG00000069282	BCL2 binding component 3
tnnc1a	9.14	6.22	ENSDARG00000011400	troponin C type 1a (slow)
atxn1b	9.04	10.21	ENSDARG00000060862	ataxin 1b
OSBP2	8.61	5.97	ENSDARG00000022772	oxysterol binding protein 2
rasl11b	8.13	4.08	ENSDARG00000015611	RAS-like, family 11, member B
mdm2	7.89	8.25	ENSDARG00000033443	transformed 3T3 cell double minute 2 homolog (mouse)
phlda3	7.65	5.89	ENSDARG00000037804	pleckstrin homology-like domain, family A, member 3
cmlc1	7.56	10.91	ENSDARG00000032976	cardiac myosin light chain-1
lnx1	7.33	6.23	ENSDARG00000043323	ligand of numb-protein X 1
crygn1	7.12	7.60	ENSDARG00000087437	crystallin, gamma N1
zak	6.37	5.53	ENSDARG00000006978	sterile alpha motif and leucine zipper containing kinase AZK
myl7	6.26	10.47	ENSDARG00000019096	myosin, light polypeptide 7, regulatory

ms4a17a.1	6.11	8.88	ENSDARG00000043798	membrane-spanning 4-domains, subfamily A, member 17A.1
vrk2	6.09	5.42	ENSDARG00000021547	vaccinia related kinase 2
cdkn1a	6.02	4.20	ENSDARG00000076554	cyclin-dependent kinase inhibitor 1A
tp53	5.89	4.79	ENSDARG00000035559	tumor protein p53
rps27.2	5.87	5.68	ENSDARG00000090186	ribosomal protein S27, isoform 2
gtpbp1l	5.71	6.15	ENSDARG00000042900	GTP binding protein 1, like
tnni1b	5.61	2.22	ENSDARG00000052708	troponin I, skeletal, slow b
fhl2a	5.50	7.16	ENSDARG00000042018	four and a half LIM domains 2a
tnnt2a	5.50	5.59	ENSDARG00000020610	troponin T2a, cardiac
foxo3b	5.34	4.79	ENSDARG00000042904	forkhead box O3b
ccng1	4.88	4.83	ENSDARG00000076667	cyclin G1
ace	4.73	3.64	ENSDARG00000079166	angiotensin I converting enzyme (peptidyl-dipeptidase A)
nppa	4.67	7.30	ENSDARG00000052960	natriuretic peptide precursor A
bmb	4.67	4.78	ENSDARG00000096603	brambleberry
gadd45aa	4.64	4.23	ENSDARG00000043581	growth arrest and DNA-damage-inducible, alpha, a
TAF1C	4.36	4.18	ENSDARG00000096310	TATA box binding protein (TBP)-associated factor, RNA polymerase I, C, 110kDa
loxhd1b	4.35	9.29	ENSDARG00000074638	lipoxygenase homology domains 1b
mat2al	4.35	5.01	ENSDARG00000063665	methionine adenosyltransferase II, alpha-like
slc8a1a	4.27	4.51	ENSDARG00000013422	solute carrier family 8 (sodium/calcium exchanger), member 1a
rnf169	4.16	2.86	ENSDARG00000042825	ring finger protein 169
sesn3	4.12	3.87	ENSDARG00000015822	sestrin 3
rlbp1b	4.10	2.98	ENSDARG00000045808	retinaldehyde binding protein 1b
ITPR1	4.04	2.91	ENSDARG00000074149	inositol 1,4,5-trisphosphate receptor, type 1
zbtb38	3.96	8.70	ENSDARG00000077426	zinc finger and BTB domain containing 38
igf2a	3.90	2.64	ENSDARG00000018643	insulin-like growth factor 2a
ms4a17a.4	3.88	3.25	ENSDARG00000014024	membrane-spanning 4-domains, subfamily A, member 17A.4
nfe2l2b	3.88	3.04	ENSDARG00000089697	nuclear factor (erythroid-derived 2)-like 2b

pik3r3a	3.84	2.78	ENSDARG00000071219	phosphoinositide-3-kinase, regulatory subunit 3a (gamma)
ms4a17a.5	3.70	3.77	ENSDARG00000092204	membrane-spanning 4-domains, subfamily A, member 17A.5
cpn1	3.59	2.56	ENSDARG00000096728	Carboxypeptidase N, polypeptide 1
isg15	3.56	30.88	ENSDARG00000086374	ISG15 ubiquitin-like modifier
lrrc10	3.52	3.56	ENSDARG00000045612	leucine rich repeat containing 10
cenpv	3.34	3.82	ENSDARG00000092285	centromere protein V
mmp13b	3.23	2.54	ENSDARG00000015797	matrix metalloproteinase 13b
tspan18a	3.20	2.23	ENSDARG00000056656	tetraspanin 18a
lyrm1	3.19	3.77	ENSDARG00000026281	LYR motif containing 1
asic1a	3.19	3.01	ENSDARG00000008329	acid-sensing (proton-gated) ion channel 1a
TRIM29	3.16	2.18	ENSDARG00000034707	tripartite motif containing 29
gig2p	3.09	2.38	ENSDARG00000088260	grass carp reovirus (GCRV)-induced gene 2p
mmp2	3.08	2.35	ENSDARG00000017676	matrix metalloproteinase 2
abcc5	3.08	2.30	ENSDARG00000061233	ATP-binding cassette, sub-family C (CFTR/MRP), member 5
METRNL	3.04	2.38	ENSDARG00000007289	meteorin, glial cell differentiation regulator-like
fsta	3.04	2.17	ENSDARG00000052846	follistatin a
nudt6	2.88	3.18	ENSDARG00000087321	nudix (nucleoside diphosphate linked moiety X)-type motif 6
rnf24	2.83	2.44	ENSDARG00000036965	ring finger protein 24
vmhc	2.82	3.16	ENSDARG00000079564	ventricular myosin heavy chain
isg20	2.79	2.66	ENSDARG00000079783	interferon-stimulated protein
f8	2.78	2.02	ENSDARG00000015247	coagulation factor VIII, procoagulant component
cdkn1ba	2.75	2.07	ENSDARG00000029018	cyclin-dependent kinase inhibitor 1Ba
PNPLA2	2.70	4.81	ENSDARG00000073955	patatin-like phospholipase domain containing 2
parp3	2.70	3.01	ENSDARG00000003961	poly (ADP-ribose) polymerase family, member 3
cacna2d4b	2.64	4.10	ENSDARG00000023886	calcium channel, voltage-dependent, alpha 2/delta subunit 4b
rd3	2.47	2.13	ENSDARG00000031600	retinal degeneration 3
PRSS56	2.32	2.14	ENSDARG00000053158	protease, serine, 56
adarb2	2.32	2.10	ENSDARG00000071823	adenosine deaminase, RNA-specific, B2 (RED2 homolog rat)

gene			id	description
ms4a17a.6	2.32	2.10	ENSDARG00000007018	membrane-spanning 4-domains, subfamily A, member 17A.6
fhit	2.25	2.36	ENSDARG00000068850	fragile histidine triad gene
tnfaip6	2.24	2.36	ENSDARG00000093440	tumor necrosis factor, alpha-induced protein 6
baxa	2.11	2.65	ENSDARG00000020623	bcl2-associated X protein, a
gpd1a	2.06	2.27	ENSDARG00000043701	glycerol-3-phosphate dehydrogenase 1a
sb:cb252	2.01	2.44	ENSDARG00000058206	sb:cb252

DOWNREGULATED GENES

Polr1c: Top 100 downregulated genes with p < 0.01

gene	Fold Change	p-value	id	description
qrfpra	-63.355	1.10E-06	ENSDARG00000039349	pyroglutamylated RFamide peptide receptor a
LTB4R (1 of 2)	-10.789	0.002317	ENSDARG00000032631	leukotriene B4 receptor
lepb	-9.636	0.000469	ENSDARG00000045548	leptin b
P2RY2 (1 of 3)	-9.213	0.0069	ENSDARG00000063545	purinergic receptor P2Y, G-protein coupled, 2
H2AFX	-9.117	0.005718	ENSDARG00000087235	H2A histone family, member X
RPS6KA2	-8.515	0.000117	ENSDARG00000028469	Ribosomal protein S6 kinase
TRIM29	-7.779	0.000484	ENSDARG00000087711	tripartite motif containing 29
ATP6V1C2	-7.604	0.005796	ENSDARG00000070440	ATPase, H+ transporting, lysosomal 42kDa, V1 subunit C2
hspb2	-7.527	0.000442	ENSDARG00000052450	heat shock protein, alpha-crystallin-related, b2
ch25hl1.2	-7.247	0.001622	ENSDARG00000068138	cholesterol 25-hydroxylase like 1, tandem duplicate 2
elnb	-6.667	0.000193	ENSDARG00000069017	elastin b
nyx	-6.462	1.66E-05	ENSDARG00000061791	nyctalopin
mrap	-6.317	0.007977	ENSDARG00000091992	melanocortin 2 receptor accessory protein
cyp8b2	-6.175	0.009526	ENSDARG00000097556	cytochrome P450, family 8, subfamily B, polypeptide 2
TGFBR3L	-5.926	0.003366	ENSDARG00000088795	transforming growth factor, beta receptor III-like

polr1c	-5.868	1.19E-29	ENSDARG00000039400	polymerase (RNA) I polypeptide C
plaua	-5.709	0.000254	ENSDARG00000075265	plasminogen activator, urokinase a
bgna	-5.549	0.003626	ENSDARG00000017884	biglycan a
spns3	-5.456	6.04E-05	ENSDARG00000035459	spinster homolog 3 (Drosophila)
EYS	-5.370	0.000225	ENSDARG00000089257	eyes shut homolog (Drosophila)
wisp1b	-4.653	0.005759	ENSDARG00000076685	WNT1 inducible signaling pathway protein 1b
fgfbp2a	-4.559	0.00131	ENSDARG00000039964	fibroblast growth factor binding protein 2a
mtnr1al	-4.273	0.000605	ENSDARG00000012057	melatonin receptor type 1A like
kcnj14	-4.272	0.006623	ENSDARG00000075914	potassium inwardly-rectifying channel, subfamily J, member 14
SLC39A8	-4.216	0.00151	ENSDARG00000056757	solute carrier family 39 (zinc transporter), member 8
slc25a4	-4.197	5.96E-08	ENSDARG00000027355	solute carrier family 25 (mitochondrial carrier; adenine nucleotide translocator), member 4
FBXO40	-4.135	2.76E-06	ENSDARG00000091119	F-box protein 40
steap4	-4.096	0.000114	ENSDARG00000055901	STEAP family member 4
YIPF7	-3.994	2.22E-11	ENSDARG00000039726	Yip1 domain family, member 7
lrrc18b	-3.900	0.002651	ENSDARG00000076236	leucine rich repeat containing 18b
stat1b	-3.880	0.007446	ENSDARG00000076182	signal transducer and activator of transcription 1b
il11a	-3.871	0.001106	ENSDARG00000037859	interleukin 11a
ifih1	-3.870	0.006252	ENSDARG00000018553	interferon induced with helicase C domain 1
clcn1a	-3.828	3.19E-05	ENSDARG00000062084	chloride channel 1a
prph2a	-3.802	0.003308	ENSDARG00000038018	peripherin 2a (retinal degeneration, slow)
bmf2	-3.778	0.000508	ENSDARG00000041414	Bcl2 modifying factor 2
Tat	-3.739	0.000388	ENSDARG00000069630	tyrosine aminotransferase
asb16	-3.710	5.19E-05	ENSDARG00000056468	ankyrin repeat and SOCS box-containing 16
pfkma	-3.687	2.87E-07	ENSDARG00000014179	phosphofructokinase, muscle a

PTAFR	-3.676	0.005925	ENSDARG00000042370	platelet-activating factor receptor
hsc70	-3.608	0.001232	ENSDARG00000012381	heat shock cognate 70
mettl11b	-3.573	1.17E-05	ENSDARG00000042033	methyltransferase like 11B
ERBB4	-3.465	0.000163	ENSDARG00000089167	erb-b2 receptor tyrosine kinase 4
tlr19	-3.464	0.009153	ENSDARG00000070392	toll-like receptor 19
scn4ba	-3.462	0.009201	ENSDARG00000062416	sodium channel, voltage-gated, type IV, beta a
c1qc	-3.459	0.007903	ENSDARG00000095627	complement component 1, q subcomponent, C chain
sult1st6	-3.287	0.008468	ENSDARG00000006811	sulfotransferase family 1, cytosolic sulfotransferase 6
KRT23	-3.255	0.009238	ENSDARG00000044973	keratin 23 (histone deacetylase inducible)
nlgn1	-3.234	0.001918	ENSDARG00000077710	neuroligin 1
pvalb1	-3.221	1.19E-05	ENSDARG00000037789	parvalbumin 1
neu3.5	-3.219	0.001601	ENSDARG00000096368	sialidase 3, tandem duplicate 5
fancl	-3.204	5.78E-08	ENSDARG00000007885	Fanconi anemia, complementation group L
asb15a	-3.187	0.001112	ENSDARG00000045633	ankyrin repeat and SOCS box containing 15a
CAPN1	-3.145	0.000171	ENSDARG00000055338	calpain 1, (mu/I) large subunit
col8a1b	-3.123	0.004463	ENSDARG00000003533	collagen, type VIII, alpha 1b
cbx7a	-3.114	0.000902	ENSDARG00000038025	chromobox homolog 7a
knca7	-3.105	0.000303	ENSDARG00000086571	potassium voltage-gated channel, shaker-related subfamily, member 7
c1qa	-3.089	0.001888	ENSDARG00000044613	complement component 1, q subcomponent, A chain
cdnf	-3.078	0.000443	ENSDARG00000075501	cerebral dopamine neurotrophic factor
SRMS	-3.059	0.000504	ENSDARG00000077783	src-related kinase lacking C-terminal regulatory tyrosine and N-terminal myristylation sites
MYOM2	-3.044	1.09E-05	ENSDARG00000091099	myomesin 2
PLEKHA4	-3.017	3.58E-06	ENSDARG00000071460	pleckstrin homology domain containing, family A (phosphoinositide binding specific) member 4
sycp2	-3.006	0.002451	ENSDARG00000088950	synaptonemal complex protein 2

aqp4	-3.002	1.32E-05	ENSDARG00000010565	aquaporin 4
myhz2	-2.965	3.94E-05	ENSDARG00000012944	myosin, heavy polypeptide 2, fast muscle specific
tcap	-2.963	0.005061	ENSDARG00000007344	titin-cap (telethonin)
rxfp3.3b	-2.919	0.005661	ENSDARG00000059348	relaxin/insulin-like family peptide receptor 3.3b
evi5a	-2.911	4.26E-05	ENSDARG00000077666	ecotropic viral integration site 5a
irf1b	-2.887	0.009384	ENSDARG00000032768	interferon regulatory factor 1b
glis1b	-2.847	0.006496	ENSDARG00000027933	GLIS family zinc finger 1b
b4galt5	-2.841	0.00625	ENSDARG00000037815	UDP-Gal:betaGlcNAc beta 1,4- galactosyltransferase, polypeptide 5
PDE2A	-2.827	8.06E-05	ENSDARG00000079064	phosphodiesterase 2A, cGMP-stimulated
myhc4	-2.812	2.10E-05	ENSDARG00000035438	myosin heavy chain 4
prkcg	-2.805	0.009304	ENSDARG00000004561	protein kinase C, gamma
myha	-2.769	1.67E-05	ENSDARG00000095930	myosin, heavy chain a
fgf6a	-2.765	0.000121	ENSDARG00000009351	fibroblast growth factor 6a
tnfaip2b	-2.752	0.003025	ENSDARG00000094072	tumor necrosis factor, alpha-induced protein 2b
myhz1.1	-2.751	5.70E-05	ENSDARG00000067990	myosin, heavy polypeptide 1.1, skeletal muscle
myoz1a	-2.725	6.76E-06	ENSDARG00000056209	myozenin 1a
IGFN1	-2.723	0.001856	ENSDARG00000097613	immunoglobulin-like and fibronectin type III domain containing 1
st6galnac5a	-2.703	0.006686	ENSDARG00000039220	ST6 (alpha-N-acetyl-neuraminyl-2,3-beta-galactosyl-1,3)-N-acetylgalactosaminide alpha-2,6-sialyltransferase 5a
MYOM2	-2.697	0.000242	ENSDARG00000089850	myomesin 2
arl14	-2.695	0.000871	ENSDARG00000063223	ADP-ribosylation factor-like 14
myhz1.2	-2.689	6.23E-05	ENSDARG00000067995	myosin, heavy polypeptide 1.2, skeletal muscle
myhz1.3	-2.675	0.000119	ENSDARG00000067997	myosin, heavy polypeptide 1.3, skeletal muscle
socs2	-2.662	0.007856	ENSDARG00000045557	suppressor of cytokine signaling 2
ryr3	-2.639	3.80E-06	ENSDARG00000071331	ryanodine receptor 3

gene	Fold Change	p-value	id	description
crtac1a	-2.637	0.002687	ENSDARG00000059826	cartilage acidic protein 1a
arl13a	-2.622	0.010937	ENSDARG00000052575	ADP-ribosylation factor-like 13a
pyroxd2	-2.612	1.33E-16	ENSDARG00000014101	pyridine nucleotide-disulphide oxidoreductase domain 2
casq1a	-2.579	4.36E-06	ENSDARG00000038716	calsequestrin 1a
CMYA5	-2.577	1.24E-05	ENSDARG00000077716	cardiomyopathy associated 5
clic5a	-2.561	0.00026	ENSDARG00000075993	chloride intracellular channel 5a
opn3	-2.533	0.001905	ENSDARG00000052775	opsin 3
SYNPO2	-2.529	0.000519	ENSDARG00000077157	synaptopodin 2
tgm2l	-2.506	0.003651	ENSDARG00000093381	transglutaminase 2, like
COLQ	-2.491	7.45E-05	ENSDARG00000074216	collagen-like tail subunit (single strand of homotrimer) of asymmetric acetylcholinesterase
tnnt3b	-2.483	0.000209	ENSDARG00000068457	troponin T3b, skeletal, fast
kcnma1a	-2.482	0.00017	ENSDARG00000079840	potassium large conductance calcium-activated channel, subfamily M, alpha member 1a
asb14	-2.479	0.001108	ENSDARG00000087741	ankyrin repeat and SOCS box containing 14

Polr1d: downregulated genes with p < 0.01

gene	Fold Change	p-value	id	description
crygm2d18	-29.103	0.004923	ENSDARG00000086912	crystallin, gamma M2d18
polr1d	-21.319	4.42E-72	ENSDARG00000037570	polymerase (RNA) I polypeptide D
tmem173	-17.487	0.000156	ENSDARG00000091058	transmembrane protein 173
drd3	-9.466	0.001728	ENSDARG00000032131	dopamine receptor D3
TRBV28	-8.787	0.001939	ENSDARG00000091233	T cell receptor beta variable 28
arl13a	-7.704	1.07E-06	ENSDARG00000052575	ADP-ribosylation factor-like 13A
CD6	-7.012	0.009592	ENSDARG00000075723	CD6 molecule
crygmxl2	-6.838	0.001979	ENSDARG00000074001	crystallin, gamma MX, like 2
crygm2d12	-6.748	0.009967	ENSDARG00000069801	crystallin, gamma M2d12

crygm2d7	-6.313	0.0099	ENSDARG00000076572	crystallin, gamma M2d7
ltc4s	-6.054	1.63E-06	ENSDARG00000062598	leukotriene C4 synthase
crygm2d17	-5.800	0.003894	ENSDARG00000076693	crystallin, gamma M2d17
aqp10b	-5.577	0.006091	ENSDARG00000058678	aquaporin 10b
crygmx	-5.523	0.004565	ENSDARG00000053862	crystallin, gamma MX
gria2b	-4.693	7.39E-11	ENSDARG00000052765	glutamate receptor, ionotropic, AMPA 2b
capn3a	-4.203	0.007203	ENSDARG00000041864	calpain 3a, (p94)
nitr10a	-3.937	0.006304	ENSDARG00000042968	novel immune-type receptor 10a
mchr2	-3.858	0.003466	ENSDARG00000036117	melanin-concentrating hormone receptor 2
zgc:113364	-3.560	6.34E-08	ENSDARG00000037192	zgc:113364
bscl2l	-3.443	4.33E-09	ENSDARG00000025912	Bernardinelli-Seip congenital lipodystrophy 2, like
FBXO40	-3.429	0.001496	ENSDARG00000091119	F-box protein 40
itga6l	-3.424	0.001439	ENSDARG00000056018	integrin, alpha 6, like
BRINP3	-3.335	0.008396	ENSDARG00000075352	bone morphogenetic protein/retinoic acid inducible neural-specific 3
sst6	-3.326	0.008252	ENSDARG00000093804	somatostatin 6
tcap	-3.293	0.002647	ENSDARG00000007344	titin-cap (telethonin)
spon2b	-3.269	9.26E-05	ENSDARG00000002732	spondin 2b, extracellular matrix protein
slc25a4	-3.231	1.77E-05	ENSDARG00000027355	solute carrier family 25 (mitochondrial carrier; adenine nucleotide translocator), member 4
rab3b	-3.215	0.003084	ENSDARG00000042803	RAB3B, member RAS oncogene family
pvalb1	-3.192	1.54E-05	ENSDARG00000037789	parvalbumin 1
crfb15	-3.040	0.000921	ENSDARG00000096495	cytokine receptor family member B15
MAF	-2.970	0.00902	ENSDARG00000076520	v-maf avian musculoaponeurotic fibrosarcoma oncogene homolog
FNDC7	-2.787	0.002275	ENSDARG00000075676	fibronectin type III domain containing 7]
tnnt3b	-2.775	3.64E-05	ENSDARG00000068457	troponin T3b, skeletal, fast
MYOM2	-2.747	0.000206	ENSDARG00000091099	myomesin 2
cabp2b	-2.731	0.000233	ENSDARG00000052277	calcium binding protein 2b
PLCB1	-2.704	0.009327	ENSDARG00000090084	phospholipase C, beta 1 (phosphoinositide-specific)

asb2a.1	-2.676	0.000606	ENSDARG00000003797	ankyrin repeat and SOCS box-containing 2a, tandem duplicate 1
crtac1a	-2.651	0.003999	ENSDARG00000059826	cartilage acidic protein 1a
pfkma	-2.628	0.000304	ENSDARG00000014179	phosphofructokinase, muscle a
FAM149A	-2.453	0.003022	ENSDARG00000073709	family with sequence similarity 149, member A
OCEL1	-2.419	0.008566	ENSDARG00000061800	occludin/ELL domain containing 1
gla	-2.359	0.000628	ENSDARG00000036155	galactosidase, alpha
tm4sf18	-2.321	0.009841	ENSDARG00000060668	transmembrane 4 L six family member 18
casq1a	-2.307	7.86E-05	ENSDARG00000038716	calsequestrin 1a
CENPU	-2.262	1.58E-06	ENSDARG00000088924	centromere protein U
rhoua	-2.197	2.87E-09	ENSDARG00000019709	ras homolog gene family, member Ua
pvalb3	-2.191	0.00437	ENSDARG00000022817	parvalbumin 3
GDPD2	-2.150	6.58E-06	ENSDARG00000073870	glycerophosphodiester phosphodiesterase domain containing 2
tubb6	-2.149	0.010827	ENSDARG00000055649	tubulin, beta 6 class V
smtnl1	-2.114	0.001993	ENSDARG00000041257	smoothelin-like 1
cry5	-2.099	3.30E-06	ENSDARG00000019498	cryptochrome 5
capn3b	-2.086	0.00051	ENSDARG00000043035	calpain 3b
CPXM1	-2.069	0.000255	ENSDARG00000073716	carboxypeptidase X (M14 family), member 1
cacng4	-2.024	0.006359	ENSDARG00000074669	calcium channel, voltage-dependent, gamma subunit 4

Appendix B: Polr1a RNA-Seq Data

The top 100 upregulated genes in common between *polr1a* mutants at 15 hpf and 24 hpf are listed below. All values are significant at p < 0.005. FC = fold change.

gene	15 hpf FC	24 hpf FC	id	description
ifit8	146.67	856.30	ENSDARG00000057173	interferon-induced protein with tetratricopeptide repeats 8
CDKN2B	185.39	335.34	ENSDARG00000037262	cyclin-dependent kinase inhibitor 2B (p15, inhibits CDK4)
rspo1	43.28	59.39	ENSDARG00000039957	R-spondin homolog (Xenopus laevis)
isg15	53.23	52.24	ENSDARG00000086374	ISG15 ubiquitin-like modifier
NAMPT	6.04	38.16	ENSDARG00000078738	nicotinamide phosphoribosyltransferase
RNF14	25.06	34.89	ENSDARG00000078683	ring finger protein 14
gig2p	19.57	34.75	ENSDARG00000088260	grass carp reovirus (GCRV)-induced gene 2p
ANKRD34C	36.52	30.77	ENSDARG00000093286	ankyrin repeat domain 34C
kcnq4	20.45	27.38	ENSDARG00000089490	potassium voltage-gated channel, KQT-like subfamily, member 4 [
cxcr3.1	22.64	26.67	ENSDARG00000007358	chemokine (C-X-C motif) receptor 3, tandem duplicate 1
atxn1b	34.86	22.32	ENSDARG00000060862	ataxin 1b
mdm2	25.28	22.32	ENSDARG00000033443	transformed 3T3 cell double minute 2 homolog (mouse)
phlda3	16.27	21.22	ENSDARG00000037804	pleckstrin homology-like domain, family A, member 3
ccdc88aa	20.18	20.70	ENSDARG00000078440	coiled-coil domain containing 88Aa
rbl2	38.95	19.23	ENSDARG00000045636	retinoblastoma-like 2 (p130)
casp8	18.12	18.52	ENSDARG00000058325	caspase 8, apoptosis-related cysteine peptidase
bbc3	17.43	18.09	ENSDARG00000069282	BCL2 binding component 3
cdkn1a	8.54	17.50	ENSDARG00000076554	cyclin-dependent kinase inhibitor 1A
NAMPT	2.63	16.40	ENSDARG00000076694	nicotinamide phosphoribosyltransferase
ms4a17a.5	11.57	14.45	ENSDARG00000092204	membrane-spanning 4-domains, subfamily A, member 17A.5

lnx1	18.16	14.40	ENSDARG00000043323	ligand of numb-protein X 1
cbln12	11.78	14.25	ENSDARG00000068232	cerebellin 12
mat2al	18.18	13.62	ENSDARG00000063665	methionine adenosyltransferase II, alpha-like
bmb	9.73	13.38	ENSDARG00000096603	brambleberry
LTB4R	15.31	13.02	ENSDARG00000032631	leukotriene B4 receptor
zak	14.72	12.60	ENSDARG00000006978	sterile alpha motif and leucine zipper containing kinase AZK
ghrh	7.92	12.43	ENSDARG00000069481	growth hormone releasing hormone
crygn1	2.87	11.97	ENSDARG00000087437	crystallin, gamma N1
gadd45aa	15.59	11.81	ENSDARG00000043581	growth arrest and DNA-damage-inducible, alpha, a
zbtb38	7.49	11.36	ENSDARG00000077426	zinc finger and BTB domain containing 38
SHISA8	9.41	11.09	ENSDARG00000088204	shisa family member 8
ace	15.88	10.73	ENSDARG00000079166	angiotensin I converting enzyme (peptidyl-dipeptidase A) 1
sesn3	21.13	10.20	ENSDARG00000015822	sestrin 3
rasl11b	4.72	10.17	ENSDARG00000015611	RAS-like, family 11, member B
LTB4R	15.01	9.68	ENSDARG00000061094	leukotriene B4 receptor
foxo3b	21.15	9.63	ENSDARG00000042904	forkhead box O3b
rps27.2	4.42	9.37	ENSDARG00000090186	ribosomal protein S27, isoform 2
bcl3	7.18	9.30	ENSDARG00000087832	B-cell CLL/lymphoma 3]
OSBP2	6.79	8.77	ENSDARG00000022772	oxysterol binding protein 2
ppp4r4	5.45	8.64	ENSDARG00000010407	protein phosphatase 4, regulatory subunit 4
oscp1a	2.65	8.63	ENSDARG00000094130	organic solute carrier partner 1a
gtpbp1l	8.44	8.29	ENSDARG00000042900	GTP binding protein 1, like
mmrn2b	14.59	7.92	ENSDARG00000073711	multimerin 2b
rpz5	18.32	7.43	ENSDARG00000075718	rapunzel 5
eva1bb	2.87	7.42	ENSDARG00000067742	eva-1 homolog Bb (C. elegans)
ccng1	4.37	7.24	ENSDARG00000076667	cyclin G1
vrk2	7.61	7.20	ENSDARG00000021547	vaccinia related kinase 2
TAF1C	5.03	7.05	ENSDARG00000096310	TATA box binding protein (TBP)-associated factor, RNA polymerase I, C, 110kDa
rnf169	8.65	7.01	ENSDARG00000042825	ring finger protein 169
igfbp7	6.13	6.94	ENSDARG00000017389	insulin-like growth factor binding protein 7
TRIM29	10.61	6.93	ENSDARG00000034707	tripartite motif containing 29
parp3	7.24	6.91	ENSDARG00000003961	poly (ADP-ribose) polymerase family, member 3

rd3	8.35	6.84	ENSDARG00000031600	retinal degeneration 3
tp53	3.66	6.55	ENSDARG00000035559	tumor protein p53
ms4a17a.1	14.02	6.45	ENSDARG00000043798	membrane-spanning 4-domains, subfamily A, member 17A.1
ms4a17a.2	10.63	6.28	ENSDARG00000093546	membrane-spanning 4-domains, subfamily A, member 17a.2
cenpv	5.54	6.20	ENSDARG00000092285	centromere protein V
prdm1b	15.02	6.09	ENSDARG00000053592	PR domain containing 1b, with ZNF domain
tnfaip6	5.40	6.07	ENSDARG00000093440	tumor necrosis factor, alpha-induced protein 6
lzts2b	5.91	6.02	ENSDARG00000077207	leucine zipper, putative tumor suppressor 2b
crfb1	4.01	5.96	ENSDARG00000068681	cytokine receptor family member b1
ITPR1	6.81	5.86	ENSDARG00000074149	inositol 1,4,5-trisphosphate receptor, type 1
pik3r3a	7.33	5.80	ENSDARG00000071219	phosphoinositide-3-kinase, regulatory subunit 3a (gamma)
PNPLA2	13.51	5.74	ENSDARG00000073955	patatin-like phospholipase domain containing 2
lyrm1	4.06	5.63	ENSDARG00000026281	LYR motif containing 1
abcc5	10.32	5.57	ENSDARG00000061233	ATP-binding cassette, sub-family C (CFTR/MRP), member 5
RNF14	7.33	5.56	ENSDARG00000090710	ring finger protein 14
dcdc2b	4.15	5.25	ENSDARG00000053744	doublecortin domain containing 2B
cica	6.20	5.20	ENSDARG00000071150	capicua homolog a (Drosophila)
METRNL	4.10	5.19	ENSDARG00000007289	meteorin, glial cell differentiation regulator-like
pappaa	2.77	5.16	ENSDARG00000059544	pregnancy-associated plasma protein A, pappalysin 1a
gpd1a	3.12	5.05	ENSDARG00000043701	glycerol-3-phosphate dehydrogenase 1a
PRSS56	15.24	5.01	ENSDARG00000053158	protease, serine, 56
igf2a	5.50	5.01	ENSDARG00000018643	insulin-like growth factor 2a
CD274	8.29	4.81	ENSDARG00000059310	CD274 molecule
NIM1K	14.20	4.79	ENSDARG00000074087	NIM1 serine/threonine protein kinase
slc1a8b	6.37	4.79	ENSDARG00000032465	solute carrier family 1 (glutamate transporter), member 8b
isg20	3.10	4.68	ENSDARG00000079783	interferon-stimulated protein
matn1	3.53	4.57	ENSDARG00000030215	matrilin 1
fosl1a	3.43	4.57	ENSDARG00000015355	FOS-like antigen 1a
fgf2	5.44	4.51	ENSDARG00000075031	fibroblast growth factor 2

247

slc5a5	2.16	4.47	ENSDARG00000005392	solute carrier family 5 (sodium iodide symporter), member 5
nudt6	2.21	4.44	ENSDARG00000087321	nudix (nucleoside diphosphate linked moiety X)-type motif 6
nfe2l2b	12.31	4.44	ENSDARG00000089697	nuclear factor (erythroid-derived 2)-like 2b
ms4a17a.4	8.06	4.38	ENSDARG00000014024	membrane-spanning 4-domains, subfamily A, member 17A.4
foxi1	2.88	4.32	ENSDARG00000019659	forkhead box i1
tspan18a	3.71	4.31	ENSDARG00000056656	tetraspanin 18a
ankef1b	4.98	4.24	ENSDARG00000060211	ankyrin repeat and EF-hand domain containing 1b
atf5a	4.62	4.21	ENSDARG00000068096	activating transcription factor 5a
lpcat2	4.11	4.19	ENSDARG00000053010	lysophosphatidylcholine acyltransferase 2
rhoub	2.11	4.13	ENSDARG00000012968	ras homolog gene family, member Ub
upb1	2.74	3.97	ENSDARG00000011521	ureidopropionase, beta
slc1a2a	3.47	3.97	ENSDARG00000052138	solute carrier family 1 (glial high affinity glutamate transporter), member 2a
mmp13b	18.92	3.93	ENSDARG00000015797	matrix metalloproteinase 13b
batf3	2.23	3.92	ENSDARG00000042577	basic leucine zipper transcription factor, ATF-like 3
cpn1	2.54	3.87	ENSDARG00000096728	carboxypeptidase N, polypeptide 1
es1	4.15	3.86	ENSDARG00000094516	es1 protein
arrdc1b	2.96	3.82	ENSDARG00000079839	arrestin domain containing 1b
RNF14	4.41	3.80	ENSDARG00000002794	ring finger protein 14

DOWNREGULATED GENES IN *POLR1A* MUTANTS

The following table shows a list of the top 100 genes that are downregulated in both 15 hpf and 24 hpf *polr1a* mutant embryos. FC = fold change.

gene	15 hpf FC	24 hpf FC	id	description
zgc:162144	-9.07	-9.97	ENSDARG00000037603	zgc:162144
polr1a	-6.18	-10.89	ENSDARG00000029172	polymerase (RNA) I polypeptide A
fads2	-5.88	-6.94	ENSDARG00000019532	fatty acid desaturase 2
rxfp3.2b	-5.35	-2.85	ENSDARG00000061846	relaxin/insulin-like family peptide receptor 3.2b
PAX7 (3 of 3)	-4.89	-2.23	ENSDARG00000091353	paired box 7
slc6a15	-4.67	-2.89	ENSDARG00000062821	solute carrier family 6 (neutral amino acid transporter), member 15
kcnj14	-4.61	-4.71	ENSDARG00000075914	potassium inwardly-rectifying channel, subfamily J, member 14
cyp4v7	-4.49	-2.13	ENSDARG00000061585	cytochrome P450, family 4, subfamily V, polypeptide 7
pax7a	-4.36	-2.36	ENSDARG00000005173	paired box gene 7a
cx44.1	-4.06	-2.10	ENSDARG00000015076	connexin 44.1
mipb	-3.99	-20.93	ENSDARG00000013963	major intrinsic protein of lens fiber b
mipa	-3.74	-7.21	ENSDARG00000037285	major intrinsic protein of lens fiber a
zgc:165604	-3.62	-2.55	ENSDARG00000021241	zgc:165604
GRM2 (2 of 2)	-3.60	-3.16	ENSDARG00000007195	glutamate receptor, metabotropic 2
prtgb	-3.58	-3.64	ENSDARG00000040442	protogenin homolog b (Gallus gallus)
nr2f1b	-3.55	-3.05	ENSDARG00000017168	nuclear receptor subfamily 2, group F, member 1b
DLK1	-3.55	-2.48	ENSDARG00000077725	delta-like 1 homolog (Drosophila)
otomp	-3.45	-2.12	ENSDARG00000040306	otolith matrix protein
il15	-3.41	-2.93	ENSDARG00000052361	interleukin 15

lrrtm2	-3.38	-2.47	ENSDARG00000071374	leucine rich repeat transmembrane neuronal 2
lrrtm2	-3.35	-2.76	ENSDARG00000090425	leucine rich repeat transmembrane neuronal 2
adamts15b	-3.34	-1.71	ENSDARG00000033544	ADAM metallopeptidase with thrombospondin type 1 motif, 15b
bcl11ab	-3.27	-5.52	ENSDARG00000063153	B-cell CLL/lymphoma 11Ab
lrrtm1	-3.24	-2.05	ENSDARG00000052713	leucine rich repeat transmembrane neuronal 1
cdca7a	-3.22	-2.80	ENSDARG00000077620	cell division cycle associated 7a
zgc:194261	-3.21	-1.63	ENSDARG00000035340	zgc:194261
lrrc4.2	-3.00	-1.70	ENSDARG00000003020	leucine rich repeat containing 4.2
helt	-2.96	-4.66	ENSDARG00000056400	hey-like transcription factor
foxd1	-2.94	-1.72	ENSDARG00000029179	forkhead box D1
crygn2	-2.91	-2.75	ENSDARG00000030411	crystallin, gamma N2
plp1a	-2.89	-4.86	ENSDARG00000057770	proteolipid protein 1a
atp2a1l	-2.87	-2.71	ENSDARG00000035458	ATPase, Ca++ transporting, cardiac muscle, fast twitch 1 like
foxg1d	-2.81	-1.56	ENSDARG00000070053	forkhead box G1d
spon2b	-2.78	-7.24	ENSDARG00000002732	spondin 2b, extracellular matrix protein
wdr76	-2.76	-2.48	ENSDARG00000053554	WD repeat domain 76
hells	-2.76	-2.34	ENSDARG00000057738	helicase, lymphoid-specific
vsx1	-2.69	-2.93	ENSDARG00000056292	visual system homeobox 1 homolog, chx10-like
dmbx1b	-2.67	-2.03	ENSDARG00000002510	diencephalon/mesencephalon homeobox 1b
atp1b4	-2.66	-3.76	ENSDARG00000053262	ATPase, (Na+)/K+ transporting, beta 4 polypeptide
ccdc153	-2.66	-3.52	ENSDARG00000077161	coiled-coil domain containing 153
mcm5	-2.64	-2.10	ENSDARG00000019507	MCM5 minichromosome maintenance deficient 5 (S. cerevisiae)
bcat1	-2.64	-2.44	ENSDARG00000045568	branched chain aminotransferase 1, cytosolic
GPR112	-2.62	-10.97	ENSDARG00000087813	G protein-coupled receptor 112
gsx2	-2.62	-1.71	ENSDARG00000043322	GS homeobox 2
nkx1.2lb	-2.62	-2.38	ENSDARG00000012697	NK1 transcription factor related 2-like,b
ccng2	-2.61	-4.14	ENSDARG00000017602	cyclin G2
stmn1a	-2.57	-2.66	ENSDARG00000004169	stathmin 1a

suv39h1a	-2.56	-2.95	ENSDARG00000026799	suppressor of variegation 3-9 homolog 1a
phf19	-2.53	-2.14	ENSDARG00000078050	PHD finger protein 19
psmd10	-2.53	-1.63	ENSDARG00000015628	proteasome (prosome, macropain) 26S subunit, non-ATPase, 10
dab1b	-2.52	-2.74	ENSDARG00000003290	disabled homolog 1b (Drosophila)
csf1b	-2.52	-1.46	ENSDARG00000068263	colony stimulating factor 1b (macrophage)
mcm6	-2.52	-2.01	ENSDARG00000057683	MCM6 minichromosome maintenance deficient 6, mitotin (S. cerevisiae)
vax1	-2.52	-2.56	ENSDARG00000021916	ventral anterior homeobox 1
rx3	-2.51	-1.53	ENSDARG00000052893	retinal homeobox gene 3
mcm3	-2.51	-2.06	ENSDARG00000090802	MCM3 minichromosome maintenance deficient 3 (S. cerevisiae)
mcm3	-2.47	-2.11	ENSDARG00000024204	MCM3 minichromosome maintenance deficient 3 (S. cerevisiae)
barhl1b	-2.47	-2.59	ENSDARG00000019013	BarH-like 1b
dnmt1	-2.45	-1.85	ENSDARG00000030756	DNA (cytosine-5-)-methyltransferase 1
NBL1	-2.45	-1.84	ENSDARG00000031898	neuroblastoma 1, DAN family BMP antagonist
hoxc13b	-2.43	-1.44	ENSDARG00000090023	homeo box C13b
FGFBP3	-2.43	-2.32	ENSDARG00000040162	fibroblast growth factor binding protein 3
ndst3	-2.43	-4.70	ENSDARG00000041776	N-deacetylase/N-sulfotransferase (heparan glucosaminyl) 3
msh6	-2.41	-1.48	ENSDARG00000011666	mutS homolog 6 (E. coli)
cdkn2d	-2.41	-2.62	ENSDARG00000094176	cyclin-dependent kinase inhibitor 2D (p19, inhibits CDK4)
nr2e1	-2.39	-3.09	ENSDARG00000017107	nuclear receptor subfamily 2, group E, member 1
ldb2b	-2.38	-1.55	ENSDARG00000034896	LIM-domain binding factor 2b
ccne2	-2.36	-2.32	ENSDARG00000027918	cyclin E2
prim1	-2.36	-1.80	ENSDARG00000040163	primase polypeptide 1
esco2	-2.34	-1.77	ENSDARG00000014685	establishment of cohesion 1 homolog 2
pou3f3b	-2.30	-2.59	ENSDARG00000095896	POU class 3 homeobox 3b
unga	-2.29	-1.87	ENSDARG00000042527	uracil-DNA glycosylase a

zgc:110540	-2.29	-2.10	ENSDARG00000054929	zgc:110540
mab21l2	-2.29	-1.49	ENSDARG00000015266	mab-21-like 2
asf1ba	-2.29	-1.90	ENSDARG00000087313	ASF1 anti-silencing function 1 homolog Ba (S. cerevisiae)
rpl22l1	-2.27	-2.82	ENSDARG00000010244	ribosomal protein L22-like 1
zgc:174719	-2.27	-1.62	ENSDARG00000074395	zgc:174719
fancc	-2.26	-1.61	ENSDARG00000055232	Fanconi anemia, complementation group C
rx2	-2.26	-5.60	ENSDARG00000040321	retinal homeobox gene 2
alpl	-2.25	-1.55	ENSDARG00000015546	alkaline phosphatase, liver/bone/kidney
mcm4	-2.25	-2.01	ENSDARG00000040041	MCM4 minichromosome maintenance deficient 4, mitotin (S. cerevisiae)
tubb1	-2.24	-1.66	ENSDARG00000053066	tubulin, beta 1 class VI
asf1ba	-2.23	-1.87	ENSDARG00000020435	ASF1 anti-silencing function 1 homolog Ba (S. cerevisiae)
orc4	-2.22	-1.40	ENSDARG00000029014	origin recognition complex, subunit 4
wdhd1	-2.21	-1.77	ENSDARG00000015998	WD repeat and HMG-box DNA binding protein 1
pde9a	-2.20	-1.65	ENSDARG00000060280	phosphodiesterase 9A
hoxa13b	-2.20	-1.82	ENSDARG00000036254	homeo box A13b
ccl25b	-2.19	-4.22	ENSDARG00000070873	chemokine (C-C motif) ligand 25b
arhgap4b	-2.19	-1.81	ENSDARG00000015003	Rho GTPase activating protein 4b
DACT3 (2 of 2)	-2.19	-2.58	ENSDARG00000088409	dishevelled-binding antagonist of beta-catenin 3
uhrf1	-2.18	-1.71	ENSDARG00000091448	ubiquitin-like, containing PHD and RING finger domains, 1
dlx1a	-2.18	-2.87	ENSDARG00000013125	distal-less homeobox gene 1a
pou3f1	-2.18	-3.09	ENSDARG00000009823	POU class 3 homeobox 1
sox21b	-2.18	-2.78	ENSDARG00000008540	SRY-box containing gene 21 b
hoxa13a	-2.17	-1.88	ENSDARG00000007609	homeo box A13a
st8sia2	-2.17	-2.35	ENSDARG00000018788	ST8 alpha-N-acetyl-neuraminide alpha-2,8-sialyltransferase 2
uhrf1	-2.16	-1.72	ENSDARG00000009946	ubiquitin-like, containing PHD and RING finger domains, 1
pogza	-2.16	-1.81	ENSDARG00000054778	pogo transposable element with ZNF domain a
syngr1a	-2.15	-1.34	ENSDARG00000002564	synaptogyrin 1a
orc6	-2.15	-1.45	ENSDARG00000075682	origin recognition complex, subunit 6

| rrm2 | -2.14 | -2.35 | ENSDARG00000078069 | ribonucleotide reductase M2 polypeptide |

Appendix C: Publications and Abstracts

The following appendix lists my four publications from the Trainor lab, selected abstracts that I presented, and some of the awards I received.

<small>PUBLICATIONS</small>

The first paper listed has recently been submitted to Plos Genetics; the other three papers are already published.

Noack Watt KE, Achilleos A, Neben C, Merrill-Brugger A, Trainor PA. The roles of RNA Polymerase I subunits Polr1c and Polr1d in craniofacial development and the pathogenesis of Treacher Collins syndrome. (submitted)

Weaver KN*, **Noack Watt KE***, Hufnagel RB, Navajas Acedo J, Linscott LL, Sund KL, Bender PL, König R, Lourenco CM, Hehr U, Hopkin RJ, Lohmann DR, Trainor PA, Wieczorek D, Saal HM. 2015. Acrofacial Dysostosis, Cincinnati Type, a Mandibulofacial Dysostosis Syndrome with Limb Anomalies, Is Caused by POLR1A Dysfunction. The American Journal of Human Genetics 96(5):765-774. (*co-first authors)

Aoto K, Sandell LL, Butler Tjaden NE, Yuen KC, **Noack Watt KE**, Black BL, Durnin M, Trainor PA. 2015. Mef2c-F10N enhancer driven β-galactosidase (LacZ) and Cre recombinase mice facilitate analyses of gene function and lineage fate in neural crest cells. Developmental Biology 402(1):3-16.

Noack Watt KE, Trainor PA. 2014. Chapter 17 - Neurocristopathies: The Etiology and Pathogenesis of Disorders Arising from Defects in Neural Crest Cell Development. In: Trainor PA, editor. Neural Crest Cells. Boston: Academic Press. p 361-394.

The following section lists presentations I gave at a variety of international meetings and some of the awards I received.

Invited Oral Presentations:

Watt K, Achilleos A, Trainor PA. The roles of RNA polymerase subunits Polr1c and Polr1d in craniofacial development and the pathogenesis of Treacher Collins syndrome. GRC on Craniofacial Morphogenesis and Tissue Regeneration, Lucca, Italy. April, 2014.

Watt K, Achilleos A, Trainor PA. The RNA polymerase subunits Polr1c and Polr1d play critical roles in craniofacial development and the pathogenesis of Treacher Collins syndrome. GRS on Craniofacial Morphogenesis and Tissue Regeneration, Ventura, CA. March, 2012.

Poster presentations:

Watt K, Achilleos A, Trainor PA. Examination of the roles of RNA Polymerase I subunits during craniofacial development. Society of Craniofacial Genetics and Developmental Biology, La Jolla, CA. October, 2014.

Watt K, Achilleos A, Trainor PA. Examining the roles of RNA Polymerase subunits Polr1c and Polr1d in Treacher Collins syndrome and craniofacial development. International Conference on Zebrafish Development and Genetics, Madison, WI. June, 2014

Watt K, Achilleos A, Trainor PA. The roles of RNA polymerase I subunits Polr1c and Polr1d in craniofacial development and Treacher Collins syndrome. Society of Craniofacial Genetics and Developmental Biology, Boston, MA. October, 2013.

Awards

Ruth Kirschstein-NRSA Predoctoral Fellowship, National Institute of Dental and Craniofacial Research**,** 2013-2015.

First Place Award, oral presentation, Young Investigator Science Retreat, Stowers Institute for Medical Research, April 2015.

First Place Award, poster presentation, Society for Craniofacial Genetics and Developmental Biology, La Jolla, CA, October 2014.

First Place Award, oral presentation, Student Research Forum, University of Kansas Medical Center, March 2013.